Investigating mitochondrial dysfunction in the nervous system

Gatt, Ariana Pia

Awarding institution:
King's College London

Investigating mitochondrial dysfunction in the nervous system

Thesis submitted to King's College London for the degree of Doctor of Philosophy in Neuroscience

Ariana Pia Gatt

Wolfson Centre for Age-Related Diseases

The Institute of Psychiatry, Psychology & Neuroscience (IoPPN)

King's College London

2011-2015

Declaration

I hereby declared that all the work presented in this thesis is a result of my own research and has not been accepted for any other degree. Contributions from anyone else have been clearly stated throughout the text.

Ariana Gatt

March 2015

Abstract

Mitochondria play critical roles in the generation of cellular energy, apoptosis, calcium buffering, and mitochondrial dysfunction is strongly implicated in common neurodegenerative diseases such as Alzheimer's and Parkinson's disease. However, we still have a very poor understanding of the consequences of mitochondrial dysfunction in neurons *in vivo*. This thesis investigates mitochondrial dysfunction in patients with neurodegenerative disease and in a novel *Drosophila* model of neuronal mitochondrial dysfunction.

I found that a single nucleotide polymorphism (SNP) in the gene *mitochondrial transcription factor A* (*TFAM,* SNP rs2306604 A>G) is associated with Parkinson's disease dementia (PDD), but not with dementia with Lewy bodies (DLB). I have shown that mitochondrial DNA levels are significantly reduced in the frontal cortex of PDD patients, compared to controls. Furthermore, I have characterised the expression of TFAM and representative components of the mitochondrial electron transport (ETC) chain at the protein level in patients with Parkinson's disease with and without dementia to determine whether rs2306604 A>G affects TFAM or ETC protein expression.

In order to investigate mitochondrial dysfunction in a genetically tractable model system I have used a novel model of neuronal-specific mitochondrial dysfunction in *Drosophila*. I have used overexpression of *TFAM*, or expression of a mitochondrially-targeted restriction enzyme *mitoXhoI*, to cause mitochondrial dysfunction specifically in neurons. I have analysed the changes in mitochondrial DNA and mitochondrial gene expression in this model as well as characterising the behavioural and synaptic phenotypes.

Using this model I performed microarray analysis to characterise the mitochondrial retrograde response in the *Drosophila* nervous system. This analysis revealed that neuronal mitochondrial dysfunction alters the expression of over 300 genes. I have validated the

changes in expression of several of these genes *in vivo*. I have also characterised the involvement of the transcription factor hypoxia inducible factor alpha (HIFα) in the mitochondrial retrograde response in *Drosophila*. I found that HIFα regulates the expression of several retrograde response genes and that modulation of HIFα expression ameliorates some of the phenotypes associated with mitochondrial dysfunction.

Acknowledgements

First of all, I would like to express my utmost gratitude to my primary supervisor Dr. Joe Bateman; his support and guidance throughout the past four years have helped me greatly. I would also like to thank my secondary supervisor Prof. Clive Ballard for the constructive feedback and amazing support, as well as Prof. Paul T. Francis for taking the time to discuss experimental data and showing great interest in the proceedings of this study.

I must also thank Julie Vallortigara for all her assistance in post-mortem tissue studies, especially in western analysis and Emma Jones for guiding me through DNA extraction and SNP genotyping. Thank you also to David Howlett for carrying out immunohistochemistry analysis on some of the cases utilised in the study. Additional thanks go to Dr. Johannes Attems for carrying out neuropathological analysis.

I must thank past and present lab members who have walked with me every step of the way. Special thanks go to past members Amélie Avet-Rochex who guided me throughout my first months in the department, and Umut Cagin who was a crucial help in the lab and a great initiator of multiple mitochondrial discussions. An additional huge thank you goes to my current partner in mitochondrial crime Olivia Duncan – thank you for all the laughs, the singing, the dancing, the cups of coffee and for introducing me to the Northumbrian countryside. I must also thank my favourite Austrian princess Katja and the most recent additions to the Bateman lab Elin and Rachel H. Thank you girls – It was a pleasure!

There is a great number of other Wolfson CARD members who I am happy to call dear friends. Pippa, Rach, Kat, Emily, Ed, Merrick, Nick, Ify, Holly, Liz, Andrea, Louise…Thank you all for the fun nights out and the highly intellectual (and non!!) conversations over beer and pizza. I must especially mention Prav who was a tremendous help in teaching me all he knows regarding western blot analysis, Thanos for all his scientific qPCR wisdom, Fiona for being a constant support and John for all the de-stressing smiles.

A huge thank you to my Maltese friends and family for all the support from miles away – thank you to 'Ilsien in-nisa' and 'the cousins' for all the uplifting texts and chat. An equally huge thank you to my London family – thank you to the Abbeville crew for all the tea and the wine, Lizzy, Antonia and Deedee, I am honoured to have shared such a beautiful home with you! Thank you to the Dulwich and Clapham boys and girls for all the laughs, the dancing and the cottage weekends away. Thank you to beautiful Erin, smiley Homen and energiser-bunny Kate for being my London sisters.

Finally and most importantly, thank you to my lovely family: sister Carla for being the other stress-head in the family and papa Charlie for being just the way he is. Thank you for all the calls and the visits, for all the home-cooked food and for giving me the strength to go on.

This work is dedicated to the memory of Frances Gatt, an amazing mum and an even greater friend.

Table of Contents

List of figures

List of Tables

List of Abbreviations

4E-BP1	4E-binding protein 1
AD	Alzheimer's disease
ADP	adenosine diphosphate
AICD	APP intracellular domain
ALS	Amylotrophic lateral sclerosis
AMP	adenosine monophosphate
ANT	adenine nucleotide transporter
AOX	alternative oxidase
ApoE	Apolipoprotein E
APP	amyloid precursor protein
ATP	adenosine triphosphate
Aβ	Amyloid beta
AβO	amyloid beta oligomers
BA9	Brodmann area 9
BDNF	Brain derived neurotrophic factor
Brp	Bruchpilot
BSA	Bovine serum albumin
CCAP	crustacean cardioactive peptide
CCCP	carbonyl cyanide m-chlorophenylhydrazone
CERAD	Consortium to Establish a Registry for Alzheimer’s Disease
CNS	central nervous system
CoQ	Coenzyme Q
CoVa	Complex IV subunit Va
COX	cytochrome c oxidase
DA	diamide
DGUOK	deoxyguanosine kinase
dInR	*Drosophila* Insulin receptor
DLB	Dementia with Lewy bodies
D-loop	displacement loop
dNTPs	deoxyribonucleotides
Drp1	dynamin related protein-1
DSAD	Down’s Syndrome with AD-like dementia
DTT	Dithiothreitol
EGCG	Epigallocatechin gallate
EOAD	Early onset Alzheimer's disease
ETC	electron transport chain
$FADH_2$	flavine adenine dinucleotide
FDA	US Food and Drug Administration
Fis1	mitochondrial fission-1 protein
FMN	flavin mononucleotide
GO	Gene ontology

GRX	Glutaredoxin
GPxI	Glutathione peroxidase
GSH	Glutathione
GSSG	Glutathione disulfide
GSK-3β	glycogen synthase kinase-3β
GWAS	Genome wide association study
HD	Huntington's disease
HMG	High mobility group
HSP	heavy strand promoter
IHC	immunohistochemistry
IMM	Inner mitochondrial membrane
IPCs	Insulin producing cells
LBD	Lewy body diseases
L-dopa	Levodopa (L-3,4-dihydroxyphenylalanine)
LHON	Leber's hereditary optic neuropathy
LIDs	Levodopa induced dyskinesias
LOAD	Late onset Alzheimer's disease
LRRK2	Leucine rich repeat kinase 2
LSP	Light strand promoter
MCI	Mild cognitive impairment
MELAS	Mitochondrial encephalopathy lactic acidosis, and stroke-like episodes
MERRF	myoclonus epilepsy and ragged-red fibers
MFN	Mitofusin
MNGIE	mitochondrial neurogastrointestinal encephelomyopathy
MnSOD	manganese superoxide dismutase
MPP+	1-methyl-4-phenylpyridinium
MPPP	1-methyl-4-phenyl-4-propionoxy-piperidine
MPTP	1-methyl-4-phenyl-1,2,5,6-tetrahydropyridine
mtDNA	mitochondrial DNA
MTERF 1-4	mitochondrial transcription termination factor 1-4
mTOR	mechanistic target of Rapamycin
mTORC1	mTOR complex 1
MTRPOL	mitochondrial RNA polymerase
NADH	nicotinamide adenine dinucleotide
NEM	N-ethylmaleimide
NFT	Neurofibrillary tangles
NMDA	N-methyl-D-aspartate
NMJ	neuromuscular junction
NRF1	nuclear respiratory factor 1
O_H	origin of replication of the heavy strand
O_L	origin of replication of the light strand
OMM	Outer mitochondrial membrane
OPA1	optic atrophy 1
ORP1	oxidant receptor peroxidise 1
OXPHOS	oxidative phosphorylation
p53R2	ribonucleotidereductase subunit

PD	Parkinson's disease
PDD	Parkinson's disease dementia
PEO	progressive external ophthalmoplegia
PGC1-α	Peroxisome proliferator-activated receptor gamma coactivator 1-alpha
PHF	Paired helical filaments
PINK1	Phosphatase and tensin homolog-induced putative kinase 1
PMD	post-mortem delay
pol γ	polymerase gamma
redox	reduction / oxidation
REM	rapid eye movement
RITOLS	RNA Incorporated Through Out the Lagging Strand
ROS	reactive oxygen species
SNP	single nucleotide polymorphism
SNpc	Substantia nigra pars compacta
SOD	Superoxide dismutase
SSBP	single strand binding protein
TBS-T	Tris-buffered saline with 0.1% Tween20
TFAM	mitochondrial transcription factor A
TFB2M	mitochondrial transcription factor B2
TIM	translocase of inner membrane
TK2	thymidine kinase
TOM	Translocase of outer membrane
TOPO	topoisomerase
TP	thymidine phosphorylase
UPR^{mt}	mitochondrial unfolded protein response
VNC	ventral nerve cord

1. Introduction

1.1. Dementia facts and figures

Dementia is one of the largest and most devastating current global health challenges. The World Alzheimer Report 2013 states that dementia affects 35 million people worldwide and that this frequency is expected to double by 2030 and triple by 2050 (Prince et al., 2013).

The global annual costs of dementia in 2010 were estimated to be of US $ 604 billion, equivalent to 1% of the World's Gross Domestic Product (Prince et al., 2013). Dementia costs will increase proportionally to the number of people affected by the disease and is therefore estimated to double to a cost of US $ 1,117 billion by 2030. In the UK, there are currently over 800,000 people living with dementia, costing the UK economy £23 billion per year (Kane and Cook, 2013).

1.2. Alzheimer's Disease (AD)

Alzheimer's disease (AD) was first described by psychiatrist and neuropathologist Alois Alzheimer in 1906. He had been treating a patient with progressive memory loss, and while carrying out an autopsy upon her death he noticed severe atrophy in her cerebral cortex, as well as neurofibrillary tangles and neuritic plaques (Ramirez-Bermudez, 2012). These histopathological features are today recognised as the pathological hallmarks of the disease.

AD is the most prevalent form of dementia, accounting for 50-75% of all dementia cases in the elderly. Age is a well-known risk factor for all forms of dementia and, in fact, the most common cases of Alzheimer's disease are late-onset (LOAD), with symptoms developing above the age of 65. Early-onset cases (EOAD), which develop earlier than the age of 65, are less prevalent and are commonly familial, therefore clustering within families.

Epidemiological studies have identified additional risk factors for the disease relating to general lifestyle, and a family history of the disease. Indeed, history of AD in the family leads to a 3-4 fold increased risk of developing the disease, suggesting the existence of genetic risk factors associated with AD. A well-established genetic associate of AD is the lipid-binding apolipoprotein E (ApoE), a polymorphic protein with three isoforms: E2, E3 and E4. The presence of at least one copy of the *ApoE* E4 variant has been established as a genetic risk factor for AD (Hutton et al., 1998).

1.2.1. Clinical symptoms and diagnosis of AD

Since AD is a progressive disease, symptoms tend to worsen over time. The earliest sign of AD is memory loss and changes in mood, which will worsen over progression of the disease and will be accompanied by increased disorientation and confusion. Additional symptoms developed over progression of the disease may include trouble with sleep, poor vision, delusions and hallucinations, problems with language and weight loss amongst others. Ultimately, at the latest stages of the disease, patients will require full-time care as they lose the ability of looking after themselves.

Clinically, a diagnosis of probable AD is made upon a thorough investigation of the symptoms and medical history of the patient, as well as neuropsychological assessments that establish a progressive loss of memory, executive function and cognitive impairment. However, a definitive diagnosis of AD can only be reported upon histological examination of the post-mortem brain specimen of the individual.

At autopsy, AD brains typically present substantial cerebral cortical atrophy, usually involving the frontotemporal association cortex. Atrophied brain tissue in AD also tends to result in symmetrical dilation of the lateral ventricles, and atrophy of the hippocampus is usually associated with dilation of the temporal horn of the lateral ventricle.

1.2.2. Neuropathology of AD

Microscopically, AD is characterised by the presence of extracellular cortical 'plaques' containing amyloid beta (Aβ) and intracellular 'tangles' containing hyperphosporylated tau protein in the brain, granulo-vacuolar degeneration, and eosinophilic rod-like inclusions (Perl, 2010) (Figure 1.1A,B).

Cortical plaques are mainly composed of Aβ, which is a 4-kDa protein with a beta-pleated sheet configuration. It is derived from the fragmentation of the highly conserved transmembrane amyloid precursor protein (APP) which, upon the action of secretases, is cleaved into a 42–amino acid chain ($A\beta_{1–42}$), which is deposited within senile plaques and a 40–amino acid chain ($A\beta_{1–40}$), which tends to localise in cerebral cortical and cerebellar blood vessels (Prelli et al., 1988).

Neurofibrillary tangles are usually present as paired helical filaments, the main component of which is a hyperphosphorylated version of the microtubule-associated protein tau. The extent and distribution of these tangles within the brain has been shown to be indicative of the severity and duration of the disease (Arriagada et al., 1992; Bierer et al., 1995). Although neurofibrillary tangles are considered to be a clinical hallmark for AD, they are also observed in other neurodegenerative diseases, including post-traumatic dementia, dementia pugalistica, amyotrophic lateral sclerosis/parkinsonism dementia complex of Guam and post-encephalitic parkinsonism, as well as, the lysosomal storage disorder, Niemann-Pick disease, type C (Perl, 2010). In 1991, Heiko Braak established a staging method for tracking AD progression through tau pathology. The presence of neurofibrillary tangles in the transentorhinal region of the brain is typical of Braak stages I and II, whilst stages III and IV are representative of tangle presence in the limbic regions including the hippocampus. Finally, Braak stages V and VI are indicative of more severe pathology, with tangles being present also in the neocortical regions (Braak and Braak, 1991).

1.2.3. The amyloid cascade hypothesis

The 'amyloid cascade hypothesis', first proposed in 1992 (Hardy and Higgins, 1992), identified Aβ as the main causative factor in AD pathology, stating that its aggregation following APP cleavage leads to a neurotoxic cascade, resulting in neurofibrillary tangles, cell loss, vascular damage and dementia (Figure 1.1 C).

The amyloid cascade hypothesis was partly based on the observations that mutations in APP cause hereditary, EOAD (Chartier-Harlin et al., 1991; Goate et al., 1991; Murrell et al., 1991; Naruse et al., 1991; van Duijn et al., 1991). Furthermore, a few years later, mutations in presenilin genes *PSEN1* and *PSEN2* were also identified as causative mutations of familial AD (Cruts et al., 1996). PSEN1 and PSEN2 are major components of the γ-secretase complex, and are therefore responsible for APP cleavage. Therefore, the association of *PSEN1/2* mutations in AD, further re-established the role of APP cleavage in AD and further supported the amyloid cascade hypothesis. Subsequently, the hypothesis led to a series of studies and investment from the pharmaceutical industry that targeted Aβ removal as a treatment for AD.

In 2012, a whole-genome sequence data analysis on 1,795 Icelanders was published, revealing the identification of a protective variant of *APP*. The A673T substitution in *APP* was found to have a strong protective effect against AD and against cognitive decline in the elderly. This substitution was then identified as being adjacent to a protease β-site in APP, thereby resulting in reduced processing of the APP protein within the β-site and a lower production of $A\beta_{1-42}$ and $A\beta_{1-40}$. This study was therefore also suggested as being proof of the amyloid cascade hypothesis (Jonsson et al., 2012).

Additionally, a recent study using a three-dimensional human neural cell culture model of AD provided further supporting evidence for the amyloid cascade hypothesis as phosphorylated tau was shown to accumulate in ReNcell VM human neural stem cells

expressing familial AD mutations, following accumulation of Aβ aggregates (Choi et al., 2014). Similarly, a recent study showed that Aβ aggregates formed upon intracerebroventricular injection of Aβ oligomers, induced tau phosphorylation and formation of neurofibrillary tangles in non-human primates (Forny-Germano et al., 2014).

However, whilst Aβ aggregates and tau hyperphosphorylation are recognised as being conducive to neuronal dysfunction in AD, the exact mechanism by which the two factors interact to cause this neuronal deficit is not well elucidated. Several studies have suggested that Aβ aggregation precedes, and induces tau hyperphosphorylation and that glycogen synthase kinase-3β (GSK-3β) is required to mediate this response. Indeed, studies have suggested that Aβ aggregates result in elevated activity of the serine/threonine kinase GSK-3β, (Takashima et al., 1993; Takashima et al., 1996) which has been previously identified as a tau kinase I, potentially phosphorylating tau in several sites that are found to be hyperphosphorylated in AD tangles. GSK-3β levels are in fact found to be upregulated in the hippocampus of AD patients (Blalock et al., 2004). Furthermore, GSK-3β is an important negative regulator of the Wnt signalling pathway, and dysfunctional Wnt signalling has been associated with neuronal degeneration and synaptic impairment in AD. Treatment with Lithium, a GSK-3β inhibitor, has been shown to be neuroprotective and preventive of AD neurodegeneration, both *in vitro a*nd *in vivo* (Alvarez et al., 1999; Zhang et al., 2011). Additionally, expression of Wnt ligands, leading to permanent activation of the Wnt pathway also exerts a neuroprotective effect (Cerpa et al., 2009). This suggests that the downstream effects of the amyloid cascade might be prevented via inhibition of GSK-3β and activation of the Wnt signalling pathway.

Other studies, however, argue that whilst the amyloid cascade hypothesis might hold true for the familial form of AD, the sporadic cases might be due to more than just accumulation of amyloidogenic proteins (Hardy and Mayer, 2011). Since the sporadic form of AD is

responsible for the vast majority of cases, it is imperative that other factors linked to AD, apart from the amyloid cascade hypothesis, are better investigated and looked at as potential therapeutic targets.

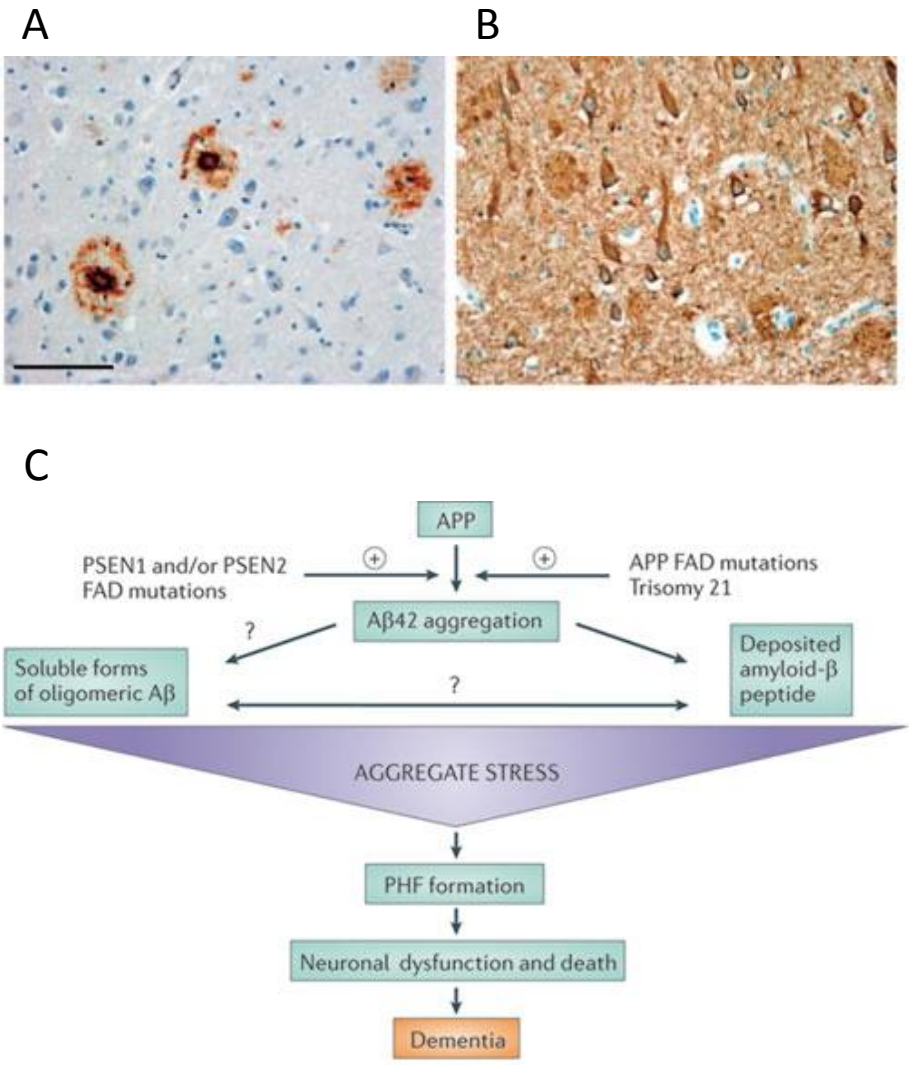

Figure 1.1 Neuropathology of Alzheimer's Disease
(A) Aβ positive senile plaques and (B) tau-positive neurofibrillary tangles and neuropil threads in a typical AD brain (Haass and Selkoe, 2007). (C) The amyloid cascade hypothesis identifies Aβ as the main causative factor in AD. Autosomal dominant mutations in presenilins *PSEN1, PSEN2* and amyloid precursor protein *APP* are associated with early onset familial AD (EOAD). The presence of these mutations leads to APP being cleaved into the neurotoxic $A\beta_{1-42}$, leading to Aβ aggregation, formation of tau paired helical filaments (PHF) and eventually resulting in neuronal death. Adapted from (Karran et al., 2011).

1.2.4. Current AD treatment

Medications currently administered to AD patients are aimed at alleviating certain symptoms and improving cognition, behaviour and everyday function.

The nucleus basalis of Meynert, the origin of cortically-projecting cholinergic neurons, is highly involved in the early stages of AD pathology. AD is, in fact, associated with a decline in acetylcholine synthesis capacity and cholinesterase inhibitor drugs are the most administered drug in AD treatment, acting to increase levels of acetylcholine in the brain (Farlow and Cummings, 2007).

Out of five total medications approved by the US Food and Drug Administration (FDA), four are cholinesterase inhibitors and the fifth is an N-methyl-D-aspartate (NMDA) receptor antagonist (Schneider, 2013). Tacrine was the first ever cholinesterase inhibitor to be approved for AD treatment but is nowadays very rarely administered due to risks of hepatotoxicity. Currently, the cholinesterase inhibitors Donepezil, Rivastigmine and Galantamine are most commonly used to treat symptoms in mild to moderate AD and are shown to be effective in improving memory, confidence, motivation and general daily living. Memantine is a commonly used NMDA receptor antagonist, acting to reduce excessive excitatory activity (Corbett and Ballard, 2012). It is used in more severe cases of AD, and is associated with improved cognitive testing and behaviour. AD behavioural symptoms are also often treated with neuropsychiatric medication including antidepressants, anxiolytic medications and neuroleptic drugs (Corbett and Ballard, 2012).

Since all current treatments for AD only provide symptomatic benefit and do not modulate the actual course of the disease, current studies are looking for agents that decrease Aβ production and/or aggregation or increase Aβ clearance from the brain.

More recently, because of a series of failures of Aβ-based compounds in clinical trials, tau has emerged as a therapeutic target. However, only one anti-tau treatment has made it into clinical phase III trials thus far. Additional tau-targeting therapies are still in development stages, including immunotherapies and inhibition of GSK-3β. Preliminary studies in humans with lithium have been fairly promising, but lithium administration is controversial and risky and therefore progress on this potential treatment has been slow (Macdonald et al., 2008). Similarly, treatment with the tau aggregate inhibitor, methylene blue, was encouraging but did not lead to major conclusions (Gura, 2008).

Therapies aimed at improving neuronal function have also been investigated. Treatment with nerve growth factors has been proposed as a beneficial therapeutic method, and candidates such as ladostigil have made it to phase II clinical trials (Weinreb et al., 2011). Similarly, a 5-HT6 receptor antagonist, aimed at improving cholinergic neurotransmission and cognition, has also made it to trials (Maher-Edwards et al., 2010). Treatments using antihypertensives, antibiotics and brain insulin receptors are also currently being investigated (Corbett and Ballard, 2012).

Since finding effective treatments for AD has proven difficult and many drugs have failed to pass all clinical trials, it is imperative for new potential therapeutic avenues to be explored. More importantly, emerging evidence strongly suggests that the initial changes occurring in AD must be addressed as potential therapeutic targets. Eliminating plaques and tangles from the brain once they have already developed might be too late to allow for a full recovery.

1.3. Parkinson's Disease (PD)

Parkinson's disease (PD) was first described in 1817 in 'An assay on the shaking palsy' written by the English doctor James Parkinson (Parkinson, 1817). Today, it is the second most common age-related neurodegenerative disorder following AD. It is estimated to

affect 1% of the population aged over 60, equivalent to approximately 127,000 individuals in the UK, and up to 5% of the population aged over 85 (de Lau and Breteler, 2006; Reeve et al., 2014). Whilst the vast majority of PD cases are sporadic and idiopathic, 5% of all cases are familial early-onset, with symptoms presenting prior to the age of 60. Such cases can be due to autosomal dominant or recessive mutations, affecting mostly protein metabolism or mitochondrial function (Reeve et al., 2014).

1.3.1. Clinical symptoms, neuropathology and etiology of PD

Symptomatically, Parkinsonian disorders are characterised by the presence of bradykinesia, tremor, rigidity and postural instability. Pathologically, parkinsonian disorders are characterised by loss of dopaminergic neurons in the substantia nigra pars compacta (SNpc) which project to the putamen, leading to reduced activity in the dopaminergic nigrostriatal pathway. This neuronal loss correlates with the loss of the black pigmentation in SNpc, due to less neuromelanin being generated as a by-product of dopamine (Figure 1.2A). Pigment loss is also observed in the locus ceruleus in PD, correlating with a loss of noradrenergic neurons.

PD is distinguished by the presence of neuronal inclusions composed of the presynaptic protein α-synuclein. These are referred to as Lewy bodies when found in neuronal perikarya, or Lewy neurites when found in neuronal processes (Figure 1.2B). Classical Lewy bodies are found within the brain stem region of the brain, however occasionally Lewy bodies are encountered in less affected brain regions such as the cortex and the amygdala. These are referred to as cortical Lewy bodies (Ikeda et al., 1978) and are thought to precede the classical Lewy bodies, thereby being termed ‘pre-Lewy bodies’.

Within Lewy bodies, α-synuclein is arranged as straight filaments that are 10-15 nm in diameter. Such filaments, consisting of a beta-sheet conformation, have been observed *in vitro* with wild-type and mutant α-synuclein (Conway et al., 2000). Native α-synuclein is

thought to be relatively unfolded and conformational changes may lead to its fibrillation (Perrin et al., 2000). A central hydrophobic region within the α-synuclein structure has been shown to be crucial in fibril formation and is also a characteristic feature that distinguishes α-synuclein from its beta (β) and gamma (γ) synuclein homologues (Giasson et al., 2001). β-and γ-synuclein lack any fibrillation capacity and have, in fact, never been observed in Lewy bodies or associated to any other pathologic structures. The factors that make α-synuclein gain this fibrillar conformation are unknown, however post-translational modifications such as phosphorylation, truncation and oxidative damage are thought to play a role in the process (Giasson et al., 2000; Fujiwara et al., 2002; Tofaris et al., 2003; Anderson et al., 2006).

α-synuclein pathology is also present in some AD patients, with most pathology being restricted to the amygdala. These amygdala-only patterns are thought to differ from the α-synuclein distribution observed in PD and therefore are thought to represent a separate disease process (Iseki, 2004; Leverenz et al., 2008; Dickson et al., 2010).

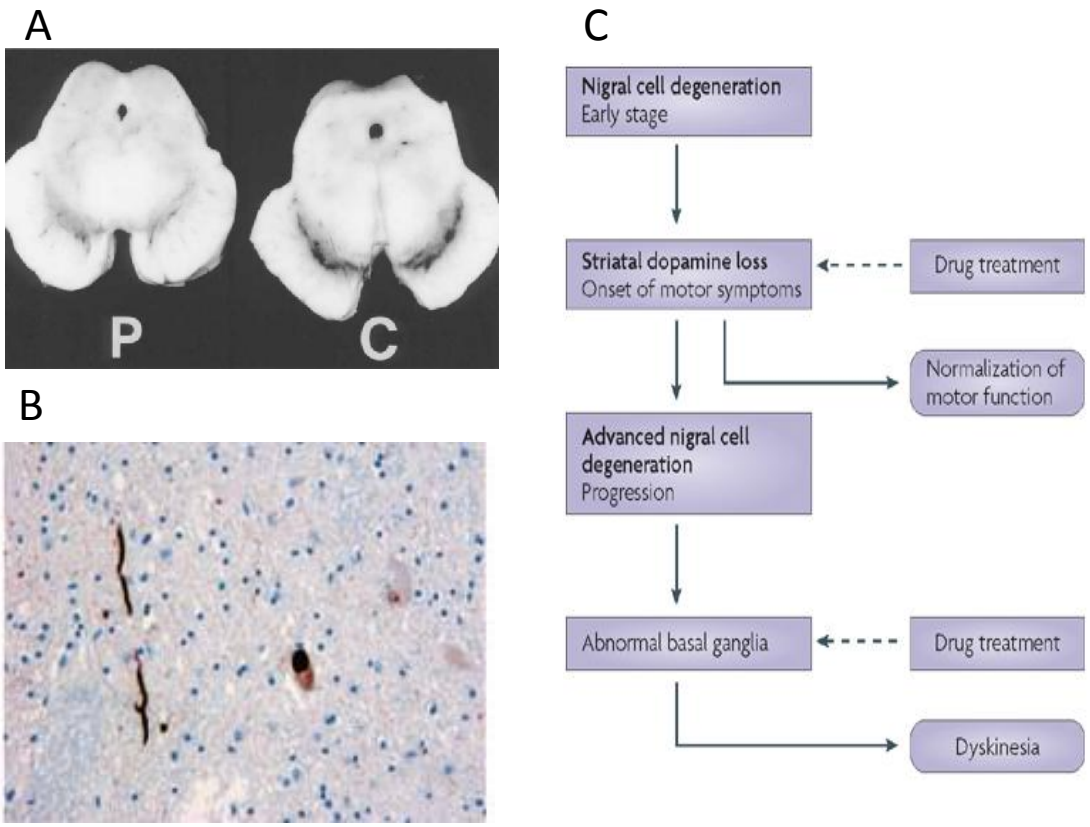

Figure 1.2 Neuropathology of Parkinson's disease
(A) Horizontal sections from the midbrain showing loss of pigment in the SNpc of a PD patient, P, compared to a healthy control, C (Mackenzie, 2001). (B) α-synuclein positive Lewy neurite (left) and Lewy body (right) in the SNpc of a PD patient (Haass and Selkoe, 2007). (C) L-dopa (L-3,4-dihydroxyphenylalanine) is the most commonly used dopamine-replacement therapy in PD, acting to improve motor symptoms. Upon further degeneration, however, treatment with L-dopa will also induce abnormal involuntary movements known as L-dopa induced dyskinesias (LIDs) (Jenner, 2008).

1.3.2. Genetic causes of PD

α-synuclein was identified as the main constituent of Lewy bodies in 1997 (Spillantini et al., 1997). In the same year, the Ala53Thr missense mutation in the *SNCA* gene, encoding α-synuclein, was shown to result in a dominantly inherited form of PD with Lewy pathology (Polymeropoulos et al., 1997). Subsequently, other substitutions in the gene, including Ala30Pro, Glu46Lys, His50Gln, and Gly51Asp, were also associated with PD (Polymeropoulos et al., 1997; Kruger et al., 1998; Zarranz et al., 2004; Appel-Cresswell et al., 2013; Lesage et al., 2013; Proukakis et al., 2013). Duplications of the *SNCA* gene have also been attributed to familial, late-onset PD (Singleton et al., 2003; Chartier-Harlin et al., 2004; Ibanez et al., 2004; Fuchs et al., 2007; Nishioka et al., 2009), and additional copies of *SNCA* have also been linked to a more severe Lewy body disease and a greater frequency of dementia (Singleton et al., 2003; Ross et al., 2008).

However, the most common genetic cases of PD are linked to dominantly-inherited missense mutations in *LRRK2*, a large gene comprising 51 exons which is located close to the centromere on chromosome 12. It encodes leucine rich repeat kinase 2, a kinase with well-established roles in striatal neurotransmission, neuronal arborisation, endocytosis, autophagy and immunity (Cookson, 2012). Dominantly inherited substitutions in *LRRK2* including Asn1437His, Arg1441Cys/Gly/His, Tyr1699Cys, Gly2019Ser and Ile2020Thr have been linked to an idiopathic PD-like clinical phenotype (Paisan-Ruiz et al., 2004; Zimprich et al., 2004; Kachergus et al., 2005; Aasly et al., 2010). *LRRK2* PD is typically associated with nigral neuronal loss and gliosis, along with Lewy body or neurofibrillary tangle pathology. The Gly2019Ser mutation in *LRRK2* has been shown to induce neuronal dysfunction via alteration of mitochondrial dynamics *in vitro* (Niu et al., 2012), and is associated with reduced mitochondrial membrane potential and adenosine triphosphate (ATP) levels in PD patients (Mortiboys et al., 2010). Expressing a *LRRK2* mutant in *C. elegans* also resulted in

enhanced mitochondrial dysfunction and susceptibility to oxidative stress (Saha et al., 2009).

The role of mitochondrial-associated genes in PD is further discussed in section 1.12.2.

1.3.3. Current PD treatment

Due to the predominant dopaminergic deficit, symptomatic PD therapy for motor symptoms is mainly focused on regenerating levels of dopamine in the brain. Neuroprotective or disease-modifying therapies aim to slow or block the loss of dopamine neurons. Thus far there is no proven neuroprotective treatment, though drugs such as monoamine oxidase (MAO)-B inhibitors, creatine and isradipine are currently under investigation (Obeso et al., 2010).

To date, the most frequently administered drug for symptomatic treatment of PD is L-dopa. Following its introduction as an anti-parkinsonian agent in 1968 (Cotzias, 1968), L-3,4-dihydroxyphenylalanine (Levodopa or L-dopa) is now the most commonly used dopaminergic drug. Even though it is the most efficacious drug treatment known for PD, its benefits are quite short-lived and long-term administration can lead to sensitisation of the dopaminergic system, resulting in motor-response complications including involuntary movements known as levodopa-induced dyskinesias (LIDs) (Figure 1.2C). Whilst L-dopa provides a mainly phasic dopaminergic stimulation, other dopamine agonists used in treating PD (e.g. pramipexole, ropinirole, pergolide) provide a more tonic stimulation and present different affinities for different dopamine receptors (Poletti and Bonuccelli, 2013). Additionally, other neurotransmitter systems such as acetylcholine, serotonin and noradrenaline are also implicated in PD and might provide alternative avenues for therapeutic targets.

Apart from the characteristic motor symptoms, PD cases are also characterised by additional non-motor symptoms which can be categorised into three groups: neuropsychiatric (including psychotic episodes, amnesia, anxiety, depression, fatigue), autonomic (including urinary incontinence and excessive sweating) and sensory (including pain and numbness). Since most non-motor symptoms are frequently found in conjunction with motor symptoms, most methods of treatment are anti-parkinsonian therapies. Analgesics might be used to treat pain and alpha-blockers might be used for dysautonomic symptoms whilst anti-anxiety agents might be used to treat neuropsychiatric symptoms. Overall, treatment for non-motor symptoms is also predominantly symptomatic and no neuroprotective treatments are yet available.

1.4. Dementia with Lewy bodies (DLB) and Parkinson's disease dementia (PDD)

A frequently encountered non-motor symptom of PD which is of great distress to the patients and their carers is a decline in cognitive function.

84% of PD patients are estimated to develop cognitive decline throughout their disease, with 60% of men and 45% of women with PD developing Parkinson's disease dementia (PDD) by the age of 75 (Buter et al., 2008). In fact, PD patients are at a six-fold increased risk of developing dementia compared to controls of the same age. The most commonly diagnosed cognitive changes occurring in PD patients include impairments in executive function and deficits in attention and visuospatial recognition. Some cases are also associated to an impairment in memory, which might be a consequence of a deficit in executive function (Irwin et al., 2013). It has therefore been suggested that impairments in executive function in PD are due to dopaminergic loss in the frontal cortex, whilst subsequent neuropathology in the temporal and parietal cortices correlate to deficits in

visuospatial recognition and semantic memory, and represent an increased risk of PDD (Williams-Gray et al., 2009).

Since the cognitive decline within a PD diagnosis appears to be gradual, recent developments have led to the establishment of a clinical diagnosis of PD-MCI (PD with mild cognitive impairment), which is defined as cognitive impairment within PD patients who are still functionally independent (Emre et al., 2007; Litvan et al., 2012). MCI tends to affect executive function, attention or memory and represents a risk factor for developing full-blown PDD, which is associated with further cognitive decline in the visuospatial domain (Gasca-Salas et al., 2014). PDD is diagnosed on two levels – possible or probable PDD. Probable PDD diagnosis requires the presence of both PDD core features (diagnosis of PD as well as dementia syndrome) and impairment in at least two of four cognitive domains (executive function, attention, memory, visuospatial function), usually supported by the presence of behavioural symptoms. Possible PDD, on the other hand, is associated with the presence of the two core features and impairment in at least one cognitive domain (Emre et al., 2007).

Structural and cellular changes correlating with these cognitive alterations have yet to be elucidated. However, atrophy in the hippocampus, amygdala, caudate nucleus, cingulate gyrus, and the temporal and prefrontal lobes, has been observed to correlate with dementia, in PD*, in vivo* (Hwang et al., 2013). Furthermore, the role of cortical Lewy bodies has been well established in PD cognitive decline. Several groups have correlated presence of cortical Lewy bodies to cognitive severity (Hurtig et al., 2000; Mattila et al., 2000), whilst others have argued that a co-existing AD-like pathology is required to cause decline in cognition (Harding and Halliday, 2001). Indeed, a recent study has suggested that whilst α-synuclein pathology in cortical areas tends to correlate significantly with a decline in cognitive ability, the presence of Aβ plaques and phospho-tau tangles are also indicative of

cognitive impairement, suggesting that multiple pathologies might play a role in cognitive decline (Howlett et al., 2014). Cognitive symptoms in PDD and AD may also be quite similar; however PDD is usually distinguished by the presence of hallucinations, depression, sleep disturbance and cognitive fluctuations.

Age is recognised as being a prominent risk factor for PDD, and studies show that age of PD onset does not play a role in risk of dementia development (Aarsland et al., 2007). Therefore patients tend to develop PDD at a similar age, regardless of when they first developed motor symptoms (Kempster et al., 2010). On the other hand, the severity of motor symptoms is correlated to cognitive decline (Braak et al., 2005). Furthermore, male gender, low levels of education and visual hallucinations as well as prominent axial rigidity and bradykinesia are thought to be risk factors for PDD (Irwin et al., 2013). Diagnosis of PDD is, however, not always clear-cut due to the similarities it shares with the more common form of dementia; dementia with Lewy bodies (DLB).

DLB is a relatively recently established form of dementia which exhibits symptoms associated with both AD and PD. As a result of combined symptoms and pathologies, researchers believe that DLB cases are under-diagnosed and may in reality make up to 10-15% of all dementia cases in the elderly, making DLB the second most common form of degenerative dementia following AD. As in AD, DLB patients also tend to exhibit cortical amyloid plaques and neurofibrillary tangles (Howlett et al., 2014). The presence of tau aggregates is linked to an increased chance of Lewy body formation especially in susceptible brain areas such as the amygdala, and in fact, as previously mentioned, Lewy bodies are also found in numerous cases of familial or sporadic AD (Lippa et al., 1998; Hamilton, 2000).

The third report of the DLB consortium published in 2005 aimed to highlight the similarities and the importance of establishing better boundaries between PDD and DLB (McKeith et

al., 2005). Pathologically, both PDD and DLB are characterised by widespread α-synuclein in the brain stem, neocortex and the limbic and forebrain regions. PDD patients tend to suffer more neuronal loss in the SNpc than DLB patients, whilst α-synuclein pathology might be greater in the striatum in DLB patients compared to PDD (Lippa et al., 2007). Neuropsychological profiles exhibited are also very similar in the two syndromes, though DLB patients tend to suffer more psychoses and hallucinations, and more conceptual and attentional errors than PDD patients (Lippa et al., 2007).

These two syndromes are distinguished diagnostically purely via the temporal sequence of appearance of symptoms. The 'one year rule' states that if cognitive symptoms arise within the same year as the motor symptoms, the diagnosis should be DLB, whilst in PDD, cognitive symptoms should appear longer than a year after the onset of motor symptoms. In fact, most PDD patients tend to develop dementia 10 years or more after the onset of motor symptoms. Nevertheless, the 'one year rule' has been criticised by some suggesting that the two types of dementia are simply different stages within a common spectrum of Lewy body disease. The consortium therefore concluded that whilst distinct PDD and DLB may be used in diagnosing more clear-cut cases and in particular areas of research, studies in clinical research, development of therapeutics and genetics might require the use of the collective term Lewy body disease (LBD) or α-synucleinopathy (McKeith et al., 2005).

The consortium also revisited the criteria used for DLB diagnosis which had previously been established in the first publication of Consensus criteria for clinical and pathologic diagnosis of DLB (McKeith et al., 1996). The most recent criteria require a central feature of progressive cognitive decline leading to concordant memory impairment and additional core features including a fluctuating cognitive impairment with varying levels of attention and alertness, prominent visual hallucinations and parkinsonism. In addition to cognitive decline, the presence of one core feature is indicative of possible DLB whilst the presence

of two core features is required for a diagnosis of probable DLB (McKeith et al., 2004; McKeith et al., 2005). Other features that may be present in DLB include rapid eye movement (REM) sleep behaviour disorder, neuroleptic sensitivity, severe autonomic dysfunctions, delusions, depression and occurrence of syncope and loss of consciousness (McKeith et al., 2005).

DLB patients exhibit both cortical and subcortical neuropsychological impairments with a prominent dysfunction in visuospatial processing. In fact this is a feature that helps to distinguish between DLB and AD patients, as DLB patients tend to have a better verbal memory but a more pronounced visuospatial impairment. Similarly to PDD, DLB patients suffer from psychiatric manifestations such as visual hallucinations, associated with a decline in cortical acetylcholine (Perry et al., 1991), a prominent number of Lewy bodies in the anterior and inferior temporal lobe (Harding et al., 2002), as well as delusions, apathy and anxiety early on in the course of the disease. Unlike PDD cases, however, 25% of DLB cases might progress through the disease without ever exhibiting any extrapyramidal symptoms, suggesting that parkinsonism is not always present in this form of dementia. In fact the absence of motor symptoms upon clinical visits, might be a major factor leading to the previously mentioned under-diagnosis of DLB (McKeith et al., 2000b) or a differential diagnosis of AD, vascular dementia, atypical parkinsonian syndromes or Creutzfeldt-Jakob disease. In DLB, when present, extrapyramidal signs tend to show an axial bias towards greater postural instability and facial impassivity compared to tremor, and this is consistent with a 'non-dopaminergic' motor involvement (McKeith et al., 2004).

The ongoing debate regarding similarities and distinctions between DLB and PDD prompted the formation of a DLB/PDD working group which, following the third report of the DLB consortium, published a report discussing boundary issues in PDD and DLB. This group concluded that PDD and DLB are indeed more similar than they are different, and that the

main distinction lies in the onset of cognitive symptoms in relation to motor deficits. They therefore reiterate that whilst the one-year rule should aim to distinguish between the two for clinical classification, the umbrella term of LBD should be used in understanding underlying molecular mechanisms. More importantly, the group suggests that since cholinergic deficits are a prominent feature in both these syndromes, and they are more severe than in other dementias, such as AD, biomarkers for cholinergic abnormalities should be investigated for use in diagnosis of these disorders. Furthermore, the need for the development of clinical biomarkers for α-synuclein and Lewy bodies, as well as the need of more communication between groups researching movement disorders and dementia is emphasized (Lippa et al., 2007).

1.4.1. Lewy body staging

In 1984, Kosaka and colleagues were the first to publish a standardized scoring system for brain pathology assessment in DLB (Kosaka et al., 1984). This was the first publication suggesting that the clinical manifestation of the disease correlates with the anatomical distribution of the pathological features. In 1996, the Consortium on DLB International Workshop published more detailed instructions on how to score disease progression following Kosaka's suggestions, based on the presence of pathology in the brainstem, limbic and neocortical regions (McKeith et al., 1996).

Following the identification of α-synuclein as a central factor in DLB and PD neurodegeneration, Braak and colleagues published a proposed staging scheme for PD based on the distribution of α-synuclein, utilising α-synuclein immunohistochemistry (IHC). According to the Braak scheme, PD progresses in six neuropathological stages, with the pathology starting in the dorsal motor nucleus of the vagus in the medulla and the anterior olfactory nucleus and progressing onto the locus ceruleus and the substantia nigra, basal forebrain, amygdala and the medial temporal lobe and finally reaching the cortical areas

(Braak et al., 2003) (Figure 1.3A-C). The DLB consortium, subsequently published a revised version of the diagnostic protocol and established α-synuclein pathology as the preferred method of evaluating pathology (McKeith et al., 2005). Moreover, the consortium recommended a semi-quantitative scoring method for Lewy body pathology in the cerebral cortex thereby establishing a cortical severity model with Lewy body staging ranging from stage 1 to 4. Stage 1 represents a sparse presence of Lewy bodies and Lewy neurites whilst stage 4 represents numerous Lewy bodies and Lewy neurites in the cerebral cortex.

The most recent protocol published by the BrainNet Europe Consortium aims to consolidate the criteria established by Braak and McKeith, proposing a method whereby Braak stages 1-3 correspond to the McKeith brainstem stage, whilst the limbic stage incorporates Braak stages 3-5 and finally Braak stage 6 corresponds to the neocortical stage (Alafuzoff et al., 2009) (Figure 1.3D).

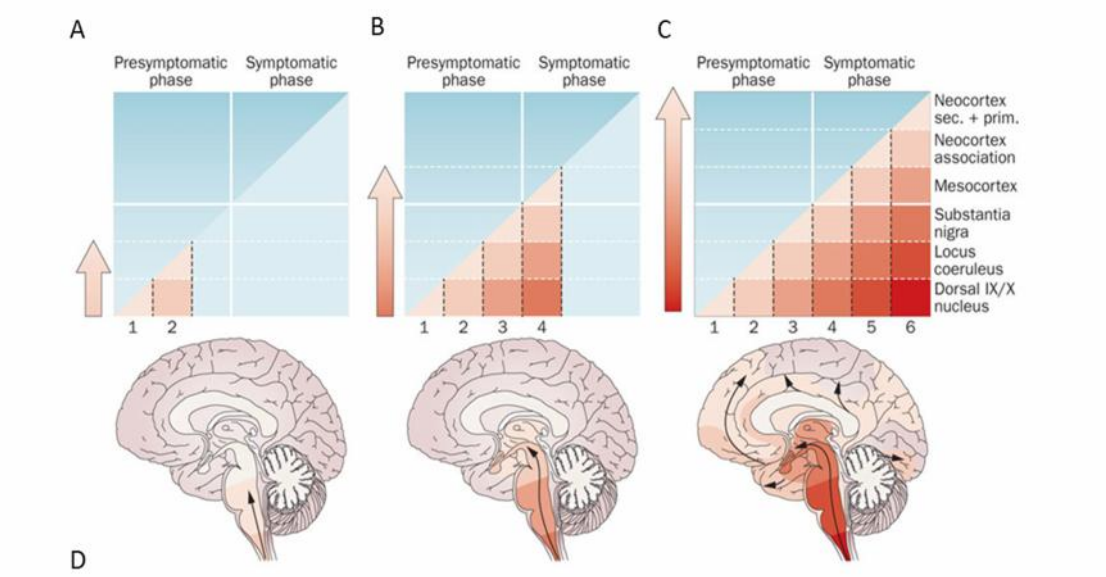

Sampled brain areas	Medulla		Pons		Midbrain	Basal Forebrain		Hippocampus		Gyrus cinguli	Temporal cortex	Frontal cortex	Parietal cortex
Anatomical region	dmV	irx	LC	R	SN	nbM	AC	CA2	TOcx	grey matter	grey matter	grey matter	grey matter
Braak stage	1	1	2	2	3	3	4	3	4	5	5	6	6
McKeith type	BRAINSTEM					LIMBIC						NEOCORTICAL	
Amygdala predominant							AC predominant						
Lesion type requested	LBs and / or LNs						LBs	LNs		LBs			

Figure 1.3 The different stages of Lewy body pathology
(A) Braak stages 1 and 2 correspond to lesions in the olfactory bulb, the anterior olfactory nucleus and/or the dorsal motor nuclei of the vagal and glossopharyngeal nerves in the brainstem as well as the locus coeruleus, magnocellular nucleus of the reticular formation, and lower raphe nuclei. (B) In Braak stages 3 and 4, the pathology reaches basal forebrain, SNpc, the hypothalamus, portions of the thalamus and the mesocortex, and the first clinical symptoms of PD appear. (C) In the later Braak stages 5 and 6, pathology reaches neocortical high-order association areas, first-order association areas and primary fields (Goedert et al., 2013). (D) The proposed BrainNet Europe protocol for assigning α-synuclein pathology. dmV: Dorsal motor nucleus of vagus, irx: intermediate reticular zone, LC: locus coeruleus, R: raphe, SN: substantia nigra, nbM: nucleus basalis of Meynert, AC: amygdala, CA2: cornu ammonis of hippocampus, region 2 TOcx: temporo-occipital cortex, LN: Lewy neurites (Alafuzoff et al., 2009).

1.4.2. Current PDD and DLB treatment

As in most other dementias, treatments for DLB and PDD are symptomatic. In the cases of these particular dementia types, treatment strategies might be especially problematic as they might enhance psychotic side effects to which these patients are sensitive.

The only treatment currently licensed in PDD is the use of rivastigmine, the cholinesterase inhibitor commonly used in AD treatment, which has been shown to cause substantial long-term improvement in areas of memory, language, praxis and executive function (McKeith et al., 2000a; Emre et al., 2004). An additional cholinesterase inhibitor, donepezil, has also shown improvement in cognition and general status in PDD patients in several clinical trials (Ishikawa et al., 2014). Atomoxetine, a selective noradrenaline reuptake inhibitor, is also at advanced stage clinical trials, after having shown to improve cognitive function in animal models (Athauda and Foltynie, 2015).

The NMDA receptor antagonist memantine has also been tested in PDD clinical trials, and showed improvement in cognitive function, sleep and general quality of life (Broadstock et al., 2014). However, additional studies on memantine found insufficient improvement on symptoms upon drug treatment and the Movement Disorder Society concluded in 2011 that although deemed safe, memantine does not exhibit strong enough evidence as a candidate for PDD treatment (Seppi et al., 2011).

Cholinesterase inhibitors, such as rivastigmine and donepezil have also been tested on DLB patients and improvements in neuropsychiatric symptoms and in cognitive screening tests were reported (Broadstock et al., 2014). In 2011, the British Association of Psychopharmacology concluded that cholinesterase inhibitors are effective in treating neuropsychiatric symptoms of PDD and DLB patients (O'Brien and Burns, 2011). As in PDD, treatment of DLB patients with memantine gave inconclusive results, although one study did suggest an improvement in Clinical Global Impression and Neuropsychiatric Inventory

(Emre et al., 2010). L-dopa has also been tested to reduce motor symptoms in DLB, however the treatment was not as efficient as it is in PD, and was associated with an increased risk of psychotic symptoms (Ballard et al., 2011).

A neuroprotective therapeutic strategy which is currently under investigation is immunisation against α-synuclein. Monoclonal antibodies against α-synuclein have been proven to promote clearance of toxic α-synuclein in animal models, leading to the development of antibodies such as PRX002 and AFFITOPE® PD01 which are currently being tested in clinical trials (Athauda and Foltynie, 2015).

Epigallocatechin gallate (EGCG), a catechin found in tea with antioxidant properties, is also being tested for therapeutic use in neurodegeneration. EGCG is thought to act via the inhibition of formation of α-synuclein oligomers (Lorenzen et al., 2014).

Additionally, since there is substantial evidence linking coffee-drinking to a reduced risk of PD, caffeine treatment has been recently investigated as a potential therapeutic strategy (Rivera-Oliver and Diaz-Rios, 2014). Pilot studies have suggested that caffeine leads to a benefit in motor impairments in PD and clinical trials underway also aim to test any benefits on cognition.

1.5. Mitochondrial dysfunction is a common factor in neurodegenerative diseases

As discussed above, most neurodegenerative diseases exhibit common overlapping pathologies and a variable degree of comorbidity, however there is no single factor known to be responsible for the causation of all neurodegenerative diseases. Age is established as the greatest risk factor in the development of neurodegeneration, and it is therefore essential for us to better elucidate the cellular changes occurring in ageing in order to better comprehend the cellular alterations leading to neurodegeneration. A key player in

the ageing paradigm, the mitochondrion, has therefore become a critical target in this field of research.

There are now increasing lines of consistent evidence linking mitochondrial dysfunction to neurodegeneration, and it is suggested that changes in bioenergetic homeostasis, influenced greatly by mitochondrial function, lie at the centre of the various facets of neurodegeneration, including loss of neuronal tissue, systemic malfunction, and an eventual deterioration of neuronal transduction and communication. Mitochondria play a major role in the apoptotic pathway and oxidative stress, which are both components in the pathway leading to neuronal death. In addition, mitochondrial dysfunction and oxidative stress are known to be strongly associated to ageing. Most neurodegenerative diseases display mitochondrial deficits early on in disease progress that may lead to a bioenergetic decline and thereby contribute to the development of the pathologies (Correia et al., 2012; Wirz et al., 2014).

In AD, the pathology-associated proteins Aβ and APP are known to interact directly with mitochondria (Pinho et al., 2014) and studies suggest that the key regulator of mitochondrial biogenesis, peroxisome proliferator-activated receptor gamma coactivator 1-alpha (PGC1-α), is down-regulated in Huntington's disease (HD), (Cui et al., 2006). In PD, mutations in the autosomal recessive genes *parkin*, *PINK1* and *DJ1* lead to increased oxidative stress and mitochondrial dysfunction (Albrecht, 2005; Andres-Mateos et al., 2007; Dodson and Guo, 2007; Devi et al., 2008; Ramsey and Giasson, 2008; Kaye et al., 2014) and in amyotrophic lateral sclerosis (ALS), mutant superoxide dismutase (SOD) has been shown to be localised in the outer mitochondrial membrane, intermembrane space and matrix (Higgins et al., 2003; Pasinelli et al., 2004; Vijayvergiya et al., 2005). It is therefore imperative that further research is carried out into better understanding the role of

mitochondrial dysfunction in neurodegenerative disease, potentially leading to the development of mitochondrial-targeted therapeutic approaches.

1.6. Mitochondrial structure and function

Mitochondria were first observed as cellular structures in the 1840s and were given the name by which they are commonly known today in 1898 by Benda (Benda, 1898). In the early 1910s it was established that cellular respiration occurs in mitochondria (Warburg, 1913). These findings led to the search for a respiratory pigment, paving the way for the discovery of what it known today as the oxidative phosphorylation (OXPHOS) respiratory chain. The late 1920s to late 1940s saw a great surge of progress in respiratory research, with the discovery of ATP as a 'molecular unit of energy currency' (Lohmann, 1929) and the citric acid cycle as the energy-generating cycle for all aerobic organisms (Krebs, 1937). In 1946, Claude isolated mitochondria for the first time using differential centrifugation (Claude, 1946), and the following decade saw mitochondria being identified as crucial in cellular respiration. In 1949, Kennedy and Lehninger found that fatty acid oxidation, as well as the citric acid cycle and ATP generation via nicotinamide adenine dinucleotide (NADH), occur exclusively in mitochondria (Kennedy and Lehninger, 1949) and in the early 1950s, the first electron micrograph of mitochondria revealed details of the morphology of the organelle (Palade, 1953). The late 1950s saw more research focused on understanding the mechanism regulating cellular respiration and in 1961 Mitchell helped to unravel the mystery with the theory of chemiosmotic coupling, which suggested that energy derived from oxidation of fuels pumps protons across the inner mitochondrial membrane, creating a 'proton motive force' (Mitchell, 1961). This concept was dismissed at first, but after being proven true by further experiments, finally led Mitchell to win a Nobel prize in 1978.

Mitochondrial structure is closely related to its function. The organelles are enclosed by an outer mitochondrial membrane (OMM), which regulates entry of large proteins into the

organelle via a large protein complex known as translocase of the outer membrane (TOM). An inter-membrane space separates the outer and inner phospholipid membranes. The inner mitochondrial membrane (IMM) is composed of several membrane infoldings known as cristae. OXPHOS, and therefore ATP generation, occurs within the IMM, and the cristae enable an enhanced surface area for optimal ATP production. A translocase of the inner membrane (TIM) complex allows transport of proteins from the IMM to the mitochondrial matrix which is the innermost space between the cristae, and is where mitochondrial DNA (mtDNA) is found (Figure 1.4A).

1.6.1. Mitochondrial origin

It is postulated that approximately two billion years ago there was a significant increase in the oxygen tension of the Earth's atmosphere, and primitive eukaryotes had to evolve mechanisms to deal with this sudden change (Kurland and Andersson, 2000). According to the endosymbiotic theory of the origins of complex life, this event lead to the origin of eukaryotic aerobes, when entities capable of aerobic respiration were introduced into ancestral eukaryotes via an endosymbiotic α-proteobacterium (Margulis, 1981). Over the past years, several evolutionary biologists have further investigated this theory and put forth their interpretations and developments to the theory. Researchers in the field are still very much puzzled by the series of events which lead to the existence of complex multicellular organisms. Some still find validity in Margulis' endosymbiotic theory, and simply state that it needs to be adapted into the modern world of microbial genomics (Zimorski et al., 2014). Others argue that there is no evidence which suggests that mitochondria evolved in order to deal with a sudden increase in atmospheric oxygen. Martin and Muller suggested an alternative 'hydrogen hypothesis' postulating that the primitive eukaryote originated from a symbiotic relationship between an anerobic autotrophic archaeon which possessed hydrogen-dependent metabolism, and a

eubacterium (future mitochondrion) capable of anaerobic respiration which generated hydrogen and carbon dioxide during the process (Martin and Muller, 1998). Evolutionary biologist Nick Lane further argues that complex life originated in the presence of natural proton gradients, possibly in alkaline hydrothermal vents, and led to the evolution of membranes capable of carrying out membrane bioenergetics that we all utilise today (Lane, 2006; Lane, 2014). Mitochondria as they are known today, contain their own genome in the form of mtDNA. According to the endosymbiotic theory, the α-proteobacterium which was engulfed by the ancestral eukaryote, carried its own genome with it, leading to the existence of mtDNA enclosed in mitochondria, isolated from its nuclear counterpart. Indeed, detailed phylogenetic studies using the mitochondrial genome of protists, the nuclear genome of *S. cerevisiae* and the genome of the α-proteobacterium *Rickettsia prowazekii* revealed that coding sequences in mitochondrial genes are descendent of α-proteobacterial homologues (Andersson et al., 2003).

Over time, the mitochondrial genome has reduced greatly in size, partly due to gene transfer from the mitochondria to the nucleus. The vast majority of mitochondrially-associated proteins are today encoded by the nuclear genome, suggesting that throughout the course of evolution, genes were transferred from the genome of the endosymbiont to that of the host.

So, why do mitochondria still carry their own genome? What is the advantage of a eukaryotic cell having two separate genomes, rather than all mitochondrial-associated genes being present on the nuclear genome? The current most widely accepted hypothesis was first put forward by John Allen in 1993 (Allen, 1993), who states that there must be great benefits offered by the presence of mtDNA within the mitochondrion for so many years and that these benefits must be related to the main function of mitochondria – respiration. The theory suggests that ATP production and ultimately energy supply is

dependent on demand and that each mitochondrion with its electron transport chain (ETC) must react individually to its needs, with speed of respiration adjusted accordingly. It therefore makes more sense for mitochondria to control their own gene expression since respiratory supply and demand might differ between mitochondria in a network and it would be too inefficient for the nuclear DNA to respond to each mitochondrion's individual needs – especially since mitochondria act as a network that is under constant turnover. In summary, the issue might be metabolic – mitochondrial gene expression might be under the direct regulation of components of the ETC or the reduction /oxidation (redox) status of the organelle.

1.6.2. The mitochondrial respiratory chain

The respiratory chain in mitochondria is composed of five different multimeric complexes (Figure 1.4B): reduced nicotinamide adenine dinucleotide (NADH) dehydrogenase-ubiquinone oxidoreductase (complex I), succinate dehydrogenase-ubiquinone oxidoreductase (complex II), ubiquinol-cytochrome c oxidoreductase (complex III), cytochrome c oxidase (complex IV) and ATP synthase (complex V) located on the IMM. Two small electron carriers; ubiquinone/coenzyme Q and cytochrome c, help to transport electrons obtained from energy substrates NADH and flavine adenine dinucleotide ($FADH_2$) along the different complexes to reach the electron acceptor, oxygen. This involves a sequential series of redox reactions, generating an electrochemical gradient, as protons are pumped into the intermembrane space, thereby resulting in the mitochondrial membrane potential. ATP synthase is composed of two functional domains; F_0 is a proton pore found embedded in the mitochondrial membrane while F_1 is located in the mitochondrial matrix and is composed of alternating alpha and beta subunits, arranged around a rotary central gamma subunit. The proton-motive force generated by the ETC triggers the transport of protons through the F_0 region of the complex, towards the rotating F_1 gamma subunit

which then causes conformational changes in associated catalytic binding sites, thereby leading to ATP synthesis. This mechanism was first explained by Paul Boyer in the late 1970s (Kayalar et al., 1977), and in 1994, the F_1 catalytic subunit of ATP synthase was crystallised by John E. Walker (Abrahams et al., 1994). In 1997 Boyer and Walker shared the Nobel prize in chemistry for their findings.

Once produced inside the mitochondrion, ATP will be translocated into the cytosol to feed energy to the cell, via the adenine nucleotide transporter (ANT) found on the IMM. This process, by which ATP is generated via the ETC is termed OXPHOS.

In the nervous system, mitochondrial ATP generation is crucial for numerous functions including the transport and release of synaptic vesicles, assembly of the actin cytoskeleton in presynaptic development, as well as, the generation of axonal and synaptic membrane potentials. Furthermore, ATP production is especially important to maintain ionic homeostasis during electrical signalling, as this process requires the action of Na^+/K^+ and Ca^{2+} plasma membrane ion pumps which are ATP consuming.

Therefore, mitochondrial ATP generation is a crucial process, however, it is prone to damage by a series of factors. Chemical treatment, Ca^{2+} overload and oxidative damage may all lead to inhibition or dysfunction of mitochondrial metabolism. In turn, this may lead to cell death, either via insufficient levels of ATP or through triggered cell death by mitochondrial released pro-apoptotic factors.

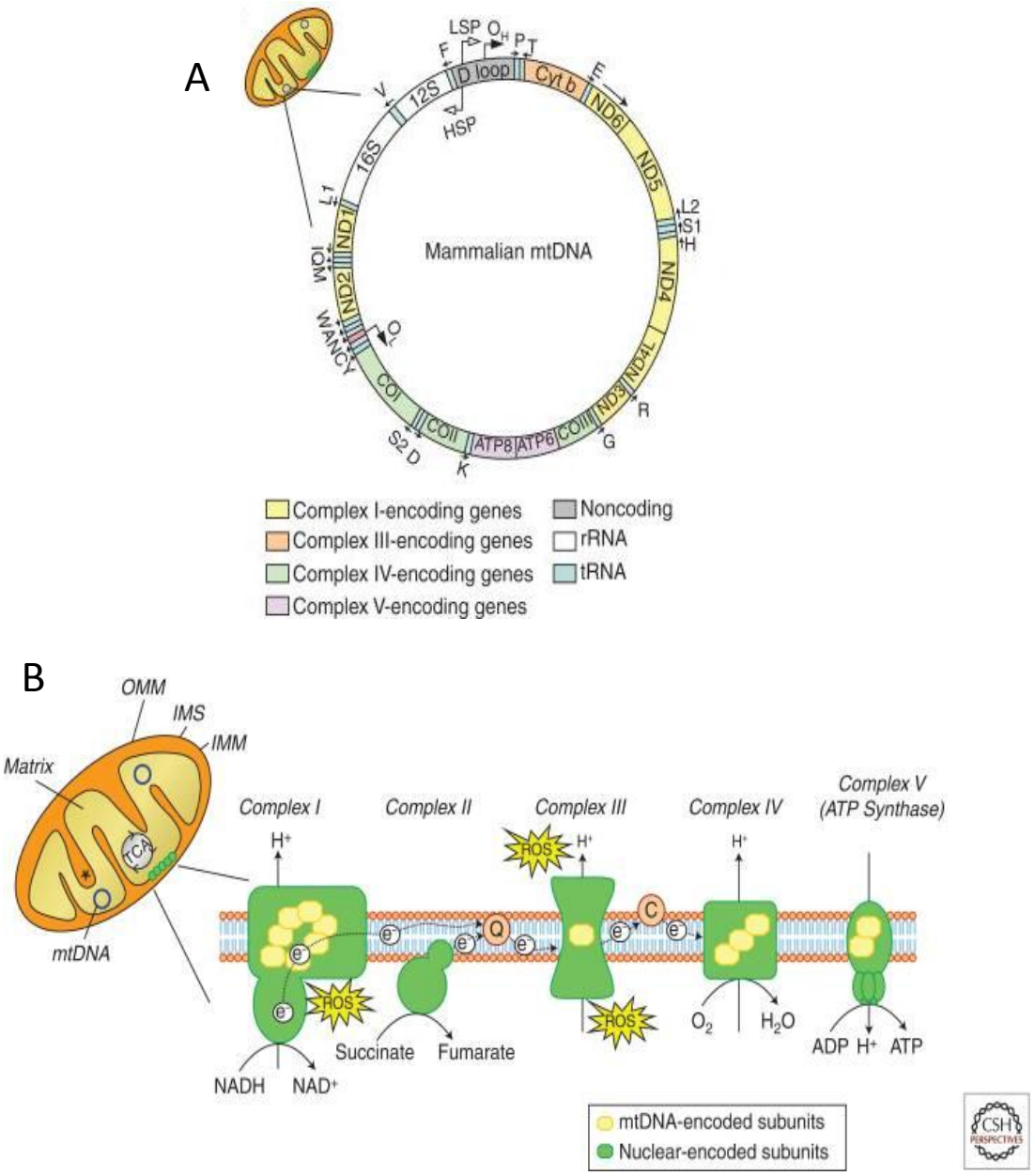

Figure 1.4 Mitochondrial DNA encodes components of the mitochondrial respiratory chain
(A) Mammalian mitochondrial DNA (mtDNA), found in the mitochondrial matrix, is a 16 kb circular genome which encodes for components of Complex I-V of the respiratory chain. (B) The ETC, located on the inner mitochondrial membrane (IMM) consists of five complexes. 13 of the proteins required for the assembly of the complexes are encoded by the mtDNA, whilst the rest are encoded by nuclear DNA. Adapted from (Perier and Vila, 2012).

1.6.3. Mitochondrial generation of reactive oxygen species

Reactive oxygen species (ROS) are produced by mitochondria during the oxidative phosphorylation process and their production is the main factor leading to oxidative damage in a range of pathologies. ROS, however, are also known to be involved in retrograde redox signalling, where they might serve a highly beneficial purpose (Gutterman, 2005; Murphy, 2009). The main ROS generated by mitochondria is superoxide ($O_2^{\bullet-}$), produced by a one-electron reduction of molecular O_2. Subsequently, $O_2^{\bullet-}$ can dismutate to form hydrogen peroxide H_2O_2, which can in turn undergo further reactions to form the hydroxyl radical HO•. $O_2^{\bullet-}$ is first produced from complex I, due to a high proton motive force in the organelle, a high NADH/NAD^+ ratio in the mitochondrial matrix and a reduced coenzyme Q (CoQ) pool. Specifically, there are two main mechanisms which explain $O_2^{\bullet-}$ production in Complex I (Murphy, 2009).

I. At complex I, a flavin mononucleotide (FMN) co-factor accepts electrons from NADH and passes them onto a series of Fe-S centres onto the CoQ reduction site. O2 will then react with the fully reduced FMN to generate $O_2^{\bullet-}$. The proportion of reduced FMN in mitochondria is determined by the NADH/NAD^+ ratio. Therefore in a situation where the respiratory chain is inhibited via mutations or other forms of damage, a low respiration rate will cause an increase in NADH/NAD^+ ratio leading to subsequent $O_2^{\bullet-}$ generation by FMN. In situations where mitochondria are undergoing normal respiration and the NADH/NAD^+ ratio is relatively low, generation of $O_2^{\bullet-}$ is highly depreciated.

II. There is also considerable $O_2^{\bullet-}$ generation at complex I via a reverse electron transport mechanism. This occurs when there is considerable electron supply acting to reduce CoQ in the presence of a large proton motive force, causing electrons to 'reverse' back into complex I, reducing NAD^+ to NADH at the FMN. The

rate of $O_2^{\bullet-}$ generation via this mechanism is highly dependent on a high proton motive force, and is therefore highly sensitive to any changes in pH which could decrease this force.

It is not entirely understood whether these two processes occur individually or simultaneously to generate $O_2^{\bullet-}$ at complex I.

An additional ETC complex which is thought to be crucial in generating ROS is complex III, which passes electrons from the CoQ pool onto cytochrome c. Generation of superoxide at this complex is thought to depend on the stability of the ubisemiquione radical in the Q_o site of CoQ, which may be modulated via changes in proton motive force, loss of cytochrome c or the redox state of CoQ. It is further important to note that $O_2^{\bullet-}$ at complex III is only substantial when the Q_i site at CoQ is directly inhibited via antimycin. Therefore under normal physiological conditions, the amount of superoxide generated at complex III is negligible compared to that produced at complex I (Andreyev et al., 2005).

Apart from complexes I and III, an additional seven mitochondrial sites have been identified as having potential in generating ROS. These are cytochrome b5 reductase and monoamine oxidases, located on the OMM, dihydroorotate dehydrogenase and dehydrogenase of *alpha*-glycerophosphate located on the outer surface of the IMM, succinate dehydrogenase located on the inner surface of the IMM, aconitase found in the mitochondrial matrix and *alpha*-Ketoglutarate dehydrogenase complex which is found on the matrix-facing side of the IMM. The role of these sites in ROS production in physiological *in vivo* conditions is however poorly understood (Andreyev et al., 2005).

ROS generation is an inevitable process that also serves a physiologically relevant purpose, as mentioned throughout this thesis. The generation of ROS by itself is not a precursor to oxidative stress. Rather, oxidative stress results from an imbalance between ROS

generation and detoxification. Multiple cellular mechanisms serve to combat oxidative stress (Cadenas and Davies, 2000; Andreyev et al., 2005). One of the predominant lines of defence against mitochondrial ROS is manganese superoxide dismutase (MnSOD), an enzyme located inside the mitochondrial matrix serving to dismutate superoxide to H_2O_2, thereby preventing any damage to the Fe-S clusters present within the mitochondria. H_2O_2 can itself be quite toxic and therefore needs to be neutralised by an additional enzyme, catalase, which converts H_2O_2 into H_2O and O_2. Glutathione peroxidase (GPxI) is another major role player in ROS detoxification. It is present in the mitochondrial matrix and the intermembrane space and also acts to detoxify H_2O_2 into H_2O and O_2 by utilising glutathione (GSH). In the process GSH is reduced to glutathione disulphide (GSSG) which can then be converted back to GSH via glutathione reductase using NADPH. The GPX scavenging system is thought to be more prevalent in cases of severe oxidative stress rather than in the neutralisation of normal physiological ROS levels. During severe oxidative stress, there is a decrease in GSH concentration, concomitant with an increase in GSSG concentration (Andreyev et al., 2005).

Several reviews written on the subject have discussed the link between mitochondrial dysfunction, oxidative stress and neurodegenerative disease as well as general ageing (Barja, 2014; Hayashi and Cortopassi, 2015; Pinto and Moraes, 2015) and several of these findings are mentioned throughout this chapter (sections 1.11 and 1.12). The exact mechanisms underlying these associations are, however, still relatively unknown and further work is required to better understand how diminishing oxidative stress in mitochondria could serve as a therapeutic strategy.

1.6.4. Mitochondrial dynamics

Mitochondria function as a dynamic network undergoing fission and fusion, mitochondrial turnover and transport (Figure 1.5). Mitochondrial distribution and motility throughout

neurons is especially heterogeneous, since neurons are polarised cells with areas of differing energy requirements. Areas with high ATP level demands such as presynaptic and postsynaptic terminals, nodes of Ranvier, active growth cones and axonal branches therefore tend to contain a higher number of mitochondria than other neuronal domains (Morris and Hollenbeck, 1993; Ruthel and Hollenbeck, 2003; Zhang et al., 2010). A recent study has shown that a resting cortical neuron uses up to 4.7 billion molecules of ATP per second (Zhu et al., 2012) and it is therefore not surprising that mitochondrial transport and distribution tend to be directly correlated to synaptic activity, with more mitochondria being detained in the presynaptic terminals and postsynaptic dendritic spines during periods of continuous synaptic activity. Mitochondrial transport towards active synapses is regulated by either ATP/adenosine diphosphate (ADP) levels, or via intracellular Ca^{2+} concentration. Indeed, mitochondria are known to slow down to a potentially stationary state in areas of a low ratio of ATP/ADP concentration (Sheng, 2014). This is because ATP has a low capacity for intracellular diffusion and therefore low energy areas require a local 'docked' pool of mitochondria for immediate ATP generation. Elevated levels of Ca^{2+} are also known to inhibit mitochondrial transport and optimal calcium levels at synapses are maintained by mitochondria which sequester intracellular Ca^{2+} (Sheng, 2014). In fact, two-thirds of mitochondria in an axonal network are thought to be stationary over an extended period of time (Kang et al., 2008).

Since neurons are particularly dependent on efficient mitochondrial dynamics, they are highly dependent on well-functioning transport, fusion, fission and turnover machinery. Mitochondrial fusion is known to be important in the exchange of contents between different mitochondria, thereby enabling a shuffling of components between healthy and damaged mitochondria allowing for an overall healthy and functional network. Mitochondrial fission on the other hand, is crucial in generating mitochondria containing damaged components, which can be easily segregated for degradation. Furthermore,

fission is highly related to transport as once mitochondria have undergone fission, the smaller daughter organelles can move along the axon at a faster pace, quickly getting to the area where required (Figure 1.5A).

Studies investigating the role of dynamin related protein-1 (Drp1), a mitochondrial dynamin-like GTPase required for mitochondrial membrane fission, show that defects in the process lead to accumulation of mitochondria in the soma and a diminished mitochondrial content in dendrites (Li et al., 2004). Studies in *Drosophila* also show that Drp1 is essential for the presence of mitochondria at neuromuscular junctions (NMJs) (Verstreken et al., 2005). Mutations in the gene encoding for mitofusin, *MFN2*, which is required for mitochondrial fusion have also been shown to disrupt anterograde and retrograde mitochondrial transport (Baloh et al., 2007). Deficiencies in fusion are therefore correlated to impaired distribution of mitochondria as well as fragmentation of the organelles. Furthermore, mitofusin has been shown to associate with the motor MIRO-Milton complex; composed of the motor adaptor complex Milton interacting with the RHO family GTPase MIRO found in the OMM. This association has also been shown to be necessary for axonal mitochondrial transport (Misko et al., 2010).

Phosphatase and tensin homolog-induced putative kinase 1 (PINK1), a mitochondrially targeted serine/threonine kinase, and Parkin, a cytosolic E3 ubiquitin ligase, are proteins involved in mitochondrial turnover by mitophagy (mitochondrial specific autophagy). Damaged mitochondria with a reduced mitochondrial membrane potential exhibit an accumulation of PINK1 on the OMM, which triggers Parkin recruitment to the mitochondrion causing ubiquitination of OMM proteins and targeting the organelle for autophagy (Figure 1.5C). Recent studies also suggest that apart from a role in mitophagy, the PINK1-Parkin pathway may also play a role in selective turnover of mitochondrial respiratory chain subunits (Vincow et al., 2013). Furthermore, the PINK1-Parkin complex

has also been shown to be associated with mitochondrial transport. More specifically, PINK1 has been shown to phosphorylate MIRO, activating its degradation, thereby arresting mitochondrial anterograde transport, in a Parkin dependent manner (Weihofen et al., 2009). This suggests that PINK1 and Parkin might also regulate mitochondrial transport, inhibiting damaged mitochondria from moving along the network, thereby allowing segregation and subsequent autophagy of the organelle.

The PINK1-Parkin pathway has been shown to promote mitochondrial fission and inhibit fusion, by downregulating *MFN2* and *OPA1*, which encodes the protein optic atrophy 1, required for fusion of the IMM (Yang et al., 2008; Yu et al., 2011). These findings have however been contradicted in several mammalian cell studies, in which loss of PINK1 correlated with an increase in mitochondrial fragmentation (Dagda et al., 2009; Lutz et al., 2009) Recent studies have also suggested that Parkin ubiquitinates mitofusin proteins, possibly inhibiting damaged mitochondria from fusing with healthy ones as an additional mode of segregation followed by mitophagy (Gegg et al., 2010; Ziviani et al., 2010).

Efficient mitochondrial transport, fission and fusion machinery are therefore required to work together in a synergistic manner facilitating mitochondrial function (Figure 1.5D), and when these processes are compromised, the ability of neurons to survive stressful stimuli and eliminate damaged cells may depreciate. Indeed, as will be discussed in sections 1.12.1 (AD) and 1.12.2 (PD), there are numerous studies linking deficits in mitochondrial dynamics to neurodegeneration.

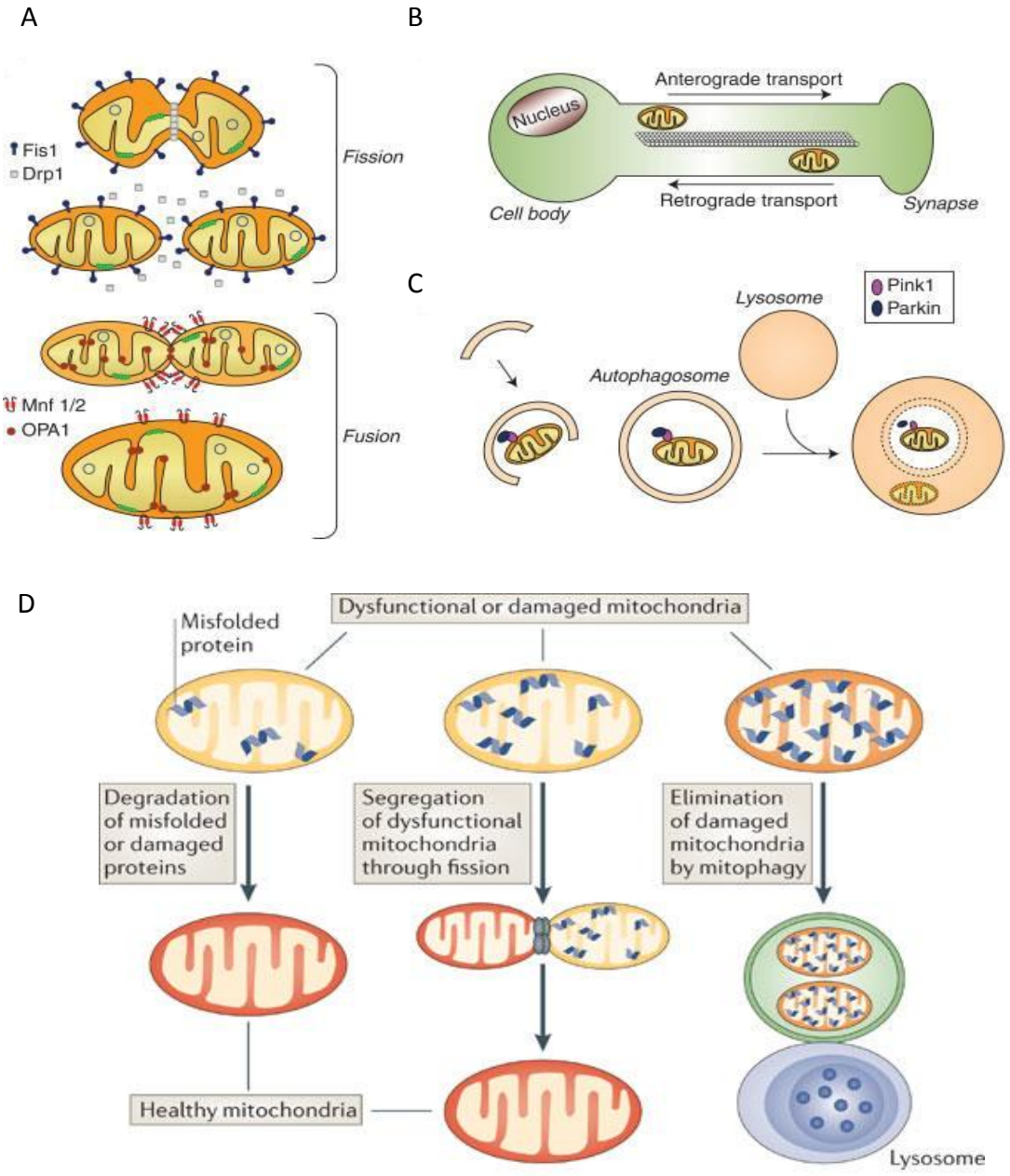

Figure 1.5 Mitochondrial dynamics
(A) Mitochondrial fission is mediated by dynamin-related protein 1 (Drp1) and mitochondrial fission-1 protein (Fis1). Fusion of the outer mitochondrial membrane (OMM) is mediated by Mitofusins (Mnf) 1 and 2 whilst fusion of the inner mitochondrial membrane (IMM) is mediated by protein optic atrophy type 1 (OPA1). (B) In neurons, mitochondria move towards the synapse via anterograde transport and back to the nucleus via retrograde transport. (C) PINK1/Parkin mediate mitochondrial quality control via mitochondria–specific autophagy (mitophagy). (A-C adapted from (Perier and Vila, 2012). (D) Mitochondrial quality control is mediated by fusion, which mixes healthy and damaged mitochondrial components, fission, which allows segregation of the damaged mitochondria and mitophagy, which degrades and eliminates the damaged mitochondria (Sheng and Cai, 2012).

1.7. The mitochondrial genome

1.7.1. mtDNA replication

The presence of DNA in mitochondria was first reported in 1963 when Margit and Sylvan Nass were studying chick embryo mitochondria under the electron microscope. They observed fibres within the mitochondria which contained DNA-like characteristics and proposed that mitochondria contained their own DNA, separate from the nuclear counterpart (Nass and Nass, 1963). A year later, in 1964, mtDNA was purified from baker's yeast (Schatz et al., 1964) and in 1966, a study reported the differentiation of nuclear and mitochondrial protein systems due to a differing susceptibility to antibiotic treatment (Clark-Walker and Linnane, 1966). A timeline of the main discoveries related to mtDNA in yeast is depicted in Figure 1.6.

The mitochondrial genome copy number in an organism is highly variable and regulated in a cell-specific manner (Phillips et al., 2014). It is estimated that there are thousands of mitochondria in most mammalian somatic cells, each containing 1 to 10 copies of mtDNA, and mammalian oocytes contain at least 100,000 copies of mtDNA per cell (Shoubridge and Wai, 2007). The mitochondrial genome, which in mammals is 16.6kb, encodes 13 polypeptides, all of which are components of the complexes of the mitochondrial respiratory chain. The energetic levels of the cell are therefore dependent on the presence of an adequate mtDNA copy number, which is sufficient to maintain the metabolic requirements of the cell.

The mtDNA replication machinery is nuclear encoded. The mitochondrial DNA polymerase (pol γ) has a catalytic and accessory subunit, termed pol γ-α and pol γ-β respectively, which are responsible for the synthesis of the new mtDNA strand. The mtDNA is unwound in the 5' to 3' direction by the mtDNA helicase, which in mammals is known as Twinkle. mtDNA

single stranded binding protein (SSBP) consequently acts to stabilize the single strand, thereby preventing rewinding of the strands (Figure 1.7).

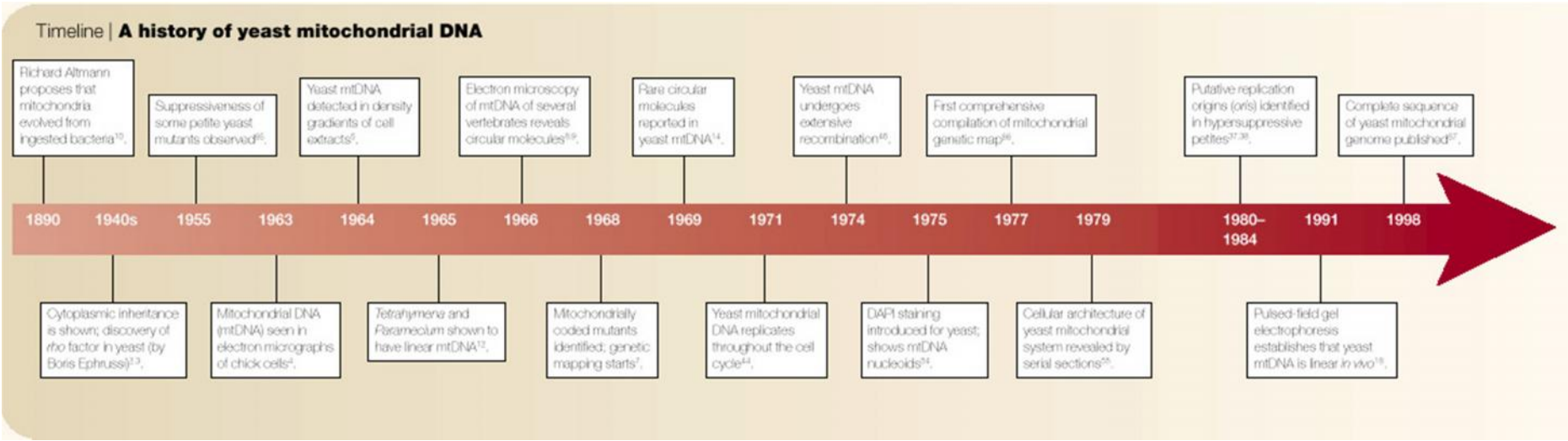

Figure 1.6 A timeline of the main discoveries in yeast mtDNA

A timeline depicting the main findings associated with mtDNA in yeast, leading to the publishing of the complete sequence of yeast mtDNA in 1998 (Williamson, 2002).

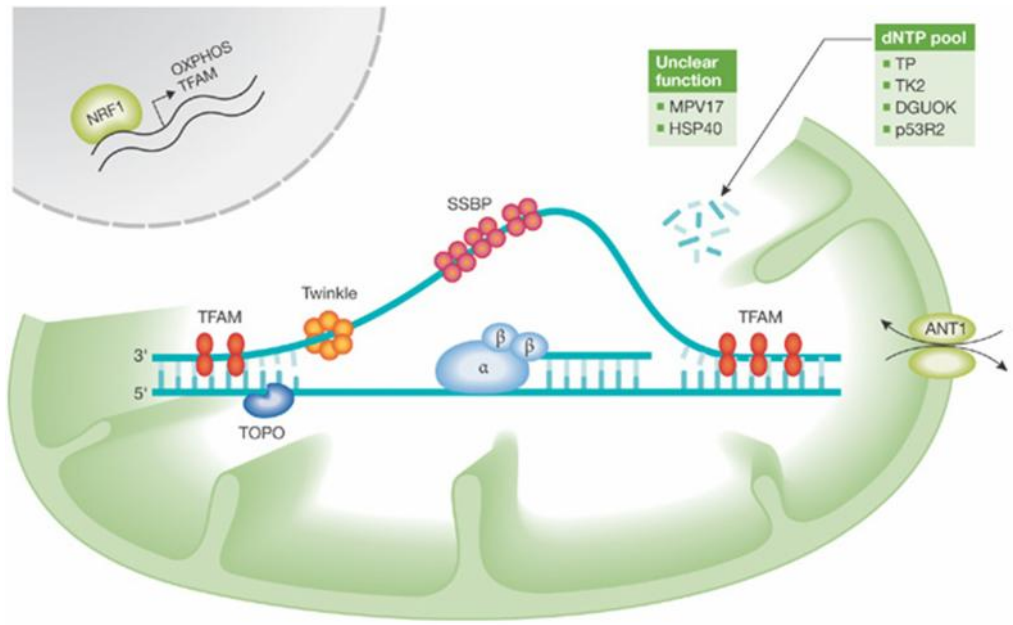

Figure 1.7 Mammalian mtDNA replication machinery

The factors required for mtDNA replication are all transcriptionally regulated by nuclear respiratory factor 1 (NRF1). MtDNA is synthesised via the mtDNA polymerase, pol γ (α and β subunits) whilst the mammalian mtDNA helicase, Twinkle, unwinds the double strand. The mtDNA single strand binding protein (SSBP) stabilises the single strand, whilst TOPO (topoisomerase) controls mtDNA winding. Mitochondrial transcription factor A (TFAM) binding to mtDNA is essential for mtDNA replication. Deoxyribonucleotides (dNTPs) required for mtDNA synthesis are supplied by TP (thymidine phosphorylase), TK2 (thymidine kinase 2), DGUOK (deoxyguanosine kinase) and p53R2 (ribonucleotide reductase subunit). Other factors including MPV17 (a mitochondrial membrane protein) and HSP40 (a mitochondrial chaperone) have an unclear function but are required for mtDNA replication. ANT1 imports ADP and exports ATP out of the mitochondrial matrix. Adapted from (Tyynismaa and Suomalainen, 2009).

In mammalian mtDNA, the circular genome consists of a heavy strand, so called because it contains a higher proportion of guanine, and a light strand. Both the heavy strand and the light strand carry an origin of replication, termed the O_H and the O_L respectively (Figure 1.8).

The strand-displacement model of mtDNA replication, which was first proposed by Clayton in 1982 (Clayton, 1982) states that DNA synthesis is initiated at the leading, heavy (H) strand from the O_H, and proceeds at the lagging, light (L) strand from the O_L, once two-thirds of the genome has been replicated by the leading strand (Figure 1.8A). This results in a displacement-loop (D-loop), unidirectional, continuous, and asymmetric replication mechanism. This model of mtDNA replication has been widely supported by both *in vitro* and *in vivo* studies (Wanrooij et al., 2007; Fuste et al., 2010; Wanrooij et al., 2012). However, later studies have challenged the validity of this model and have proposed alternative theories.

Studies using two-dimensional agarose gel electrophoresis identified the presence of replication intermediates suggesting the presence of coupled leading and lagging strand synthesis (Holt et al., 2000). The strand-coupled model proposes a bidirectional, discontinuous and symmetric mechanism in which replication is initiated in a region of about 10kb in size, downstream of the 3' end of the D-loop in the control region (Figure 1.8C) (Holt et al., 2000; Yang et al., 2002; Reyes et al., 2005). Later studies further investigated the nature of the replication intermediates and identified them as RNA segments which become incorporated into the newly synthesised lagging strand, to be later maturated into DNA. This was proposed as the RITOLS (RNA Incorporated Through Out the Lagging Strand) model of mtDNA replication (Figure 1.8B) (Yang et al., 2002; Yasukawa et al., 2006).

Therefore, there has been no conclusive study establishing the presence of a sole mode of mtDNA replication and it is unclear whether different mechanisms of mtDNA replication may be used depending on the organism or particular physiological conditions. Further study and detailed investigation is required to understand the mechanism and the regulation of mtDNA replication.

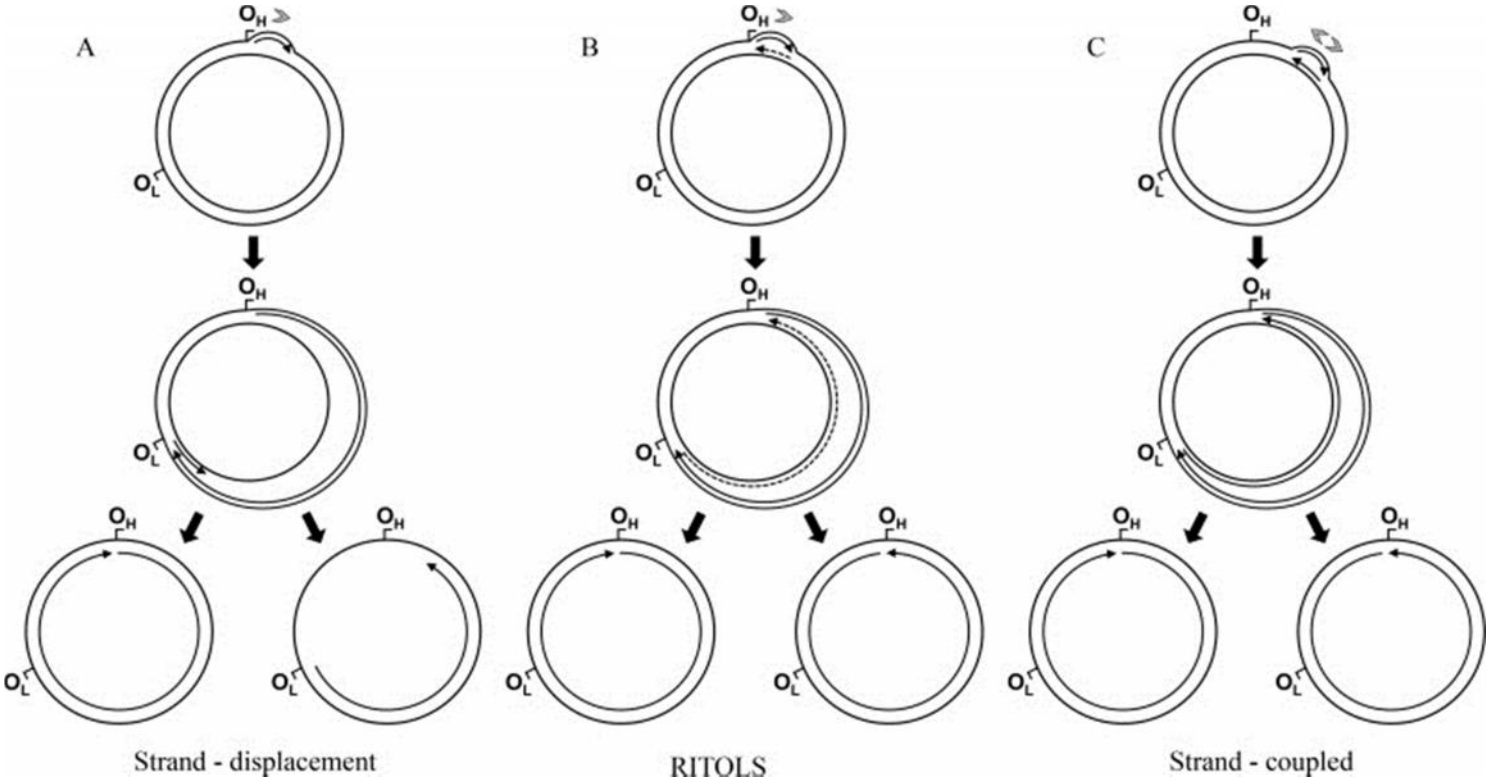

Figure 1.8 Models of mtDNA replication

(A) The strand-displacement model of mtDNA replication suggests that replication is initiated at the O_H on the heavy strand and proceeds on the light strand once the O_L is exposed, leading to a continuous unidirectional mode of replication. (B) The RITOLS model suggests the incorporation of RNA segments into the newly synthesised lagging strand. (C) The strand-coupled model suggests a bidirectional, discontinuous, symmetric mode of replication. Continuous and dashed lines represent the 5' to 3' direction of DNA and RNA synthesis respectively (McKinney and Oliveira, 2013).

1.7.2. Mitochondrial transcription

Mitochondrial transcription is dependent on factors encoded by the nuclear genome. Mitochondrial RNA polymerase (MTRPOL), mitochondrial transcription factor B 2 (TFB2M) and mitochondrial transcription factor A (TFAM) must interact and are the core proteins in the transcription machinery.

MtDNA contains three promoters; one on the light strand (LSP) which controls the expression of one protein-coding transcript (ND6), eight tRNAs and RNA primers required for mtDNA replication initiation, and two on the heavy strand – HSP1 controls the expression of two tRNAs and two rRNAs, whilst HSP2 controls the expression of the remaining 12 tRNAs and 12 protein-encoding genes (Shi et al., 2012). Transcription termination is regulated by the mitochondrial transcription termination factors 1-4 (MTERF 1-4) (Linder et al., 2005).

A recent study has suggested that the transcription process is initiated via a pre-initiation transcription complex, which has been identified and isolated (Morozov et al., 2014). This study suggests that TFAM, once bound to the N-terminal domain of MTRPOL results in the bending of promoter DNA around MTRPOL forming a pre-initiation complex, which then triggers the recruitment of TFB2M, inducing promoter melting and the assembly of a complete initiation complex. A later study also used electron microscopy to model the complete mitochondrial transcription initiation complex (Yakubovskaya et al., 2014).

TFAM is a nuclear encoded protein, containing a mitochondrial targeting sequence which is cleaved upon its import into the mitochondrion, leading to the formation of the mature protein. TFAM contains two high-mobility group (HMG) box domains, each of which is composed of three alpha-helices and two inter-connected peptide loops. When the two HMG boxes in TFAM bind to the mtDNA, they cause a kink in the structure which induces bending (Figure 1.9). The basic linker domain found in between HMG 1 and 2 will stabilise

the binding by making additional contacts with the phosphodiester backbone. The C-terminal tail found behind HMG 2 serves to activate TFAM transcriptional activity and is also involved in TFAM dimerization and positive cooperativity – a process by which TFAM binding to mtDNA triggers binding of further TFAM molecules along the chain (Kaufman et al., 2007).

Therefore, TFAM is necessary for mtDNA transcription in mammals, and is also required to bind to and bend mtDNA into particular conformations (Shi et al., 2012). Recent studies have further investigated the role of TFAM in mtDNA packaging, showing that TFAM creates a U-turn in mtDNA which results in the compaction of mtDNA (Ngo et al., 2011). The compact structure is also known to interact with other proteins to form nucleoprotein complexes known as nucleoids (Garrido et al., 2003). Super resolution imaging studies in human fibroblasts have revealed that each nucleoid, of which TFAM is a main component, has a diameter of around 100 nm and carries one copy of mtDNA (Kukat et al., 2011).

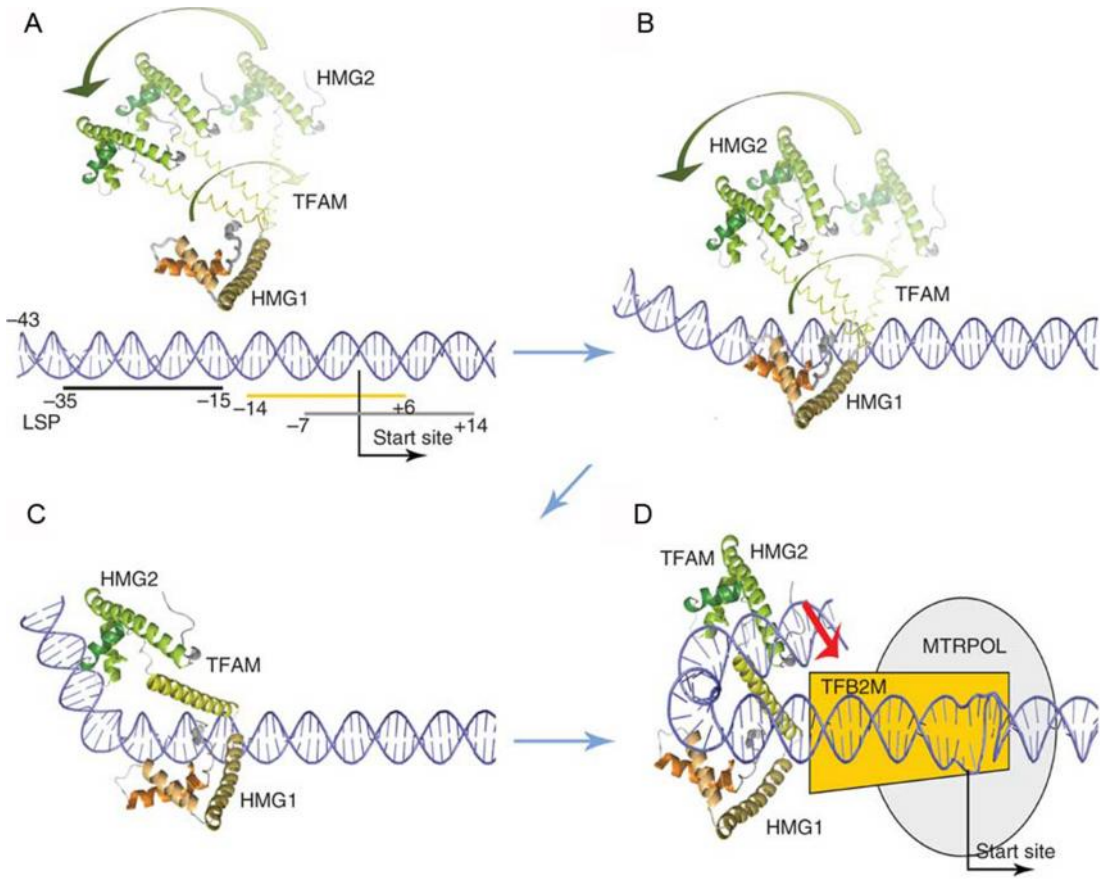

Figure 1.9 Mitochondrial transcription factor A (TFAM) binding to mtDNA is required for transcription

The model depicted in the diagram proposes a mechanism for TFAM transcriptional activity at the LSP. (A) TFAM will bind to mtDNA in the region marked by the black bar, whilst mitochondrial transcription factor B2 (TFB2M) and mitochondrial RNA polymerase (MTRPOL) bind to the regions indicated by the yellow and grey bars respectively. (B) HMG1 will bind to the mtDNA first inducing a kink. (C) The linker segment will then stabilise the first kink, leading to the binding of HMG2, which introduces a second kink, therefore forming a U-turn in the mtDNA. (D) Transcription is then initiated upon recruitment of TFB2M and MTRPOL (Rubio-Cosials et al., 2011).

Several *in vitro* studies have been carried out to further investigate the requirements for TFAM in mammalian mitochondrial transcription (Fisher and Clayton, 1988; Parisi and Clayton, 1991). It has been concluded that TFAM binding to a specific site upstream of the LSP, is necessary for transcription to occur, as alterations within this site (Dairaghi et al., 1995b; Gaspari et al., 2004) or depletion of TFAM (Shi et al., 2012) lead to transcription abolishment. Absolute TFAM requirement for transcription can be relaxed in conditions that induce DNA breathing, i.e. the spontaneous re-opening and closing of the double helix, such as low salt concentrations or negative supercoiling. Such conditions also lead to non-specific initiation of transcription at various other sites along the template (Shi et al., 2012).

The requirement for TFAM in maintenance of mtDNA and regulation of copy number has also been demonstrated in several animal models. Homozygous *TFAM*-/- mice are embryonic lethal, have reduced cytochrome c oxidase (COX) expression and abnormal mitochondrial morphology. Moreover, mtDNA copy number in these animals is greatly reduced (Larsson et al., 1998). Heterozygous *TFAM*-/+ animals are viable with a 50% reduction in TFAM levels and a concomitant reduction in mtDNA levels (Larsson et al., 1998).

TFAM binding regulates mtDNA copy number, and there are currently two models attempting to explain how this is achieved (Campbell et al., 2012). The first model is transcription-mediated and suggests that *TFAM* over-expression increases LSP activity, thereby increasing expression of the RNA priming sequence which triggers mtDNA replication (Shutt et al., 2010). This model is obviously dependent on the concentration of TFAM present relative to DNA, since saturating levels of TFAM are known to interfere with transcription. Indeed over-expression of *TFAM*, resulting in high TFAM: mtDNA ratios are thought to interfere with optimal DNA coiling, restricting access to DNA thereby reducing levels of transcription and mtDNA copy number (Dairaghi et al., 1995a; Pohjoismaki et al.,

2006; Matsushima et al., 2010; Shutt et al., 2010). Furthermore, at higher levels of TFAM, transcription would occur preferentially at the HSP1 promoter, which would not trigger replication (Shutt et al., 2010). The second model argues that TFAM covers the whole of the mtDNA (a dimer per 35 bp), not just the promoter region, and that the transcriptional activity of TFAM is not required to control mtDNA copy number (Ekstrand et al., 2004; Freyer et al., 2010). In fact, over-expressing *TFAM* lacking the C-terminal region, therefore lacking transcriptional competence, in human cell lines, has been shown to increase mtDNA copy number (Kanki et al., 2004). Similarly, over-expression of human *TFAM* in a *TFAM* knockout mouse increases the mtDNA copy number, but has no effect on mitochondrial transcript level and does not improve respiratory chain function and mitochondrial mass (Ekstrand et al., 2004). As previously mentioned, the C-terminal region in the TFAM structure is required for transcriptional activity, and since this region sequence differs in human and mouse TFAM, *hTFAM* cannot be used to activate transcription in a mouse and vice versa (Ekstrand et al., 2004). This model therefore suggests that the role of TFAM as a transcription factor is not required in the regulation of mtDNA copy number.

How is TFAM activity regulated? TFAM is known to be degraded by mitochondrial Lon protease (Matsushima et al., 2010) – an enzyme that degrades oxidised or mis-folded proteins. It is not known what triggers this TFAM degradation – the protease might recognise unfolded TFAM, or it might be targeting oxidatively-altered mtDNA, reducing TFAM binding (Canugovi et al., 2010).

Recently, Lu et al. showed that TFAM is phosphorylated, possibly via phosphate kinase A within its HMG1 domain, leading to its dissociation from mtDNA and its subsequent degradation by Lon (Lu et al., 2013). Furthermore, an additional study also demonstrated that TFAM is directly phosphorylated by extracellular-signal-regulated kinase (ERK)1/2 at Serine 177, similarly reducing its binding to the mtDNA promoter region and thereby

inhibiting its transcriptional activity (Wang et al., 2014). Other studies also demonstrate that TFAM might be post-translationally modified via acetylation at a single lysine residue. The authors speculate that since TFAM exhibits histone-like properties, its acetylation might be a way of regulating mtDNA gene expression, similar to nuclear gene regulation by histone acetylation (Dinardo et al., 2003).

Due to its crucial role in mtDNA stability, transcription and regulation of copy number, over-expression of *TFAM* has been shown to ameliorate cell function and viability in several pathology models including Type II diabetes, heart disease, PD, AD and general ageing (Ikeuchi et al., 2005; Hayashi et al., 2008; Suarez et al., 2008; Gauthier et al., 2009; Keeney et al., 2009; Xu et al., 2009; Campbell et al., 2012; Piao et al., 2012). Clearly, this is dependent on the structure of TFAM, with a compatible C-terminal tail allowing for transcription initiation, and ratios of TFAM: mtDNA, whereby an optimal balance allows for sustainable rates of transcription and replication without compromising mtDNA integrity.

1.7.3. MtDNA inheritance

MtDNA is maternally inherited, and therefore, mtDNA mutations and any associated pathologies are also derived from the maternal line. In mammals, mitochondria are randomly distributed during oogenesis in females, thereby producing oocytes with different amounts of mutant or wild-type mtDNA (Figure 1.10). A mother carrying only normal (wild-type) mtDNA will only pass on wild-type mtDNA to her progeny, and in this case all mitochondria will carry identical copies of mtDNA – this is known as homoplasmy. However, in cases where the mother is carrying mutant mtDNA, mitochondria in the progeny may harbour both wild-type and mutant mtDNA; a situation known as heteroplasmy. Therefore, in any cell, levels of heteroplasmy can vary greatly and over time somatic segregation might favour an increase in the frequency of one genotype to the other. The level of heteroplasmy is crucial because pathogenic mutations must surpass a

threshold level in order for symptoms to develop and a disease to develop (Taylor and Turnbull, 2005). The threshold level required for pathogenesis is dependent on the tissue type. Highly oxygen demanding tissue types such as the brain, heart and muscle, will have a lower threshold level for presence of mtDNA mutations as they will be particularly susceptible to mutations in mtDNA affecting the respiratory chain.

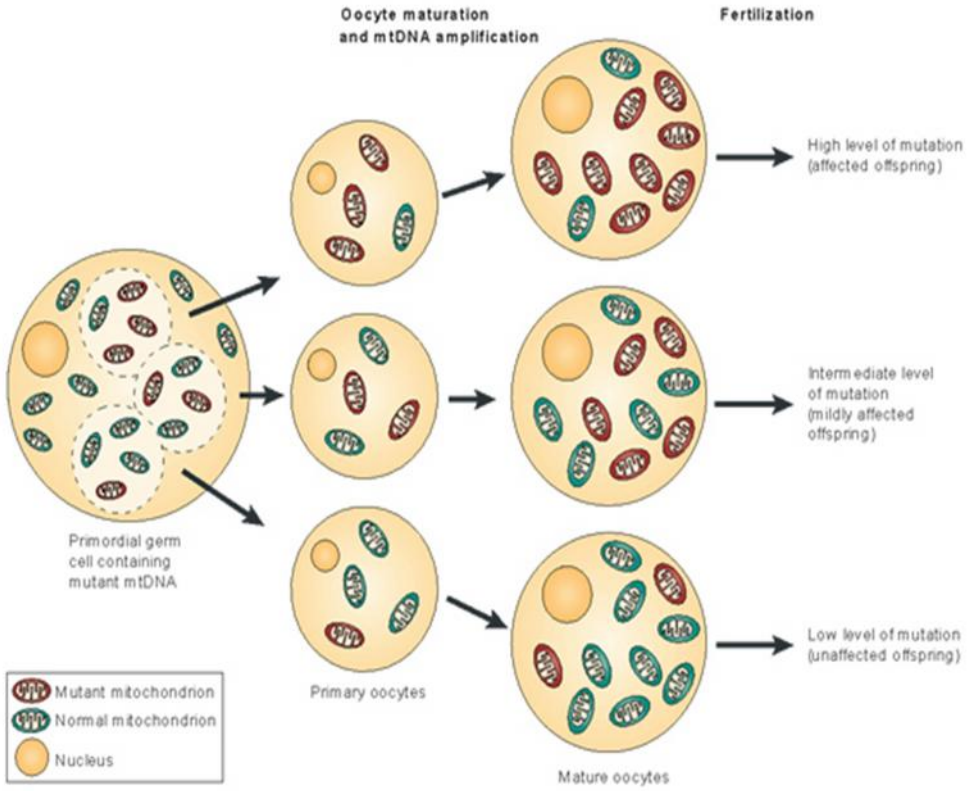

Figure 1.10 Inheritance of mtDNA
MtDNA is maternally inherited and during the production of primary oocytes. MtDNA molecules are randomly distributed to the individual oocytes. This leads to varying levels of mtDNA mutational load, with some oocytes carrying a low level and thereby giving rise to unaffected offspring and other oocytes having higher levels of mutations, surpassing the pathological threshold, therefore leading to affected offspring (Taylor and Turnbull, 2005).

1.8. Mutations in mtDNA

The mitochondrial genome, being less protected and having fewer repair mechanisms than its nuclear counterpart, is particularly susceptible to damage. Mutations in mtDNA may lead to mitochondrial dysfunction either via direct alterations in the protein-encoding genes of the genome, or via mutations in the genes affecting translation. Mutations in mtDNA can be inherited or occur spontaneously. The most well-known syndromes associated with large mtDNA deletions are; Pearson's syndrome, a rare disease characterised by sideroblastic anemia and exocrine pancreas dysfunction, Kearns-Sayre syndrome, a multisystemic mitochondrial myopathy, and progressive external ophtalmoplegia (PEO), a mitochondrial myopathy characterised by drooping of the eyelids (ptosis) and paralysis of the extraocular muscles (ophthalmoplegia) (Zeviani et al., 1988; Moraes et al., 1989; Rotig et al., 1990). Point mutations in rRNA or tRNA genes in the mitochondrial genome result in defects in the overall synthesis of mitochondrial proteins. Mitochondrial encephalopathy lactic acidosis, and stroke-like episodes (MELAS) syndrome is associated with an A to G transition, A3243G, in the mTERF binding site on tRNA, whilst an A8344G transition is associated with myoclonus epilepsy and ragged-red fibers (MERRF) (Wallace et al., 1988a; Goto et al., 1990; Shoffner et al., 1990; Larsson et al., 1992). Finally, point mutations may also occur in the protein-encoding genes in the mitochondrial genome. Leber's hereditary optic neuropathy (LHON), characterised by the degeneration of retinal ganglion cells, is a maternally inherited disease caused by one of three mutations: G3460A, G11778A and T14484C, affecting *ND1*, *ND4* and *ND6* respectively (Wallace et al., 1988b; Wallace et al., 1988a; Howell et al., 1991; Johns et al., 1992). Similarly, Leigh syndrome, also known as juvenile subacute necrotizing encephalomyelopathy, results from a mutation T8993C in the *ATP6* gene (Shoffner et al., 1992). MtDNA mutations, however, only account for 20-25% of cases of Leigh syndrome (Thorburn and Rahman, 1993). The

majority of cases are associated with a mutation in *SURF1*, a nuclear DNA encoded gene which is required for assembly and function of COX.

1.9. Mutations in nuclear DNA

Mutations in nuclear genes encoding mitochondrial targeted proteins will also affect mitochondrial function and OXPHOS. This might occur via defects in proteins regulating mitochondrial replication – autosomal dominant PEO is attributed to mutations in the catalytic subunit of pol γ, the mtDNA helicase Twinkle and ANT (Copeland, 2008). Mutations in genes encoding for TK2 and dGUOK, which are required for synthesis of dNTPs for mtDNA replication (Figure 1.7), are also associated with depletion of mtDNA levels (Mandel et al., 2001; Saada et al., 2001). Similarly, mutations in TP, resulting in a decrease in enzyme activity and an accumulation of thymidine, lead to depletion or deletions in mtDNA in patients with mitochondrial neuro gastro-intestinal encephalomyopathy (MNGIE), possibly via an aberrant regulation of thymidine availability for DNA synthesis (Nishino et al., 1999).

1.10. Animal models of mtDNA dysfunction

Mutations in *Drosophila* pol γ-α (*tamas*) and pol γ-β have been shown to lead to loss of mtDNA and developmental lethality (Iyengar et al., 1999; Iyengar et al., 2002). Similarly, homozygous *pol γ-α* knockout mice are embryonic lethal whilst heterozygous mice develop normally despite showing a slight reduction in mtDNA levels (Hance et al., 2005). Moreover, mice expressing a proofreading-deficient version of *pol γ-α*, known as 'mutator mice', exhibit an increased level of mtDNA mutations, have a shorter lifespan and exhibit premature ageing phenotypes (Trifunovic et al., 2004). Indeed, studies have identified the presence of mtDNA deletions as the driving force behind the premature phenotypes observed (Vermulst et al., 2008). However, other studies have argued that whilst there might be an increase of mtDNA deletions in pol γ mutator mice, the association with a

premature ageing phenotype might be correlative, rather than causal. Quantitative measurement of mtDNA deletions in mutator mice via analysis by single molecule PCR has revealed that, in reality, the frequency of mtDNA deletions in these mice is too low to significantly contribute to a change in physiology, such as premature ageing. Indeed, it is argued that current experimental data is not sufficient to conclude that mtDNA deletions drive premature ageing and that further work is required to investigate this association in mutator mice models (Khrapko and Vijg, 2009; Kraytsberg et al., 2009).

Overexpression of *tamas* in *Drosophila* has also been shown to cause mtDNA depletion resulting in a variety of phenotypes (Lefai et al., 2000). Overexpressing *tamas* in muscle resulted in substantial pupal lethality, with a few surviving adults having a significantly reduced lifespan concomitant with a reduced mtDNA level and a decrease in levels of TFAM (Martinez-Azorin et al., 2013). Overexpression of *tamas* in the fly nervous system also caused an increase in pupal lethality, albeit to a lower level than that observed in the muscle. Adults also exhibit a decreased lifespan, a reduced mtDNA level and lower levels of TFAM (Martinez-Azorin et al., 2008). Contrastingly, overexpression of *tamas* in *Drosophila* Schneider cells did not phenocopy these observations, and mtDNA levels and growth rate were unchanged (Lefai et al., 2000), suggesting that variable levels of pol-γ are tolerated more *in vitro* than they are when expressed in the whole organism.

Recently, downregulation of *tamas* in *Drosophila* dopaminergic neurons was shown to result in premature ageing, lower respiratory chain activity and neuronal cell loss, which was fully rescued upon expression of the alternative oxidase AOX, allowing for an alternative ETC route, bypassing complex III/IV deficiency (Humphrey et al., 2012).

In mammals, dominant mutations in the mtDNA helicase, Twinkle, are associated with adult onset PEO. Expression of these PEO patient mutations in mice resulted in ‘deletor mice’ exhibiting respiratory chain deficiency in skeletal muscles and specific neuronal

populations, as well as a reduced level of mtDNA levels in the brain. Furthermore, mitochondrial myopathy was observed in these mice at about 12 months of age, with a progressively increasing rise of mtDNA deletions with age. These 'deletor mice' however, unlike the 'mutator mice' previously discussed, do not exhibit any signs of premature ageing. Therefore, Twinkle and pol γ might influence ageing via separate mechanisms. Alternatively, high levels of mtDNA mutations, resulting specifically from *PolgA* mutations, might be required for a premature ageing phenotype (Tyynismaa et al., 2005).

Overexpression of wild-type mtDNA helicase in both mice and *Drosophila* led to an increased mtDNA copy number, but the animals did not exhibit any particular phenotypes (Tyynismaa et al., 2004; Sanchez-Martinez et al., 2012). Expression of a mtDNA helicase variant carrying a K388A mutation, which disrupts helicase activity, in *Drosophila*, however, led to a decreased mtDNA number and lethality at the third larval instar stage (Sanchez-Martinez et al., 2012). Expression of two mtDNA helicase mutations which are commonly associated with human autosomal dominant PEO: A442P and W441C, also resulted in a decrease in mtDNA copy number and a decrease in lifespan, although the results were more significant in the A442P mutants than W441C. Expression of the K388A and A442P mutations elicit defects in the mitochondrial OXHPOS process and a concomitant increase in apoptosis, suggesting that these mutations lead to a deregulation of mitochondrial-assisted programmed cell death and a reduction in cell proliferation (Sanchez-Martinez et al., 2012).

Similarly, mutations in the *lopo* gene in *Drosophila*, encoding mtDNA SSBP, result in developmental lethality, loss of respiratory function and reduced cell proliferation (Maier et al., 2001). Moreover, mutations in specific amino acids within mtDNA SSBP, which inhibit its DNA-binding activity and its interaction with pol γ, result in a loss of pol γ activity and defects in DNA synthesis.

Furthermore, as previously mentioned in Section 1.7.2, inactivation of TFAM in mouse dopaminergic neurons leads to a reduction in mtDNA levels. These 'Mito-park' mice develop parkinsonian-like phenotypes, with neuronal loss in SNpc, loss of dopamine in the striatum, abnormal mitochondrial aggregates as well as reduced movement and tremors (Ekstrand et al., 2007).

An additional model of mtDNA dysfunction was recently developed by the Moraes group, utilising a mitochondrially targeted endonuclease (*mito-PstI*) to create double stranded breaks in mtDNA in dopaminergic neurons. This model, known as 'PD-*mito-PstI*' develops a reduction in mtDNA copy number resulting in OXPHOS deficiency and a disrupted mitochondrial membrane potential. The 'PD-*mito-PstI*' mouse develops similar PD-like phenotypes to those observed in the 'Mito-park' mouse, including depletion in dopamine levels, motor symptoms and a reduction in dopaminergic neurons in the SNpc (Pickrell et al., 2011).

Taken together, these studies all demonstrate the importance of mitochondrial integrity in a functional nervous system and further validate the role of mtDNA dysfunction in neurodegenerative diseases.

1.11. Mitochondrial retrograde signalling

As discussed above, the nuclear genome plays a crucial role in the regulation of mitochondrial structure and function. The nucleus, therefore, must efficiently communicate with the mitochondria, ensuring a constant flow of information – this process is referred to as nucleus-to-mitochondria 'anterograde signalling'. In the early 1990s, pioneering work by the Butow laboratory also led to the identification of a mitochondria-to-nucleus communication pathway referred to as 'retrograde signalling' (Liao and Butow, 1993; Butow and Avadhani, 2004). Research carried out on the mitochondrial retrograde signalling pathway suggests that dysfunctional mitochondria communicate with the nucleus

to deliver information regarding their metabolic, oxidative and respiratory statuses. Such communication could ultimately lead to changes in nuclear gene expression, acting to ameliorate metabolic conditions (Figure 1.11). Therefore, mitochondrial retrograde signalling is defined as a cellular response to a change in mitochondrial function.

The mitochondrial retrograde signalling pathway was first identified in yeast, where mtDNA depletion was found to induce the upregulation of nuclear-encoded transcription factors, resulting in altered mitochondrial metabolism with upregulated fatty acid β-oxidation and activation of the glyoxylate cycle (Parikh et al., 1987; Butow et al., 1988). Later studies identified three retrograde response genes in yeast: *RTG1*, *RTG2* and *RTG3* (Liao and Butow, 1993; Jia et al., 1997; Rothermel et al., 1997; Sekito et al., 2000; Liu et al., 2003). *RTG1* and *RTG3* encode the subunits of a heterodimeric transcription factor, which bind to the sequence GTCAC (R box) in the promoters of target genes of the retrograde signalling response, stimulating transcription. RTG1-RTG3 are usually located in the cytoplasm, where RTG3 is heavily phosphorylated, but are translocated to the nucleus upon the induction of the retrograde response (Rothermel et al., 1995; Rothermel et al., 1997; Sekito et al., 2000). This requires a partial dephosphorylation of RTG3; a process which requires the presence of RTG2 (Sekito et al., 2000).

Retrograde signalling is conserved in mammals, although the molecular mechanisms might differ in different species, likely due to varying metabolic demands. Retrograde signalling in mammals was first observed in several ρ° (devoid of mtDNA) cell lines which showed increased mRNA levels for several mitochondrial proteins (Marusich et al., 1997; Wang and Morais, 1997). Further studies in mammalian cell lines, including C2C12 skeletal myoblasts (rhabdomyoblasts) (Biswas et al., 1999) and human lung carcinoma A549 cells (Amuthan et al., 2002), further established the presence of a mitochondrial stress response. Treatment with ethidium bromide or the ionophore CCCP (carbonyl cyanide m-chlorophenyl

hydrazone), resulted in altered mitochondrial membrane potential and increased levels of cytosolic free Ca^{2+}, which in turn activates the phosphatase calcineurin. Ultimately, the induced mitochondrial stress in both cell types resulted in the upregulation of nuclear-encoded genes involved in Ca^{2+} transport and storage such as Ryanodine Receptor I or II, calreticulin and calsequestrin (Biswas et al., 1999; Amuthan et al., 2001).

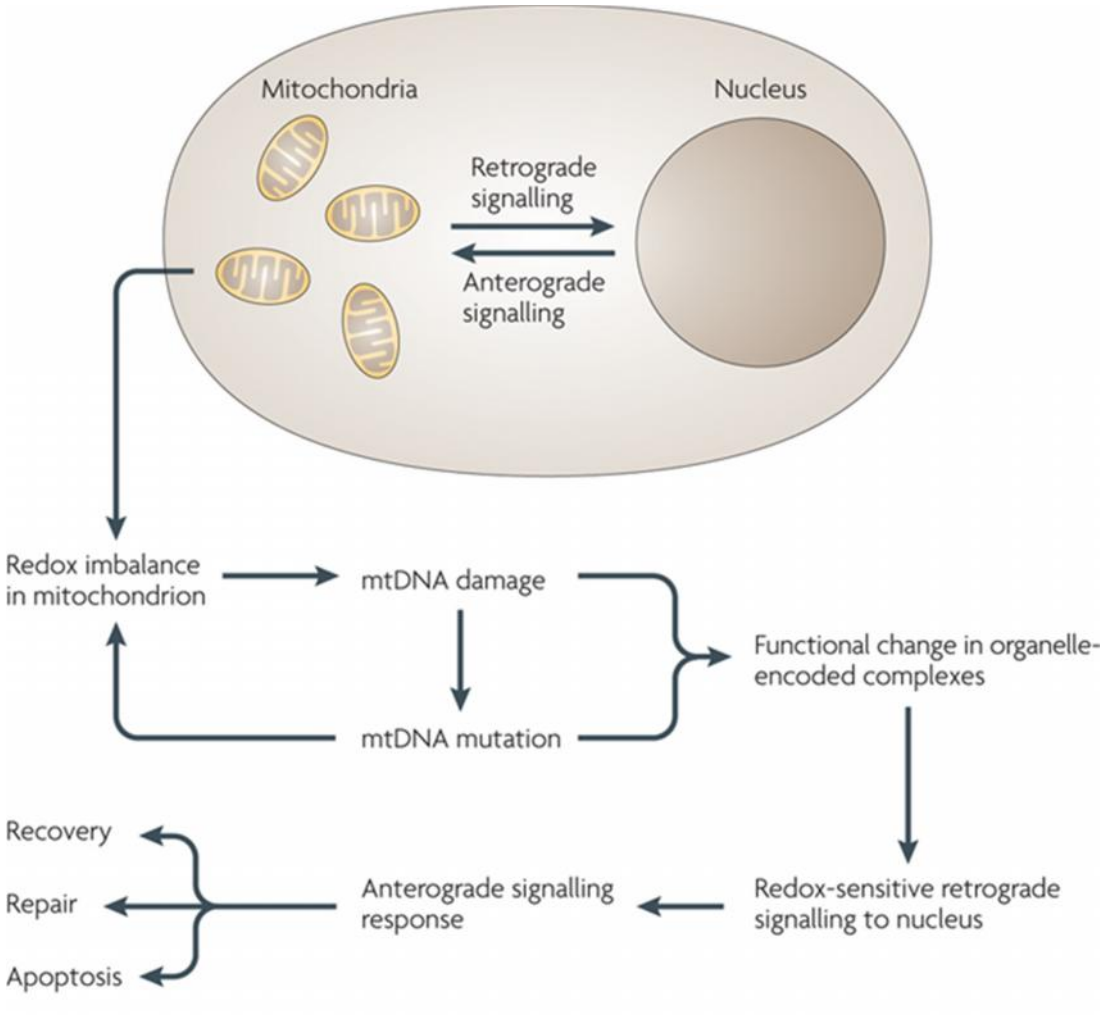

Figure 1.11 Mitochondrial retrograde signalling
MtDNA damage or the presence of mutations in mtDNA can lead to mitochondrial dysfunction, including a bioenergetic deficit due to functional changes in respiratory chain complexes. Mitochondria can relay this information back to the nucleus via a retrograde signalling pathway, which will elicit an anterograde response, acting to repair the damage or induce cell death (Wright et al., 2010).

Recently, studies have also been carried out in *Drosophila*, in order to uncover more details regarding the mechanisms of retrograde pathways which are activated upon mitochondrial dysfunction (Mandal et al., 2005; Liao et al., 2006; Freije et al., 2012). Downregulation of Complex IV (COX) subunit Va (CoVa) in the developing *Drosophila* retina, activates a retrograde pathway specifically involving AMP-activated protein kinase and tumor-suppressor protein p53 (Mandal et al., 2010). Activated p53 will transcriptionally activate archipelago, an F-box protein which will in turn ubiquitinylate Cyclin E, resulting in proteasomal degredation and a block in the cell cycle from G1 to S phase (Mandal et al., 2010; Freije et al., 2012). However, cell viability is maintained, suggesting that the retrograde signal acts to alter the metabolic state whilst favouring cell survival. Indeed, disruption of ETC genes has been reported to extend lifespan, via a retrograde signal, in *Drosophila* (Copeland et al., 2009; Liu et al., 2011) and mice (Liu et al., 2005; Dell'agnello et al., 2007; Lapointe and Hekimi, 2008).

Furthermore, studies in mammalian cells also identified an additional retrograde response, which was termed the mitochondrial unfolded protein response (UPR^{mt}). In a healthy mitochondrion, mitochondrial chaperones localised in the mitochondrial matrix act to regulate protein import and folding of proteins and complex assembly, whilst proteases in the matrix and inner membrane degrade any misfolded proteins (Tatsuta and Langer, 2008). However, several disruptions in the mitochondrial environment, such as mutations in assembly proteins, harsh environmental conditions or high levels of reactive oxygen species (ROS), might lead to the accumulation of unfolded or misfolded proteins, triggering a UPR^{mt} (Haynes and Ron, 2010). This stress response induces an upregulation of nuclear encoded mitochondrial chaperones and proteases (Martinus et al., 1996; Zhao et al., 2002). The UPR^{mt} response has also been shown to be activated upon mitochondrial stress caused by mtDNA depletion, downregulation of ETC components, depletion of mitochondrial

proteases and induction of high ROS levels in *C. elegans* (Yoneda et al., 2004; Haynes et al., 2010; Durieux et al., 2011; Nargund et al., 2012).

Recently, the theory of 'mitonuclear protein imbalance' was put forward by Houtkooper et al. (Houtkooper et al., 2013). This suggests that there is a stochiometric imbalance between proteins encoded by mitochondrial and nuclear genomes, and that this imbalance might be involved in regulating lifespan. Mitochondrial dysfunction induces this mitonuclear protein imbalance which will in turn trigger a UPR^{mt}, positively correlating with an increased lifespan in *C. elegans* (Houtkooper et al., 2013). In another *Drosophila* study, knockdown of complex I components resulted in a muscle mitochondrial phenotype while concomitantly inducing a redox – dependent upregulation of UPR^{mt} regulating genes. Expression of the insulin-like growth factor binding protein, ImpL2, was also upregulated, suggesting a decrease in insulin signalling and an increase in mitophagy. This ultimately preserved muscle activity and prolonged lifespan (Owusu-Ansah et al., 2013). Activation of the retrograde signal in *C. elegans*, has also been shown to extend lifespan, and similarly to *Drosophila*, knockdown of subunit 4 of Complex IV of the ETC (COX) has been reported to increase lifespan whilst activating a UPR^{mt} (Durieux et al., 2011). Interestingly, this study also found that mitochondrial dysfunction in the nervous system triggered a UPR^{mt} in the intestine in *C. elegans*, suggesting that the mitochondrial stress response could lead to a non-cell autonomous signal.

In mammals, retrograde signalling is known to involve the mechanistic target of rapamycin (mTOR) complex and PGC1α, which act to regulate mitochondrial biogenesis, thus maintaining adequate cellular bioenergetics (Jones et al., 2012; Chae et al., 2013; Lerner et al., 2013). Mitochondrial dysfunction might trigger a retrograde response, which acts on mTOR and PGC1-α to re-establish functional mitochondria and promote cell survival. In neurodegenerative diseases, which are characterized by neuronal cell death, this would

lead to neuroprotection, whilst in cancer, promoting cell survival might further exacerbate the pathology. Indeed, the mitochondrial retrograde response has been reported to be implicated in cellular proliferation and survival in a wide variety of tumours. Inhibition of mitochondrial ATPase has been shown to trigger a ROS-mediated retrograde response that inhibits apoptosis via upregulation of the anti-apoptotic protein Bcl-xl, promoting tumorigenesis (Formentini et al., 2012). Mutations in the mitochondrial-encoded *ATP6* and *COI* genes are also both associated with decreased mitochondrial respiration and enhanced tumour growth, following increased ROS levels (Petros et al., 2005; Shidara et al., 2005; Arnold et al., 2013), and several other studies suggest that somatic mtDNA mutations lead to increased ROS levels which are attributed to enhanced tumour metastasis (Ishikawa et al., 2008; Chang et al., 2009; Hung et al., 2010). Moreover, recent studies in cybrid cell lines have suggested that the introduction of healthy mitochondria into cancerous cells can attenuate the mitochondrial dysfunction phenotypes associated, and can restore ATP generation and oxygen consumption whilst reducing ROS levels (Kaipparettu et al., 2013). Taken together, these findings suggest that ROS-mediated retrograde signalling is implicated in tumorigenesis, introducing a role for ROS-regulation in the therapeutic intervention of cancer.

Mitochondria have also been reported to modify the epigenetics of the nuclear genome. A study has shown that peripheral blood DNA from subjects belonging to haplogroup J had higher methylation levels than samples from individuals belonging to other haplogroups. The same findings were observed in DNA from cybrid cells, where cybrids carrying DNA from J haplogroup exhibited higher methylation levels than cybrids with other haplogroup DNA (Bellizzi et al., 2012). J cybrids also generated lower levels of ATP and ROS, suggesting that mtDNA can regulate epigenetic changes in the nuclear genome and that this might possibly affect OXPHOS activity (Bellizzi et al., 2012).

Differing DNA methylation levels were also observed in mouse embryonic stem cells belonging to different mtDNA haplogroups (Kelly et al., 2012), and a human disease study, identified altered DNA methylation levels in cardiac cells from patients with dilated cardiomyopathy (Koczor et al., 2013). These findings therefore imply that a mitochondrial retrograde signalling mechanism might also be acting to modulate the epigenetic gene silencing of nuclear DNA, however, the mechanisms by which this control might occur are not yet well elucidated. Recent studies have provided some mechanistic insight by identifying the role of ROS in this epigenetic response. O'Hagan et al. found that exposure to ROS resulted in the assembly of a protein complex at regions of damaged chromatin, leading to the methylation of DNA (O'Hagan et al., 2011). A later study found that mitochondrial ROS are able to activate DNA damage response kinases, which act in the nucleus inhibiting histone demethylation (Schroeder et al., 2013). These discoveries further establish ROS as important retrograde signalling molecules, which may also play a part in the epigenetic changes induced by the mitochondria on the nucleus.

1.11.1. Mitochondrial retrograde signalling in disease

The presence of a compensatory mechanism in response to stress and mtDNA mutations, begs the question of whether an age-related malfunction of this compensatory mechanism might be implicated in the development of age-related disease.

Several animal models have demonstrated that mtDNA dysfunction leads to a retrograde signal that triggers an adaptive compensatory response. In *Drosophila*, a mutation in the ETC complex V ATP6 protein resulted in reduced OXPHOS activity but an upregulation in the rate of glycolysis, ketogenesis and citric acid cycle bioenergetics that maintained functional cellular activity while the flies were still young. However, once aged, the flies exhibited locomotor deficits and premature death (Celotto et al., 2011).

Furthermore, mitochondria isolated from platelets of AD and MCI patients had differentially expressed levels of genes that regulate mitochondrial biogenesis and activity, compared with controls (Silva et al., 2013). Mitochondrial malfunction has also been reported in embryonic neurons in AD mouse models, prior to onset of AD pathology (Yao et al., 2009). These findings therefore suggest that while a compensatory mechanism does exist, in response to mitochondrial dysfunction, it might become inadequate over prolonged periods of time, resulting in full-blown disease onset and cell death.

The previously mentioned mtDNA A3243G base substitution associated with MELAS, has also recently been shown to potentially instigate a retrograde signalling pathway acting via RXRA (retinoid X receptor α), ROS, JNK kinase (c-JUN N-terminal kinase), and the transcriptional co-activator PGC1α to mediate the response (Chae et al., 2013). Chae et al., found that in a cybrid model cell line, expression of the A3243G mutation triggered generation of reactive oxygen species which resulted in a decreased mRNA abundance of OXPHOS and translation-related genes. This pathway therefore results in a transcriptional feedback loop which further exacerbates the dysfunction in oxidative phosphorylation, further aggravating mitochondrial dysfunction and contributing to disease progression.

Therefore, the mitochondrial retrograde signalling pathway plays a crucial part in regulating the processes related to mitochondrial-associated pathologies and further understanding of the mechanism is critical to develop potential therapeutic options.

1.12. Mitochondrial dysfunction in neurodegenerative diseases

1.12.1. Mitochondria and Alzheimer's Disease

The AD mitochondrial cascade hypothesis was first proposed in 2004 by Swerdlow and Kahn (Swerdlow and Khan, 2004). The premise is that, for each individual, a genetically determined mitochondrial baseline function, along with environmental factors, will

regulate a rate of decline in mitochondrial function which will in turn determine the temporal onset of AD pathology (Figure1.12). This theorem further strengthens the ideas put forth by numerous studies which concluded a link between mtDNA mutations, mitochondrial dysfunction and AD (Parker et al., 1989; Wallace, 1992).

Unlike the amyloid cascade hypothesis, the mitochondrial cascade hypothesis clearly distinguishes between LOAD and EOAD in terms of disease development. According to this hypothesis, in LOAD, age-associated mitochondrial dysfunction leads to AD pathology, whilst in EOAD, the APP processing leading to Aβ aggregation will be the hallmark of disease onset. The proposal also further identifies the role of an ageing brain in AD development. Mitochondrial function declines with ageing, which is compensated by adaptive mechanisms. However, if compensatory mechanisms are not enough to counteract the disease development, symptoms will present (Swerdlow et al., 2013).

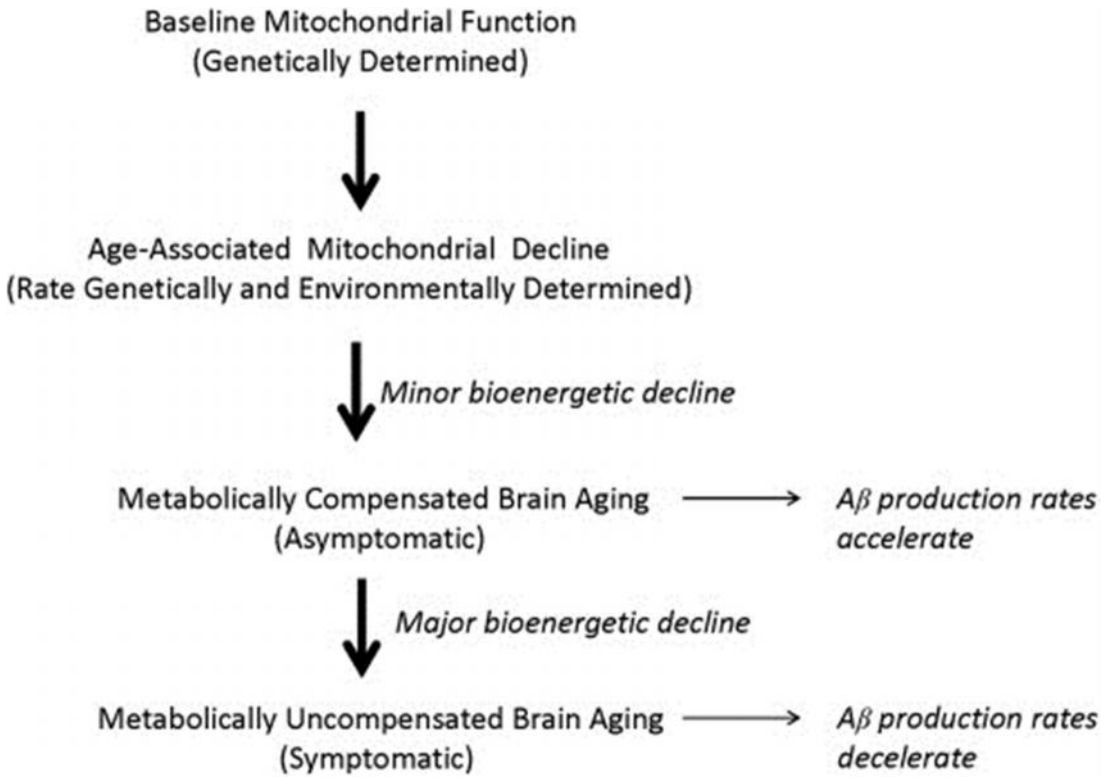

Figure1.12 The mitochondrial cascade hypothesis
The mitochondrial cascade hypothesis argues that for each individual, genetic and environmental factors determine an age-associated mitochondrial decline, which initially leads to a compensatory mechanism resulting in bioenergetic hypermetabolism. This, in turn, increases production rates of Aβ and this leads to further bioenergetic decline. When mitochondrial dysfunction is too severe, compensatory mechanisms are not adequate and symptoms develop. At this point, Aβ production rates decline (Swerdlow et al., 2013).

As previously stated, familial, EOAD cases account for less than 1% of all AD cases and are mostly associated with mutations in APP and the presenilin genes *PSEN1* and *PSEN2*. Presenilin 1 and 2 complexes regulate the cleavage of APP by γ-secretase, into $A\beta_{1–40}$ and $A\beta_{1–42}$. The toxicity of these peptides has been greatly studied, with $A\beta_{1–42}$ being identified as the most neurotoxic, especially in its aggregated form (Deshpande et al., 2006). The presenilin complex with γ-secretase has been shown to be localised to mitochondria, further confirming the importance of the organelle in the pathogenesis of the disease (Hansson et al., 2004). APP has also been found to bind to the OMM, where the APP intracellular domain (AICD), is released into the mitochondrion once cleaved by the γ-secretase complex (Pavlov et al., 2011). Moreover, Aβ is found in mitochondrial cristae, where it localises after entering the organelle via the TOM complex (Hansson Petersen et al., 2008). Indeed, in AD patients, Aβ accumulation is known to occur early on in the disease and is especially found in lysosomes, endosomes and mitochondria (Lustbader et al., 2004; Gouras et al., 2005; Manczak et al., 2006; LaFerla et al., 2007). Aβ binds to mitochondrial proteins, altering mitochondrial morphology and function. Inhibiting this interaction suppresses mitochondrial damage caused by Aβ and reduces cognitive phenotypes in mouse models of AD, suggesting that mitochondrial targets are a major contributor to AD progression (Lustbader et al., 2004; Du et al., 2008).

Aβ is thought to interfere with mitochondrial function by increasing viscosity of the mitochondrial membrane, altering levels of the phosphate to oxygen ratio, reducing levels of ETC activity, and increasing levels of ROS and release of cytochrome c (Aleardi et al., 2005). Indeed, in human cortical neurons, treatment with Aβ oligomers (AβO), composed of 15-20 monomers, resulted in a significant 89% drop in mitochondrial membrane potential and a 70% loss in ATP levels within 2 hours post-treatment, followed by an increase in caspase activation and release of cytochrome c and apoptosis initiating factor after 8 hours (Deshpande et al., 2006).

Aβ has also been shown to interfere with mitochondrial function via inhibition of the respiratory chain (Canevari et al., 1999; Crouch et al., 2005). Aβ is known to inhibit complex IV of the ETC, possibly via an interaction with the heme-containing COX unit (Atamna and Boyle, 2006). *In vivo* treatment with sodium azide, a known COX inhibitor, results in cognitive deficits and morphological changes in rat neurons (Szabados et al., 2004). Additionally, manganese superoxide dismutase (MnSOD), an enzyme acting to reduce superoxide levels in mitochondria, is also inhibited by Aβ causing an increase in oxidative stress (Massaad et al., 2010).

Studies have also suggested that Aβ accumulation in AD is linked to increased mitochondrial fission and a decrease in mitochondrial fusion, leading to a disruption in mitochondrial dynamics and subsequent neuronal damage (Wang et al., 2008).

Somatic mtDNA mutations, such as the common 5 kb deletion (mtDNA-4977) have also been linked to AD, particularly in the frontal cortex and basal ganglion (Corral-Debrinski et al., 1994). These regions are especially susceptible since they carry the highest somatic mtDNA mutation rate in the human body and they are highly energy demanding. The mutation T414G in the control region of mtDNA causes an alteration in the TFAM binding site which transcribes the *ND6* gene, encoding NADH-ubiquinone oxidoreductase chain 6 (Michikawa et al., 1999a; Murdock et al., 2000). This mutation was found to be associated with ageing in human skin fibroblasts (Michikawa et al., 1999b), and was later found to be more predominant in AD brains compared to control brains (Coskun et al., 2004). Somatic mtDNA mutations have also been found to be more frequent in DSAD (Down's Syndrome with AD-like dementia) and mtDNA/nDNA ratio levels are reduced in both DSAD and AD (Coskun et al., 2004; Coskun et al., 2010).

Interestingly, mtDNA mutations and levels were also found to correlate with Aβ metabolism. In DSAD, an increase in the somatic mutation levels in the mtDNA control

region and a decrease in mtDNA/nDNA levels, correlated with an increase in β-secretase activity (Coskun et al., 2010). Furthermore, depleting levels of mtDNA correlated with an increase in insoluble forms of $A\beta_{1-40}$. MtDNA mutations arise earlier than Aβ accumulation in progression of the disease, and may therefore play a role in increasing Aβ pathology.

AD cybrid studies have also established a link in bioenergetic decline with disease progression. Specifically AD-neuroblastoma cybrids exhibit reduced complex IV activity, increased oxidative stress, Aβ peptide secretion and fluctuations in mitochondrial membrane potential (Thiffault and Bennett Jr, 2005). Differentiated AD cybrids also develop altered mitochondrial morphology and impaired mitochondrial transport along neurites as well as increased autophagic vesicles and increased deposition of Aβ (Trimmer and Borland, 2005; Cardoso et al., 2010). Whilst transmitochondrial cybrid studies have proven extremely useful in studying the role of mitochondrial mutations in disease, it is important to note that most ρ^0 cells used in these studies are derived from aneuploid tumor cell lines. Since aneuploidy could affect nuclear DNA-mtDNA ratios and consequently nuclear DNA-mtDNA ETC subunit stoichiometry, it could significantly affect phenotypes observed in such studies. Furthermore, most tumorigenic cell lines are highly anaerobic. Therefore, in such cybrid models, the metabolic state of the original host cell might be an exerting an effect which could influence the results obtained in the studies (Swerdlow, 2007).

Studies in animal models have also established a link between mitochondrial dysfunction and AD. In a *Drosophila* model of AD, Aβ accumulates intraneuronally when expressed in the giant fibre neuron system (Zhao et al., 2010). Such treatment with Aβ was sufficient to cause age-dependent mitochondrial loss at the presynaptic terminal, concomitant with a decrease in synaptic vesicle release and increased synaptic fatigue. Axonal mitochondrial numbers were also reduced, whilst mean mitochondrial area was increased, suggesting a

defect in mitochondrial fission. Anterograde and retrograde transport of mitochondria along the axon was also observed to slow down, following presynaptic mitochondrial loss upon treatment with Aβ. Impaired transport upon Aβ treatment has also been observed in cultured hippocampal neurons (Rui et al., 2006; Vossel et al., 2010). Bruchpilot (Brp) is the *Drosophila* homolog of the Elks/CAST proteins, which function in the assembly of presynaptic active zones; areas within the presynaptic membrane where presynaptic vesicles dock and fuse to release neurotransmitters (Kittel et al., 2006; Wagh et al., 2006). Expression of the arctic mutant form of $A\beta_{1-42}$ ($A\beta_{arc}$) in the giant fiber neuron system of *Drosophila* has been shown to lead to an age-dependent decrease in Brp protein, suggesting a decrease in the amount of active zones (Huang et al., 2013). In the squid giant axon, treatment of the presynaptic region with Aβ also resulted in a reduction of docked synaptic vesicles and a subsequent loss of synaptic transmission (Moreno et al., 2009).

The temporal sequence leading to full-blown AD pathogenesis is not well elucidated. Though presynaptic mitochondrial alterations are a contributing factor, they might occur much earlier than any real synaptic dysfunction. Therefore, whilst loss of mitochondrial function and ATP deficiencies might be a result of neurodegeneration, they might also be required to trigger the damage induced upon Aβ accumulation. Furthermore, recent studies suggest that while AD pathology is necessary for cognitive decline to develop, failure of the stress response system in the brain is also a requirement (Lu et al., 2014) and other studies find compelling evidence suggesting that chromatin remodelling plays a major role in the epigenetic regulation correlated to cognitive decline (Fischer et al., 2007; Graff and Tsai, 2013; Ronan et al., 2013). Recent studies also suggest that Aβ is produced in a soluble form via APP processing in response to mitochondrial dysfunction (Jimenez et al., 2011). This response might initially serve a protective function, however, if sustained, might result in accumulation of Aβ levels leading to oligomerisation (Eckert et al., 2008). Analogously, α-synuclein might initially serve a neuroprotective purpose in PD, but later

aggregates into Lewy bodies. This would lead to further mitochondrial dysfunction and association bioenergetic deficits. In an aged individual, such deficits might rapidly result in neuronal death.

1.12.2. Mitochondria and Parkinson's Disease

In 1976, a chemistry student called Barry Kidston synthesised the drug 1-methyl-4-phenyl-4-propionoxy-piperidine (MPPP) for recreational use. However, the drug was contaminated with 1-methyl-4-phenyl-1,2,5,6-tetrahydropyridine (MPTP) and Kidston developed parkinsonian symptoms as a result. A few years later, in 1982, another six people were diagnosed with Parkinsonism after having intravenously injected the illicit drug MPPP. The neurologist J. William Langston identified MPTP as a major contaminant in the substance, and further studied the effects of the drug on primates. This led to the discovery that MPTP metabolite 1-methyl-4-phenylpyridinium (MPP+) is primarily toxic to the dopamine-producing substantia nigra cells in the brain, where it interferes with complex I of the ETC.

Later studies further investigated the structure and function of mitochondrial respiratory chain complexes in PD post-mortem tissue, and found a reduced complex I activity in the SNpc of PD patient tissue (Schapira et al., 1990a; Schapira et al., 1990b; Hattori et al., 1991; Mann et al., 1992; Janetzky et al., 1994; Hanagasi et al., 2005). Studies have also reported the presence of multiple mtDNA deletions in the SNpc of PD patients. These somatic mtDNA mutations accumulate to an extent which leads to respiratory chain deficiency and eventual neuronal loss (Bender et al., 2006; Kraytsberg et al., 2006).

Furthermore, loss of activity of the previously discussed PINK1 and Parkin has been suggested to be implicated in respiratory chain deficits, particularly in Complex I dysfunction (Mortiboys et al., 2008; Morais et al., 2009; Amo et al., 2011). As previously discussed, the PINK1-Parkin complex plays a role in mitochondrial turnover, fission and fusion and transport. The mechanism underlying the PINK1 – Parkin interaction is not yet

fully elucidated, and whilst certain studies suggest a direct binding between the two (Xiong et al., 2009; Sha et al., 2010) or that PINK1 directly phosphorylates Parkin (Kim et al., 2008; Narendra et al., 2010; Sha et al., 2010; Vives-Bauza et al., 2010), others suggest that they localise in separate complexes (Thomas et al., 2011; Lazarou et al., 2012). Recent studies also suggest that PINK1 targets Parkin to the mitochondrial membrane via phosphorylation of specific substrates, such as the primary motor/adaptor complex component Miro (Wang et al., 2011). Specific proteosomal degradation of Miro via Parkin, inhibits further mitochondrial movement and quarantines damaged mitochondria for sequestration.

PARK2, the gene encoding for Parkin, has been associated with early-onset Parkinsonism with reports of more than 120 mutations in over 600 affected families (http://www.molgen.ua.ac.be/PDmutDB/). *PARK2* mutations therefore account for most cases of autosomal recessive PD, though the mechanism by which the mutation might lead to parkinsonism is not well elucidated. Mutations in *PINK1* and the oxidative stress sensor *DJ-1*, are much less prevalent in association with PD (Spatola and Wider, 2014).

Lee et al., found that expressing mutations of Parkin known to be associated with early-onset PD, in mouse embryonic fibroblasts led to impaired clearance of defective mitochondria due to defects in recognition, transportation and ubiquitination of dysfunctional mitochondria (Lee et al., 2010). Furthermore, knock-out of Parkin in mice leads to a reduced number of mitochondrially-linked proteins and reduced respiration as well as increased susceptibility to oxidative stress (Palacino et al., 2004). In *Drosophila*, loss of Parkin led to reduced mitochondrial integrity and function (Narendra et al., 2009). Studies *in vitro* (Yu et al., 2011) and in *Drosophila* (Yang et al., 2008) have also concluded that Parkin and PINK1 regulate mitochondrial dynamics and function in dopaminergic neurons.

Similarly, knock-down of *PINK1* has been shown to decrease mitochondrial respiration and ATP synthesis, as well as increase α-synuclein aggregation in *in vitro* models of PD (Liu et

al., 2009). In murine models, *PINK1* knock-out decreases mitochondrial respiration, and increases mitochondrial dysfunction and susceptibility to oxidative stress (Gautier et al., 2008). Furthermore, alterations in *dPINK1* levels in *Drosophila* also affected mitochondrial axonal transport with *dPINK1* knock-down promoting anterograde transport, whilst *dPINK1* over-expression inhibited transport in both the anterograde and retrograde direction (Liu et al., 2012). *DJ-1* knockdown has also been associated to increased oxidative damage and dopaminergic degeneration, impaired mitochondrial respiration and morphology and an increased mitochondrial dysfunction (Lavara-Culebras and Paricio, 2007; Irrcher et al., 2010; Krebiehl et al., 2010) (Figure 1.13).

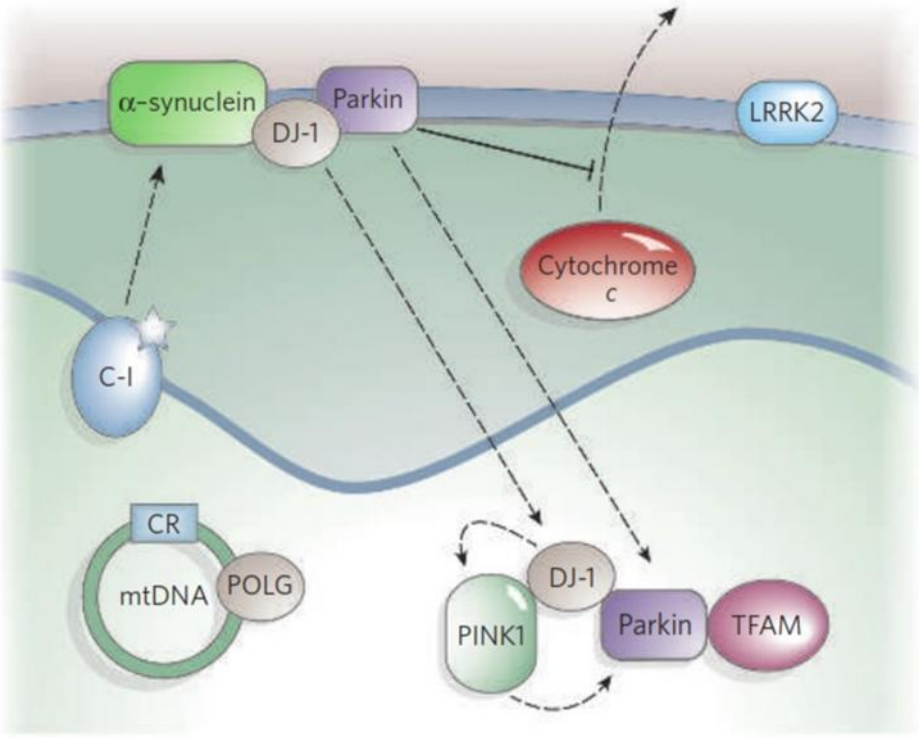

Figure 1.13 Mitochondria and Parkinson's disease
A decrease in Complex I (C-I) activity as well as mutations in *POLG* (mtDNA polymerase γ) are associated with PD. Proteins associated with PD (α-synuclein, parkin, DJ-1, PINK1, and LRRK2) are also known to be localised in the mitochondria and mutations in genes encoding these factors contribute to mitochondrial dysfunction and PD pathology. Parkin is located in the outer mitochondrial membrane where it inhibits cytochrome c release and might also associate with TFAM. It is also known to physically interact with PINK1, mediating mitochondrial quality control and the oxidative stress sensor DJ-1. LRRK2 is also localised to the mitochondria, and PD mutations are known to augment its kinase activity, disrupting mitochondrial function. Additionally, overexpression of α-synuclein has also been linked to mitochondrial dysfunction and toxicity of the mitochondrial membrane transition pore. Adapted from (Lin and Beal, 2006).

Whilst the role of ETC dysfunction in PD is well established, the presence of a mitochondrial retrograde signalling response has not been thoroughly examined. The presence of a UPR^{mt} in dopaminergic neurons is plausible since the ETC toxins, such as paraquat, known to induce parkinsonian phenotypes are also strong inducers of the UPR^{mt} (Nargund et al., 2012; Haynes et al., 2013). Furthermore, both the UPR^{mt} and PINK1-dependent mitophagy are dependent on mitochondrial import efficiency and are both activated by the same stresses (Haynes et al., 2013). Therefore, it would be of great interest to understand how these processes communicate with one another to efficiently regulate a response to mitochondrial dysfunction, and most importantly, how these mechanisms are being compromised in the context of neurodegenerative disease.

1.13. Summary

All forms of dementia lead to a devastating decline in cognitive ability and quality of life for the patients. Patients lose the ability to take care of themselves and eventually require full-time care, leading to an immense emotional burden for both patients and their carers.

The pathogenic mechanisms leading to AD, PD, DLB and PDD are all complex and are usually associated with varying levels of comorbidity. This complexity, the limited amount of efficient animal models, and the substantial side effects associated with certain drugs have led to a huge difficulty in providing efficient treatments for these diseases. Indeed, all treatments available to date are symptomatic and offer limited, and mostly temporary, benefit. The need for disease modifying therapies is crucial, especially at a time in which the world population is ageing.

Mitochondria, being the prime source of cellular energy, are critically important in our general body health and are especially crucial in maintaining adequate levels of energy in our brain, which is the most energy-demanding organ of all. Mitochondrial dysfunction is thought to be an early feature in forms of dementia, playing a role in cognitive decline and

disease progression. Therefore, mitochondria have recently become an attractive candidate for therapeutic studies since they might hold the secret to inhibiting the degeneration of neurons prior to its onset. However, the mechanisms underlying the association of mitochondrial dysfunction to neurodegeneration are not well known. Work in this thesis aims to address the potential association of a single nucleotide polyphormism (SNP) in TFAM with dementia.

Evidence suggesting the existence of a mitochondrial retrograde signalling pathway is also substantial, however the role of this pathway in neuronal maintenance and in the onset of neurodegenerative disease is not well elucidated.

Neurodegenerative diseases are progressive and most therapeutic strategies aimed at improving cognition and brain function at the later stages of the disease have not been very successful. The work outlined in this thesis therefore aims to better understand the initial response of neurons to mitochondrial dysfunction, via an examination of mitochondrial retrograde signalling in a *Drosophila* model of neuronal mitochondrial dysfunction. Investigating this response could lead to the discovery of a mechanism and therapeutic targets which inhibit the onset of neurodegeneration, thereby preventing the devastating symptoms and pathologies associated with dementia.

2. **Investigating the association of *TFAM* SNP rs2306604 A>G with dementia with Lewy bodies, Parkinson's disease and Parkinson's disease dementia.**

2.1. Introduction

The implications of mitochondrial dysfunction in neurodegeneration have been discussed in chapter 1 (Sections 1.12.1 and 1.12.2).

The human *TFAM* gene contains seven exons and six introns and covers 11.7 kb in chromosome region 10q 21.1. There are several linkage and candidate gene studies that have associated a risk of LOAD to genes present on a broad region of chromosome 10 (Zubenko et al., 1998; Bertram et al., 2000; Myers et al., 2002; Liang et al., 2007; Liang et al., 2009). Therefore, due its chromosomal location and function, *TFAM* has been of great interest in AD association studies.

The genetic variant, *TFAM* rs2306604 with a IVS4 + 113A > G SNP in intron 4, has been associated with AD in a 2007 meta-analysis of several small-scale studies and in a recent French genome wide association study (GWAS) (Bertram et al., 2007; Laumet et al., 2010). In both these studies, the A allele was associated with an increased risk of developing AD. The non-synonymous coding variant of *TFAM*, rs1937 (exon 1 variant S12T G > C), also referred to as rs11006128, has also been studied in association with the intronic variant rs2306604 (IVS4 + 113A > G) in AD, and studies show that G/G genotype of the rs1937 variant and a *TFAM* haplotype, G_{rs1937}-$A_{rs2306604}$ are significantly associated with AD.

rs2306604 has a global minor allele frequency of *A* = 0.461 and an average European minor allele frequency of *A* = 0.400. *In silico* studies have suggested that the presence of rs2306604 (IVS4 + 113A > G) creates an alternative splice variant generating a truncated TFAM protein (Günther et al., 2004). However, there are no *in vivo* studies affirming the presence of this splice variant.

The intronic variant rs2306604 (IVS4 + 113A > G) has also been studied in association with PD and was identified as a PD risk modifier in a 2010 study, with the G/G genotype leading

to an increased risk of disease development (OR 1.789, 95% CI 1.162-2.755, p=0.008) (Gaweda-Walerych et al., 2010). However, other studies, including GWAS and a meta-analysis study found no significant association of rs2306604 (IVS4 + 113A > G) with PD risk (Gaweda-Walerych and Zekanowski, 2013). These results suggest that this *TFAM* variant might be conferring different risks for AD and PD and that *TFAM* polymorphisms might be contributing to the development of dementia.

As previously described (section 1.4), up to 84% of PD patients develop cognitive impairment throughout the progression of the disease leading to PDD, which is associated with further alpha-synuclein pathology in the cortical areas, cholinergic deficits and co-morbid AD pathology including amyloid plaques. PDD is highly similar to another form of dementia; DLB. Indeed, as previously discussed, PDD and DLB patients exhibit similar symptoms and neuropsychological and neuropathological profiles. The main recognised distinguishing feature between the two dementias is the time of onset of cognitive symptoms relative to motor symptoms, with PDD cases expected to exhibit motor symptoms for longer than a year before developing cognitive impairments. DLB cases on the other hand typically develop dementia within the same year of exhibiting motor symptoms.

Importantly, the role of genetic factors in a predisposition to dementia in PD is not very well understood. Similarly, there are no studies investigating genetic differences distinguishing DLB and PDD development. Since definitions and diagnostic criteria for PDD and PD-MCI have only been established fairly recently (Emre et al., 2007; Litvan et al., 2012; Goldman et al., 2013), there have been no GWAS studies identifying genes associated with cognitive impairment in PD. However, studies on smaller cohorts have recorded an association of several genetic factors with cognitive impairment in PD. Namely, triplications in the *SNCA* gene and the presence of a E46K mutation are attributed

to an increased risk of cognitive impairment in PD (Singleton et al., 2003; Chartier-Harlin et al., 2004; Ibanez et al., 2004; Zarranz et al., 2004; Somme et al., 2011), whilst cognitive impairment in the presence of *LRRK2* mutations is thought to be less frequent than in cases of sporadic PD, suggesting that the mutations confer a reduced risk of dementia in PD (Goldwurm et al., 2006; Belarbi et al., 2010; Shanker et al., 2011; Ben Sassi et al., 2012). Similarly, the presence of mutations in mitochondrial associated *Parkin,* have been found to confer no added risk to cognitive impairment in PD (Caccappolo et al., 2011). Additionally, a study investigating the presence of mtDNA polymorphisms in PD and PDD, identified the presence of amino acid replacements in mtDNA-encoded complex I genes in haplogroup super-cluster JTIWX in both PD and PDD. However, the presence of this super-cluster was found to be even more frequent in PDD than in PD (Autere et al., 2004). Taken together, these studies therefore suggest that there might be genetic risk factors enabling a predisposition to the progression of dementia in PD.

In order to investigate whether *TFAM* rs2306604 A>G might also confer a predisposition to dementia, the distribution of *TFAM* rs2306604 A>G, and gender bias associated with its presence, in PD, PDD and DLB compared to healthy controls was studied.

2.2. Chapter aims

TFAM is a nuclear encoded protein that plays a variety of roles in mitochondria, including regulation of transcription, stability of mtDNA and regulation of mtDNA copy number. *TFAM* variants have been investigated in association with AD and PD and in particular, studies investigating an association of *TFAM* SNP rs2306604 A>G have provided contrasting evidence for AD and PD with the A allele being recognised as a risk factor for AD and a putative protective factor for PD.

In this chapter, I aim to investigate whether the intronic variant *TFAM* SNP rs2306604 A>G is associated with the other forms of dementia; PDD and DLB in comparison to non-demented PD cases and healthy controls. In particular, the prime objectives of this chapter are:

- To investigate whether *TFAM* SNP rs2306604 A>G is associated with the development of dementia in PD.
- To investigate whether the distribution of *TFAM* SNP rs2306604 A>G is significantly different in the highly similar dementias PDD and DLB.
- To investigate whether the distribution of *TFAM* SNP rs2306604 A>G is significantly different in males and females of the different diagnoses.

2.3. Materials and Methods

2.3.1. Cohort description

Post-mortem tissue from frontal cortex Brodmann area 9 (BA9), and blood samples were collected from multiple UK and Scandinavian clinical cohorts and tissue resources: postoperative cognitive decline trial, King's College London, UK; Newcastle Brain Tissue Resource, London Neurodegenerative Diseases Brain Bank and Thomas Willis Oxford Brain Collection, as part of the Brains for Dementia Research initiative, UK, Multiple Sclerosis and Parkinson's Tissue bank, UK; Demvest clinical and pathological study in Stavanger, Norway, and a dementia patient cohort in Malmö, Sweden. A total of 328 DNA samples were prepared from brain or blood of individuals for *TFAM* rs2306604 SNP genotyping. 72 DNA samples were obtained from DLB patients, 74 from PDD patients, 41 from PD patients and 141 from controls. Paraffin fixed, wax-embedded blocks, cut into sections of 7 μm and mounted onto slides, were also available for subsets of the samples for IHC.

PD cases were diagnosed based upon the presence of PD following the UK brain bank criteria (Hughes et al., 2001), whilst PDD cases were diagnosed according to DSM-IV criteria and required the presence of PD symptoms for more than one year before the onset of dementia (McKeith et al., 2005). Cases were diagnosed as DLB when cognitive impairment was developed within the same year of motor symptoms, according to the McKeith consensus criteria (McKeith et al., 2005). Controls presented no evidence of dementia-associated pathology upon post-mortem examination.

All post-mortem tissue analysis described in this chapter received ethical approval from Brains for Dementia Research, UK and the Multiple Sclerosis and Parkinson's Tissue bank, UK.

Of the total 328 samples, 158 were tissue (BA9) samples: 48 Controls, 41 PD, 22 DLB and 47 PDD whilst the rest of the cases were blood samples: 93 Controls, 50 DLB and 27 PDD (full list in Appendix 1). All 41 PD samples obtained were from brain tissue, and therefore no blood samples were used for this diagnosis group. Out of the total 158 BA9 samples, 33 controls, 41 PD, and 39 PDD samples were utilised in this study.

2.3.2. Semi-quantitative pathology scoring

Lewy body neuropathology scoring was carried out according to (Ballard et al., 2006), which is a 0 to 20 scoring system based on the previously published Lewy body scoring system from (McKeith et al., 1996), which is modified to also represent pathology in response to α-synuclein staining. For the purposes of this study, the scores were re-coded as 0 (none), 1 (brainstem predominant), 2 (limbic), 3 (neocortical) as shown in Table 1.

Table 1. Scoring system used for Lewy body neuropathology.

Category	Mc Keith scoring system (McKeith et al., 1996)	Ballard scoring system (Ballard et al., 2006)	Re-coded scores for this study
None	-	-	0
Brainstem	0	0-2	1
Limbic (transitional)	0-1	3-8	2
Neocortical	1-2	9-18 (mild) 19-20 (severe)	3

Tau neuropathology was scored according to (Braak and Braak, 1991) and recoded as 0 (Stage 0), 1 (stages I/II), 2 (stages III/IV), 3 (stages V/VI) as shown in Table 2. Aβ neuropathology was scored according to the CERAD scoring system (Mirra et al., 1991) and recoded as 0 (none), 1 (sparse), 2 (moderate) and 3 (frequent) as shown in Table 3.

Table 2. Scoring system used for tau neurofibrillary tangle (NFT) neuropathology.

Braak and Braak Staging (Braak and Braak, 1991)	Category	Re-coded scores for this study
0	None	0
I-II	NFT in transentorhinal and entorhinal cortex	1
III-IV	NFT in limbic allocortex and adjoining neocortex	2
V-VI	NFT in neocortex	3

Table 3. Scoring system used for Aβ plaque neuropathology.

Frequency of Aβ plaques (Mirra et al., 1991)	Score
None	0
Sparse	1
Moderate	2
Frequent	3

2.3.3. Measurement of pH of tissue homogenate

Brain tissue pH is known to vary depending on agonal state, brain ischaemia as well as repeated freeze/thaw cycles. It is therefore a routinely used indicator for quality of post-mortem tissue (Monoranu et al., 2009). The pH of brain tissue homogenates used in this study were measured as previously described by Kirvell et al. (Kirvell et al., 2006). Briefly, pH readings were taken using a pH meter (Thermo, Orion 3 star) calibrated at pH 4.0, 7.0 and 10.0 using standard buffer solutions (Thermo, Orion). The pH of dH_2O was taken as a baseline measurement to tare the readings. 50 mg of brain tissue was dissected and homogenised in 2 mL distilled deionised water (dH_2O) using an Ultra-Turrax tissue homogeniser (IKA Werke, Germany). The pH of each sample was measured in triplicate and the average reading was recorded.

2.3.4. DNA extraction

Genomic DNA was extracted using a commercially available kit (DNeasy blood and tissue kit, Qiagen), following the 'Animal tissue, spin column protocol'. 10 mg of BA9 tissue was

cut and placed in a 1.5 ml microcentrifuge tube and 180 µl buffer ATL were added. 20 µl of proteinase K were added and once thoroughly mixed, the sample was incubated at 56^{o}C overnight. 200 µl of Buffer AL were then added, followed by 200 µl of 100% ethanol. The mixture was then spun through a DNeasy Mini Spin column and washed with washing buffer AW1, followed by an additional spin and a wash with buffer AW2. DNA was finally eluted with 200µl elution buffer AE. The concentration of the purified DNA samples was subsequently quantified using the NanoDrop 1000 Spectrophotometer (Thermo Scientific) and stored at -20^{o}C.

2.3.5. Genotyping

The *TFAM* rs2306604 SNP was genotyped using a Taqman SNP genotyping assay (Applied Biosystems, C__1953826_1). DNA at a concentration of 20ng/µl was diluted 1 in 10 fold in DNAse-free water. A total of 5µl of DNA was then added per well in a 96-well reaction plate. A Taqman primer/probe mixture (Context sequence: AATAAAATATGGTAGAATGTC ATCA [A/G] GTATTCTTCAGTTAGGCAGAAGTGG, with the VIC reporter dye linked to the 5' end of the A allele probe, and the FAM reporter dye linked to the 5' end of the G allele probe) was prepared using a 1:2 dilution in Tris-EDTA pH7.4. A total of 1.25µl of the diluted primer/probe mixture along with 12.5µl TaqMan Universal PCR MasterMix and 6.25µl DNase-free water, were added to the 5µl DNA volume per well for a total reaction volume of 25µl. A 25µL non-template control was also included per plate. The plate was then run on an ABI PRISM 7000 Sequence Detection System (Applied Biosystems) using the following thermal cycling conditions: a 10 min hold at 95^{o}C followed by 40 cycles of (95^{o}C for 15 sec and 60^{o}C for 1 min). A substantial increase in VIC-dye fluorescence indicated homozygosity for allele A, an increase in FAM-dye fluorescence indicated homozygosity for allele B, whilst an increase in fluorescence of both dyes indicated A/G heterozygosity. An example of such an assay run is shown in Figure 2.1A.

Samples obtained from the Multiple Sclerosis and Parkinson's Tissue bank, UK at a later stage in the study were genotyped by PCR followed by restriction enzyme digestion as in (Alvarez et al., 2008a). A fragment of 230 bp was amplified with primers TAAAATATGGTAGAATGTCCTC (forward) and AGATTCTTGATACTCCTGGT (reverse) at conditions: 95^{o}C for 2 min, followed by 40 cycles of 95^{o}C for 15s, 50^{o}C for 15s and 72^{o}C for 1 min, and a final 10 min at 72^{o}C. The forward primer introduces a target site for the restriction enzyme *DdeI* in fragments containing the G-allele (Figure 2.1B). Therefore following digestion with *DdeI* (New England Biolabs UK, Ltd.) at 37^{o}C for 30 minutes, the PCR product was run on a 2% gel. An example of such a gel is shown in Figure 2.1C.

2.3.6. Statistical analysis

Statistical analyses were performed using IBM SPSS Statistics version 19 and GraphPad Prism version 5.0 (GraphPad Software Inc). When required, data were normalised by logarithmic transformation and case outliers greater than two standard deviations from the mean were not included in the analysis.

A Pearson correlative analysis was used to measure the linear correlation between post-mortem delay of patients and levels of protein and mtDNA.

Genotype distribution in DLB, PD and PDD cases compared to controls was tested using Pearson's chi-squared test whilst 2x2 contingency of allele frequencies was compared using Fischer's exact test.

In all individual analyses, a null hypothesis was postulated which asserted that there is no difference in frequency of *TFAM* SNP rs2306604 A>G amongst the different groups tested. In all cases, a result was considered statistically significant, and the null hypothesis rejected, when p value was lower or equal to 0.05 ($p \leq 0.05$).

2.4. Results

Demographic information was made available from the individual brain banks from which the case samples were obtained, and is summarised in Table 4. There was no significant difference between the mean age of death and brain pH of controls and PD, DLB, or PDD patients. Post-mortem delay (PMD) of PD samples was significantly shorter than in the other diagnostic groups, possibly due to the samples being sourced from a different brain bank (Multiple Sclerosis and Parkinson's Tissue bank, UK), however, correlation studies confirmed that the difference in PMD did not influence levels of proteins or mtDNA discussed below (data not shown).

Since only the samples obtained from the brain tissue were utilised for certain experiments, including measurement of mtDNA levels and protein levels, demographic information was also compared for the brain tissue samples only (Table 5).

Table 4. Demographic information for control, DLB, PD and PDD samples used in the study

	Control (141)	DLB (72)	PD (41)	PDD (74)
Age of death	76.34 ± 7.93 (n=141)	75.14 ± 11.26 (n=72)	79.07 ± 7.10 (n=41)	77.72 ± 6.58 (n=74)
Males (%)	56 (39.7)	36 (50.0)	26 (63.4)	38 (51.4)
PD duration (yrs)	-	4.50 ± 5.34 (n=19)	11.63 ± 6.53 (n=41)	13.31 ± 5.94 (n=31)
PD before dementia (yrs)	-	0.37 ± 4.46 (n=19)	-	9.84 ± 5.31 (n=31)
Dementia duration (yrs)	-	3.62 ± 2.52 (n=69)	-	3.86 ± 3.66 (n=72)
MMSE before death	-	18.39 ± 6.94 (n=54)	-	17.73 ± 7.63 (n=59)
Brain pH	6.47 ± 0.28 (n=25)	6.48 ± 0.36(n=22)	6.63 ± 0.14 (n=38)	6.47 ± 0.32 (n=39)
PMD (hours)	36.15± 20.11 (n=26)	37.68 ± 19.27(n=22)	15.38 ± 6.55 (n=39)	29.44 ± 15.87 (n=39)

Table 5.Demographic information for control, PD and PDD BA9 tissue samples used in the study

	Control	PD	PDD
Age of death	80.52 ± 8.86 (n=33)	79.07 ± 7.10 (n=41)	80.15 ± 5.41 (n=39)
Males (%)	18 (54.5)	26 (63.4)	23 (59.0)
PD duration (yrs)	-	11.63 ± 6.53 (n=41)	13.67 ± 5.97 (n=29)
PD before dementia (yrs)	-	-	10.07 ± 5.40 (n=29)
Dementia duration (yrs)	-	-	2.84 ± 2.60 (n=37)
MMSE	-	-	13.63 ± 7.77 (n=27)
Brain pH	6.47 ± 0.28 (n=24)	6.63 ± 0.14 (n=38)	6.45 ± 0.31 (n=37)
PMD (hours)	36.69 ± 19.99 (n=24)	15.39 ± 6.55 (n=39)	29.58 ± 16.06 (n=38)
CERAD (Aβ) score Median (IQ range)	0.00(0)	1.00 (2)	1.00 (2)
Braak (tau) stage Median (IQ range)	1.00 (1)	1.00 (0)	1.00 (1)
Lewy body (α-syn) score Median (IQ range)	0.00 (0)	2.00 (0)	3.00 (1)

2.4.1. *TFAM* SNP rs2306604 (A>G) association with PDD

Figure 2.1 shows examples of results obtained from *TFAM* SNP rs2306604 genotyping of BA9 samples, using the two methods outlined in section 2.3.5.

TFAM SNP rs2306604 genotype and allele frequencies in the different diagnostic groups, obtained using these methods, are summarised in Table 6.

Genotype frequencies were not different in control and DLB groups ($\chi 2 = 1.273$, p value = 0.5292), and similarly to the control group most samples were heterozygotes (A/G) (41.7%) compared to the A/A and G/G (33.3 and 25.0 % respectively) in the DLB group. Similarly, genotype frequencies were not significantly different in the PD group compared to controls ($\chi 2 = 4.882$, p value = 0.0871). However, the PD cohort did present a majority of cases in the A/A genotype (46.2%). This distribution was, however, not statistically different from the control cohort. In the PDD group, genotype frequency was significantly different from the control group ($\chi 2 = 9.080$, p value = 0.0107). 47.9% of the samples were of A/A genotype, suggesting that *TFAM* SNP rs2306604 (A>G) is associated with PDD in our cohort study. Combining the PD and PDD groups together in one set further strengthens the statistical significance of the genotype association compared to the control group. In fact, the genotype frequency is now significantly different from the control group with a p value of 0.0052 and a χ^2 value of 10.53. Genotype frequency distribution in the different diagnosis groups is represented graphically in Figure 2.2A.

Combining the AG and GG genotypes together, allowed for the analysis of the frequency of the AA allele compared to AG/GG. This, again, revealed no significant difference in the frequency of the AA allele in DLB compared to control population (p = 0.4290, OR = 1.308). The frequency of the AA allele was now significantly different in both the PD group (p = 0.0334, OR = 2.242) and in the PDD group (p= 0.0040, OR = 2.409) compared to controls.

Grouping the PD and PDD groups in one set, again, further strengthened the statistical difference in frequency of the AA allele compared to the control group (p = 0.0016, OR = 2.349). AA vs. AG/GG frequency distribution in the different diagnosis groups is represented graphically in Figure 2.2B.

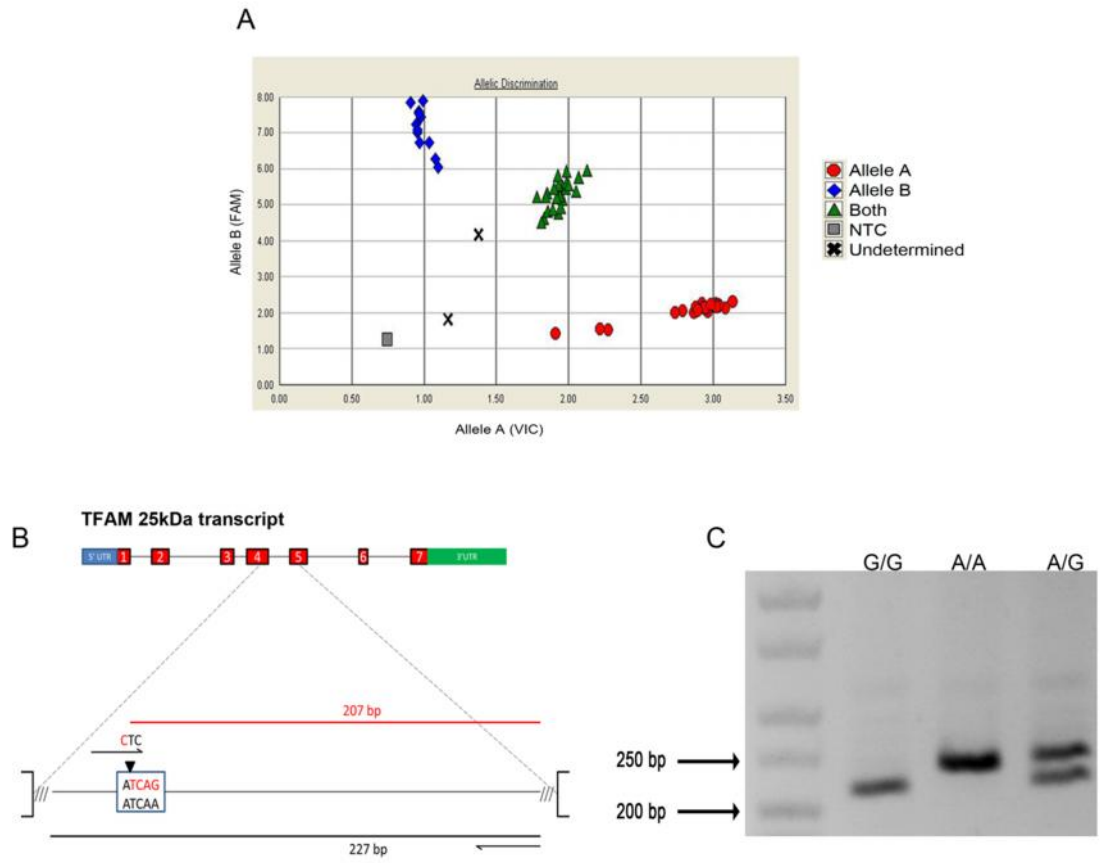

Figure 2.1 Genotyping of BA9 Control, PD, DLB and PDD samples
(A) Taqman SNP genotyping assay showing an increase in VIC-dye fluorescence indicating homozygosity for allele A (X-axis, red), an increase in FAM-dye fluorescence indicating homozygosity for allele B (Y-axis, blue), whilst an increase in fluorescence of both dyes indicates A/G heterozygosity (green). The two black crosses indicate cases whose genotype was undetermined by the assay, whilst the grey square indicates baseline fluorescence from the no template control (NTC). (B) *TFAM* 25kDa transcript with a zoomed-in insert outlining the position of the primers used and the *DdeI* restriction site. A 207 bp fragment is amplified (red) when G allele is present and fragment is subsequently cut by *DdeI.* A 227 bp fragment (black) is amplified when A allele is present. (C) PD cases were genotyped via PCR followed by restriction enzyme digestion with *DdeI*. Homozygous A/A cases gave a band at approximately 227 bp, whilst homozygous G/G cases gave a band at approximately 207 bp. Both bands were observed when cases were heterozygous.

Table 6 TFAM SNP rs2306604 (A>G) genotype distribution and allele frequency in Control, DLB, PD and PDD

	Control	**DLB**	**PD**	**PDD**	**PDD/PD**
	n=141	**n=72**	**n=39**	**n=73**	**n=112**
AA (%)	39 (27.7)	24 (33.3)	18 (46.2)	35 (47.9)	53 (47.3)
AG (%)	70 (49.6)	30 (41.7)	15 (38.5)	24 (32.9)	39 (34.8)
GG (%)	32 (22.7)	18 (25.0)	6 (15.4)	14 (19.2)	20 (17.9)
χ^2, d.f.		1.273, 2	4.882, 2	9.080, 2	10.53, 2
p-Value		0.5292	0.0871	0.0107	0.0052
	Control	**DLB**	**PD**	**PDD**	**PDD/PD**
AA	39 (27.7)	24 (33.3)	18 (46.2)	35 (47.9)	53 (47.3)
AG/GG	102 (72.3)	48 (66.6)	21 (53.8)	38 (52.0)	59 (52.7)
p-Value		0.4290	0.0334	0.0040	0.0016
Odds ratio		1.308	2.242	2.409	2.349
CI		0.708 to 2.415	1.080 to 4.651	1.336 to 4.342	1.392 to 3.965

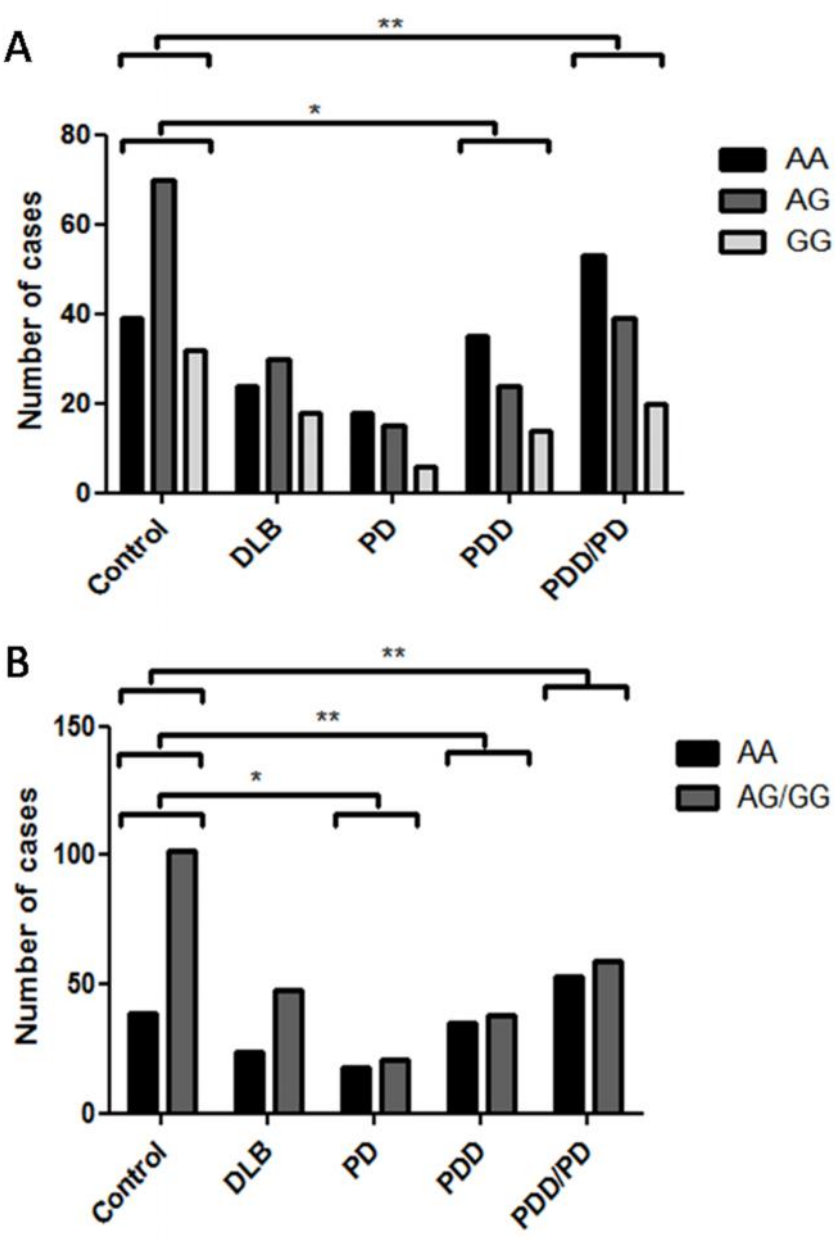

Figure 2.2 *TFAM* SNP rs2306604 A>G genotype distribution and allele frequency in control, DLB, PD and PDD

(A) *TFAM* SNP rs2306604 A>G genotype distribution is significantly different in PDD cases compared to control cases (χ^2= 9.080, p = 0.0107). When PDD and PD cases are grouped together, the genotype distribution is also significantly different compared to controls (χ^2= 10.53, p = 0.0052). (B) The AA allele compared to AG/GG cases grouped together is significantly more frequent in PD (p = 0.0334, OR = 2.242) and in PDD (p = 0.0040, OR = 2.409) cases compared to controls. PDD and PD cases grouped together also display a significant distribution of the AA allele compared to AG/GG (p = 0.0016, OR = 2.349). *=p≤0.05, **=p≤0.01.

2.4.2. *TFAM* SNP rs2306604 (A>G) is associated with males and not females

Since the presence of *TFAM* SNP rs2306604 A>G was strongly associated with PDD compared to controls, its association was also investigated in males and females separately. Cases were stratified according to gender and this revealed a strong association of the *TFAM* SNP rs2306604 A>G genotype in PDD males compared to control males, with 57.9% of the cases being homozygous for the A allele, compared to only 16.1% of the controls (χ^2 = 17.92, p value = 0.0001). Genotype frequencies were not different in control and DLB males (χ^2 = 2.821, p value = 0.2440), and as in the control group most samples were heterozygotes (A/G) (47.2%) compared to the A/A and G/G homozygotes (30.6% and 22.2% respectively). Genotype frequency in PD males was also significantly different from controls (χ^2 = 5.906, p value = 0.0522), although not as strongly as for PDD males. Grouping the PD and PDD groups into one set also gave a significantly different distribution in genotype compared to controls (χ^2 = 15.95, p value = 0.0003) (Table 7).

Investigating differences in allele frequency by comparing A/A homozygotes to A/G and G/G pooled together, again, revealed no significant difference in the frequency of the AA allele in DLB compared to control males (p = 0.1236, OR = 2.298). Allele frequencies in PD males were again significantly differentially distributed compared to controls (p = 0.0252, OR = 3.481), but this association was still weaker than that observed in PDD males. Indeed, A allele frequency in PDD males was strongly significantly different from that in controls (p = < 0.0001, OR = 7.181). Pooling PD and PDD males together into one set also revealed a strong association of the A allele frequency in this set compared to control males (p = <0.0001, OR = 5.391) (Table 7).

Contrastingly, no significantly different genotype distribution was observed in females from DLB, PD or PDD groups compared to controls (Table 8). This suggests that the presence of *TFAM* rs2306604 A allele might be a risk factor for PD and PDD in males but not in females.

TFAM SNP rs2306604 A>G frequency distribution in the different diagnosis groups, when stratified according to gender, is represented graphically in Figure 2.3.

Table 7 TFAM SNP rs2306604 A>G genotype distribution in Control, DLB, PD and PDD males.

	Control	**DLB**	**PD**	**PDD**	**PD/PDD**
	n=56	**n=36**	**n=25**	**n=38**	**n=63**
AA (%)	9 (16.1)	11 (30.6)	10 (40.0)	22 (57.9)	32 (50.8)
AG (%)	30 (53.6)	17 (47.2)	11 (44.0)	10 (26.3)	21 (33.3)
GG (%)	17 (30.4)	8 (22.2)	4 (16.0)	6 (15.8)	10 (15.9)
χ^2, d.f.		2.821, 2	5.906, 2	17.92, 2	15.95, 2
p-Value		0.2440	0.0522	0.0001	0.0003
	Control	**DLB**	**PD**	**PDD**	**PD/PDD**
AA (%)	9 (16.1)	11 (30.6)	10 (40.0)	22 (57.9)	32 (50.8)
AG/GG (%)	47 (83.9)	25 (69.4)	15 (60.0)	16 (42.10	31 (49.2)
p-Value		0.1236	0.0252	< 0.0001	< 0.0001
Odds ratio		2.298	3.481	7.181	5.391
CI		0.840 to 6.283	1.192 to 10.170	2.746 to 18.770	2.264 to 12.840

Table 8 *TFAM* SNP rs2306604 A>G genotype distribution in Control, DLB, PD and PDD females.

	Control	**DLB**	**PD**	**PDD**	**PD/PDD**
	n=85	**n=36**	**n=14**	**n=35**	**n=49**
AA (%)	30 (35.3)	13 (36.1)	8 (57.1)	13 (37.1)	21 (42.9)
AG (%)	40 (47.1)	13 (36.1)	4 (28.6)	14 (40.0)	18 (36.7)
GG (%)	15 (17.6)	10 (27.8)	2 (14.3)	8 (22.9)	10 (20.4)
χ^2, d.f.		1.953, 2	2.498, 2	0.6493, 2	1.360, 2
p-Value		0.3766	0.2867	0.7228	0.5067
	Control	**DLB**	**PD**	**PDD**	**PD/PDD**
AA (%)	30 (35.3)	13 (36.1)	8 (57.1)	13 (37.1)	21 (42.9)
AG/GG (%)	55 (64.7)	23 (63.9)	6 (42.9)	22 (62.9)	28 (57.1)
p-Value		1.0000	0.1441	0.8376	0.4607
Odds ratio		1.036	2.444	1.083	1.375
CI		0.460 to 2.336	0.775 to 7.708	0.478 to 2.454	0.669 to 2.825

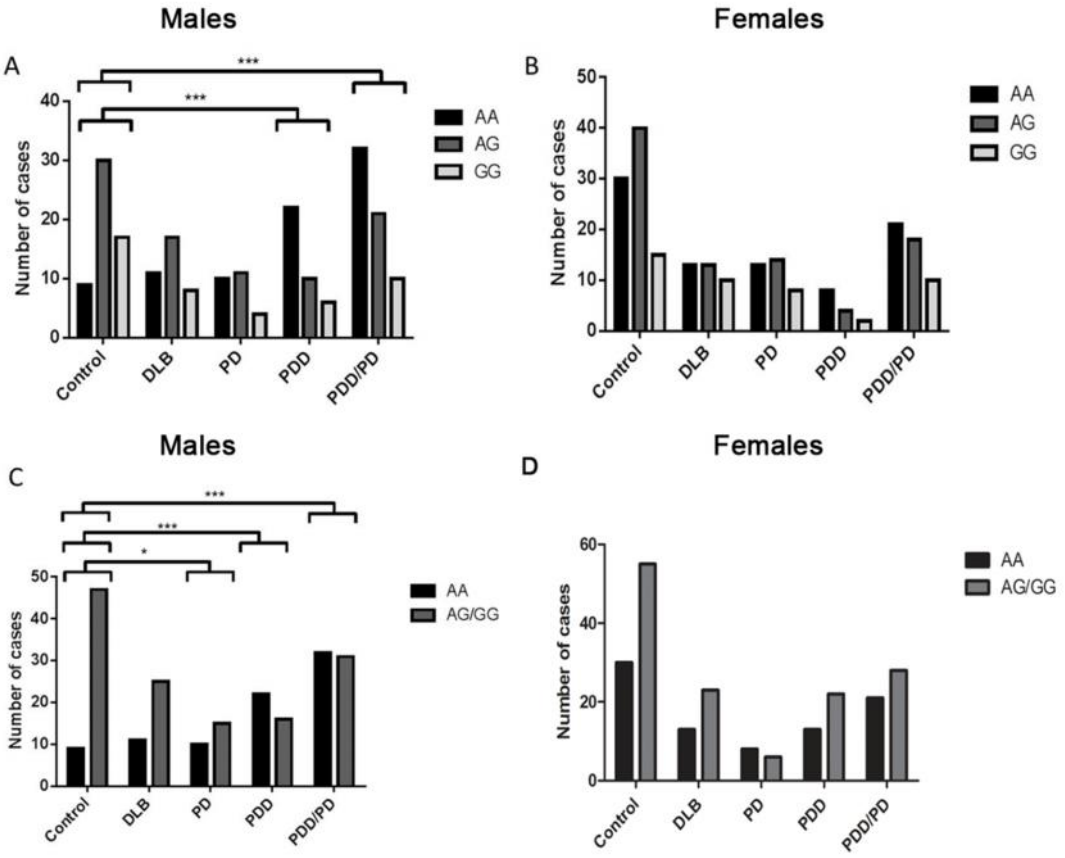

Figure 2.3 *TFAM* SNP rs2306604 A>G distribution in male and female Control, DLB, PD and PDD samples.

(A) *TFAM* SNP rs2306604 (A>G) genotype distribution is significantly different in PDD males compared to control males (χ^2= 17.92, p=0.0001). When PDD and PD cases are grouped together, the genotype distribution is also significantly different compared to controls (χ^2= 15.95, p = 0.0003). (B) *TFAM* SNP rs2306604 (A>G) genotype distribution is not significantly different in PDD females compared to control females. (C) The AA allele compared to AG/GG cases grouped together is significantly more frequent in PD (p = 0.0252, OR = 3.481) and in PDD (p = <0.0001, OR = 7.181) males compared to control males. PDD and PD cases grouped together also display a significant distribution of the AA allele compared to AG/GG (p = < 0.0001, OR = 5.391). (D) The distribution of the AA allele compared to AG/GG cases grouped together is not significantly different in females of the different diagnostic groups. *= p ≤0.05, **= p ≤0.01, ***= p ≤0.001.

2.5. Discussion

This chapter presents results from the first study investigating a genetic variant that might potentially distinguish between PDD and DLB. *TFAM* SNP rs2306604 A>G was found to confer a risk factor for PDD but not for DLB, suggesting that whilst the two forms of dementia are indeed very similar in their symptomatic, neuropsychological and neuropathological profiles, there might be different genetic factors that distinguish the two (Gatt et al., 2013). Furthermore, the *TFAM* rs2306604 A/A genotype is significantly more frequent in the PDD cohort of samples than in a non-demented PD cohort and that this association is significantly stronger in males than in females.

2.5.1. Gender bias in AD and PD

TFAM SNP rs2306604 A>G has been shown to be associated with AD in multiple studies, with the A allele identified as a risk factor for the disease, however the functional consequences of this intronic variant remain unknown. Gender bias in association with this SNP in AD has also been investigated, and whilst results reveal no significant association of rs2306604 frequency with gender, the *TFAM* SNP rs1937 G>C was found to be significantly more present in females compared to males (Günther et al., 2004; Belin et al., 2007; Bertram et al., 2007; Laumet et al., 2010). Overall, Günther et al., reported that the frequency of the haplotype G_{rs1937}-$A_{rs2306604}$ was significantly higher in AD females than AD males (Günther et al., 2004). Similarly, the APOE ε4 allele confers greater risk for AD in females than in males (Günther et al., 2004). There are no known reasons for this gender bias in APOE genotype in AD, and it is unclear whether TFAM haplotype G_{rs1937}-$A_{rs2306604}$ might be contributing to this gender bias in AD risk. Overall, AD is also known to be more common in women than in men, and again reasons for this gender link are unclear. Some studies have suggested that in women, oestrogen might play a neuroprotective role. Indeed, oestrogen carries antioxidant properties (Mooradian, 1993) and promotes growth

of dendritic spines and synapses (Naftolin et al., 1993), as well as increasing cerebral blood flow (Belfort et al., 1995). Therefore, high levels of oestrogen in women might be delaying the risk of developing AD until after menopause when oestrogen levels have been depleted. Theoretically, this would leave women at a greater risk at these later stages, whilst men at risk of dementia would have possibly suffered earlier death due to hypercholesterolemia, hypertension, or smoking (Andersen et al., 1999).

Contrastingly, PD is thought to be more common in men, with one meta-analysis suggesting that men are at a 1.5 times greater risk of developing the disease than women (Wooten et al., 2004). As in AD, no conclusion has been made as to any biological basis for this gender-associated risk. Some studies suggest that differences in brain circuitry between men and women might be playing a role in disease progression (Inestrosa et al., 1998), whilst other hypotheses include that lifestyle choices made by men make them more at risk of developing PD due to exposure to toxins and increased incidents of head trauma (Tanner and Goldman, 1996). Alternatively, genetic linkage studies suggest that the presence of a PD susceptibility gene on the X chromosome might explain the greater risk of the disease in men (Pankratz et al., 2002). Studies have also suggested that the male gender is more prevalent in PDD and DLB cases (Gillies and McArthur, 2010; Fereshtehnejad et al., 2013). In the cohort used in this study, 59% of PDD cases and 63% of PD total cases were male. In order to better understand whether gender plays a significant role in *TFAM* SNP rs2306604 A>G association, statistical analysis on cases stratified by gender was also carried out.

2.5.2. Gender bias in *TFAM* SNP rs2306604 A>G presence

Gender does not confer any association to the *TFAM* SNP rs2306604 A>G frequency in the DLB cohort, as genotype distribution is similar in males and females in this group. Contrastingly, gender stratification revealed a significant association of *TFAM* SNP

rs2306604 A>G in PDD males compared to females. Indeed, genotype A/A frequency was similar in PDD females compared to control females, suggesting that the SNP might confer a stronger risk for PDD in males than in females.

The biological basis for this gender bias is unknown. The *TFAM* SNP might genetically interact with an environmental risk factor to which men are more exposed to than women. Alternatively, it might be due to an interaction of *TFAM* with a Y-chromosomal gene such as *SRY* or *ZFY*, which have been identified as transcriptional regulators expressed in the hypothalamus, frontal and temporal cortex of the male adult brain (Mayer et al., 1998).

Furthermore, whilst the data show no association of *TFAM* SNP rs2306604 A>G with PD compared to control cases overall, stratification by gender revealed a higher frequency of the A/A genotype in males compared to controls, and this difference was close to approaching statistical significance. Indeed, when grouping A/G and G/G genotypes together, the A allele is significantly more frequent in PD males compared to control males. These data are in contrast with previous studies (Belin et al., 2007) which find no association of *TFAM* SNP rs2306604 A>G with PD, even when stratifying the cases by gender. These different results obtained might be attributed to the difference in cohort size between the different studies. This study utilised only 41 PD samples in this study, which when stratified by gender lead to a total of 26 males and 15 females, compared to a total of 300 PD subjects in the Belin et al., study (Belin et al., 2007). Thus, the caveat of a small sample number might have contributed to a bias in the result and further work is required to conclude whether there truly is an association of *TFAM* SNP rs2306604 A>G with PD.

2.5.3. *TFAM* SNP rs2306604 A>G presence might contribute to cognitive decline in PD

The association of *TFAM* SNP rs2306604 A>G is certainly much stronger in PDD than PD, suggesting that the SNP is associated with an increased risk of cognitive impairment in PD rather than the risk of PD itself.

Recently, a study carried out by Bialecka et al., investigated an association of a polymorphism in brain-derived neurotrophic factor (BDNF), a neurotrophin expressed in the mammalian brain, known to regulate neuronal survival and cognition. The BDNF G196A (Val 66 Met) polymorphism, resulting in a valine to methionine substitution at codon 66, was not significantly associated with PDD and non-demented PD patients compared to controls, however, patients expressing Met/Met alleles did perform better on a verbal learning task than patients with Val/Val alleles (Bialecka et al., 2014). Furthermore, a different group also found that PD patients carrying the BDNF 196A allele gave a better performance at a planning task than carriers of the 196G allele (Foltynie et al., 2009). Additionally, an Italian study carried out in 2009 had found a significant association of the BDNF G196A (Val 66 Met) polymorphism in cognitively impaired PD compared (MMSE >24) to non-demented PD cases (MMSE ≤ 24) (Guerini et al., 2009). The different cognitive measures used might explain the discrepancy in results obtained between the Guerini study and the Bialecka and Foltynie studies. Indeed, the latter two studies utilised more comprehensive neuropsychological assessments for measuring cognition, and therefore the results obtained cannot be directly compared. However, taken together, these data suggest that there might be multiple genetic factors that offer a predisposition to cognitive decline in PD. The data outlined above suggest that *TFAM* SNP rs2306604 A>G might offer such a risk and might contribute to the development of PDD in PD patients.

2.6. Conclusion

This study suggests that *TFAM* SNP rs2306604 A>G is observed in significantly higher prevalence in PDD, especially in males, but is not associated with DLB. This work offers new insight into a potential genetic variation distinguishing PDD from the highly similar form of dementia, DLB.

However, the absence of this association in DLB cases, also suggests that this SNP might play a role in determining the temporal onset of cognitive decline in PD. PDD and DLB are mainly distinguished by the temporal onset of cognitive decline compared to decline in motor ability, with DLB patients presenting symptoms of cognitive decline within the same year in which they present motor symptoms. Therefore, one might speculate that this finding suggests that the presence of *TFAM* SNP rs2306604 A>G might actually be exerting a 'neuroprotective' role in that it is acting to delay the onset of dementia, following onset of motor symptoms.

Cohort numbers in this study are relatively small, especially when groups are stratified by gender or genotype. Furthermore, MMSE data for some PDD and PD patients was unavailable, further limiting correlative analysis. Therefore, conclusions inferred from the results can only be speculative and further research is required to better understand the association of this SNP with different neurodegenerative diseases.

3. **Investigating changes in mitochondrial-associated proteins and mitochondrial DNA levels in Parkinson's disease and Parkinson's disease dementia compared to controls.**

3.1. Introduction

In the previous chapter of this thesis, *TFAM* SNP rs2306604 A>G was found to be associated with PDD. Previous studies have shown that the presence of this SNP also leads to an increased risk for AD. The presence of this SNP was also found to be more predominant in PDD than in PD. Taken together, these results brought us to speculate that the presence of *TFAM* SNP rs2306604 A>G might lead to a greater risk of cognitive decline.

It is known that mitochondrial ETC complex I activity is decreased in the Snpc of PD patients. However, mitochondrial function and activity in the frontal cortex in PD and in PDD are not well investigated. Since changes associated with dementia are commonly associated with frontal cortex function, it is of interest to investigate this brain region in association with cognitive decline in PD leading to PDD.

Studies in post-mortem AD tissue have revealed reduced mitochondrial mass, reduced cellular respiration, reduced expression of nuclear encoded respiratory genes, and reduced expression of mitochondrial biogenesis genes, including *TFAM*, compared to controls (Reddy et al., 2012; Sheng et al., 2012). An increased frequency of deleted mtDNA molecules has also been reported in AD cortical tissue (Lin et al., 2002; Coskun et al., 2004). Similarly, mitochondrial dysfunction is commonly implicated in PD (see section 1.12.2). As mentioned in Chapter 1 (Section 1.7.2), a study in 2007 revealed that *TFAM* knockout in mice DA neurons results in reduced mtDNA expression and respiratory chain dysfunction, concomitantly with the development of intraneuronal inclusions, leading to parkinsonian symptoms in adulthood (Ekstrand et al., 2007). This study therefore reaffirmed the role of mitochondrial dysfunction and respiratory chain disruption in the development of PD phenotypes.

Since cognitive decline in PD, in the form of PDD, exhibits neuropathological and symptomatic features similar to AD, it was of interest to investigate whether mitochondrial

dysfunction in the frontal cortex in PDD occurs as it does in AD. Moreover, it was of interest to determine whether the presence of *TFAM* SNP rs2306604 A>G elicits any changes in *TFAM* expression levels. Previous studies have also reported that the presence of this SNP might affect splicing of the *TFAM* transcript (Tominaga et al., 1993; Poulton et al., 1994). I was therefore interested in determining whether alternative TFAM spliceforms are observed in this cohort and whether the presence of the SNP causes any functional changes in terms of mtDNA levels and mitochondrial protein level in PDD compared to PD and controls.

3.2. Chapter aims

Since *TFAM* SNP rs2306604 A>G was found to be associated with PDD but not DLB in chapter 2, I aimed to investigate the functional consequences of the presence of this SNP in such cases. In particular, aims were:

- To investigate whether *TFAM* SNP rs2306604 A>G is associated with differences in mtDNA copy number and altered expression of TFAM and other mitochondrial-associated protein levels.

3.3. Materials and Methods

3.3.1. Tissue homogenate preparation

For each tissue sample, the cortical grey matter was dissected from the white matter and the meninges at 0^{o}C. Approximately 100mg of cortical grey matter was homogenised in 1mL of ice-cold homogenisation buffer using an Ultra-Turrax tissue homogeniser (IKA Werke, Germany). The homogenisation buffer contained 50mM Tris-HCl, 5mM EGTA, 10mM EDTA, (for chelation of magnesium and calcium ions), 'Complete, mini, EDTA-free, Protease inhibitor cocktail tablets' from Roche Applied Science (1 per 10mL, for inhibition of cysteine, serine, and metallo-proteases), and 20µg/mL PMSF, which was added immediately prior to use. The crude homogenates were immediately frozen on dry ice and stored at -80^{o}C for later use.

3.3.2. Protein assay

The total protein concentration in the prepared crude homogenate was determined using the Bradford protein assay method. Standards were prepared using bovine serum albumin (BSA) diluted in homogenisation buffer in a series of dilutions, resulting in the following concentrations: 0.5, 0.375, 0.250, 0.188, 0.125, 0.063, 0.031 and 0.0007 mg/mL. Each homogenate sample was also diluted in a series of 1 in 4, 1 in 8, 1 in 16, 1 in 32, and 1 in 6dilutions in homogenisation buffer. 20µL of each standard or sample dilution were then added to a 96-well plate in triplicate and 250µl of Coomassie reagent (Thermo Scientific, USA) was added. The reaction was allowed to proceed for ten minutes and absorbance was then read at 595nm using a FlexStation 3 (Molecular Devices Ltd, UK). The standard curve and concentration of protein in the samples was analysed using Soft Max Pro Software 4.5.1 (Molecular Devices Ltd, UK).

3.3.3. Semi-quantitative western blotting

Tissue samples for western blotting were prepared as previously described by Kirvell et al. (Kirvell et al., 2006). Briefly, to prepare the crude homogenate for western blotting, 20µl of 5x Laemmli buffer for SDS-PAGE (10% SDS, 20% glycerol, 0.2M Tris-HCl pH 6.8, 0.05% bromophenol blue), was added to 80µl of homogenate diluted in dH_2O, for a final volume of 100µl. All samples were prepared to a final concentration of 1µg/µl. 0.02M dithiothreitol (DTT) was added to reduce protein disulfide bonds, and the samples were then heated to 95^{o}C for 5 minutes. Once cooled, samples were stored at -20^{o}C.

Western blot samples were run on a 10% SDS-polyacrylamide gel at approximately 70 volts (V), for 30 minutes and then 100V for the rest of the run. On each gel 5µl of a pre-stained protein ladder was run (EZ Run, Prestained*Rec* Protein ladder, Fischer) in the first lane. 20µl of a control sample, selected as an inter-blot control, was loaded in the second lane of each gel. 20µl of each case sample, equivalent to 20µg of protein, were loaded in the remaining eight lanes, when running a gel of ten lanes.

Once the samples had run to the bottom of the gel, the proteins were transferred onto nitrocellulose hybond membranes (Amersham) for one hour at 25V. Non-specific binding sites on the membranes were then blocked using a one hour incubation in a solution of 10% non-fat powdered milk in tris-buffered saline with 0.1% Tween20 (TBS-T). The membranes were then incubated with the primary antibody (listed in Table 9) overnight at 4^{o}C in 5% milk in TBS-T. The following day, excess antibody was removed with three 10 minute washes in TBS-T. Fluorescently labelled secondary antibodies (anti-mouse IR dye 700 (Rockland) and anti-rabbit IR dye 800 (LI-COR)) in 5% milk in TBS-T were added for one hour at room temperature and blots were then scanned and analysed using an Odyssey infrared scanner (LI-COR, Version 3.0).

Table 9. Primary antibodies used in western blot (WB) analysis of BA9 homogenates

Antibody	WB dilution	Species	Company/Source	Secondary antibody (all at 1 in 5000 dilution)
Histone H3	1 in 1000	Ms	Abcam ab24834	Ms 700
TFAM	1 in 5000	Rbt	Wiesner Lab	Rbt 800
ATP Synthase (ATP5A)	1 in 5000	Ms	Abcam ab14748	Ms700
β-Actin	1 in 4000	Rbt	Cell Signalling 4967S	Rbt 800
OXPHOS cocktail	1 in 200	Ms	Abcam ab110411	Ms 700
Porin	1 in 2000	Ms	Abcam ab14734	Ms700

Odyssey infrared imaging systems application software version 3.0.25 was used to quantify the intensity of the bands on the blots. Signal intensity of each individual band was measured using the box tool on the Odyssey software (drawn while in 'detailed view' mode). The band intensity was then normalised to the intensity of the corresponding inter-blot control band for each protein. Furthermore, the intensity of each band was normalised to the corresponding band of histone H3 or β-Actin, which served as loading controls.

3.3.4. mtDNA deletion assay

A Long Range PCR dNTPack (Roche) was used to amplify a 10.4kb fragment spanning the major arc of the mitochondrial genome (Bender et al., 2006). 20µl reactions were setup consisting of 4µl 5x reaction buffer (Roche),1µl PCR nucleotide mix, 0.6µl each of forward primer (nt5367-5386; ACCTCAATCACACTACTCCC) and reverse primer (nt129-110; AGATACTGCGACATAGGGTG) (Sigma-Aldrich) at 10µM each, 0.6µl of DMSO, 0.28µl of polymerase, 8.92µl of dH_2O and 4µl of non-sonicated DNA at 10ng/µl. Amplifications were

carried out using a PTC-200 Thermal Cycler using the following conditions; 2 min at 92^{o}C; 10 cycles of (10 sec at 92^{o}C, 15 sec at 58^{o}C and 10 min at 68^{o}C), 20 cycles of (10 sec at 92^{o}C, 15 sec at 58^{o}C, 10 min at 68^{o}C with an additional 20sec per cycle) and a final extension of 7 min at 68^{o}C. Amplified products were then run on a 0.8% agarose gel containing ethidium bromide and visualised using UV light.

3.3.5. Quantitative real-time PCR (qPCR) for measurement of mtDNA / nuclear DNA ratio.

3.3.5.1. Standard curve preparation

A set of mitochondrial-specific, CACTTTCCACACAGACATCA (hMito forward) and TGGTTAGGCTGGTGTTAGGG (hMito reverse) and nuclear-specific; GTTCCTGCTGGGTAGCTCT (hB2M forward) and CCTCCATGATGCTGCTTACA (hB2M reverse) primers, (Malik et al., 2011) were used to amplify mtDNA and nuclear DNA fragments within a control DNA sample, using a GoTaq (Promega) PCR reaction. PCR products of the predicted band size were then cut out using sterile scalpel blades under UV light. Once the pieces were weighed, DNA was isolated and purified using the 'Qiaquick' spin column gel extraction kit (Qiagen). A NanoDrop spectrophotometer was again used to calculate DNA concentration in ng/µl. A stock solution of 1x10^{9} copies of DNA per 2µl was prepared and a set of six dilutions were then prepared to set up solutions of concentration 10^{7} to 10^{2} copies.

3.3.5.2. Sample preparation

DNA samples from the individual cases were diluted to 10ng/µl in a 50µl volume, and sonicated for 10 minutes in a bath sonicator, as suggested in (Malik et al., 2011). Ultimately, samples were diluted further to a concentration of 5ng/µl in water containing tRNA (10µg/ml) in a total volume of 50µl.

3.3.5.3. qPCR reaction and analysis

Real-time qPCR was carried out using a Sybrgreen reaction mix (qPCRSygreen mix Lo-ROX, PCR Biosystems) in a LightCycler 480 Real-time PCR system (Roche). A 10µl total reaction mixture containing 5µl qPCR Bio Sybrgreen master mix,0.4µl each of reverse and forward primers (at 10µM) and 4.2ul of DNA (at 5ng/µl) was prepared for each sample, once using the hMito primers and another using the hB2M primers. Reactions were run along with all standard curve reactions and non-template controls. qPCR conditions used were; 95^{o}C for 10 min followed by 40 cycles of (95^{o}C for 15 sec, 57^{o}C for 15 sec and 72^{o}C for 15 sec) followed by a melting cycle going up to 95^{o}C. The LightCycler 480 Real-time PCR System (Roche) was used to calculate mtDNA and nuclear DNA copy numbers by extrapolating values using the standard curves obtained, using an absolute quantification method. Ratios of mtDNA/ nDNA levels were calculated and transformed to $\log_{10}$ values for statistical analysis.

3.3.6. Statistical analysis

Analysis to compare means in multiple groups was carried out by one-way analysis of variance (ANOVA) followed by Bonferroni's post-hoc multiple comparison test. If data did not fit a normal distribution, a Kruskal-Wallis test followed by Dunn's multiple comparison test was carried out.

A two-way ANOVA followed by Tukey's multiple comparison tests was used to compare mtDNA levels in the different diagnostic groups and assess the influence of *TFAM* SNP rs2306604 A>G on this mean.

A student un-paired t-test was used to compare means between two individual groups. If data did not fit a normal distribution, a non-parametric Mann-Whitney test was carried out.

In all individual analyses, a null hypothesis was postulated which asserted that there is no difference in mitochondrial protein levels, mtDNA levels or neuropathology scores amongst the different diagnostic groups tested. In all cases, a result was considered statistically significant, and the null hypothesis rejected, when p value was lower or equal to 0.05 ($p \leq 0.05$).

3.4. Results

3.4.1. Mitochondrial protein levels are not altered in control, PD and PDD cases and are not associated with *TFAM* rs2306604 A>G genotype.

Since *TFAM* SNP rs2306604 (A>G) was found to be associated with PD and PDD but was not associated with DLB, further analysis was only carried out using controls, PD and PDD cases.

In order to assess whether TFAM protein levels were altered in the different diagnostic groups, BA9 homogenates from control, PD and PDD cases were analysed by western blot (Figure 3.1). In order to investigate any changes in protein levels of respiratory chain components, protein levels of ETC complex I subunit NDUFB8 (nuclear encoded), the complex II 30kDa subunit (nuclear encoded), complex III subunit core 2 (nuclear encoded), complex IV subunit II (mitochondrially encoded), and ATP synthase (complex V) subunit alpha (nuclear encoded) were also quantified. β-actin and histone H3 levels were used as total protein loading controls.

Overall, no difference was observed in the average protein levels in controls compared to PD and PDD samples, suggesting that expression levels are unaltered in the different diagnoses. However, comparing protein levels of the mitochondrial outer membrane channel protein porin (VDAC1) amongst the different diagnostic groups revealed that, on average, expression levels were statistically significantly higher in PD cases (an average of 10.5% increased expression) compared to controls (Kruskal-Wallis test, followed by Dunn's multiple comparisons test, $p = 0.0087$), suggesting that the average expression of VDAC1 is increased in PD (Figure 3.2).

Furthermore, stratification of the diagnostic groups according to genotype also revealed that there is no significant difference in expression levels for the proteins listed above, as one-way ANOVA analysis revealed no association of genotype with protein levels within the individual diagnostic groups (Figure 3.3).

3.4.2. Mitochondrial protein levels are not altered in control, PD and PDD cases and are not associated with *TFAM* rs2306604 A>G genotype in males.

Since *TFAM* SNP rs2306604 A>G was found to be more prevalent in PDD and PD males compared to females, we also investigated whether a difference in protein levels would be found in control, PD and PDD males and whether any difference would be associated with the *TFAM* genotype in this gender group only.

This data shows that in males only, there is no difference in β-actin, TFAM and OXPHOS complex protein levels between controls, PD and PDD samples. Stratification of values by gender and *TFAM* SNP rs2306604 A>G genotype, did reduce the numbers in the individual data sets considerably, especially since G/G cases in the individual diagnostic groups were very rare. Therefore, stratifying the values by diagnosis, gender and *TFAM* genotype would have not allowed a reliable statistical analysis. In order to overcome this limitation, association of protein levels to genotype in males was tested by grouping the A/A, A/G and G/G samples together, independent of diagnosis (Figure 3.4). This revealed that overall, there was no difference in protein levels amongst A/A, A/G and G/G males in our whole cohort.

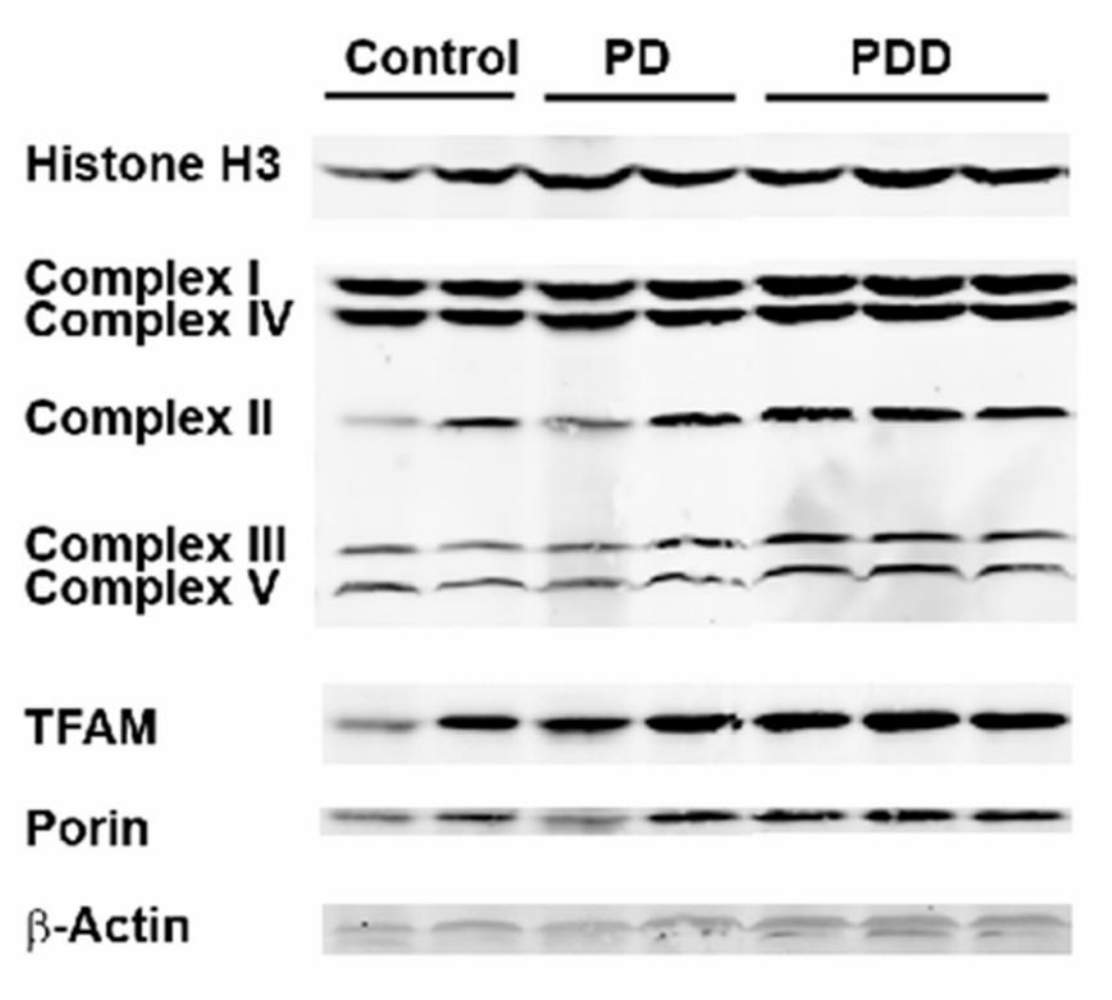

Figure 3.1 Representative western blot of control, PD and PDD BA9 homogenate samples
A representative western blot showing bands obtained using antibodies for histone H3 (used as loading control), subunits of Complex I, II, III, IV and V, TFAM, porin and β-actin.

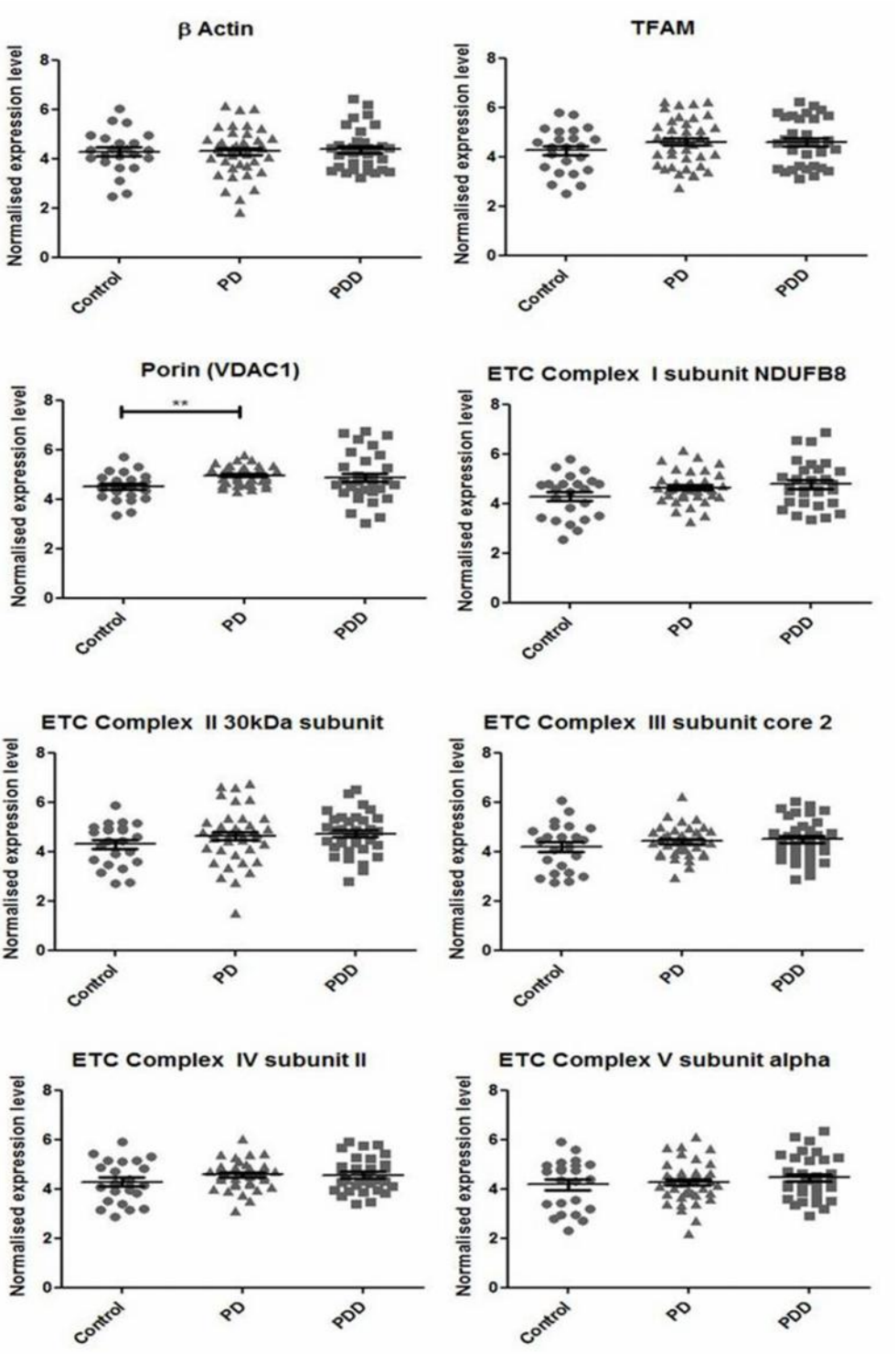

Figure 3.2 Protein levels in control, PD and PDD frontal cortex homogenates.
β actin, TFAM and ETC complex I-V subunit protein levels are unchanged in control (n=23), PD (n=40) and PDD (n=33) frontal cortex homogenates, according to one-way ANOVA analysis. Porin (VDAC1) expression levels are significantly increased in PD samples compared to controls. All values are normalised to levels of histone H3 and to an inter-blot control. Lines on the scatter plots represent mean with SEM. **= p≤0.01

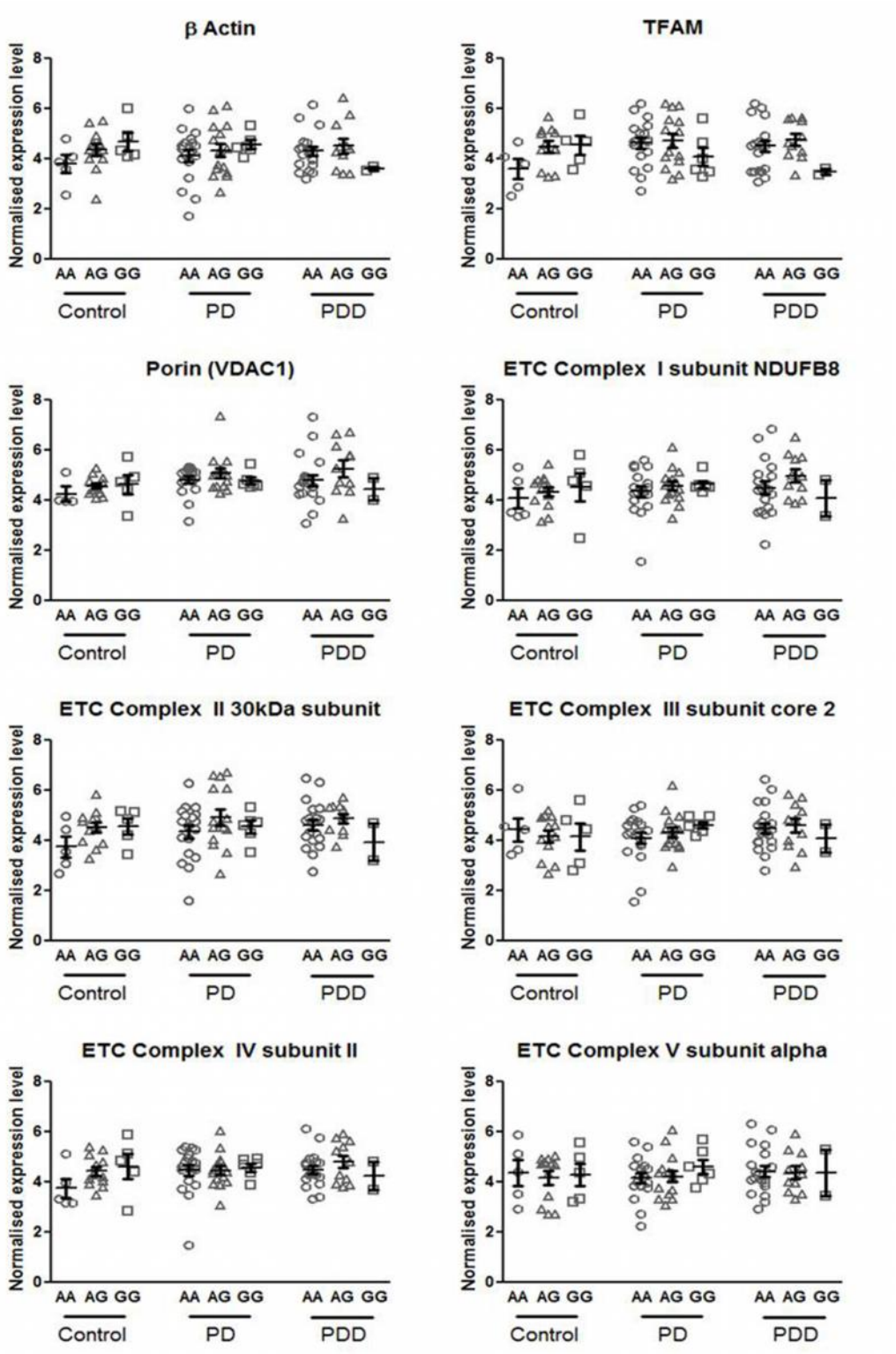

Figure 3.3 Protein levels in control, PD and PDD frontal cortex homogenates according to TFAM SNP rs2306604 A>G genotype.

No difference in expression levels of β-actin, TFAM, porin (VDAC1) and ETC complex I-V subunit proteins is observed when diagnostic groups are stratified according to *TFAM* SNP rs2306604 A>G genotype. There is no statistical difference between control AA (n= 5), AG (n=12), GG (n=5), and PD AA (n=18), AG (n=15), GG (n=6), and PDD AA (n=19), AG (n=11), GG (n=2) samples by one-way ANOVA analysis. Lines on the scatter plots represent mean with SEM.

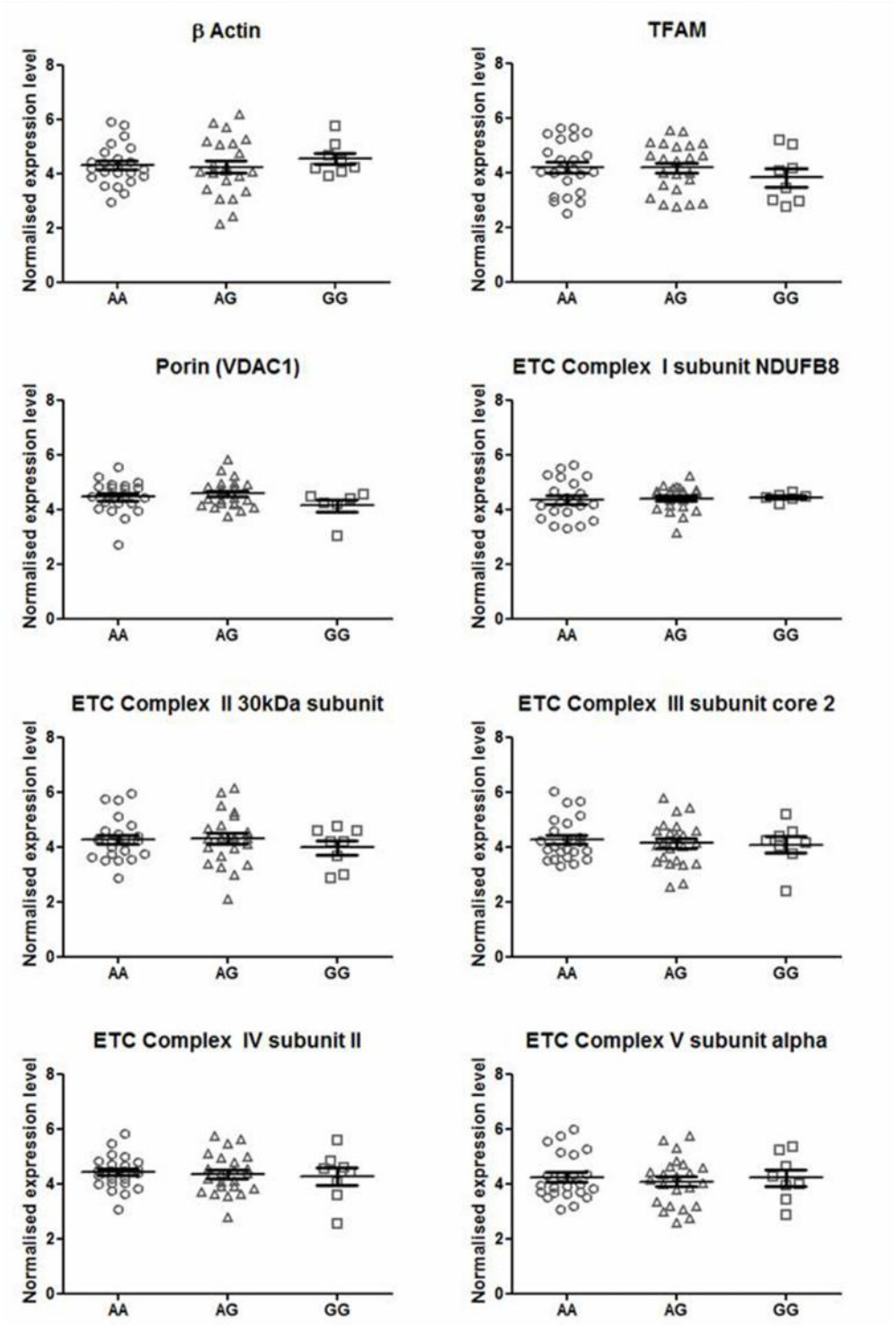

Figure 3.4 Protein levels in frontal cortex homogenates according to TFAM SNP rs2306604 A>G genotype in males.

No difference in expression levels of β-actin, TFAM, porin (VDAC1) and ETC complex I-V subunit proteins is observed between frontal cortex homogenate samples of *TFAM* SNP rs2306604 A>G genotype AA (n=23), AG (n=23) or GG (n=8) in males, by one-way ANOVA analysis. Values are not divided by diagnostic group due to small n numbers. Lines on the scatter plots represent mean with SEM.

3.4.3. *TFAM* rs2306604 A>G SNP is not associated with an alternative splice form.

Studies have suggested that the presence of the intronic SNP rs2306604 in the *TFAM* transcript might lead to the generation of an alternative splice form which produces a truncated form of the protein.

Western blot analysis of control, PD and PDD samples did not reveal the presence of any truncated forms of the TFAM protein and only bands corresponding to the 24 kDa mature form of the protein were observed (Figure 3.5).

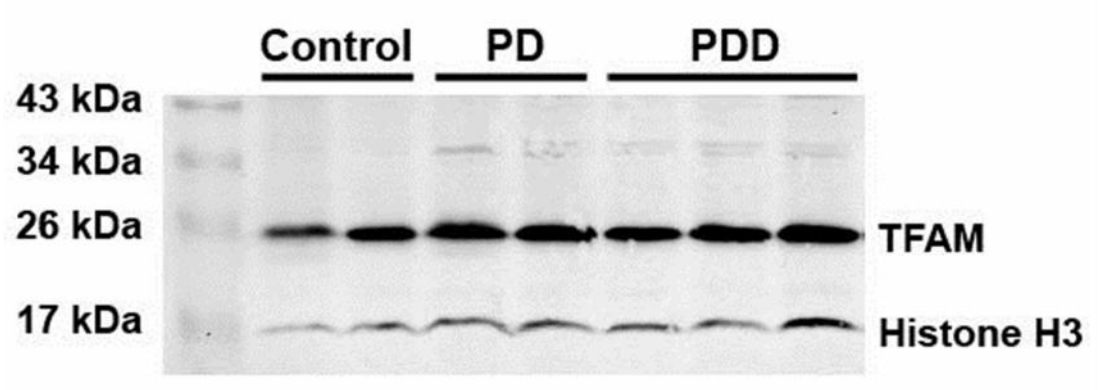

Figure 3.5 No alternative splice isoform of TFAM is observed in control, PD and PDD BA9 homogenates by western blot analysis.
A representative western blot shown that only TFAM bands corresponding to the mature 24 kDa form of the protein were observed in control, PD and PDD BA9 brain homogenates. No alternative smaller splice form of the protein was observed.

3.4.4. mtDNA levels are reduced in PDD

In order to investigate whether mtDNA levels differ in the different diagnostic groups, and whether any correlation with the genotype presence is found, mtDNA copy number as a ratio of nuclear DNA copy number was measured in control, PD and PDD BA9 samples.

A non-parametric one – way ANOVA (Kruskal-Wallis) analysis revealed that median mtDNA levels were significantly reduced in PDD cases ($p = 0.0304$) with an average reduction of 18%. MtDNA levels were not reduced in PD cases compared to controls. When grouped according to *TFAM* rs2306604 A>G genotype, a two-way ANOVA revealed a non-significant interaction p value and no overall significant difference in mtDNA levels between the different genotypes in the diagnostic groups. However, Bonferroni post-hoc tests did reveal a significant difference in mtDNA levels between PD AG and PDD AG heterozygotes, with the mtDNA levels being reduced in the PDD cases (Figure 3.6).

Since a significant association with *TFAM* rs2306604 A>G genotype was observed in PDD and PD males, mtDNA levels in the different genotypes in the diagnostic groups was also investigated exclusively in male cases. This revealed no difference between the diagnostic groups upon performing a Kruskal-Wallis test ($p = 0.0629$), however a Mann-Whitney test revealed a significant reduction in mtDNA levels in PDD male cases compared to controls ($p = 0.0391$). A two-way ANOVA analysis revealed a non-significant interaction p value, and no significant difference in mtDNA levels according to *TFAM* rs2306604 A>G genotype (Figure 3.7). mtDNA levels in females did not change in the different diagnostic groups and no association with *TFAM* SNP rs2306604 A>G was revealed (Figure 3.7).

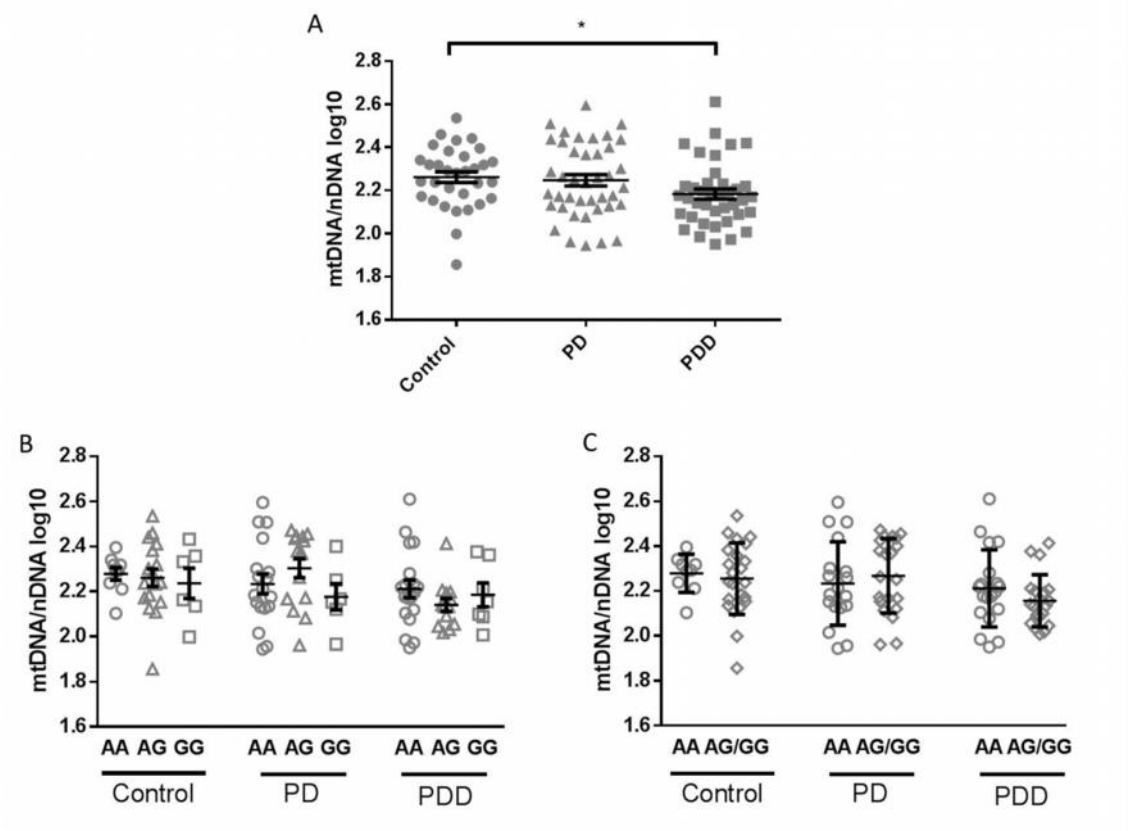

Figure 3.6 mtDNA/nDNA levels are significantly reduced in PDD cases.

(A) mtDNA/nDNA levels are significantly reduced in PDD cases, but not in PD cases, compared to control ($p = 0.0304$, Kruskal-Wallis test followed by Dunn's multiple comparisons test). (B) mtDNA/nDNA levels are not significantly changed according to *TFAM* rs2306604 A>G genotype in the different diagnostic groups (Two-way ANOVA followed by Tukey's multiple comparisons test). (C) mtDNA/nDNA levels are not significantly changed according to *TFAM* rs2306604 A>G genotype in the different diagnostic groups, when grouping AG and GG together compared to AA (Two-way ANOVA followed by Tukey's multiple comparisons test). Lines on the scatter plots represent mean with SEM. *= $p \leq 0.05$.

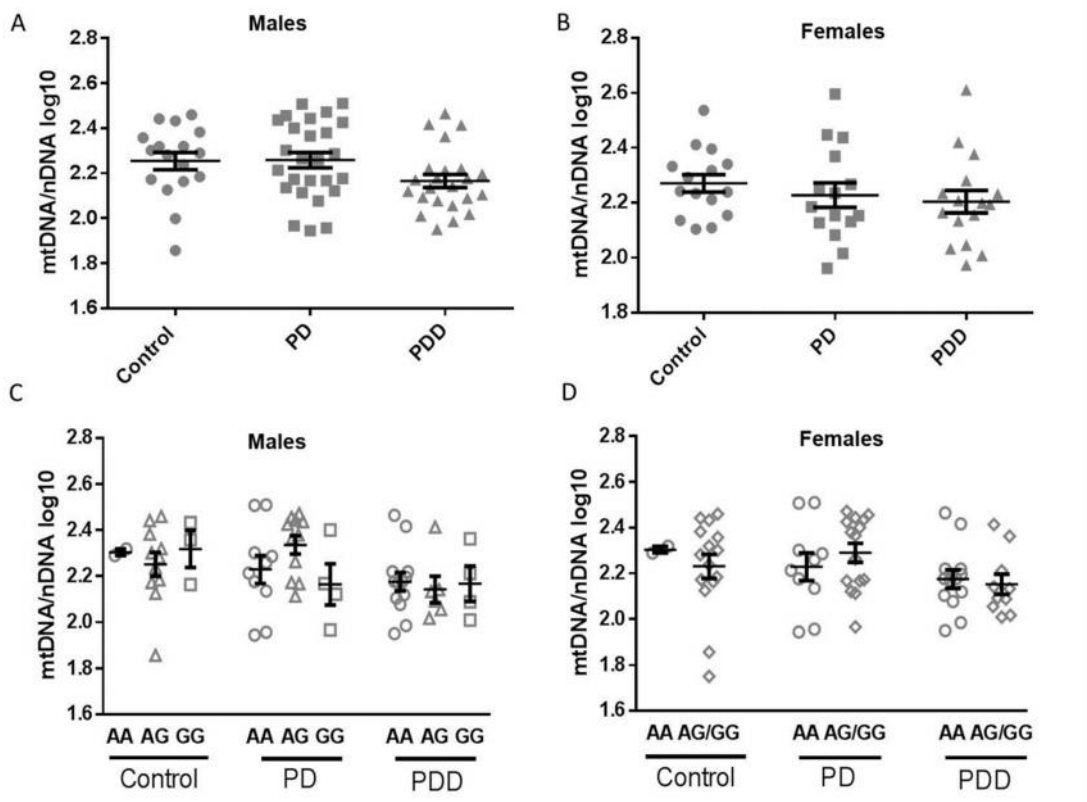

Figure 3.7 mtDNA/nDNA levels in male and female Control, PD and PDD samples.
(A) mtDNA/nDNA levels are not significantly changed in Control, PD and PDD males (p = 0.0629, Kruskal-Wallis test followed by Dunn's multiple comparisons test). A non-parametric t-test reveals that mtDNA/nDNA levels are reduced in PDD male cases compared to controls (p = 0.0391, Mann-Whitney test). (B) mtDNA/nDNA levels are not significantly changed in female Control, PD and PDD cases (One-way ANOVA followed by Dunn's multiple comparisons test, p=0.4897). A non-parametric t-test reveals that mtDNA/nDNA levels are not changed in PDD female cases compared to controls (p = 0.1284, Mann-Whitney test). (C) mtDNA/nDNA levels are not significantly changed according to *TFAM* rs2306604 A>G genotype in the different diagnostic groups in males (Two-way ANOVA followed by Tukey's multiple comparisons test). (D) mtDNA/nDNA levels are not significantly changed according to *TFAM* rs2306604 A>G genotype in the different diagnostic groups in females, when grouping AG and GG together compared to AA (two-way ANOVA followed by Tukey's multiple comparisons test). Lines on the scatter plots represent mean with SEM.

3.4.5. mtDNA deletions are not observed in control, PD and PDD samples.

As described in Section 1.8, mtDNA mutations, including deletions in the genome, are commonly found in neurodegenerative diseases (Kraytsberg et al., 2006; Krishnan et al., 2007; Krishnan et al., 2008; Nicholas et al., 2009). In order to assess whether mtDNA deletions are present in any of the PD, PDD and aged control cases used in this study, a 10.4 kb fragment of mtDNA was amplified, thereby allowing for the observation of all possible deletions within the major arc of the mitochondrial genome.

Figure 3.8 shows a representative image of a gel, in which one strong intensity band is observed for each sample, at the full length PCR product length of approximately 10 kb. Additional low intensity bands can also be observed at shorter lengths in some cases (Figure 3.8), however, as previously observed in literature, such 'background' bands could represent deletions that are generated by the polymerase enzyme during the PCR reaction (Khrapko et al., 1999).

The study by Khrapko et al., which measured the amount of mtDNA deletions in myocytes, also compared mtDNA deletion analysis in tissue homogenates compared to single cells. The authors suggest that in a homogenate, the number of cells containing a substantial amount of mtDNA deletions will be few in comparison to the cells containing wild-type mtDNA. Therefore any deletions will only be represented on the gels as low intensity bands, and would be hard to distinguish from the 'background' bands explained above.

Therefore, it is hard to conclude whether any mtDNA deletions were truly present in these homogenate samples, and analysis at the single—cell level would be required to fully confirm or deny the presence of any mtDNA deletions.

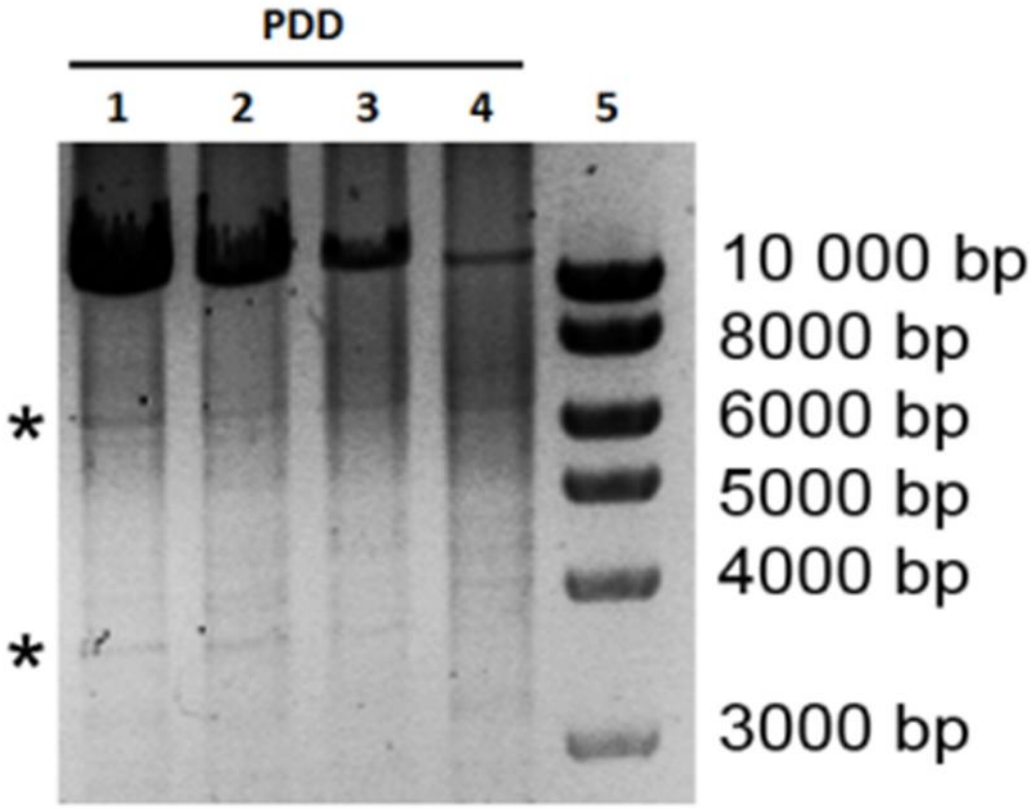

Figure 3.8 No mtDNA deletions are observed in control, PD and PDD BA9 homogenate samples
A representative 0.8% agarose gel showing bands obtained from DNA extracted from individual PDD BA9 homogenates using a long-template PCR (lanes 1-4). This gel revealed only one major PCR product for each sample corresponding to the full-length mtDNA major arc (approximately 10kb), as suggested by the ladder shown in lane 5, implying the absence of any deleted mtDNA. Multiple low intensity bands do appear in some cases (shown in *), however these are likely to correspond to deletions being generated during the PCR reaction.

3.5. Discussion

Chapter 2 concluded that the genetic variant *TFAM* SNP rs2306604 A>G confers a risk factor for PDD, especially in males. In this chapter I investigated whether the presence of this SNP leads to functional consequences in terms of mitochondrial-associated protein levels and mtDNA copy number. I find that mtDNA levels are significantly reduced in PDD compared to control BA9 tissue. However, mitochondrial-associated protein levels were unchanged in PDD and PD compared to controls.

3.5.1. TFAM and OXPHOS complex protein levels are unchanged in PD and PDD samples compared to controls and are not associated with *TFAM* SNP rs2306604 A>G genotype

In order to investigate whether *TFAM* SNP rs2306604 A>G is altering expression levels of TFAM and other OXPHOS complex proteins, I carried out a western blot analysis on brain homogenates of control, PD and PDD BA9 samples. Whilst western blot analysis can only be semi-quantitative and there are a lot of factors within a western blot protocol that lead to variable results, I argue that a high enough 'n' number of samples run, such as ones used in this study, allows for a reliable statistical analysis in which one can test for normal distribution and undergo suitable statistical tests to check for difference in expression between the different diagnostic groups. The data presented in this chapter showed no difference in protein levels of β-actin, TFAM and subunits of OXPHOS complexes I – V between control, PD and PDD BA9 samples. However, a significant increase in porin (VDAC1) protein levels was observed in PD cases compared to controls.

Recently an increase in VDAC1 protein levels has been reported in AD post-mortem brains (Reddy, 2013), with the authors suggesting that increased VDAC1 levels might be implicated in the progression of AD. The same authors determined that VDAC1 interacts

with Aβ and phosphorylated tau, leading to reduced transport between the mitochondria and the external environment in the cell. I therefore postulate that an increase in VDAC1 levels in PD might offer some interesting insight into the role of porins in neurodegeneration, and that whilst VDAC1 levels were not significantly increased in PDD cases compared to controls, further work is required to fully elucidate whether there is an association of VDAC1 with PD disease progression as is postulated to be in AD. Importantly, any alteration in protein levels was not significantly associated to *TFAM* SNP rs2306604 A>G, as one-way ANOVA analysis in the individual diagnostic groups revealed no significant difference in protein levels between A/A, A/G or G/G carriers.

The use of whole brain BA9 homogenates imposes a limit of detection in this study. IHC on the individual case samples could potentially serve to expose any difference in expression levels of the individual proteins in different cell types.

3.5.2. mtDNA levels are reduced in PDD but are not associated with *TFAM* SNP rs2306604 A>G genotype

Increased oxidative damage in nuclear and mitochondrial DNA has been associated with AD, PD (Sanders et al., 2014) and MCI (Wang et al., 2006), and elevated levels of mtDNA mutations have been attributed to cognitive decline (Inczedy-Farkas et al., 2014). Furthermore, frontal cortex mtDNA levels have been shown to be depleted in AD (Rodriguez-Santiago et al., 2001) and a reduction of mitobiogenesis genes in the frontal cortex in PD has also been reported (Thomas et al., 2012). The data presented in section 3.4.4 reveal no alteration in mtDNA copy number in the frontal cortex of PD cases compared to controls. However, a significant reduction in mtDNA levels in PDD compared to control is observed. Additionally, mtDNA levels appeared to be more reduced in PDD males than in PDD females. However, this reduction in mtDNA levels was not attributable to an association with *TFAM* SNP rs2306604 genotype, and was therefore only due to

diagnosis. Moreover, no alteration in protein levels of TFAM, or mitochondrial encoded ETC components (COXII), were observed by western blot analysis in PDD or PD cases compared to controls. It has been reported that a 60-90% reduction in mtDNA levels is required for a threshold level to be exceeded, and therefore for biochemical defects to become apparent (Tuppen et al., 2010). Therefore, it is probable that the average 18% reduction in mtDNA levels observed in the PDD cases compared to controls was not sufficient to induce significant loss of mitochondrial proteins. However, since a significant reduction was only observed in PDD and not in PD, the decline in mtDNA copy number might be related to a decline in cognitive impairment. This suggests that an elevation of AD-related pathology in the brain, as observed in PDD, might be the link to a reduced mtDNA level.

It is important to note that while a decrease in mtDNA levels was observed in the pre-frontal cortex of PDD cases, no analysis was carried out on other brain regions. It would therefore be imperative to compare mtDNA levels in other brain regions in both PD and PDD samples, to investigate whether alterations in mtDNA levels in additional brain areas might be contributing to cognitive decline in PD.

Since mtDNA damage in the SNpc has also been observed in PD, including an increase of mtDNA deletions, we investigated whether we would observe increased mtDNA deletions in the frontal cortex of PD and PDD patients. Amplification of a major arc of the mitochondrial genome by long-template PCR revealed that all PCR products contained a majority of the wild-type full length (10 kb) amplicons, without any obvious abundant deletions giving rise to smaller PCR products. As argued in Section 3.4.5, this might be due to the fact that DNA used in the PCR reaction was extracted from brain homogenate, possibly containing cells of widely varying mtDNA mutation levels. In order to determine whether our samples contain mtDNA deletions and whether frequency of such deletions

differs between the diagnostic groups, the samples would have to be analysed at the single cell level, using laser capture microdissection.

3.5.3. No alternative isoform of TFAM is observed in controls, PD and PDD samples by western blot analysis

Western blot analysis also revealed that only the mature 24 kDa form of TFAM was observed in our control, PD and PDD homogenate samples. A 1993 study by Tominaga et al., examining the levels of steady state mRNA of TFAM in cultured HeLa cells, identified the presence of a smaller isoform of the transcript (Tominaga et al., 1993). This isoform, containing a 96 base deletion in exon 5 of the transcript, was present in most tissues and constituted 30% of the total TFAM mRNA. Later studies identified this as an alternative splice variant which generated a 22 kDa isoform (Poulton et al., 1994), 3 kDa smaller than the wild-type 25 kDa polypeptide (Fisher and Clayton, 1988).

Furthemore, *in silico* studies have suggested that *TFAM* SNP rs2306604 (A>G) might generate an alternatively spliced form of the protein for the G-allele (Günther et al., 2004; Belin et al., 2007). However, no alternative isoforms were predicted for the risk A allele. This suggests that the A allele might be conferring an increased risk of neurodegeneration via linkage disequilbrium with other causal variants and that such a disequilbrium could be leading to mtDNA dysfunction, thereby inducing neuronal cell death. We observed no smaller forms of the protein in our samples via western blot analysis; however, we cannot exclude that alternative splice variants might simply not be visible using this technique.

Certainly, it is possible that the splice variant is expressed at levels that are below the threshold required for visibility by western blot analysis. Additionally, the splice isoform might undergo a rapid turnover rendering it difficult to detect at steady state levels.

It is also important to note that as previously mentioned in section 1.7.2, TFAM is known to be phosphorylated, possibly via different kinases, and that this phosphorylation might trigger its degradation by Lon proteases (Lu et al., 2013). No differentially sized forms of TFAM were detected in the samples analysed by western blot analysis, suggesting that the presence of the *TFAM* SNP rs2306604 A>G plays no role in determining phosphorylation state of the protein. However, the lack of observation of different phosphoforms could again be due to the technique utilised, and therefore more in-depth investigation would be required to make a conclusive statement regarding an association of *TFAM* SNP rs2306604 A>G with phosphorylation states.

3.6. Conclusion

The presence of the *TFAM* SNP rs2300604 A>G was not associated with mtDNA copy number, protein levels of TFAM itself or other OXPHOS complex proteins or pathology levels in the brain in PDD, PD or control BA9 cases. Therefore, the functional consequences of this SNP presence remain unknown.

The association of this SNP to PDD, and AD, might be a result of linkage disequilbrium with other gene variants, however, further investigation is required in order to reach such conclusions. Moreover, any biochemical effects resulting from the SNP presence might be limited to a subset of neurons, with the consequence that any functional change is diluted out and becomes undetectable when analysing whole homogenate samples. Therefore, isolation of specific neural subtypes using laser microdissection might circumvent this issue and might lead to the discovery of a functional role of *TFAM* SNP rs2300604 A>G.

4. Developing *Drosophila* models of neuronal mitochondrial dysfunction.

4.1. Introduction

As discussed in detail in Section 1.10, mtDNA mutations and mitochondrial dysfunction have been studied in a variety of animal models, including *Drosophila*. The initial response of the nervous system to mitochondrial dysfunction, however, is not well elucidated. This chapter outlines the generation and use of *Drosophila* models to investigate this initial response to neuronal mitochondrial dysfunction.

The *Drosophila* neuromuscular junction (NMJ) is a widely used model system for investigating synaptic transmission, especially since this mechanism is highly conserved between flies and mammals (Frank et al., 2013). Inducing mitochondrial dysfunction in the motor neuron system of the fly allows us to investigate alterations in the neuron cell bodies, along the axons, as well as at the NMJs, where neurotransmitter release occurs at the synapses. Furthermore, since motor neurons are particularly energy demanding and therefore dependent on mitochondrial activity, and since reduced mitochondrial activity at the synapses is known to lead to neuronal dysfunction (Du et al., 2012), they are a particularly suitable cell type for studying mitochondrial dysfunction.

Indeed, synaptic mitochondria are known to play a crucial role in maintaining neuronal and synaptic activity, and defects in synaptic mitochondria are associated with reduced synaptic function. Synaptic mitochondria are also known to be particularly susceptible to oxidative damage and calcium damage during ageing. Therefore, synaptic mitochondrial damage has been investigated in relation to neurodegenerative diseases, and several studies have revealed that synaptic deficits are an early feature in AD and PD, with synaptic failure thought to directly contribute to cognitive decline (Selkoe, 2002; Reddy and Beal, 2008).

As previously discussed, TFAM is a major regulator of mtDNA replication, mitochondrial copy number and transcription (Section 1.7.2). Since mitochondrial function is crucial for

efficient synaptic activity, altered levels of TFAM might contribute to mitochondrial deficiency at the synapses.

Several studies have provided support for a potential therapeutic use of *TFAM* overexpression, as elevated levels of *TFAM* have been shown to improve survival after myocardial infarction and reduce age-related memory loss and mtDNA damage in microglia in mice (Ikeuchi et al., 2005; Hayashi et al., 2008). However, overexpression of human *TFAM* in mice has also been shown to result in enlarged nucleoid size in muscle and heart tissue concomitant with an increased generation of mtDNA deletions. Furthermore, these mice exhibited reduced levels of respiratory chain complex I and IV in skeletal muscle and showed COX-deficient fibres in skeletal muscle and heart (Ylikallio et al., 2010).

Similarly to *TFAM* overexpression, expression of a mitochondrially-targeted restriction enzyme, *XhoI*, also results in mitochondrial dysfunction. *XhoI* targets mtDNA at a single restriction site located in the cytochrome c oxidase subunit I (*Co*I) locus in *Drosophila,* resulting in the linearization of the circular mtDNA. Targeting *XhoI* to mitochondria has been shown to cleave the majority of mtDNA molecules, and when expressed in a ubiquitous manner using a tubulin (*tub-Gal4)* driver, leads to embryonic lethality. Expressing *mitoXhoI* selectively in the eye, using an *eyeless-Gal4* driver, resulted in the complete loss or significant reduction of the eye (Xu et al., 2008).

In this chapter, I present data obtained using *Drosophila* models of neuronal mtDNA dysfunction. I further investigate the mitochondrial retrograde response initiated upon mitochondrial dysfunction using microarray analysis.

4.2. Chapter aims

Overexpression of *TFAM* and expression of the restriction enzyme *mitoXhoI* have both been shown to cause mitochondrial dysfunction in previous animal studies. Targeting their expression specifically in the fly nervous system, would allow for the investigation of mtDNA dysfunction at the cellular level in a tissue-specific manner.

Work previously carried out by Umut Cagin verified that overexpression of *TFAM* and expression of *mitoXhoI* cause mitochondrial dysfunction in *Drosophila* motor neurons (Cagin, 2013). In this thesis chapter I outline how these tools were used to further investigate the initial response of neurons to mitochondrial dysfunction.

Therefore the general aims of this chapter include:

- To investigate the consequences of *TFAM* overexpression and *mitoXhoI* expression on mtDNA levels and mitochondrial-associated proteins.
- To investigate synaptic mitochondrial phenotypes generated by these tools via analysis of the NMJ.
- To investigate the oxidation/reduction status of the mitochondria and cytosol at the NMJs in the mtDNA dysfunction models.
- To investigate alterations in gene expression in *Drosophila* models of neuronal mitochondrial dysfunction by microarray analysis.

4.3. Materials and Methods

4.3.1. Fly food

R1 recipe: 64g Agar (Fischer), 160g ground yellow corn, 640g glucose (Sigma), 400g Brewer's yeast (MP Biomed Europe) in a total volume of 10L dH_2O

R2 recipe: 64g Agar (Fischer), 160g ground yellow corn, 640g glucose (Sigma), 800g Brewer's yeast (MP Biomed Europe) in a total volume of 10L dH_2O

The ingredients were mixed in a SystecMediaPrep media steriliser and cooled to a temperature below 60^{o}C. 18g methyl 4-hydroxybenzoate (Sigma), 30mL propionic acid (Fischer Scientific) and 160mL ethanol were then added. Once well mixed, the food was dispensed into vials and bottles (Regina Industries Ltd) which were stored in a cold room at 4^{o}C.

4.3.2. Fly breeding

Virgin female flies were collected five days a week and were kept at 18^{o}C in R1 food. Experimental crosses using the *Gal4*/UAS system were set up on R2 food, and were kept at 25^{o}C for three days. The adults were then removed and the embryos were allowed to develop at 29^{o}C. Dissections and behavioural analysis of wandering larvae were carried out on the third day at 29^{o}C, unless stated otherwise. In all cases, unless otherwise stated, the control used in experiments was the *Gal4* driver line specified in the experiment crossed to the Drosophila background strain, w^{1118}.

In *Drosophila*, the *Gal4*/UAS system is an efficient way of selectively expressing genes of interest in specific tissues. Expression of the yeast transcriptional activator *Gal4* is under the control of a promoter. When activated, *Gal4* directs the transcription of an upstream activation sequence (UAS) which leads to the expression of the gene of interest.

Importantly, *Gal4* activation will not lead to expression of the target gene unless UAS is present. Similarly, in the UAS-target gene line, the target gene is not expressed unless activated by the *Gal4*. Therefore both lines are required and the target gene will only be expressed in the tissue specified by the *Gal4* system in the progeny (Brand and Perrimon, 1993).

Since ubiquitous overexpression of *TFAM* and expression of *mitoXhoI* cause early developmental lethality, a temperature-sensitive $Gal80^{ts}$ system was used to express *Tub-Gal4. Gal80* is a *Gal4* inhibitor and by using a temperature sensitive *Gal80* ($Gal80^{ts}$) one is able to cause temporal regulation of the *Gal4*/UAS system in a temperature sensitive manner. The $Gal80^{ts}$ allele suppresses *Gal4* activity at temperatures of 18^{o}C and then allows *Gal4* activity upon the temperature being elevated to 29^{o}C, as the $Gal80^{ts}$ allele is rendered inactive at this temperature (Figure 4.1) (Lee and Luo, 1999). This allowed for a temporally controlled overexpression of *TFAM* and expression of *mitoXhoI*, in order to obtain third instar larvae for qPCR and western blot analysis. Experimental crosses were set up and embryos laid at 18^{o}C for three days. The embryos were then left to incubate at 18^{o}C for an additional five days, and then put at 29^{o}C before being homogenised at the wandering third larval instar stage.

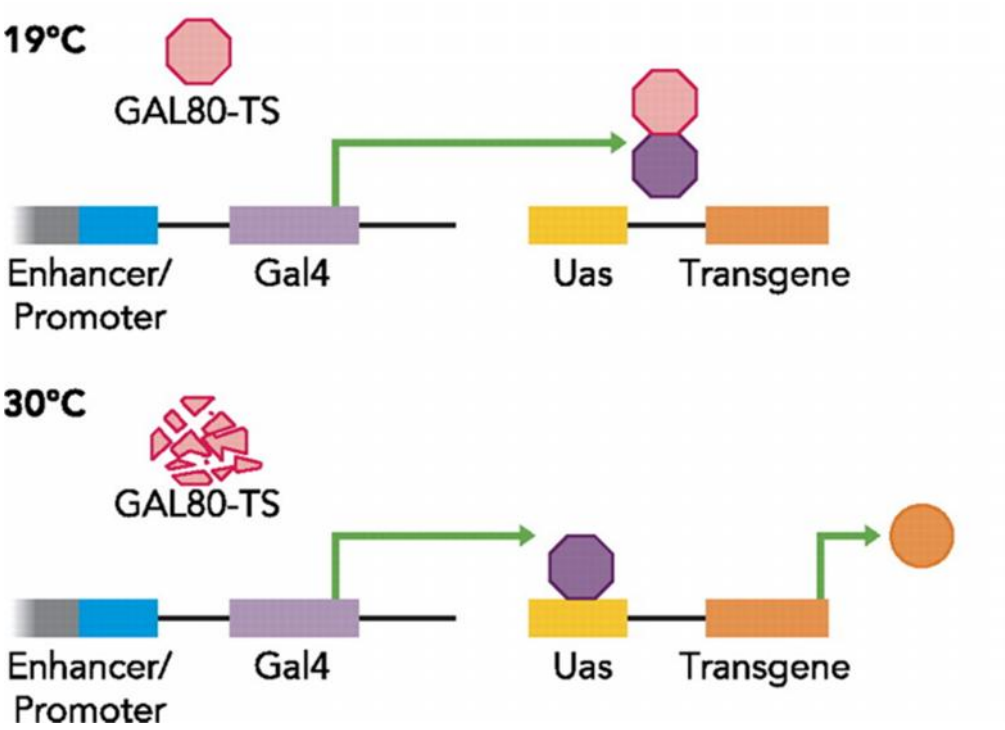

Figure 4.1 Temporal control of the *Gal4*/UAS system
At low temperatures (19°C) *Gal80^{ts}* suppresses *Gal4* activity thereby inhibiting expression of the transgene which is under control of the UAS. At higher temperatures (30°C) the *Gal80^{ts}* is rendered inactive. *Gal4* now binds to UAS activating transcription of the transgene. Adapted from (Busto et al., 2010).

4.3.3. Fly stocks

***Gal4* driver lines:**

nSyb-Gal4 (Sousa-Nunes Lab) – post-mitoticneurons (synaptobrevin expressing)

Da-Gal4 (Perrin et al., 2003)– daughterless (ubiquitous expression)

OK371-Gal4 (Bloomington,26160) – glutamatergic neurons

Tub-Gal80^{ts} (Bloomington, 7018) – Tubulin (temperature sensitive *Gal4*)

Tub-Gal4 (Bloomington, 5138) - Tubulin (ubiquitous expression)

Background strain:

w^{1118} (Bloomington, 6326)

UAS Stocks :

UAS-TFAM 3M (chromosome II, generated by Umut Cagin, Bateman Lab) – *TFAM* overexpression

UAS-mitoGFP (Bloomington, 8442) – GFP mitochondrial marker

UAS-mitoXhoI (O'Farrell lab) – restriction enzyme targeting *mtDNA:CoI*

UAS-CD8GFP (Tear lab) – GFP expression in neuronal membranes

RNAi lines:

ATPSyn-Cf6 dsRNA (VDRC, CG4412 107826) – RNAi of ATP synthase Coupling factor 6

GFP fluorescent probes:

Mito-roGFP2-Grx1 (Albrecht et al., 2011) – measurement of glutathione redox potential in the mitochondrial matrix

Mito-roGFP2-ORP1 (Albrecht et al., 2011) – measurement of hydrogen peroxide levels in the mitochondrial matrix

Cyto-roGFP2-Grx1 (Albrecht et al., 2011) – measurement of glutathione redox potential in the cytosol.

4.3.4. Measurement of mtDNA levels by quantitative PCR (qPCR).

5 wandering third instar larvae were briefly washed in cold dH_2O to remove excess food. The larvae were then placed in an empty tube on ice and kept cold. 250µl of homogenisation buffer (Tris-Cl 0.1M, pH 9.0, EDTA 0.1M, SDS 1%) were added, and the larvae were homogenised using a small pestle. Once homogenised, the tubes were immediately returned to ice and then incubated for 30 minutes at 70°C. 35µl of potassium acetate were then added and the solution was shaken. The tubes were left on ice for 30 minutes and then spun for 15 minutes at 13000 rpm. The supernatant was then transferred into a new tube and 1 volume of Phenol: Chloroform (1:1) was added. The tubes were shaken thoroughly and spun at 13000 rpm for 5 minutes. The supernatant was again transferred onto a new tube and the phenol: chloroform and centrifuge steps repeated. The supernatant was then isolated and 150µl of isopropanol added. The solution was shaken and spun for 5 minutes at 10000 rpm. The supernatant was then discarded and 1ml of 70% ethanol added. Following a final 5 minute spin at 13000 rpm, the pellet was left to dry at room temperature and then resuspended in 100µl of Tris-EDTA.

Real time qPCR was performed on a Corbett Rotor-Gene RG-3000 machine. LightCycler® FastStart DNA MasterPLUS SYBR Green I (Roche) reaction mixture and gene specific primers (mitochondrial: cytochrome c oxidase subunit I (*mt:CoI*) and nuclear: glyceraldehyde 3-phosphate dehydrogenase (*Gapdh1*)) were used (Table 10). The PCR reaction consisted of 40 cycles with a 10s denaturing step at 95°C, followed by 15s of annealing at 60°C, an extension step at 72°C for 20s and a final melting step with a temperature increase from 72°C to 95°C.

Standard curves for *mt:CoI* and *Gapdh1* were generated using a series of 8 dilutions of genomic DNA to ensure primer efficiency. The relative mtDNA level for each sample was calculated by measuring the ΔCT of *Gapdh1* to *CoI* expression.

Table 10. Primer sequences for measuring mtDNA levels in *Drosophila*

Gene	Primers	Sequence
Mt: CoI	Forward primer	5'-GAGCTGGAACAGGATGAACTG-3`
	Reverse primer	5'-TTGAAGAAATCCCTGCTAAATGT-3`
Gapdh1	Forward primer	5`-GACGAAATCAAGGCTAAGGTCG-3`
	Reverse primer	5`-AATGGGTGTCGCTGAAGAAGTC-3`

4.3.5. Western blot analysis

25 third instar larvae (per genotype) were homogenised in 150µl of 1x SDS PAGE loading buffer (2% SDS, 10% glycerol, 50mM Tris-HCl pH 6.8, 0.1% bromophenol blue). 0.1% DTT was then added to the supernatant and the samples were boiled at 95^{o}C for 5 min and stored at -20^{o}C.

Western blot samples, at a known concentration of protein, were run on a 12% SDS-polyacrylamide gel at approximately 70 volts (V), for 30 minutes and then 100V for the rest of the run. On each gel, 5µl of a pre-stained protein ladder was run (EZ Run, Prestained*Rec* Protein ladder, Fischer) in the first lane.

The proteins were transferred onto nitrocellulose hybond membranes (Amersham) for one hour at 25V. The membranes were then incubated with the primary antibody overnight at 4^{o}C in 5% milk in TBS-T. Primary antibodies used were rabbit anti-*Drosophila* TFAM (Abcam ab47548, 1:500), mouse anti-ATP5A (Abcam ab14748, 1:5000), mouse anti-MTCOI (Abcam ab14705, 1:1000) and rabbit anti-Actin (Cell Signalling, 1:4000). Western blots were developed via chemiluminescence using an ECL Prime western detection reagent (Amersham). Band intensities, corresponding to protein levels, were quantified using Image J 1.45s software. The intensity of each band was normalised to the corresponding level of actin.

4.3.6. Larval flat preps

Wandering third instar larvae were briefly placed in ice-cold PBS (Oxoid, Thermo Scientific) to rinse away food and to reduce muscle contractions. The larvae were then transferred to a drop of PBS on a Sylgard dish and pinned down dorsal side up using micro-pins (Entomoravia) placed on the anterior and posterior tips of the larva. Iridectomy scissors (Fine Science Tools) were then used to cut the larval body wall from the posterior to the anterior end, and intestines, fat bodies and the tracheal system were carefully removed using a pair of forceps. The larvae were then pinned flat using additional micro-pins, maintaining the nervous and muscle system intact. The flat preps were then fixed in 4% formaldehyde (FA) /PBS for 30-45 minutes and the pins were removed. The preps were then transferred into a 1.5ml microcentrifuge tube containing PBST (PBS, 0.1% Triton X 100) and washed three times at ten minute intervals. The tissue was then blocked in 10% NGS for 30 minutes. Anti-horseradish peroxidase (goat anti-HRP-Cy3, Stratech), used as a marker for neuronal membranes (Jan and Jan, 1982), was then added at a concentration of 1 in 250µl and the preps were left to incubate overnight at 4^{o}C on a shaking platform. The larval preps were then washed again three times in PBST. Once mounted in vectashield (Vector labs), the slides were stored at 4^{o}C in the dark. The NMJ synapses on muscle group 4 in segment A3 of the larva were imaged using a Zeiss LSM710 confocal microscope.

4.3.7. Microscopy and Image Processing

All slides were imaged using a Zeiss LSM710 confocal microscope using ZEN Software (2010, Version 6.0). Images were taken at a resolution of 1024 x 1024 pixels and 4 times averaging, with a 7x speed. Lenses used were 10x with a numerical aperture (NA) of 0.30, 20x with a NA of 0.50 and 40x, NA of 1.30 (oil immersion).

Images were processed and analysed using the Volocity Software (v5.5, Perkin Elmer) program. An image projection scanning the entire NMJ was used for analysis and a

specified measurement protocol in which objects greater than 0.02 μm^3 were selected. Additionally, an average size guide of 0.05 μm^3 was set for separating touching objects. A region of interest was selected, outlining the NMJ structure, and the number of mitochondria and their respective volume were measured. Intensity threshold levels were adjusted independently for each experiment.

4.3.8. Larval locomotion assay

A 1.5% agarose (Fischer Scientific) in PBS solution was poured into 15 cm petri dishes and allowed to cool and solidify at room temperature. Larval locomotion assays were carried out in a dark room under safe light. Wandering third instar larvae were picked up using a moist paint brush and briefly washed in water. The larvae were then transferred to an agarose plate for a 30 second acclimatisation period. Finally, the larvae were placed on a 15cm petri dish for 2 minutes, and their trail was followed and marked using a marker pen. The petri dishes were then scanned and the trail analysed as distance travelled using Image J 1.45s software.

4.3.9. NMJ dissections for redox level measurement

This dissection protocol was adapted from the method outlined by Albrecht et al. (Albrecht et al., 2011). Wandering third instar larvae were briefly placed in cold dH_2O to wash away excess food. In order to obtain preps of fully reduced larvae, dissections as in 4.3.6 were carried out in 20mM thiol reducing agent DTT and then left to incubate for 10 minutes. The DTT was then removed and replaced with 20mM thiol blocker N-ethylmaleimide (NEM) for an additional 10 minutes. After one rinse with PBS, the preps were fixed in 4% FA in PBS for 15 minutes. Once fixed, the preps were again rinsed in PBS and washed three times in PBST for 10 minute intervals. The preps were then incubated for 40 minutes with anti-HRP-Cy3 (Stratech), PBST and 10% NGS, followed by three 10 minute interval washes in PBST

and a final wash in PBS. The preps were then mounted on slides in vectashield. The same procedure was repeated for preps of fully oxidised larvae, utilising 2mM thiol oxidising agent diamide (DA) instead of DTT. Control and test larvae were not treated with DA or DTT but were directly dissected in 20mM NEM and left for 10 minutes. The rest of the procedure was the same as outlined above. Reduced, oxidised, control and test larvae were imaged on the confocal microscope on the same day as dissection and mounting.

4.3.10. Microarray experiments and analysis

The central nervous system (CNS) from 15 wandering third instar control (*nSyb-Gal4>w1118*), *TFAM* overexpressing *(nSyb-Gal4>UAS-TFAM 3M*) or *ATPSyn-Cf6* dsRNA expressing (*nSyb-Gal4>ATPSyn-Cf6 ds*RNA) larvae were dissected in PBS. The brains were then transferred into 100µl of lysis buffer from the Absolutely RNA Microprep kit (Stratagene) and vortexed for 5 seconds. Total RNA was then prepared following the kit instructions. Triplicate RNA samples were prepared for each genotype and stored at -80^{o}C.

RNA integrity was measured using an Agilent 2100 Bioanalyzer instrument (version 2.6, Agilent Technologies, Inc.), and cDNA was prepared from 500ng of total RNA using the Ambion WT Expression kit.

An Affymetrix Terminal Labelling kit on *Drosophila* Gene 1.0 ST Arrays (Affymetrix) was used to perform the probe hybridisations. Imaging of the arrays was performed using the Affymetrix GCS3000 microarray system. The data was processed using a Robust Multichip Average (RMA) algorithm (Bolstad et al., 2003) and analysed using the Omics Explorer package (Qlucore) using a false discovery rate (FDR) of 0.2%.

Gene ontology (GO) analysis was carried out using Database for Annotation, Visualization and Integrated Discovery (DAVID) v6.7 (Huang da et al., 2009). Results obtained via

functional annotation clustering were visualised as a chart and graphically represented as a histogram using Microsoft Excel (2007 version).

The data obtained have been uploaded on NCBI's Gene Expression Omnibus and are accessible via GEO Series accession number GSE53509.

4.3.11. Statistical analysis

Statistical analysis of data and generation of graphs were performed using GraphPad Prism version 5.0 (GraphPad Software Inc).

Comparison of data between two individual groups was carried out using a two-tailed unpaired t-test, when variances in the groups passed the equality test. When variances were considered unequal, a t-test with Welch's correction for unequal variances was carried out. When the data in one or both of the individual groups compared did not fit a normal distribution, a non-parametric Mann-Whitney test was carried out.

Analysis to compare means in multiple groups was carried out by one-way analysis of variance (ANOVA) followed by Tukey's post-hoc multiple comparison test. If data did not fit a normal distribution, a Kruskal-Wallis test followed by Dunn's multiple comparison test was carried out.

In all experimental analysis, data was considered significantly different when the p value was lower or equal to 0.05 ($p \leq 0.05$).

4.4. Results

4.4.1. Ubiquitous overexpression of *TFAM* and expression of *mitoXhoI* result in mtDNA dysfunction

Previous studies have suggested that overexpression of *TFAM* and expression of the mitochondrially-targeted restriction enzyme, *mitoXhoI* could be used as efficient tools to induce mitochondrial dysfunction (Xu et al., 2008; Ylikallio et al., 2010). Work by Umut Cagin, outlined in his PhD dissertation (Cagin, 2013) suggested that the use of these tools causes synaptic and behavioural phenotypes which are consistent with mtDNA dysfunction in *Drosophila*.

To further characterise the effects of *TFAM* overexpression and *mitoXhoI* expression as tools of mtDNA dysfunction, they were expressed ubiquitously under the control of a daughterless (*Da-Gal4*) driver. This resulted in lethality in early development stages in both cases. *TFAM* overexpression resulted in lethality at the first instar larval stage, whilst *mitoXhoI* expression caused lethality at the embryonic or early first instar larval stage (Table 11).

Using the *Gal80^{ts}* system, *TFAM* was ubiquitously overexpressed for three days following the start of the second larval instar stage. This did not result in a significant alteration in mtDNA levels when compared to controls (Figure 4.2 A). However, western blot analysis revealed that increased protein levels of TFAM (Figure 4.2 B,C) were accompanied by a significant reduction in protein levels of the mitochondrially encoded CoxI (Figure 4.2 B,D). Contrastingly, there was no change observed in protein levels of the nuclear encoded ATP synthase α subunit (Figure 4.2 B,E). This therefore suggests that overexpression of *TFAM* results in unaltered mtDNA levels but reduced mitochondrial gene expression.

Similarly, since UAS-*mitoXhoI* caused early developmental lethality under the control of *Da-Gal4*, a temperature-sensitive *Tub-Gal80 ($Gal80^{ts}$)* construct was used to induce *Gal4* activity in a temporally controlled manner. Flies expressing *mitoXhoI* ubiquitously exhibited reduced levels of mtDNA (Figure 4.3 A,B). However, mtDNA levels were only found to be statistically significantly reduced when utilising primers that spanned the restriction site within the *coxI* gene in the mitochondrial genome (Figure 4.3 A,C). This suggests that while the *XhoI* enzyme efficiently linearises the mtDNA, it does not significantly deplete mtDNA levels compared to control.

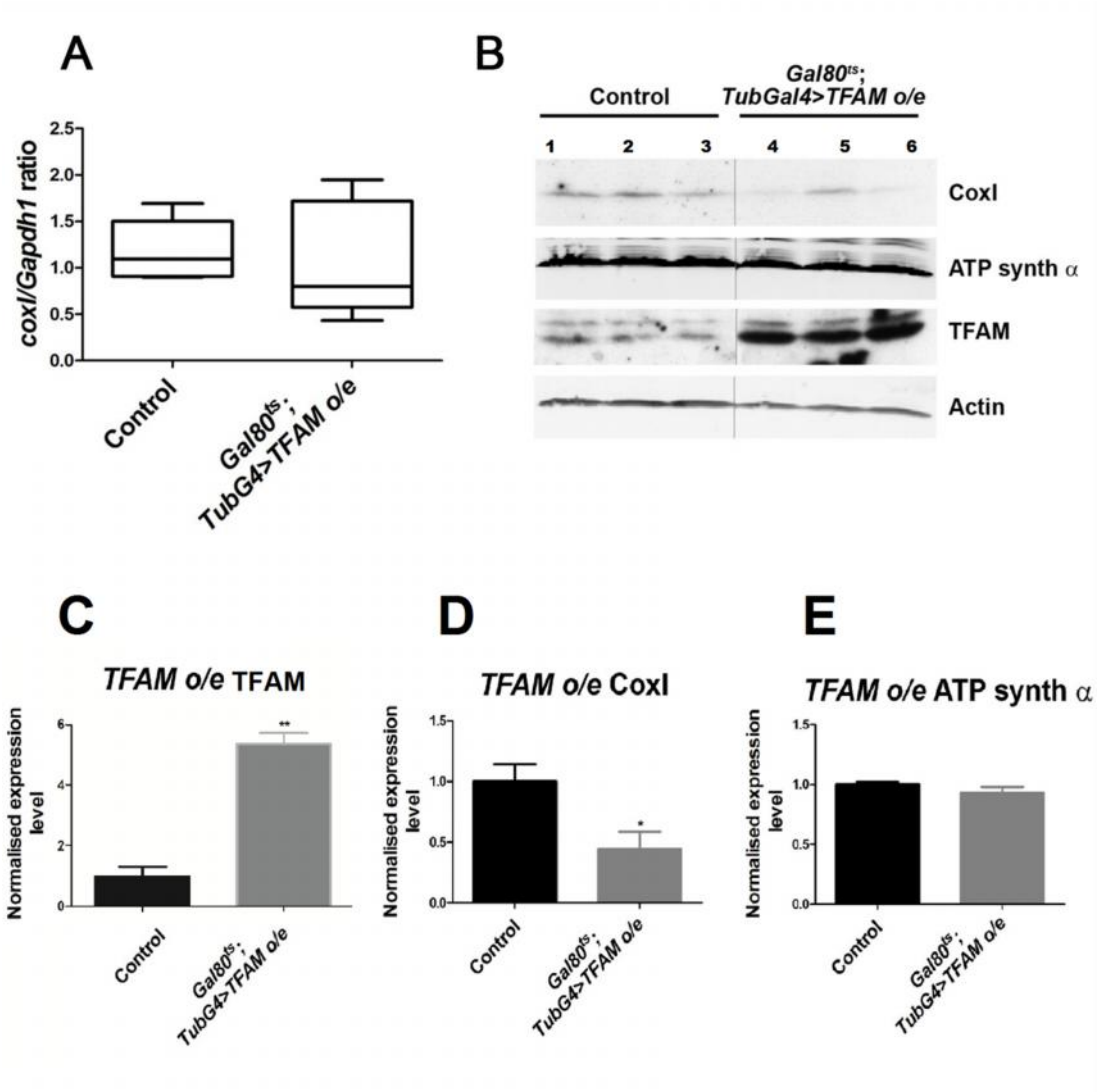

Figure 4.2 MtDNA levels and mitochondrial-encoded protein levels in larvae overexpressing *TFAM*. (A) mtDNA (*coxI*) /nDNA (*Gapdh1*) levels are not significantly different from control in flies ubiquitously overexpressing *TFAM* using *Tub-Gal80ts; Tub-Gal4*. Control n=8, *TFAM* overexpression n=8. The horizontal line in box and whisker plots represents the median whilst whiskers represent the 5th and 95th percentile. (B) Western blot analysis of third instar larvae from control (lanes 1-3) and *TFAM* overxpressing (lanes 4-6) flies. Protein levels were normalised to Actin expression levels. (C) Quantification of protein levels of TFAM. (D) Quantification of protein levels of CoxI. (E) Quantification of protein levels of ATP synthase α. Control n=3, *TFAM* overexpression n=3. Lines on the bar graphs represent mean with SEM. *=p=≤0.05. In all cases, control represents *Tub-Gal80ts; Tub-Gal4>wIII8.*

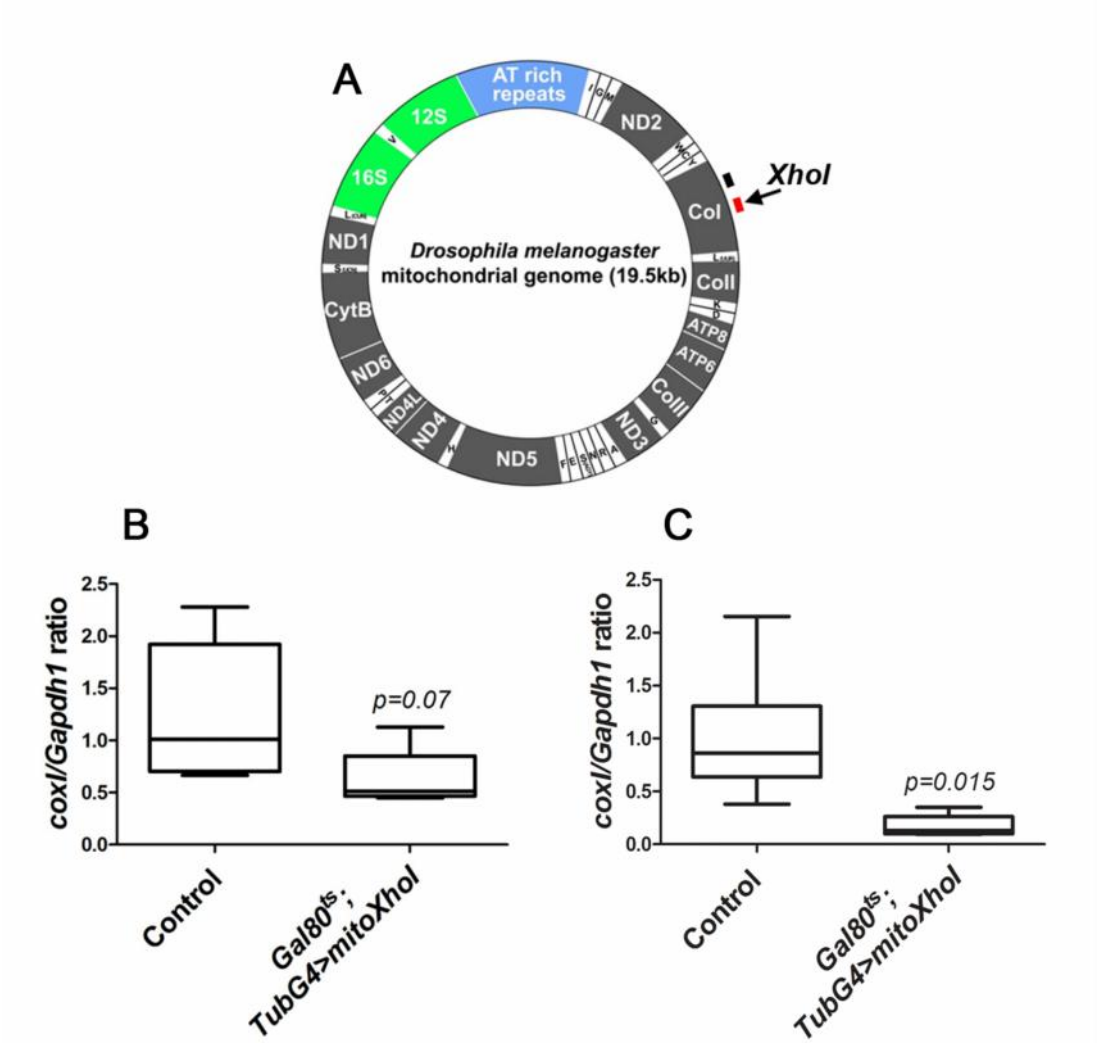

Figure 4.3 MtDNA levels in larvae expressing *mitoXhoI*.
(A)The *Drosophila melanogaster* mitochondrial genome. Protein coding genes are represented in grey, the AT rich repeat region is shown in blue and the rRNAs and tRNAs are represented in green and white respectively. (B) Quantification of mtDNA/nDNA levels in flies ubiquitously expressing *mitoXhoI* using *Tub-Gal80ts; Tub-Gal4,* using *coxI* primers that span the amplicon indicated by the black line in (A). (C) Quantification of mtDNA/nDNA levels in flies ubiquitously expressing *mitoXhoI* using *Tub-Gal80ts; Tub-Gal4,* using *coxI* primers that span the amplicon indicated by the red line in (A) which also spans the *XhoI* site in *coxI,* Control n=7, *mitoXhoI* n=5. The horizontal line in box and whisker plots represents the median whilst whiskers represent the 5th and 95th percentile. In all cases, control represents *Tub-Gal80ts; Tub-Gal4>wIII8.*

4.4.2. Overexpression of *TFAM* and expression of *mitoXhoI* in the fly motor neuron system results in loss of synaptic mitochondria

Once the tools for inducing mtDNA dysfunction were established, the motor neuron driver *OK371-Gal4* was used to drive their expression specifically in this neural population. Overexpression of *TFAM* in motor neurons resulted in late pupal lethality at 29^{o}C. Most progeny was also late pupal lethal at 25^{o}C, with few eclosed adults. Expression of *mitoXhoI* in motor neurons resulted in late pupal lethality when the experiments were performed at 25^{o}C, and earlier pupal lethality when performed at 29^{o}C (Table 11).

In order to assess whether mitochondrial dysfunction results in synaptic abnormalities, the NMJs in muscle 4 of segment A3 were investigated. The number of boutons, which are sites of neurotransmitter release, is an indicator of NMJ development and size. This was unchanged in flies overexpressing TFAM and those expressing *mitoXhoI* (Figure 4.4).

To investigate whether there was any change in mitochondrial number and volume at the NMJ, *mitoGFP* was used to quantify these parameters. Both mitochondrial number and volume were significantly reduced in NMJs of flies overexpressing *TFAM* compared to controls (Figure 4.4). Expression of *mitoXhoI* in the *Drosophila* motor neuron system also results in a reduced number of significantly smaller mitochondria at the synapses (Figure 4.4)

Table 11. Viability of *Drosophila* overexpressing *TFAM* or expressing *mitoXhoI* under the control of ubiquitous driver *Da-Gal4* and motor neuron driver *OK371-Gal4*.

	***TFAM* overexpression**	***MitoXhoI* expression**
Da-Gal4 (ubiquitous expression)	First instar larval lethal	Embryonic/early first instar larval lethal
OK371-Gal4 (motor neuron expression) at 25^{o}C	Late pupal lethal / viable adults that die within one week	Late pupal lethal
OK371-Gal4 (motor neuron expression) at 29^{o}C	Late pupal lethal	Pupal lethal

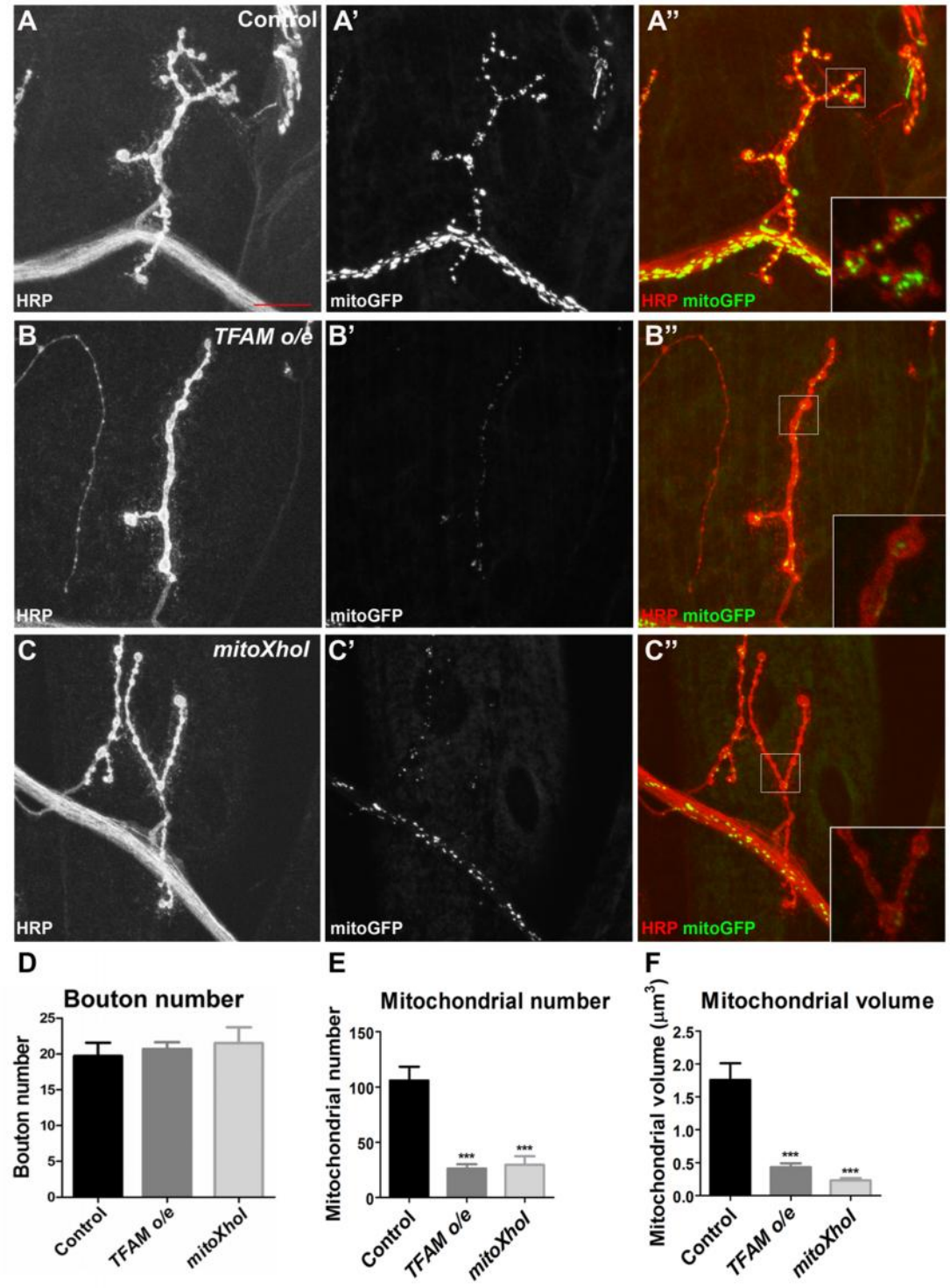

Figure 4.4 Synaptic mitochondria in flies overexpressing *TFAM* and *mitoXhoI.*
NMJs of muscle 4 in segment A3 in control (A), *TFAM* overexpressing (B), and *mitoXhoI* expressing (C) third instar larvae. *MitoGFP* was driven in motor neurons via expression of the glutamatergic driver *OK371-Gal4* to visualise mitochondria, whilst anti-HRP was used to visualise neuronal membranes. Quantification of bouton number (D), mitochondrial number (E) and mitochondrial volume (F) in larvae overepxressing *TFAM* or *mitoXhoI* compared to control. Bouton number, mitochondrial number and volume were quantified in 10-12 muscle 4 NMJs for each genotype. Data are represented as mean +/- SEM, ***=p=≤0.001. In all cases, control represents *OK371-Gal4>wIII8*.

4.4.3. Redox homeostasis in flies overexpressing *TFAM* and expressing *mitoXhoI*

As previously discussed in Section 1.5, oxidative stress and antioxidant levels are widely suspected to be involved in disease progression and are also believed to be involved in the process of ageing. Despite these theories, however, redox changes *in vivo* are not very well studied and the mechanism underlying the involvement of oxidants in physiological changes is still poorly understood.

Recently, Albrecht et al., developed a method allowing quantitative *in vivo* mapping of oxidative changes in a tissue-specific, pH-independent manner in *Drosophila* (Albrecht et al., 2011). The method utilises redox sensitive GFPs (roGFPs) (Dooley et al., 2004; Hanson et al., 2004), fused to glutaredoxin (GRX); a glutathione co-factor in the glutathione system. RoGFPs contain a dithiol/disulphide switch which responds to changes in redox potential giving a measurable fluorescent change. The fusion with GRX allows for a sensitive response to glutathione redox changes thereby allowing for a readable glutathione redox potential (E_{GSH}). Furthermore, since the GRX and roGFPs are engineered as exogenous constructs, the E_{GSH} measurement is independent of endogenous GRX.

The use of *mito-roGFP2-GRX1* constructs under the control of the *OK371-Gal4* driver allows for the measurement of E_{GSH} redox potential specifically in the mitochondrial matrix of motor neurons. Exposure of the brain tissue to exogenous reductant (DTT) or oxidant (DA) allowed for the measurement of a full redox potential range between fully reduced and fully oxidised cases.

The redox state in control larvae was close to the reduced end of the measuring range, suggesting that in a wild-type situation, glutathione is in a mostly reduced state. The redox potential was even further reduced in flies overexpressing *TFAM* and in flies expressing

mitoXhoI. This suggests that upon mitochondrial dysfunction, the E_{GSH} redox potential in the mitochondrial matrix is significantly reduced compared to control (Figure 4.5).

Similarly, a *cyto-roGFP2-GRX1* construct allowed for the measurement of E_{GSH} redox potential specifically in the cytosol of the NMJs. Unlike the mitochondrial-targeted construct, the cytosolic probe showed no difference in redox potential between controls and flies overexpressing *TFAM* or *mitoXhoI* (Figure 4.6). While this result might suggest that cytosolic E_{GSH} redox potential is unchanged under these conditions of mitochondrial dysfunction, it is important to note that the 405/488m ratio in controls was not significantly different than in the maximally reduced controls (Red (DTT)). This suggests that the redox potential in the control NMJ is already at the limit of reduced potential detection. Therefore, if the redox potential is further reduced in flies overexpressing *TFAM* or expressing *mitoXhoI*, the change could remain undetected using this technique.

An alternative roGFP fused to the microbial H_2O_2 sensor oxidant receptor peroxidise 1 (ORP1) can be used to measure redox levels of the major oxidant species involved in redox regulation, H_2O_2 (Albrecht et al., 2011). Expression of a *mito-roGFP2-ORP1* construct in the motor neurons using an *OK371-Gal4* driver revealed that there was no change in the measurement of H_2O_2 levels in the mitochondrial matrix of flies expressing *mitoXhoI* compared to controls. However, similar to what was observed for *cyto-roGFP2-GRX1* measurement, the level in controls was similar to that in the maximally reduced larvae, suggesting that the H_2O_2 levels in the control mitochondria at the NMJ is also at the limit of reduced potential detection (Figure 4.7). Therefore, it could also be that further alterations in H_2O_2 levels in larvae expressing *mitoXhoI* are outside the measurable range and therefore undetectable using this technique.

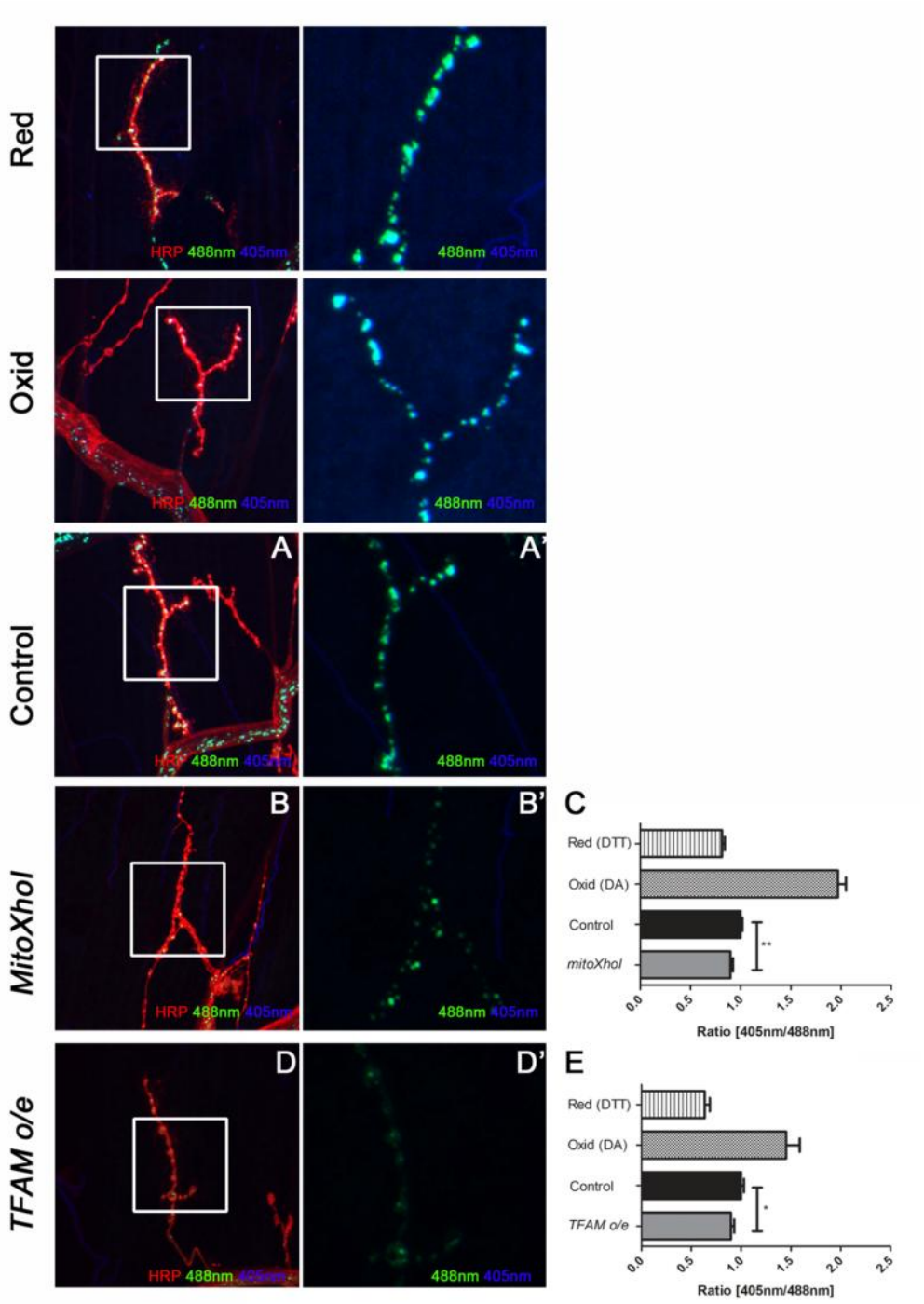

Figure 4.5 Glutathione redox potential in the mitochondrial matrix in the motor neurons of *mito-roGFP2-GRX1* flies.

Images and respective quantifications of 405/488 nm ratio in NMJs of muscle 4 in segment A3 in control (A), *mitoXhoI* expressing (B, C) (DTT n=9, DA n=11, Control n=13, *mitoXhoI* n=21), and *TFAM* overexpressing (D, E) (DTT n= 14, DA n=8, Control n=15, *TFAM* overexpression n=12) third instar larvae. Reduced (red) images represent control larvae treated with the reductant DTT, which exhibit a low 405/488 nm ratio. Oxidised (Oxid) images represent control larvae treated with the oxidant DA, which exhibit a high 405/488 nm ratio... Data are represented as mean +/- SEM, *=p=≤0.05, **=p≤0.01. In all cases, control represents *OK371-Gal4 >mito-roGFP2-GRX1.*

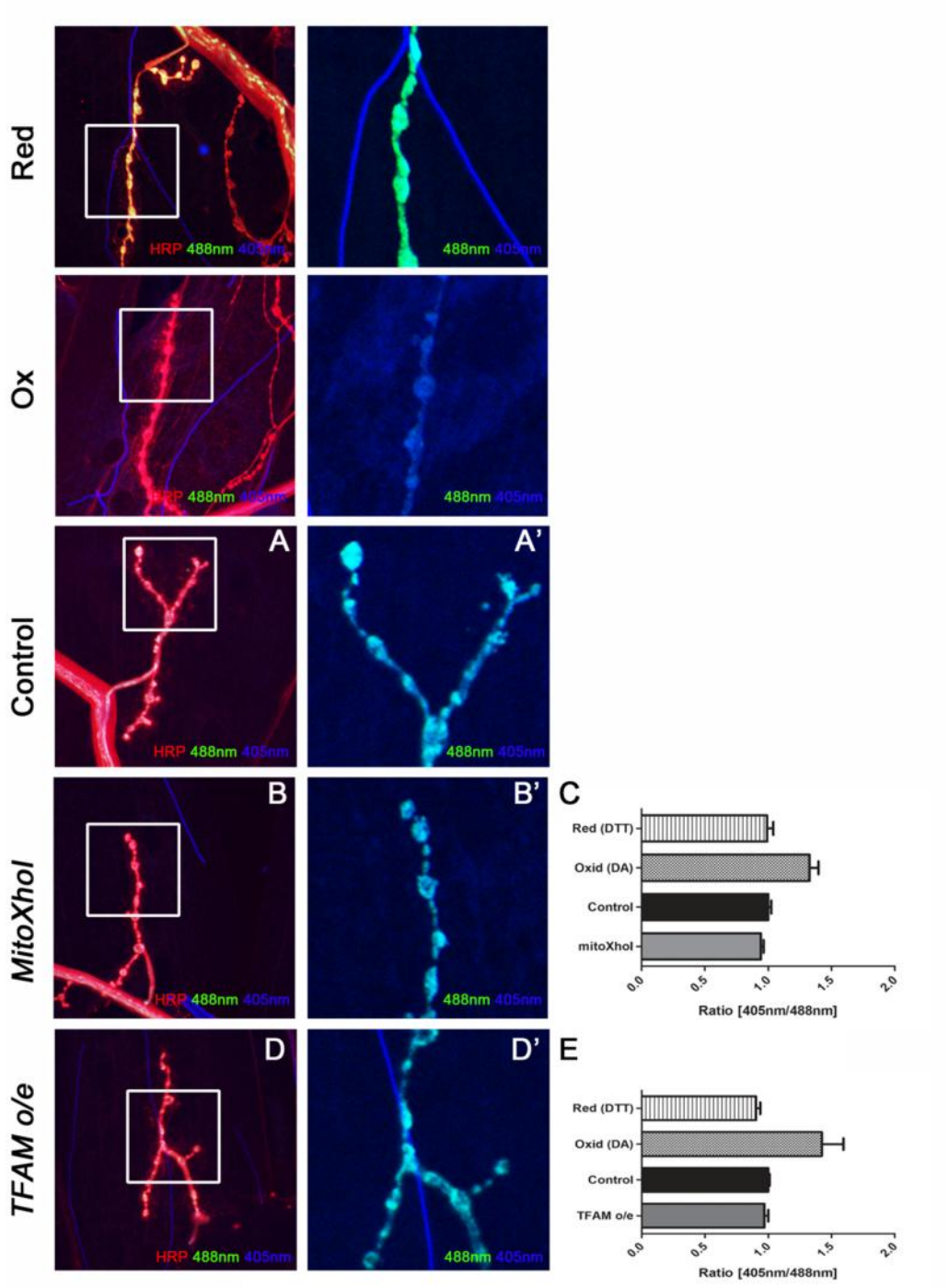

Figure 4.6 Glutathione redox potential in the cytosol in the motor neurons of *cyto-roGFP2-GRX1* flies

Images and respective quantifications of 405/488 nm ratio in NMJs of muscle 4 in segment A3 in control (A), *mitoXhoI* expressing (B, C) (DTT n=8, DA n=8, Control n=20, *mitoXhoI* n=12), and *TFAM* overexpressing (D, E) (DTT n=10, DA n=3, Control n=17, *TFAM* overexpression n=19) third instar larvae. Reduced (red) images represent control larvae treated with the reductant DTT, which exhibit a low 405/488 nm ratio. Oxidised (Oxid) images represent control larvae treated with the oxidant DA, which exhibit a high 405/488 nm ratio. Data are represented as mean +/- SEM. In all cases, control represents *OK371-Gal4 >cyto-roGFP2-GRX1.*

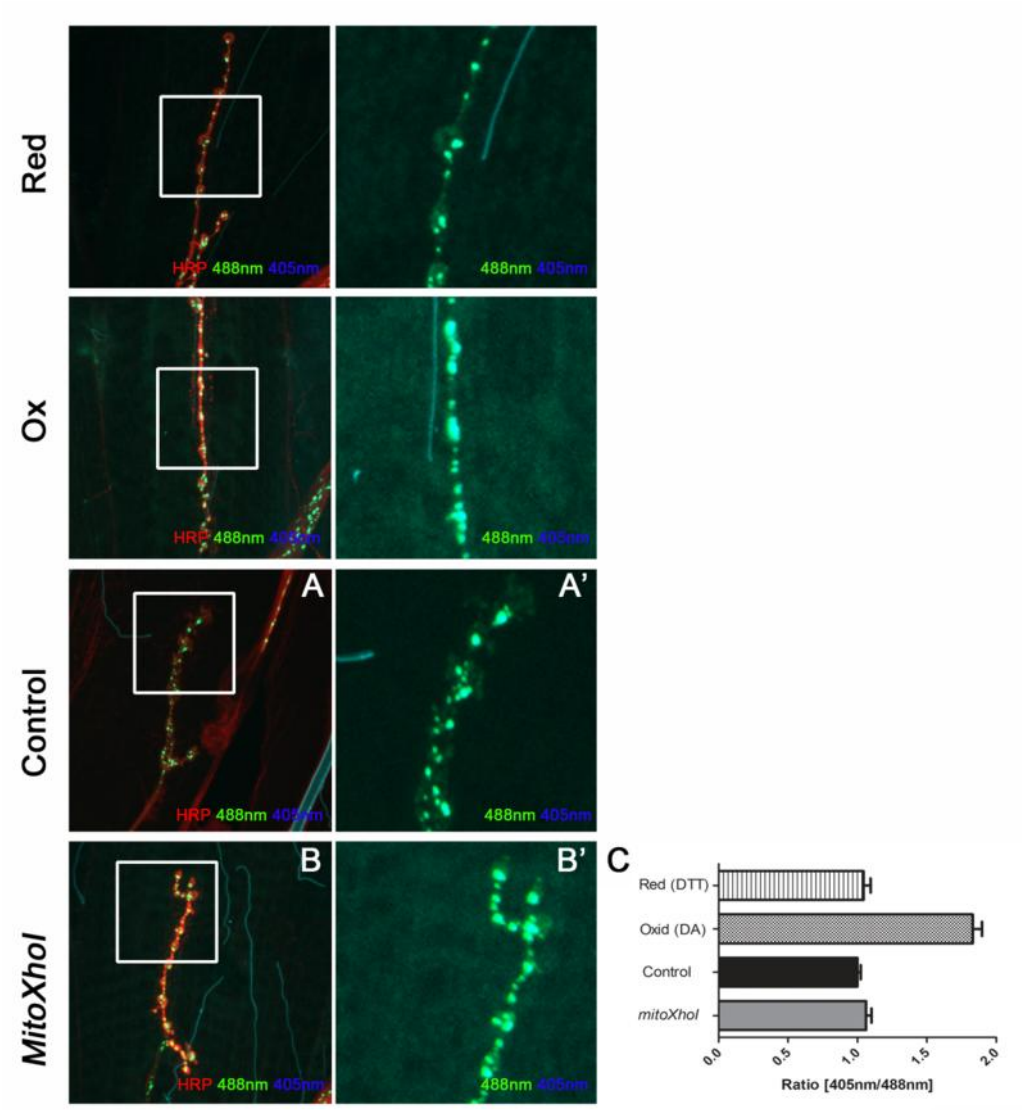

Figure 4.7 Hydrogen peroxide levels in the mitochondrial matrix in the motor neurons of *mito-roGFP2-ORP1* flies

Images and respective quantifications of 405/488 nm ratio in NMJs of muscle 4 in segment A3 in control (A) and *mitoXhoI* (B,C) (DTT n=10, DA n=8, Control n=12, *mitoXhoI* n=14) expressing third instar larvae. Reduced (red) images represent control larvae treated with the reductant DTT, which exhibit a low 405/488 nm ratio. Oxidised (Oxid) images represent control larvae treated with the oxidant DA, which exhibit a high 405/488 nm ratio. Data are represented as mean +/- SEM. Control represents *OK371-Gal4 >mito-roGFP2-ORP1.*

4.4.4. Characterisation of the mitochondrial retrograde response in the *Drosophila* CNS.

In order to better understand the molecular mechanisms underlying mitochondrial dysfunction, a microarray analysis was carried out to investigate altered gene expression in the late larval CNS, upon induction of mitochondrial dysfunction. The genechip *Drosophila* genome 2.0 Array from Affymetrix contains 18,880 probe sets and allows investigation of the expression profiles of more than 18,500 *Drosophila* transcripts (Affymetrix).

The *nSyb-Gal4* driver, driving expression in all post-mitotic neurons, was used to induce pan-neuronal mitochondrial dysfunction. Expression of *mitoXhoI* using *nSyb-Gal4* resulted in mid-larval lethality and this tool was, therefore, not used for this study. Expression of dsRNA against ATP synthase Coupling factor 6 (*ATPSyn-Cf6* dsRNA) was therefore used as an alternative method of inducing mitochondrial dysfunction. The F6 subunit of the complex is found in the F_0 unit, which is the proton channel component of ATP synthase, and is required for the interaction of the F_0 subunit with the F_1 subunit. Larvae expressing *ATPSyn-Cf6* dsRNA display similar synaptic and behavioural phenotypes to *mitoXhoI* and *TFAM* overexpressing flies (Cagin et al., submitted). Therefore, larvae overexpressing *TFAM* and larvae expressing *ATPSyn-Cf6* dsRNA were chosen as candidates for the microarray study.

Overexpression of *TFAM* and knockdown of *ATPSyn-Cf6* in post-mitotic differentiated neurons resulted in late pupal lethality in both cases. Behavioural analysis of larvae from *nSybGal> TFAM*o/e and *nsybGal4> ATPSyn-Cf6* dsRNA showed that larval locomotion was significantly reduced in both cases when compared to controls. Larval locomotion in larvae expressing *ATPSyn-Cf6* dsRNA was even more significantly reduced than in larvae overexpressing *TFAM* (Figure 4.8).

RNA from larval CNS tissue was used for microarray analysis. Overall, data analysis revealed that gene regulation following mitochondrial dysfunction was highly correlated in larvae overexpressing TFAM and those expressing *ATPSyn-Cf6* dsRNA ($r = 0.72$, $p = \leq 0.0001$, Figure 4.9), suggesting that genes responded in a similar manner to the two methods of mitochondrial dysfunction. Using a false discovery rate of 0.2%, microarray analysis revealed that 340 probes, corresponding to 293 genes were differentially regulated in *TFAM* overexpressing larvae (Appendix 2.1), whilst 424 probes, corresponding to 371 genes were differentially regulated in larvae expressing *ATPSyn-Cf6* dsRNA (Appendix 2.2). 142 of the genes were commonly differentially regulated in both cases (Appendix 2.3) (Figure 4.9). A correlation analysis on these 142 genes, again revealed a highly significant positive correlation ($r = 0.93$, $p = \leq 0.0001$, Figure 4.9)

Heat map E in Figure 4.9 shows the 20 genes that were most upregulated in *TFAM* o/e flies compared to *ATPSyn-Cf6* dsRNA flies, whilst heat map F shows the 20 genes that were most upregulated in *ATPSyn-Cf6* dsRNA flies compared to *TFAM* overexpressing flies. Heatmap G shows 20 genes that were commonly differentially regulated in *TFAM* overexpressing larvae and larvae expressing *ATPSyn-Cf6* dsRNA compared to controls.

Among the common differentially regulated genes in the *TFAM* o/e and *ATPSyn-Cf6* dsRNA expressing larvae, were the ones listed in Table 12.

Figure 4.10 depicts histograms representing gene ontology analysis carried out on genes differentially regulated in larvae expressing *ATPSyn-Cf6* dsRNA (Figure 4.10A), larvae overexpressing TFAM (Figure 4.10B), and genes which were commonly regulated in the two cases (Figure 4.10C). Detailed charts listing the names of the genes annotated to each cluster and relative enrichment scores can be found in appendices 2.4, 2.5 and 2.6.

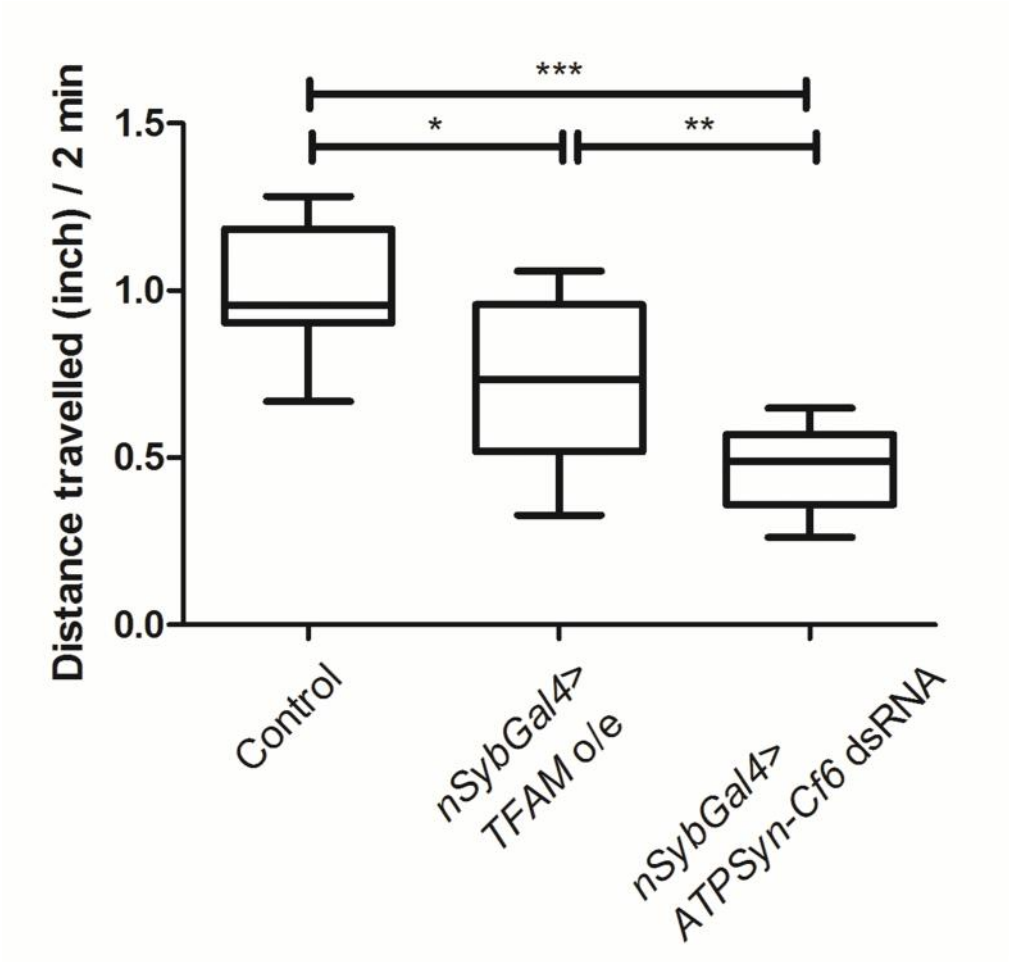

Figure 4.8 Larval locomotion in larvae overexpressing *TFAM* and *ATPSyn-Cf6* dsRNA.
Larval locomotion is significantly reduced in larvae overexpressing *TFAM* and in larvae expressing *ATPSyn-Cf6* dsRNA (One-way ANOVA followed by Tukey's multiple comparison test) n=10 for Control, *TFAM* o/e and *ATPSyn-Cf6* dsRNA. The horizontal line in box and whisker plots represents the median whilst whiskers represent the 5th and 95th percentile. *=p≤0.05, **=p≤0.01, ***=p≤0.001. Control represents *nSybGal4>WIII8.*

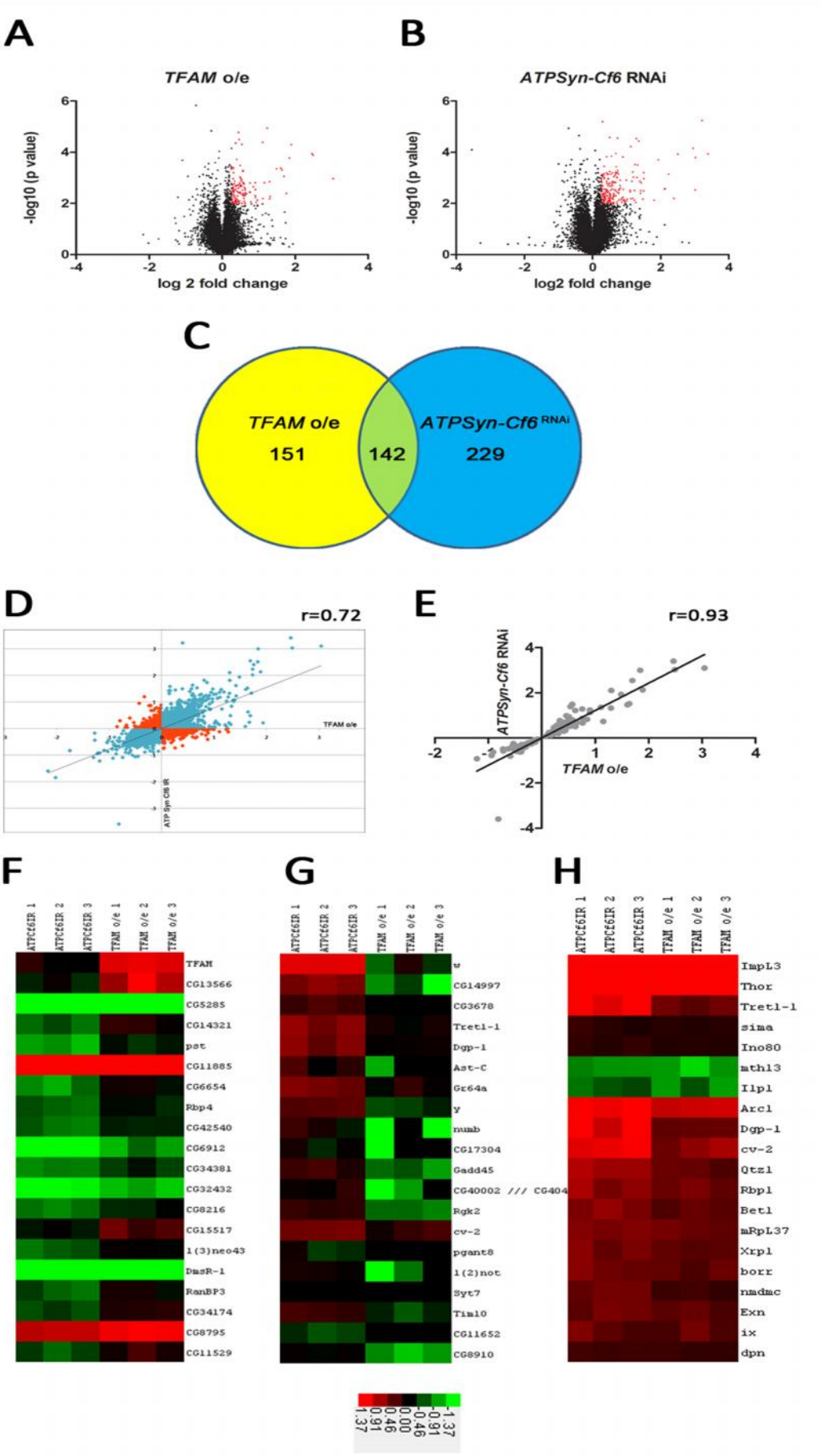

(Figure legend on next page)

Figure 4.9 Microarray analysis reveals mitochondrial retrograde response upon *TFAM* overexpression or *ATPSyn-Cf6* knockdown.
(A,B) Volcano plots of gene expression levels in flies expressing *TFAM o/e* (A) or *ATPSyn-Cf6 ds*RNA (B). Genes whose expression was significantly increased ≥1.2 fold with a p value ≤0.01 are shown in red. (C) Venn diagram depicting the number of genes whose expression was significantly changed with a p value ≤0.01 in larval CNS of flies overexpressing *TFAM* (*TFAM o/e*) (n = 151), *ATPSyn-Cf6* dsRNA (n=229) and in both conditions (n=142). (D) Correlation plot of all *ATPSyn-Cf6* dsRNA vs. *TFAM o/e* gene expression levels. Blue scatter dots represent genes which display positive correlation between the two conditions. Red scatter dots represent genes which are inversely correlated and are therefore upregulated in one condition whilst being downregulated in another. (E) Correlation plot of genes which were statistically commonly regulated upon *ATPSyn-Cf6* dsRNA and *TFAM o/e*. (F,G) Heat maps showing expression levels of 20 genes whose expression was significantly upregulated in *TFAM o/e* flies (F) and in *ATPSyn-Cf6* dsRNA flies (G). (H) Heat map showing expression level of 20 genes whose expression was similarly regulated in *ATPSyn-Cf6* dsRNA and *TFAM o/e* flies.

Table 12. Selected common differentially regulated genes in the TFAM o/e and ATPSyn-Cf6 dsRNA expressing larvae

***TFAM* o/e fold change**	**Gene**	**Function**	***ATPSyn-Cf6* dsRNA fold change**
3.584	*Impl3*	Ecdysone-inducible gene L3 – L-lactate dehydrogenase activity	7.971
1.486	*Tret1-1*	Trehalose transporter	2.813
3.235	*Thor*	4E-BP –eukaryotic initiation factor 4E binding	5.832
0.607	*Ilp1*	Insulin-like peptide – Insulin Receptor Signalling pathway	0.711

Impl3 encodes lactate dehydrogenase, which converts pyruvate, the final product of glycolysis, to lactate when oxygen is limiting. Trehalose is the primary circulating sugar in insects and is taken up into the various cellular systems via the facilitated trehalose transporter, *Tret1-1*. Both *Impl3* and *Tret1-1* were upregulated in larvae overexpressing *TFAM* and expressing *ATPSyn-Cf6* dsRNA suggesting a common upregulation of glycolysis induced upon mitochondrial dysfunction.

Thor, encoding for eukaryotic translation initiation factor 4E-binding protein 1 (4E-BP1) was also highly upregulated in both conditions, whilst *Drosophila* insulin-like peptide 1 (*Ilp1*)

was significantly downregulated in both larvae overexpressing TFAM and those expressing *ATPSyn-Cf6* dsRNA. *Ilp3* was additionally significantly downregulated in the latter group. Together, these findings suggest a downregulation of the mTOR pathway in response to mitochondrial dysfunction. These genes were consequently selected as indicative of a mitochondrial retrograde signalling mechanism. Validation of the differential regulation of these genes and further investigation into their role in mitochondrial retrograde signalling is further described in Chapter 5.

A *ATPSyn-Cf6* dsRNA

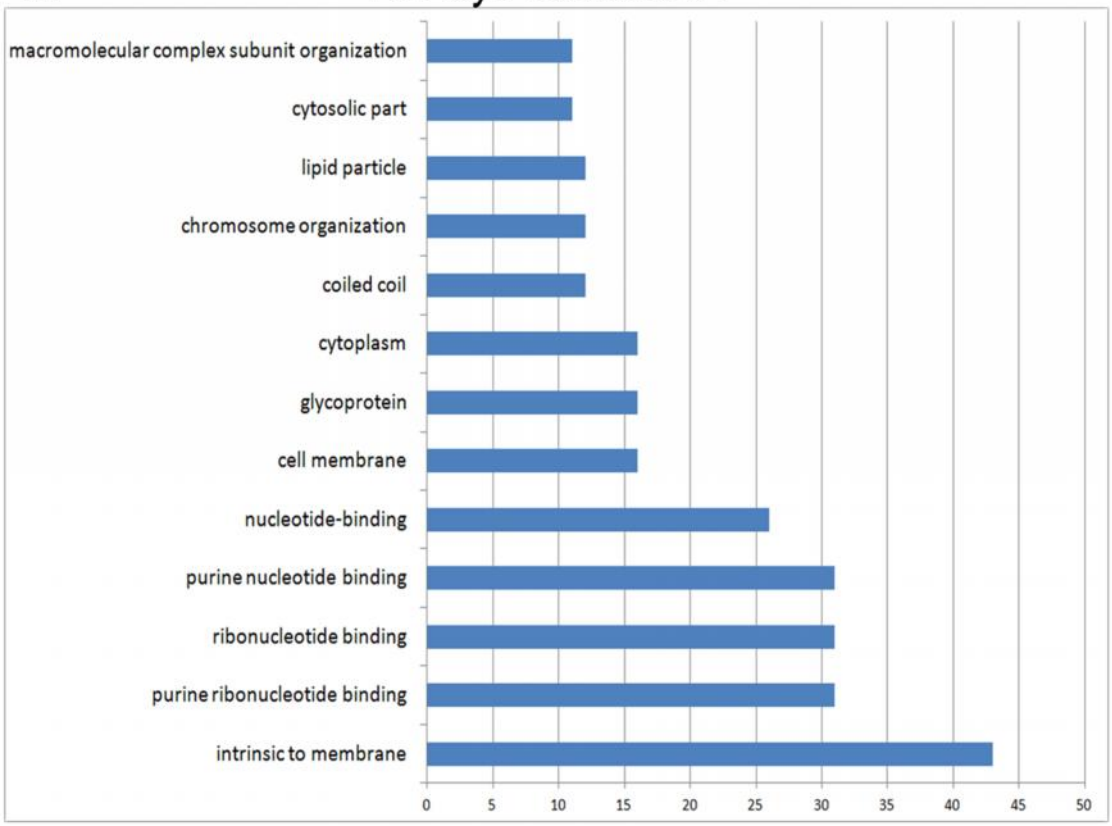

B *TFAM o/e*

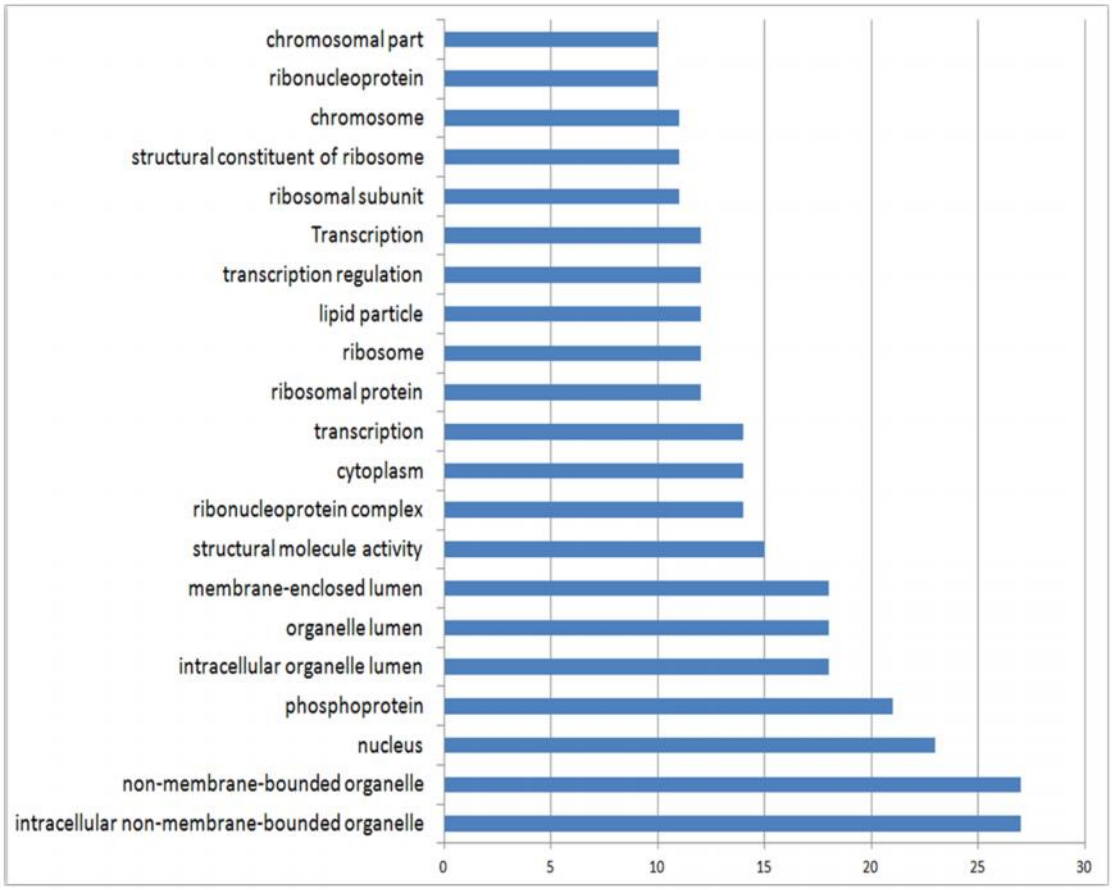

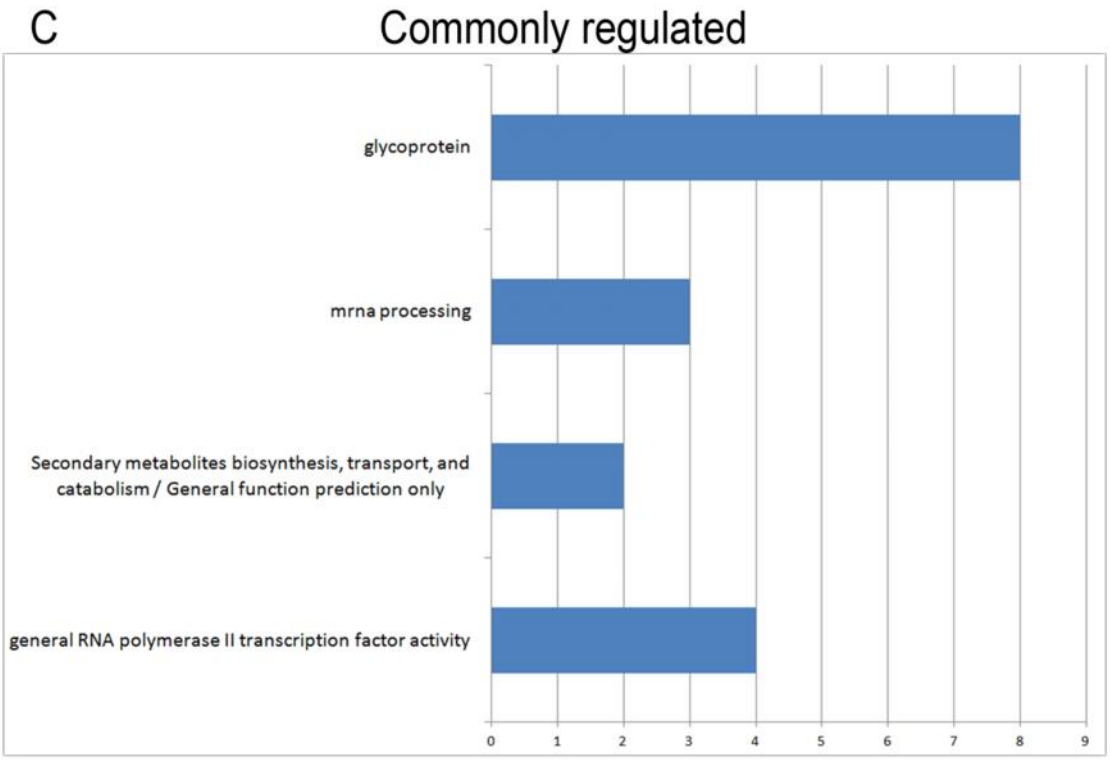

Figure 4.10 Gene ontology (GO) analysis, based on functional annotation clustering, of genes differentially or commonly regulated in larvae expressing *ATPSyn-Cf6* dsRNA or overexpressing *TFAM*.

Histograms representing functional annotation clusters resulting from GO analysis of genes significantly differentially regulated in larvae expressing *ATPSyn-Cf6* dsRNA (A) or over-expressing *TFAM* (B). Only clusters which included a count of gene number ≥ 10 are represented in charts A and B. (C) A histogram representing functional annotation clusters from GO analysis of genes that were commonly regulated upon expression of *ATPSyn-Cf6* dsRNA or *TFAM* overexpression. The x-axis represents the number of genes represented in each cluster. The y-axis represents the functional annotations which were found to be enriched by GO analysis using DAVID v6.7.

4.5. Discussion

Overexpression of *TFAM* and expression of the mitochondrially-targeted restriction enzyme *mitoXhoI* proved to be efficient tools for inducing mitochondrial dysfunction in *Drosophila*. In this study, these tools were used to induce mitochondrial dysfunction specifically in the nervous system of the fly, thus creating a novel neuronal model of mitochondrial dysfunction. As in previous studies, overexpression of *TFAM* resulted in a reduction of mitochondrial gene expression whilst expression of *mitoXhoI* resulted in linearization of mtDNA. In a *Drosophila* motor neuron model, mtDNA dysfunction caused a reduction in the number of synaptic mitochondria and a reduction in the glutathione redox potential within the mitochondrial matrix.

4.5.1. Overexpression of *TFAM* and expression of *mitoXhoI* result in mtDNA dysfunction

Previous studies have shown that the effects of overexpression of *TFAM* can be different depending on cell type, model organism and most importantly the ratio of the protein to mtDNA (Falkenberg et al., 2002; Ekstrand et al., 2004; Maniura-Weber et al., 2004; Pohjoismaki et al., 2006; Ylikallio et al., 2010). The results outlined in this study show that in *Drosophila*, when *TFAM* is in excess, mtDNA copy number is similar to control, however gene expression of mtDNA is compromised. Indeed, complex IV COX I protein levels were significantly reduced in wandering larvae overexpressing *TFAM*.

It is important to note that whilst TFAM overexpression did clearly result in mtDNA dysfunction, the methodologies used cannot allow us to conclude that the phenotypes observed are due to overexpression of TFAM itself rather than any other mitochondrial protein. Whilst studies in literature do emphasise that TFAM levels are crucial in determining mitochondrial function, it is also true that overexpression of several

mitochondrially- targeted proteins could affect mitochondrial function and result in disruption of the ETC. Several experiments outlined in this chapter would have therefore benefitted from the use of a mitochondrial-targeted control, such as over-expression of an inert mitochondrial target (for example, mito-GFP) which could have helped to validate the choice of TFAM overexpression as a tool of mitochondrial dysfunction.

Expression of *mitoXhoI* did not cause a statistically significant reduction in mtDNA levels, however it did cause a linearization of mtDNA. MtDNA is transcribed as two polycistronic mRNAs. Therefore, transcription of the majority of the mtDNA encoded genes is probably inhibited as *XhoI* cuts the strands at the *coxI* restriction site.

Overexpression of *TFAM* and expression of *mitoXhoI* specifically in the motor neurons of the fly resulted in a reduction in the number of mitochondria at the synapses at the third instar larval stage. Mitochondria at the synapses were quantified using a mitochondrial-targeted mitoGFP construct. Ideally, mitochondrial numbers would have been counted using an endogenous marker such as porin, however this was not possible as the porin antibody available was not efficient for use in immunohistochemistry, at least not to an extent that allowed for reliable quantification.

Overexpression of TFAM in the motor neurons also led to late pupal lethality in most cases, and the few adults which eclosed out of their pupal cases only survived for the first week. Flies overexpressing *mitoXhoI* in motor neurons did not survive past the late pupal stage, suggesting that mitochondrial dysfunction in these flies had an even more severe impact.

It could be that the phenotypes observed are directly due to the loss of synaptic mitochondria. Indeed, flies expressing a mutant form of the mitochondrial fission gene *drp1*, have also been shown to exhibit a loss of synaptic mitochondria at the larval NMJ, similar to what is observed in these models. Furthermore they also exhibit locomotor

defects at the adult stage (Verstreken et al., 2005). These mutant flies have reduced levels of ATP which is required for reserve pool tethering and release. Therefore, they exhibit a reduction in synaptic reserve pool vesicle mobilisation, which could be causing the synaptic and locomotor phenotypes. Further investigation is required to study whether a similar mechanism is occurring in the *TFAM* overexpressing and *mitoXhoI* expressing flies.

Neurotransmitter release at the synapses occurs at active zones found within individual boutons at the NMJ. In flies overexpressing *TFAM* or *mitoXhoI*, bouton number was not significantly altered. This suggests that the synaptic and behavioural phenotypes observed are due to a bioenergetic deficit resulting from a reduced number of mitochondria, rather than due to dysfunctional development of the NMJ as a structure.

As previously argued in section 1.12, studies on AD and PD models and post-mortem tissue have implicated a loss of synaptic activity and structure in the disease process. Therefore, overall our results support the theory that neuronal mitochondrial dysfunction might contribute significantly to these neuropathologies.

4.5.2. Redox state changes in flies overexpressing *TFAM* and expressing mito*XhoI*.

Since overexpression of *TFAM* and expression of *mitoXhoI* caused mitochondrial dysfunction at the synapses, it was of interest to investigate any redox changes in these mitochondria and surrounding cytosol. It is generally thought that dysfunctional mitochondria and oxidative stress are an inter-linked phenomenon and alterations in cellular redox state, towards a more pro-oxidative state, are regularly associated with ageing and neurodegeneration.

The results obtained in this study, however, suggest that when investigating redox changes specifically in the *Drosophila* motor neuron system, no pro-oxidative change is observed upon mitochondrial dysfunction.

Similar to observations reported by Albrecht et al., cytosolic glutathione redox potential in wild-type flies was more towards the reduced state in the motor neuron NMJs (Albrecht et al., 2011). Furthermore, cytosolic E_{GSH} was not significantly different in larvae overexpressing *TFAM* and expressing *mitoXhoI*. Therefore, these results support the findings of Albrecht et al., which suggest that cytosolic E_{GSH} is close to the lower end of the roGFP2 measuring range all throughout the organism, and that this lack of variation is suggestive of a stable and robust steady-state glutathione redox potential, which prevents the excessive oxidation of thiols on cytosolic proteins. However, as argued in section 4.4.3, it is possible that a further reduction in cytosolic glutathione redox potential in larvae overexpressing *TFAM* or expressing *mitoXhoI*, would have been undetected due to limitations of the technique used. In conclusion, the parameters set by this experiment might not be adequate for the efficient measurement of cytosolic glutathione redox potential in NMJs of larvae with mitochondrial dysfunction. An additional caveat to this experiment is that the use of such probes could potentially alter the mitochondrial membrane potential leading to reduced mitochondrial import. This could have been tested by using porin as a marker for mitochondrial number as well as integrity of the organelle. However, as previously stated (section 4.5.1) the porin antibody available was not found to be efficient in use for IHC.

Previous studies in *Drosophila* have also shown that during ageing, glutathione is present at a more oxidised state and hydrogen peroxide levels are increased in the whole organism (Rebrin et al., 2004; Cocheme et al., 2011). Albrecht et al., however, find that the observed steady-state cytosolic glutathione redox potential is also maintained in aged *Drosophila*,

suggesting that in this experimental setup, ageing does not directly correlate with a pro-oxidative state. Similarly, the data presented in this study indicate that cytosolic glutathione redox potential is also maintained in a steady reduced state in conditions of mitochondrial dysfunction.

Albrecht et al., also argue that mitochondrial E_{GSH} is much more variable in different tissue types (Albrecht et al., 2011). Similarly, data presented here suggests that the mitochondrial E_{GSH} in motor neurons was even more reduced in flies overexpressing *TFAM* and in flies expressing *mitoXhoI* than in controls. Therefore, mitochondrial dysfunction in motor neurons does not cause excessive oxidation within mitochondria, but conversely results in a more reduced state within the organelle. This might be due to the reduced number of functional mitochondria at the NMJ. Since the method used for inducing mitochondrial dysfunction results in a reduced expression of mitochondrial-encoded genes, as seen by the reduced levels of COXI, it is possible that the respiratory chain in these mitochondria is not as efficient and therefore generates less oxidative stress than in wild-type mitochondria.

Furthermore, studies have shown that knockdown of different complexes of the OXPHOS chain cause differential regulation of ROS levels. In 2008, Owusu-Ansah et al., showed that, in *Drosophila*, downregulation of the complex I gene *Pdsw* results in cell-cycle arrest at the G1 phase and a five-fold increase in ROS. Conversely, knockdown of the *CoVa* gene in complex IV resulted in a 20% decrease in ROS, whilst still blocking the cell cycle at G1 phase (Owusu-Ansah et al., 2008). Similarly, deletion of another gene required for complex IV assembly, *COX10*, in a mouse model of AD also resulted in a reduction in oxidative stress (Fukui et al., 2007), whilst an AD-*mitoPstI* mouse model exhibit no alteration in mitochondrial hydrogen peroxide production, suggesting that mitochondrial dysfunction did not trigger an upregulation of ROS. This further suggests that ROS regulation upon mitochondrial dysfunction is a complex process, and further work is required to elucidate

the role of ROS in the mitochondrial retrograde response. Investigating the mitochondrial and cytosolic redox states in larvae expressing *ATPSyn-Cf6* dsRNA might offer some insight into whether mitochondrial dysfunction induced upon downregulation of a Complex V gene, causes a differential regulation of ROS compared to overexpression of *TFAM* or expression of *mitoXhoI*.

4.5.3. Mitochondrial dysfunction leads to a transcriptional retrograde response.

A microarray analysis revealed that in the third larval stage, neuronal mitochondrial dysfunction leads to alterations in the nuclear transcriptome which clearly underline a mitochondrial retrograde response.

Indeed, both overexpression of *TFAM* and expression of *ATPSyn-Cf6* dsRNA, led to an increased expression of lactate dehydrogenase (*Impl3*) and trehalose transporter (*Tret1-1*) in post-mitotic neurons. Upregulation of *Impl3* and *Tret1-1* suggest a compensatory mechanism to upregulate glycolysis upon mitochondrial dysfunction, as an alternative to oxidative phosphorylation. Inhibition of OXPHOS is known to trigger a metabolic switch towards an upregulated rate of glycolysis (Freije et al., 2012). Downregulation of the gene encoding subunit Va of the OXPHOS complex IV (*CoVa*) in *Drosophila* S2 cells, has also been shown to induce increased glycolysis, with an upregulated expression of *Impl3* and *Tret1-1*. Glycolytic capacity of the cells was also overall increased upon *CoVa* knockdown (Freije et al., 2012). Additionally, studies of the mitochondrial retrograde signalling pathway in mammalian cancer cell lines have also revealed a metabolic shift towards glycolysis as well as upregulation of genes involved in mitochondrial biogenesis, cell adhesion, cytoskeletal markers, invasiveness, metabolism, transcription factors and alternative splicing (Guha et al., 2010; Guha and Avadhani, 2013) .

Such a metabolic shift towards glycolysis has already been shown to act in response to mitochondrial dysfunction in human *in vitro* studies, and lactic acidemia, an excess of lactic acid in the blood, is also known to occur in patients with mitochondrial diseases (Robinson, 2006; Distelmaier et al., 2015).

The microarray analysis also revealed an upregulation of the transcription factor *sima*, as well as a down-regulation of *Drosophila* insulin-like peptide *Ilp1* and *Ilp3*, and an upregulation of *Thor*, *Drosophila* 4E-BP. This is suggestive of a mitochondrial retrograde signal which is acting towards a downregulation of the mTOR (mechanistic target of rapamycin) pathway.

The mTOR pathway, the main component of which is the mTOR serine/threonine protein kinase, regulates cell growth, cell proliferation, cell motility, cell survival, protein synthesis, and transcription. Furthermore, it also regulates mitochondrial biogenesis and the translation of nuclear-encoded mitochondrial proteins via its inhibitory effects on the downstream translation suppressor, eukaryotic translation initiation factor 4E-BP1 (Zoncu et al., 2011).

Flies overexpressing *TFAM* and flies expressing *ATPSyn-Cf6* dsRNA demonstrate a down-regulated expression of *Ilp1* and *Ilp3*, ligands known to activate the mTOR pathway, as well as an upregulated expression of the translation suppressor *Thor*. Therefore, this might suggest that as an initial neuronal response, mitochondrial dysfunction exerts an inhibitory effect on the process of mitochondrial biogenesis and protein translation. This might be a neuroprotective response aiming to protect the nervous system from too much energy expenditure during such stressful conditions.

4.6. Conclusion

Overexpression of *TFAM* and expression of the restriction enzyme *mitoXhoI* specifically in the motor neurons in *Drosophila* results in mitochondrial dysfunction which elicits a synaptic phenotype at the NMJ.

A microarray analysis revealed that the induction of mitochondrial dysfunction specifically in the *Drosophila* post-mitotic nervous system, results in a mitochondrial retrograde response which encompasses an upregulation of *sima*, the *Drosophila* homologue of *HIF1α*, a downregulation of the mTOR pathway and an upregulation of the translational inhibitor *4E-BP*.

In order to better understand this mechanism, these microarray results were validated and this retrograde response was further investigated in *in vivo* models of *Drosophila* mitochondrial dysfunction. This data is presented in Chapter 5.

5. *In vivo* investigation of neuronal mitochondrial retrograde signalling in *Drosophila*

5.1. Introduction

As argued in Chapter 1, section 1.11, mitochondrial retrograde signalling is a phenomenon, mostly well known in yeast, in which mitochondria communicate back to the nucleus exerting an effect on nuclear gene expression.

This arrangement appears to be conserved throughout animal species; however the exact mechanism and signal transducers involved might differ. Recent studies have highlighted the presence of such a system in mammals, with several studies suggesting that an adaptive compensatory mechanism acts in response to mitochondrial malfunction. Such compensatory mechanisms observed include an increase in the expression of ETC complex subunits, increase in mtDNA biogenesis, alterations in nuclear DNA methylation and alterations in oxidative stress (Cannon et al., 2011; Bellizzi et al., 2012; Kao et al., 2012; Ling et al., 2012).

An overall incapability of maintaining these compensatory mechanisms might therefore result in the loss of cellular homeostasis and organism health. Alternatively, a long-term upkeep of such compensatory response might be toxic to the cellular environment and could therefore result in disease onset. Indeed, disruption of the mitochondrial retrograde response and compensatory mechanisms may contribute to several diseases including forms of cancer, type II diabetes and neurodegenerative disease such as AD and PD (Horan and Cooper, 2014).

In Chapter 4, I demonstrated that utilising *TFAM* overexpression as well as knockdown of the ETC complex V subunit *ATPSyn-Cf6* as tools of mitochondrial dysfunction in *Drosophila* post-mitotic neurons triggered a mitochondrial retrograde response causing differential expression of around 300 genes in both of the mitochondrial dysfunction models. Moreover, microarray analysis also revealed 142 of these genes were commonly differentially regulated suggesting that differential expression of some genes is a response

to general mitochondrial dysfunction, whilst other genes are regulated in response to a specific perturbation in mitochondrial function.

This chapter focuses on the genes whose expression is commonly regulated by mitochondrial dysfunction induced by overexpression of *TFAM* or knockdown of *ATPSyn-Cf6*. The regulation of these genes could offer insight into a retrograde mechanism which acts in response to mitochondrial dysfunction.

5.2. Chapter aims

Overexpression of *TFAM* and knockdown of *ATPSyn-Cf6* result in mitochondrial dysfunction which elicits a mitochondrial retrograde response, altering the expression of the nuclear transcriptome. Data presented in this chapter aim to validate the results obtained in a microarray carried out on *Drosophila* models of neuronal mitochondrial dysfunction. Furthermore, this *in vivo* setup was used to better understand the interaction of these differentially expressed genes to develop a working mechanism of mitochondrial retrograde signalling.

Therefore the general aims of this chapter include:

- To validate microarray results *in vivo*, in the *Drosophila* nervous system using bacterial *lacZ* reporters.
- To better elucidate the retrograde mechanism acting in response to mitochondrial dysfunction.
- To identify ways in which modulation of this retrograde response can be used to rescue behavioural and synaptic phenotypes in *Drosophila* models of mitochondrial dysfunction.

5.3. Materials and Methods

5.3.1. Fly stocks

Flies used for the experiments described in this chapter were fed and bred as outlined in 4.3.1 and 4.3.2.

Stocks used were:

Gal4 driver lines:

nSyb-Gal4 (Pospisilik et al., 2010) – post-mitotic neurons (synaptobrevin expressing)

OK371-Gal 4 (Bloomington,26160) – glutamatergic neurons

D42-Gal4 (Bloomington, 8816) – motor neurons

Background strain:

w^{1118} (Bloomington, 6326)

UAS Stocks :

UAS-TFAM 3M (chromosome II, generated by Umut Cagin, Bateman Lab) – *TFAM* overexpression

UAS-TFAM 10M (chromosome III, generated by Umut Cagin, Bateman Lab) – *TFAM* overexpression

UAS- mitoXhoI (Xu et al., 2008) – restriction enzyme targeting *mtDNA:CoI*

UAS-CD8GFP (Tear lab) – GFP expression in neuronal membranes

UAS-sima (Bloomington, 9582) – *sima* overexpression

RNAi lines:

Sima ^{HMS00832}(Bloomington, 33894) – *sima* RNAi

Sima ^{HMS00833}(Bloomington, 33895) – *sima* RNAi

LacZ reporter lines:

Thor-lacZ (Bloomington, 9558) – reporting expression of *Thor*

Ilp3-lacZ (Ikeya et al., 2002) – reporting expression of *Ilp3*

5.3.2. Larval CNS dissections

Wandering third instar larvae were briefly placed in ice-cold PBS (Oxoid, Thermo Scientific) to rinse away food. The larvae were then dissected with fine forceps (Agar Scientific) under a dissection microscope. The dissected brains were placed in a 1.5ml microcentrifuge tube containing 4% formaldehyde (Thermo Scientific) / PBS and left to fix for 30-45 minutes while on a shaking platform (Rotarod). Once fixed, the brains were washed for ten minutes three times in PBST (PBS, 0.1% Triton X 100). The brains were then blocked in 10% normal goat serum (NGS, Sigma-Aldrich) for 30 minutes. Once blocked, primary antibodies in 10% NGS/PBST were added to the brains (anti-beta-galactosidase (β-Gal), 1 in 1000, Abcam, 9361) and left to incubate overnight on a shaking platform at 4^{o}C. The tissue was then washed three times in PBST at ten minute intervals on a shaking platform at room temperature. Secondary antibodies (Goat anti-Chk AlexaFlour 555 (A21437), Life Technologies, 1 in 1000) were then added at the appropriate dilution and left to incubate for 1.5 hours whilst wrapped in aluminium foil so as to protect the fluorescent signal. The brains were again washed three times in PBST at ten minute intervals, prior to mounting onto slides. The brains were then fully dissected on the slide in PBS. Excess PBS was then removed and 15ul of Vectashield mounting media (Vector Laboratories) were added. Cover slips were then carefully placed to cover the tissues and the slides were stored at 4^{o}C until imaging. All tissue was imaged using a Zeiss LSM710 confocal microscope.

5.3.3. Microscopy and image processing

CNS tissue was dissected and imaged on a Zeiss LSM710 confocal microscope. Quantifications were carried out on maximum intensity projections which encompassed the whole region of interest.

Thor-lacZ expression in motor neuron cell bodies of VNC was measured as intensity of β-Gal using the point tool on Image J. The intensity was measured in approximately 24 motor neuron cell bodies and the average expression in each VNC was then calculated. *Thor-lacZ* expression in each experimental VNC was then normalised to expression levels in controls.

Ilp3-lacZ expression in CNS neurosecretory cells in the optic lobes was measured as intensity using the point tool on Image J. The intensity was measured in all 14 cells per brain (7 insulin secreting cells per hemisphere). Average expression in each CNS was then calculated and normalised to expression levels in controls.

5.3.4. Climbing (Negative geotaxis) assay

Climbing assays were carried out on males only. Males were collected, using CO_2 gassing, upon eclosion and kept separately from females in a vial with fresh food. The males were left at 25^{o}C for 24 hours, a time interval deemed sufficient to regain mobility and a normal metabolic profile following CO_2 anaesthesia (Colinet and Renault, 2012). The assay was then carried out on one-day old males between the hours of 8 am and 10 am in the morning, so as to record climbing ability at a standard time and circumvent variability due to the fly circadian clock.

An individual male fly was aspirated, via a mouth aspirator, into a 5mL Falcon pipette with a cut-off tip. The pipette was then tapped on the bench so that the fly fell to the bottom of the graduated pipette. The timer was started as soon as the fly starting climbing the pipette wall. The time was stopped after 10 seconds and the distance climbed was recorded. Trials

in which the flies paused or walked down the pipette were ignored. The climbing distance of each individual male was recorded 3 times and 10-14 flies were tested per genotype.

5.3.5. Wing inflation assay

D42-Gal4 driver was used to drive overexpression of *TFAM* (*TFAM o/e*), knockdown of *sima* (*sima* ^{HMS00832}), or *sima* RNAi in flies overexpressing *TFAM* (*sima* ^{HMS00832}*;TFAM o/e*). The progeny of each cross was left to develop at 25^{o}C. The wing phenotype of the adults was checked 24 hours after eclosion. The phenotype of the wings of both male and female flies was classified as inflated (normal), half-way inflated or folded. The data from two separate trials was pooled and the frequency calculated as a percentage.

5.4. Results

5.4.1. *Thor* expression is upregulated in *in vivo Drosophila* models of mitochondrial dysfunction

Microarray analysis on CNS tissue from third instar larvae overexpressing *TFAM* or knocked down *ATPSyn-Cf6* revealed an upregulation of *Thor,* encoding the cap-dependent translation inhibitor and mTOR downstream target 4E-BP1.

I wanted to validate whether such an upregulation is also observed *in vivo*, following mitochondrial dysfunction. Immunofluorescence using a 4E-BP antibody proved difficult as no clear signal, which would allow for efficient quantification, was observed. In *Drosophila*, gene expression can also be measured *in vivo* by monitoring the expression of the gene of interest that is under the control of a reporter gene such as bacterial *lacZ*. *LacZ* encodes beta-galactosidase (β-gal) and an anti- β-gal antibody was therefore used to measure levels of the gene product by immunofluorescence. Therefore, overexpression of *TFAM* or expression of *mitoXhoI*, were driven specifically in the motor neurons, and *lacZ* reporters

were used to measure the endogenous expression of genes of interest. This allowed for the validation of microarray results obtained *in vivo*.

Control flies exhibited a low level expression of *Thor* in motor neuron cell bodies in the ventral nerve cord (VNC). However, this expression was strongly upregulated in both flies overexpressing *TFAM* ($p = \leq 0.001$, Figure 5.1) and those expressing *mitoXhoI* ($p = \leq 0.001$, Figure 5.2). These results therefore validate the data obtained in the microarray and confirm that *Thor* expression is upregulated upon *Drosophila* mitochondrial dysfunction. Furthermore, the fact that its upregulation is also observed in flies expressing *mitoXhoI* suggests that this response is conserved in other cases of mitochondrial dysfunction.

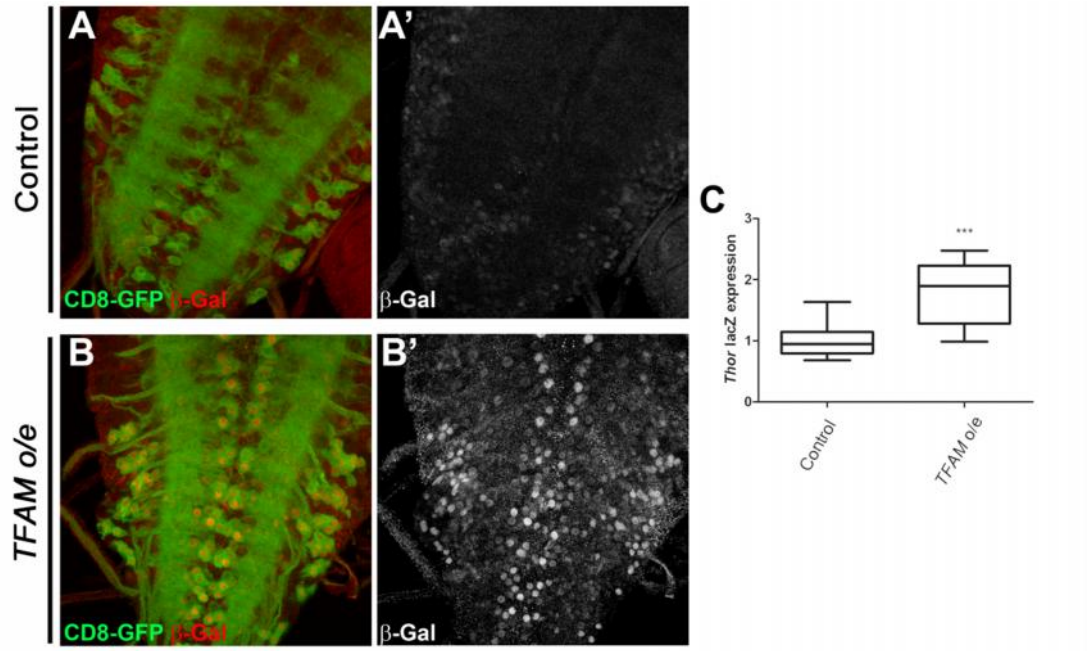

Figure 5.1 *Thor* expression is upregulated in flies overexpressing *TFAM*

Expression of *Thor-lacZ*, measured by β-Gal immunostaining, in motor neurons in VNC of control larvae (A-A') and in larvae overexpressing *TFAM* (B-B') using *OK371-Gal4, CD8-GFP*. Quantification of *Thor* expression levels normalised to control is shown in (C) (Unpaired t-test). Control n=21, *TFAM* overexpression n=16. ***= p = ≤0.001. The horizontal line in box and whisker plots represents the median whilst whiskers represent the 5th and 95th percentile. Control represents *OK371-Gal4, CD8-GFP>WIII8.*

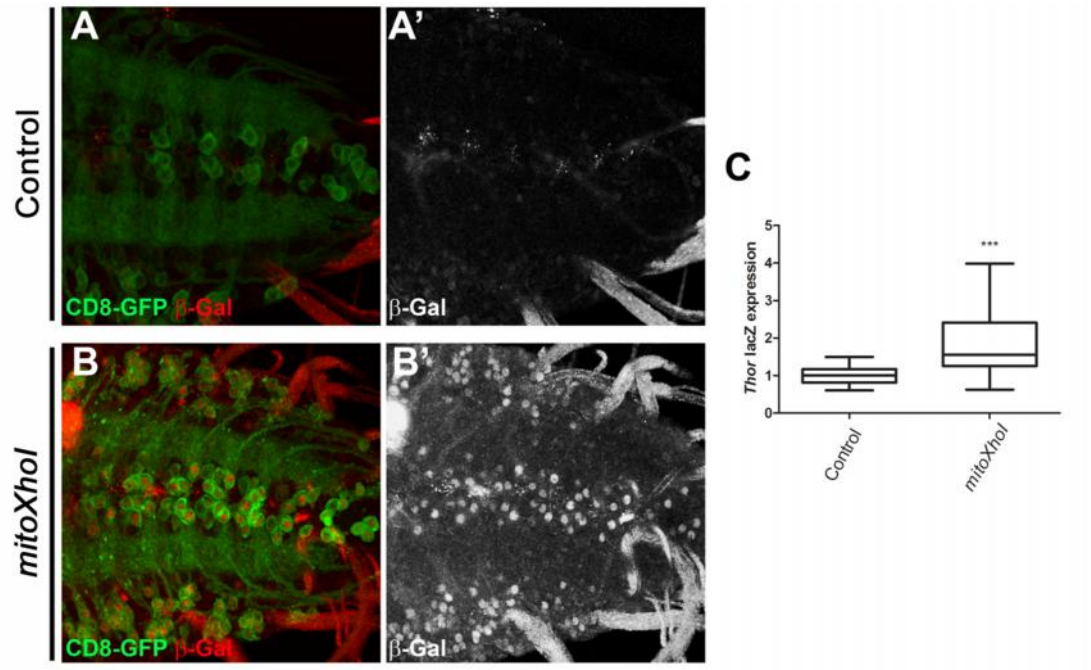

Figure 5.2 *Thor* expression is upregulated in flies expressing *mitoXhoI*

Expression of Thor-lacZ, measured by β-Gal immunostaining, in motor neurons in VNC of control larvae (A-A') and in larvae expressing *mitoXhoI* (B-B') using OK371-Gal4, CD8-GFP. Quantification of *Thor* expression levels normalised to control is shown in (C) (Unpaired t-test). Control n=18, *mitoXhoI* n=18. ***=p=≤0.001. The horizontal line in box and whisker plots represents the median whilst whiskers represent the 5th and 95th percentile. Control represents *OK371-Gal4, CD8-GFP>WIII8.*

5.4.2. *Ilp3* expression is downregulated in *in vivo Drosophila* models of mitochondrial dysfunction

Microarray analysis on third instar larvae overexpressing *TFAM* or expressing *ATPSyn-Cf6* dsRNA also revealed a downregulated expression of two *Drosophila* Ilps; *Ilp1* (fold change = 0.607 in *TFAM* o/e and 0.711 in *ATPSyn-Cf6* dsRNA) and *Ilp3* (fold change = 0.681 in *TFAM* o/e and 0.499 in *ATPSyn-Cf6* dsRNA).

In order to validate these results *in vivo, Ilp3* expression was measured in control larvae as well as larvae overexpressing *TFAM* and expressing *mitoXhoI* under the control of an *nSyb-Gal4* driver. *Ilp3* was found to be expressed in median neurosecretory cells and *Ilp3-lacZ* levels were found to be significantly decreased in *TFAM* overexpressing ($p=0.0012$) and *mitoXhoI* expressing larvae ($p=<0.0001$) compared to controls (Figure 5.3).

These results validate the data obtained by the microarray and also suggest that general modes of mitochondrial dysfunction might trigger a downregulation of *Ilp3* expression.

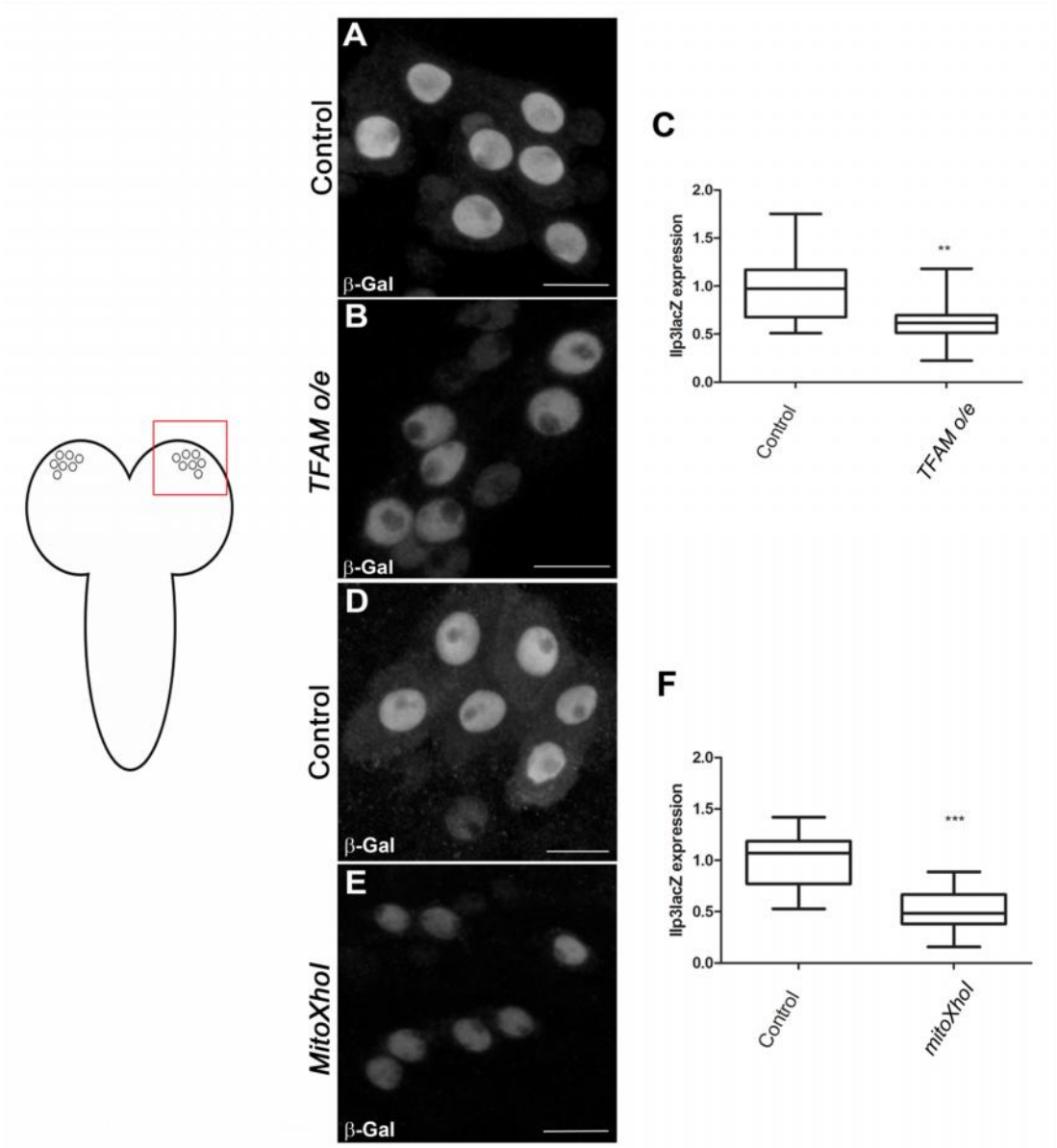

Figure 5.3 *Ilp3* expression is downregulated in flies overexpressing *TFAM* and flies expressing *mitoXhoI*.

Expression of *Ilp3-lacZ*, measured by β-Gal immunostaining, in neurosecretory cells in CNS of control larvae (A, D) and in larvae overexpressing *TFAM* (B) or expressing *mitoXhoI* (E), using *nSyb-Gal4*. Quantification of *Ilp3* expression levels in flies overexpressing *TFAM* normalised to control is shown in (C) (Unpaired t-test). Control n=15, *TFAM o/e* n=20. **=p≤0.01. Quantification of *Ilp3* expression levels in flies expressing *mitoXhoI* normalised to control is shown in (F) (Unpaired t-test). Control n=15, *mitoXhoI* n=15. ***=p=≤0.001. The horizontal line in box and whisker plots represents the median whilst whiskers represent the 5th and 95th percentile. In all cases, control represents *nSyb-Gal4>WIII8.*

5.4.3. *Ilp3* expression is downregulated upon overexpression of *sima*.

Multiple genes which were found to be differentially regulated in the microarray analysis are known targets of the transcription factor hypoxia inducible factor (HIF). HIF is a primary sensor of cellular oxygen levels and regulates cellular responses to hypoxia, including an upregulation of glycolytic processes (Majmundar et al., 2010). *Impl3*, a known *HIFα* target which encodes LDH in Drosophila (Firth et al., 1995; Lavista-Llanos et al., 2002), was upregulated in both *TFAM* overexpressing and *ATPSyn-Cf6* dsRNA flies (Table 12).

Similar (sima) is the Drosophila orthologue of *HIFα*. I hypothesised that sima is playing a role in the differential regulation of several genes in response to mitochondrial dysfunction. Therefore, in order to assess whether *sima* is acting to induce the downregulation of *Ilp3* upon mitochondrial dysfunction, *nSyb-Gal4* was also used to monitor *Ilp3-lacZ* expression in flies overexpressing *sima*.

This revealed that *Ilp3* expression is also significantly downregulated in flies overexpressing *sima*, ($p = 0.0003$, Figure 5.4) suggesting that the upregulation of *sima* upon mitochondrial dysfunction is the trigger for a downregulated *Ilp3* expression response.

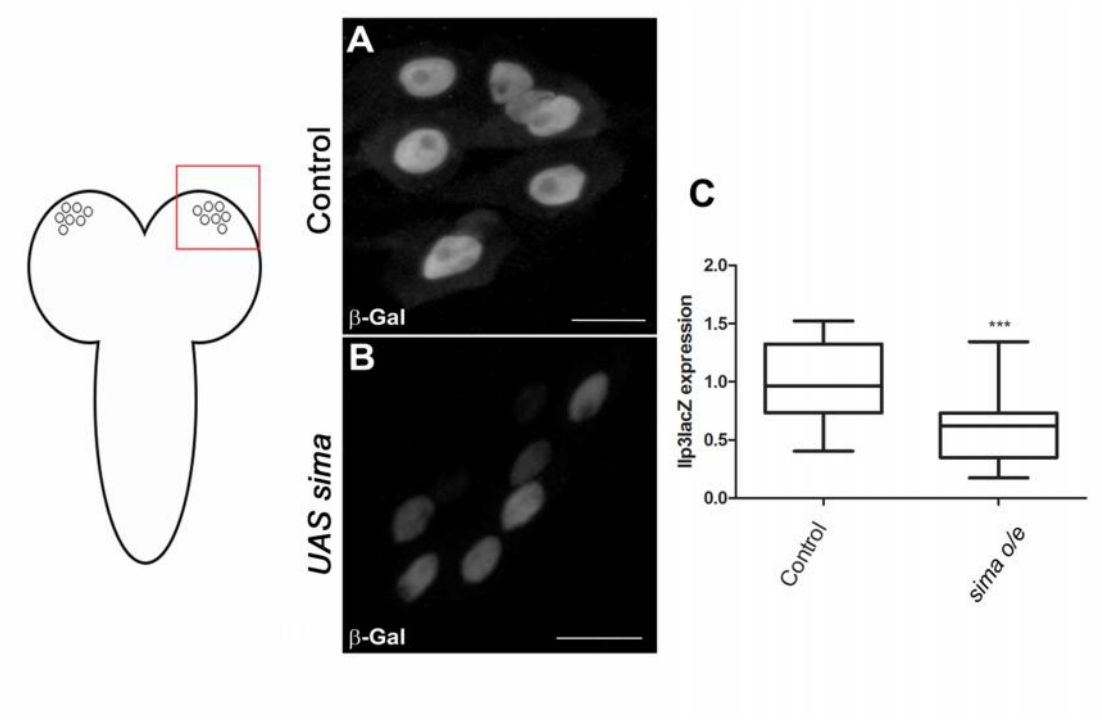

Figure 5.4 *Ilp3* expression is downregulated upon overexpression of *sima*
Expression of *Ilp3-lacZ*, measured by β-Gal immunostaining, in neurosecretory cells in CNS of control larvae (A) and in larvae overexpressing *sima* (B) using *nSyb-Gal4*. Quantification of *Ilp3* expression levels in flies overexpressing *sima* normalised to control is shown in (C) (Unpaired t-test). Control n=18, *sima o/e* n=22. ***=p=≤0.001. The horizontal line in box and whisker plots represents the median whilst whiskers represent the 5th and 95th percentile. Control represents *nSyb-Gal4>WIII8.*

5.4.4. *Thor* expression is upregulated upon overexpression of *sima*.

Since *sima* is a transcription factor, and since *Thor* was also upregulated in response to *TFAM* overexpression and *ATPSyn-Cf6* RNAi, it was of interest to investigate whether *sima* might be the factor responsible for the upregulation of *Thor* in such conditions.

Thor expression was found to be highly significantly upregulated upon overexpression of *sima* in *Drosophila* motor neurons (p = ≤0.001, Figure 5.5) suggesting that *Sima* acts to upregulate the expression of *Thor* upon mitochondrial dysfunction.

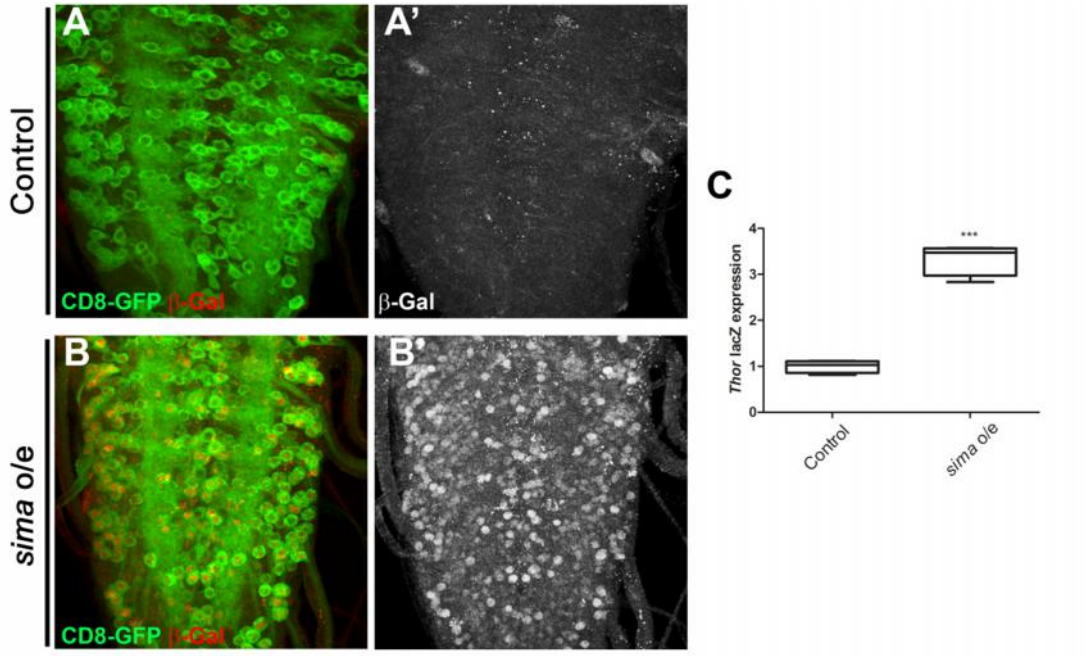

Figure 5.5 *Thor* expression is upregulated in flies overexpressing *sima*
Expression of *Thor-lacZ*, measured by β-Gal immunostaining, in motor neurons in VNC of control larvae (A-A') and in larvae overexpressing *sima* (B-B') using *OK371-Gal4, CD8-GFP*. Quantification of *Thor* expression levels normalised to control is shown in (C) (Unpaired t-test). Control n=4, *sima o/e* n=4. ***=p=≤0.001. The horizontal line in box and whisker plots represents the median whilst whiskers represent the 5th and 95th percentile. Control represents *OK371-Gal4, CD8-GFP >WIII8.*

5.4.5. Knockdown of *sima* restores *Thor* expression to control levels in flies overexpressing *TFAM*.

Since data described above suggested that *sima* might be the transcription factor involved in upregulating *Thor* expression upon mitochondrial dysfunction, this hypothesis was also tested *in vivo* by investigating how *Thor* expression is altered upon mitochondrial dysfunction in *Drosophila* CNS in which *sima* is knocked down.

Downregulation of *sima* in *sima* RNAi flies appeared to have no effect on *Thor* expression, as these flies exhibited similar levels of *Thor* expression as in controls, in VNC motor neuron cell bodies. As previously stated, *Thor* expression was significantly upregulated in flies overexpressing *TFAM*. However, when *OK371-Gal4* was used to drive *Thor-lacZ* in flies overexpressing *TFAM* and *sima* knock-down (*OK371-Gal4,Thor-lacZ > Sima RNAi; UAS-TFAM*), these flies exhibited similar *Thor* expression levels to control flies, and to flies expressing *sima* RNAi ($p=\leq 0.001$, Figure 5.6). Furthermore, *Thor* expression was significantly reduced when compared to flies overexpressing *TFAM* ($p=\leq 0.001$, Figure 5.6). This suggests that *sima* is necessary in order for *Thor* expression to be upregulated upon mitochondrial dysfunction induced by *TFAM* overexpression.

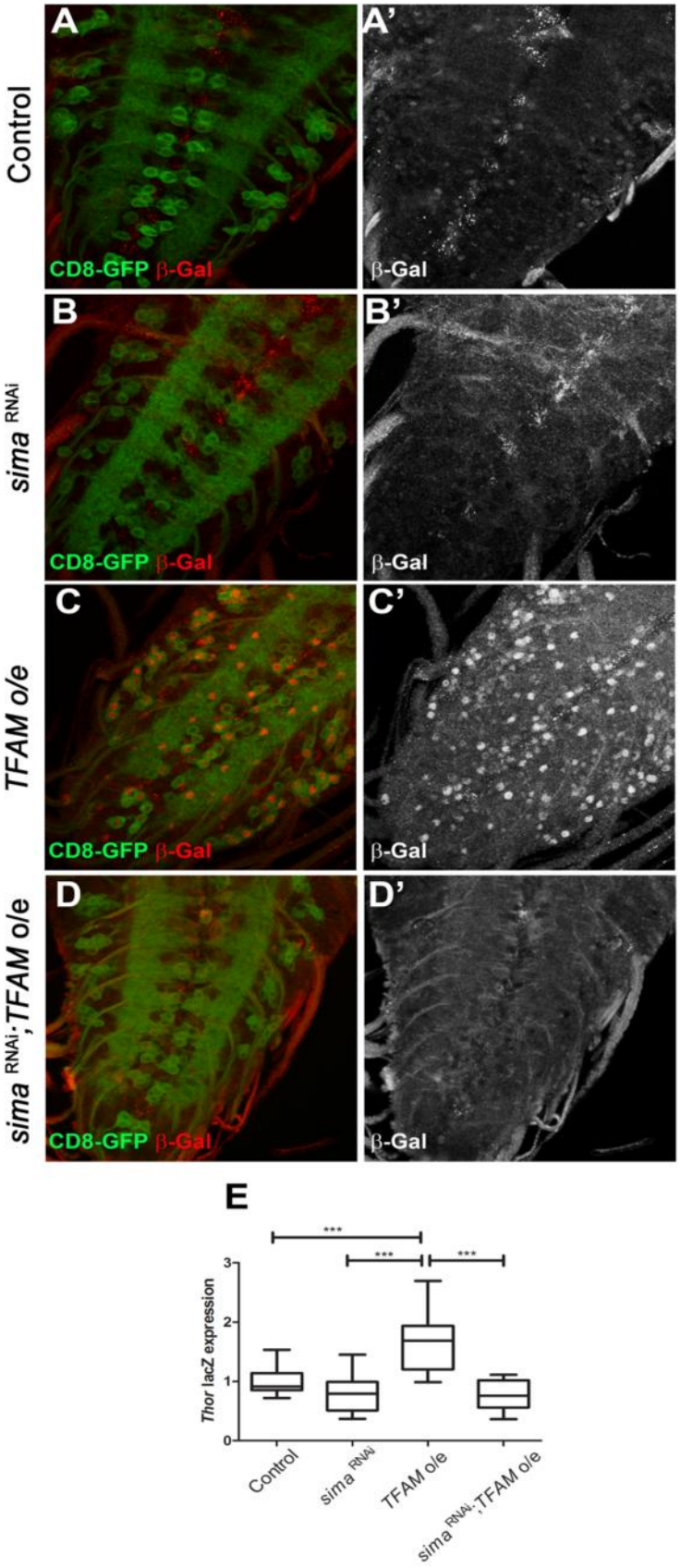

(Figure legend on next page)

Figure 5.6 *sima* RNAi inhibits upregulation of *Thor* in *TFAM* overexpressing flies.
Expression of *Thor-lacZ* levels, measured by β-Gal immunostaining, in motor neurons in VNC of control larvae (A-A'), in larvae expressing *sima* RNAi (B-B'), in larvae overexpressing *TFAM* (C-C') and in larvae expressing *sima RNAi; TFAMo/e* (D-D') using *OK371-Gal4, CD8-GFP*. Quantification of *Thor* expression levels normalised to control is shown in (E) (One-way ANOVA followed by Tukey's multiple comparison test). Control n=10, *sima* RNAi n=10, *TFAM o/e* n = 12, *sima RNAi; TFAM o/e* n=13. ***= p =≤0.001. The horizontal line in box and whisker plots represents the median whilst whiskers represent the 5th and 95th percentile. Control represents *OK371-Gal4, CD8-GFP >WIII8.*

5.4.6. Knockdown of *sima* has no effect on *Ilp3* expression flies overexpressing *TFAM*.

Overexpression of *sima* in larval CNS tissue was found to result in a reduced expression of *Ilp3* in neurosecretory cells, suggesting that upregulated levels of *sima* induced upon mitochondrial dysfunction could be responsible for the downregulated *Ilp3* levels observed. In order to further investigate the role of *sima* in the regulation of *Ilp3* expression, the *nSyb-Gal4* driver was used to drive *TFAM* overexpression and *sima* knockdown in post-mitotic neurons. The levels of the secreted peptide were then measured in the larval CNS of larvae.

Ilp3 levels in flies expressing *sima* knockdown were found to be similar to controls. Furthermore, the knockdown of *sima* bore no effect on the levels of *Ilp3* expression in larvae overexpressing *TFAM*, as *Ilp3* expression was still significantly decreased when compared to control (Figure 5.7).

This suggests that knockdown of *sima* alone is not sufficient to restore *Ilp3* expression to control levels in larvae with mitochondrial dysfunction.

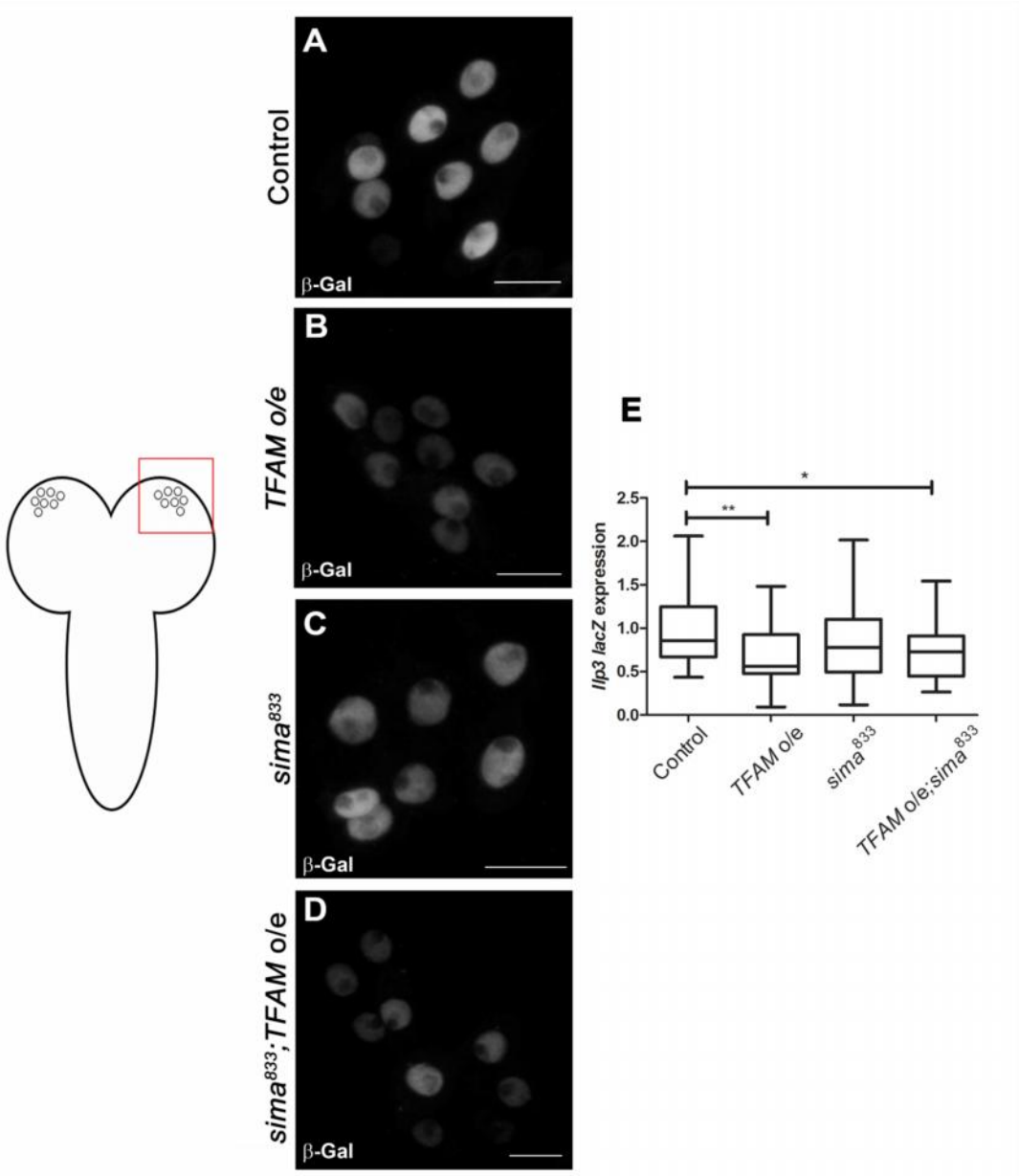

Figure 5.7 *sima* RNAi does not restore *Ilp3* expression levels in flies overexpressing *TFAM*.
Expression of *Ilp3-lacZ*, measured by β-Gal immunostaining, in neurosecretory cells in CNS of control larvae (A-A'), in larvae overexpressing *TFAM* (B-B'), in larvae expressing *sima* RNAi (C-C'), and in larvae expressing *sima RNAi; TFAMo/e* (D-D') using *nSyb-Gal4*. Quantification of *Ilp3* expression levels normalised to control is shown in (E) (One-way ANOVA followed by Tukey's multiple comparison test). Control n=37, *TFAM o/e* n = 32, *sima* RNAi n=27, *sima RNAi; TFAM o/e* n=29. *= p ≤0.05, **= p ≤0.01. The horizontal line in box and whisker plots represents the median whilst whiskers represent the 5th and 95th percentile. Control represents *nSyb-Gal4 >WIII8.*

5.4.7. Knockdown of *sima* partially rescues climbing and wing inflation ability of flies overexpressing *TFAM*.

In Section 5.4.5, mitochondrial dysfunction in *Drosophila* was found to elicit an upregulated expression of the cap-dependent translation inhibitor *Thor*, and the nuclear transcription factor *sima* was required for this upregulation to occur. In order to assess whether *sima* is also required for behavioural phenotypes exhibited upon mitochondrial dysfunction, the climbing ability of flies overexpressing *TFAM* in a *sima* RNAi background was assessed.

Flies overexpressing *TFAM* in motor neurons, under the control of a *D42-Gal4* driver, exhibit a significantly reduced climbing ability (Figure 5.8A). Flies expressing *sima* RNAi, exhibited no climbing phenotype and indeed climbed to similar distances as in control flies. Interestingly, flies overexpressing *TFAM* and downregulated *sima* (*sima*^{832}*;TFAM o/e*) exhibited a significantly improved climbing ability when compared to *TFAM* overexpressing flies. This suggests that functional *sima* is required for climbing ability to be compromised in flies overexpressing *TFAM*, and furthermore this also suggests that knockdown of *sima* partially rescues the locomotor defect observed upon mitochondrial dysfunction.

The *D42-Gal4* driver used to assess climbing ability is also expressed in bursicon-secreting neurons: crustacean cardioactive peptide (CCAP) neurons. The neuropeptide bursicon plays an important role in wing maturation during the last stages of metamorphosis. CCAP neurons activate the release of bursicon into the hemolymph during ecdysis, resulting in wing inflation and hardening of the wing cuticle. Inability to release bursicon due to inhibition of CCAP neuronal activity results in blocked wing inflation leading to adult wings which remain folded (Luan et al., 2006; Vanden Broeck et al., 2013).

Overexpression of *TFAM* under the control of the *D42-Gal4* driver resulted in a 54% reduction of inflated wings, with 15% having a partial inflation defect (Figure 5.8B,D) and

39% of wings being fully-folded (Figure 5.8B,E). Knockdown of *sima* in a *TFAM* overexpression background, however, significantly restored wing inflation ability with 93% of wings being inflated (Figure 5.8 B,C), 3% half-way inflated (Figure 5.8 B,D) and only 4% which remained folded (Figure 5.8 B,E). This suggests that mitochondrial dysfunction results in partial inhibition of CCAP neuronal activity which is restored upon knockdown of *sima*.

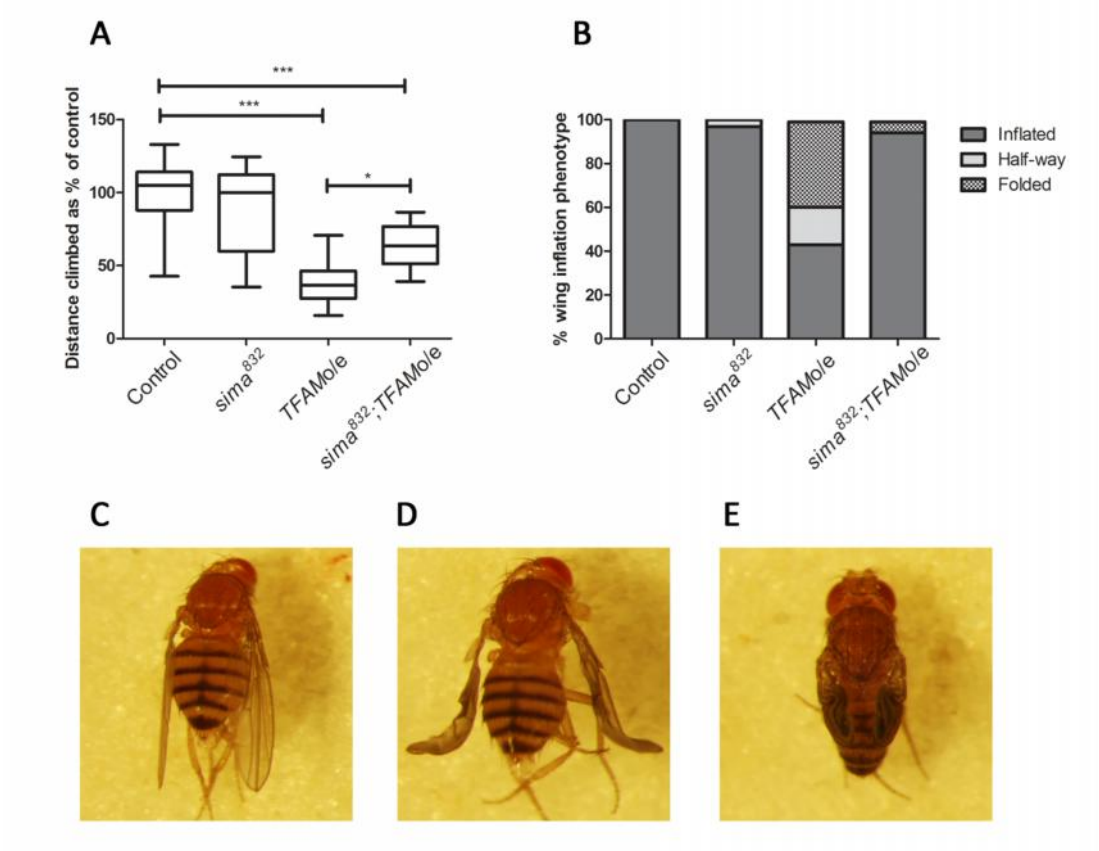

Figure 5.8 *sima* RNAi restores climbing and wing inflation ability in flies overexpressing *TFAM*.
(A) Climbing ability in flies expressing *sima* RNAi, *TFAM o/e*, and *sima* RNAi; *TFAM o/e* compared to control. n=13 for all. *=p=≤0.05, ***=p=≤0.001. The horizontal line in box and whisker plots represents the median whilst whiskers represent the 5th and 95th percentile. (B) Graphical representation of the proportion of flies with the different wing inflation phenotypes in control flies, flies expressing *sima* RNAi, flies overexpressing *TFAM* and flies expressing *sima* RNAi whilst overexpressing *TFAM*. (C-E) Representative images of flies with inflated wings (C), wings inflated half-way (D) and folded wings (E). In all cases control represents *D42-Gal4>WIII8*.

5.5. Discussion

In the final section of chapter 4, a microarray gene expression analysis showed that mitochondrial dysfunction elicits a mitochondrial retrograde response in the *Drosophila* larval nervous system. Amongst the genes differentially regulated upon mitochondrial dysfunction were ones pertaining to the mTOR pathway. The expression of two *Drosophila* insulin-like peptides, *Ilp1* and *Ilp3*, was downregulated whilst the expression of the *Drosophila* homologue of *4E-BP, Thor*, was significantly upregulated suggesting that mitochondrial dysfunction triggers nuclear transcriptional changes which result in a downregulation of the mTOR pathway.

In order to validate this work *in vivo*, I investigated levels of *Thor* expression in motor neuron cell bodies in the larval VNC and levels of *Ilp3* expression in neurosecretory cells in the larval CNS. *Ilp3* was also expressed at low levels throughout the VNC, although not at levels which were easily quantifiable.

5.5.1. The transcription factor *sima* mediates the downregulation of the mTOR pathway upon mitochondrial dysfunction.

In section 5.4.1, mitochondrial dysfunction, induced via overexpression of *TFAM* or expression of *mitoXhoI*, was shown to trigger an upregulation of *Thor* in *Drosophila* larval motor neurons. Similarly, in section 5.4.2, expression levels of *Ilp3* were found to be significantly reduced in *Drosophila* overexpressing *TFAM* and expressing *mitoXhoI*, thereby validating the microarray results in *in vivo* models of mitochondrial dysfunction.

Since several of the genes which were found to be differentially regulated upon mitochondrial dysfunction in the microarray were also transcription targets of the transcription factor *sima*, the *Drosophila* homologue of *HIF1α*, I also investigated its involvement *in vivo*. Overexpression of *sima* in an otherwise wild-type background resulted

in downregulated levels of *Ilp3* and upregulated levels of *Thor*, suggesting that *sima* is an upstream inhibitor of the mTOR pathway.

The next step was therefore to further investigate whether *sima* is in fact responsible for the differential regulation of *Ilp3* and *Thor* in the context of mitochondrial dysfunction. The knockdown of *sima* in larvae overexpressing *TFAM* resulted in *Thor* expression being restored to control levels. Therefore, *sima* is necessary to trigger an upregulation of *Thor* in response to mitochondrial dysfunction. Knockdown of *sima* was, on the other hand, not sufficient to restore *Ilp3* expression levels in larvae with mitochondrial dysfunction.

5.5.2. *Sima* knockdown is not sufficient to restore *Ilp3* expression levels upon mitochondrial dysfunction.

Eight insulin-like peptides and one insulin receptor (dInR) have been identified in *Drosophila* (Fernandez et al., 1995; Brogiolo et al., 2001; Gronke et al., 2010; Colombani et al., 2012; Garelli et al., 2012). Ilps 1, 2, 3 and 5 are secreted by the 14 brain insulin producing cells (IPCs) in the larval central brain, in both a systemic and paracrine fashion, acting to induce growth and differentiation (Geminard et al., 2009; Nassel et al., 2013).

The regulation of the secretion of the different Ilps in response to environmental and systemic stimuli is not well elucidated. Certainly, Ilp release acts in response to nutrient availability. After feeding, elevated glucose and amino acid levels in the circulation are sensed by the fat body which, as a consequence, releases signals into the hemolymph. These signals then reach the brain and the IPCs, which in turn regulate secretion of the Ilps (Geminard et al., 2009). The expression and functionality of the different Ilps appears to be quite complex and they appear to exert a certain degree of functional redundancy, with Ilps compensating for each other's expression levels. Furthermore, studies also suggest that Ilps themselves might provide feedback onto the brain IPCs. Overexpression of *Ilp6* has been

shown to lead to reduced levels of *Ilp2* and *Ilp5* (Bai et al., 2012), whilst knockdown of *Ilp2* leads to increased levels of *Ilp3* and *Ilp5* mRNA (Broughton et al., 2008).

Therefore, since *Ilp* expression is regulated by a multitude of factors, it is not surprising that knockdown of *sima* was not sufficient to restore *Ilp3* expression upon mitochondrial dysfunction. In order to better understand the consequences of Ilp regulation upon mitochondrial dysfunction, one must investigate the expression levels of other Ilps to identify any compensatory regulation. Furthermore, one must also note that feeding behaviour was not monitored in the mitochondrial dysfunction models described in this study. It would be of interest to investigate whether differential regulation of *Ilp* expression is a direct consequence of mitochondrial dysfunction and regulation by *sima*, or whether mitochondrial dysfunction is causing a disturbance to the feeding behaviour or to the nutrient-sensing pathway to the IPCs, thereby indirectly causing a reduced *Ilp3* expression.

Another important note to take into consideration is that the different Ilps expressed in the IPCs are independently transcriptionally regulated. Could different stress responses, such as mitochondrial dysfunction, trigger a differential transcription regulation of one *Ilp* versus the other? If this were the case would the differential regulation be beneficial because of a particular affinity for the one known dInR, or could it be because the differentially regulated Ilp could exert a function which is beneficial to the organism in response to the insult?

5.5.3. Mitochondrial dysfunction triggers a downregulation of cap-dependent mRNA translation

Overexpression of *TFAM* and knockdown of *ATPSyn-Cf6* both triggered a transcriptional upregulation of *Thor*, encoding *Drosophila* 4E-BP1, which was further shown to be upregulated *in vivo* in response to expression of *mitoXhoI*. This suggests that mitochondrial

dysfunction triggers a downregulation of the mTOR pathway resulting in downregulated cap-dependent translation.

Under normal physiological conditions, activated mTOR will act to inhibit 4E-BP1 via phosphorylation, which will allow for cap-dependent mRNA translation to proceed. If mTOR is inhibited, 4E-BP1 will be hypophosphorylated, allowing it to bind to eIF4E, thereby inhibiting the formation of the eIF4F complex which is required for protein synthesis (Figure 5.9). Therefore, essentially, downregulation of the mTOR pathway and consequent upregulation of active 4E-BP1, results in decreased protein synthesis.

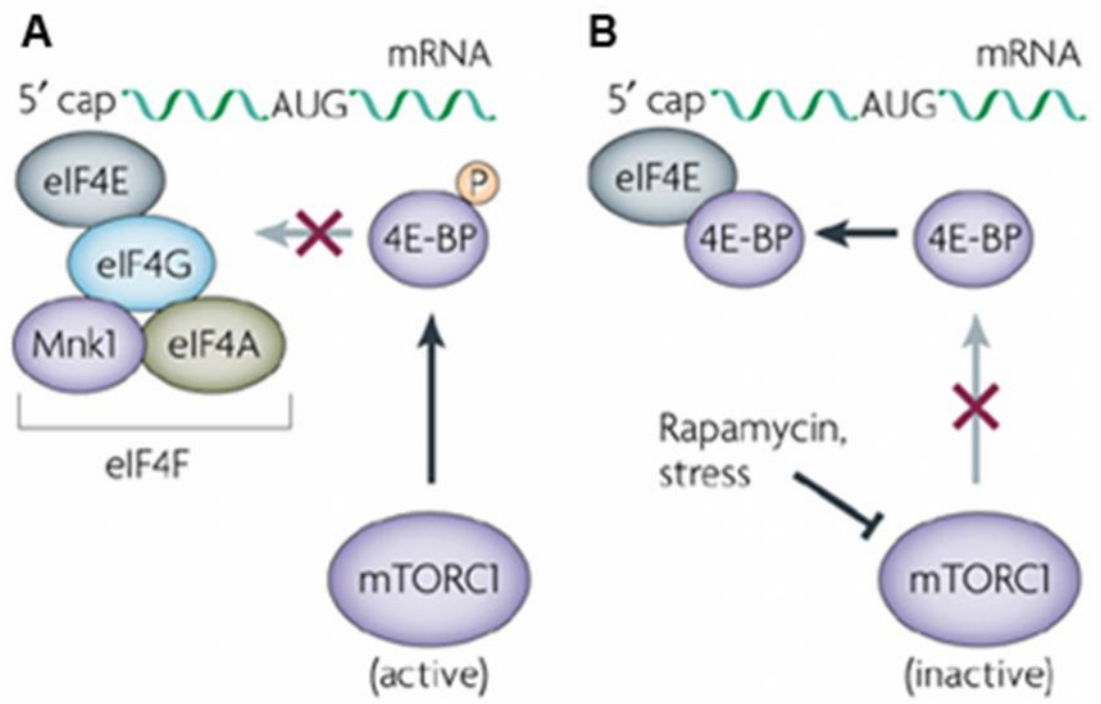

Figure 5.9 Active mTORC1 phosphorylates 4E-BP, promoting 5' cap-dependent mRNA translation
mTORC1 controls 4E-BP phosphorylation thereby regulating its binding to eIF4E. (A) When mTORC1 is active, it phosphorylates 4E-BP, rendering it unable to bind to eIF4E. EIF4E is therefore free to bind to eIF4G, which upon binding with the other components, mitogen-activated protein kinase-interacting kinase 1 (Mnk1), and the RNA helicase eIF4A, completes the eIF4F complex at the 5' cap. Translation is now able to be initiated. (B) When mTORC1 is inactive, 4E-BP becomes hypophosphorylated and can bind to eIF4E. EIF4E is therefore now dissociated from the rest of the eIF complex and translation cannot proceed (Buchkovich et al., 2008).

How does this relate to the context of mitochondrial dysfunction in neurodegeneration? If the initial retrograde response to mitochondrial dysfunction involves an upregulation of *sima* and a subsequent downregulation of cap-dependent mRNA translation, one would think that this is a stress response mechanism which aims to minimise activity which requires a high degree of energy expenditure whilst maintaining a minimal neuronal activity. Inhibition of this response via downregulation of *sima*, resulted in 4E-BP1 levels being restored to control levels and rescue of climbing and wing inflation ability. Therefore *sima* knockdown restores cap-dependent protein translation, whilst also promoting locomotor activity as well as CCAP neuronal activity. Further work is required to understand whether downregulation of *HIF1α* could be used therapeutically to treat mitochondrial dysfunction in the context of neurodegeneration, or whether restoration of an enhanced neuronal activity would actually be more harmful than beneficial in a prolonged mitochondrial dysfunction scenario. This is further discussed in section 6.

6. Conclusions and general discussion

6.1. Summary of findings

The brain is the most energy demanding organ in the human body and is therefore highly reliant on efficient mitochondrial function and ATP production. Mitochondrial dysfunction is linked to an array of diseases and is commonly associated with neurodegenerative diseases including AD and PD.

In this thesis, a SNP in mitochondrial transcription factor A, *TFAM* SNP rs2306604 A>G, is shown to be associated with an increased risk of PD in males. Furthermore, this association was even greater in males who were diagnosed with PDD. No such association was found with DLB, a form of dementia which develops shortly after the onset of motor symptoms in PD. This is the first study which reports a genetic association that might distinguish PDD from DLB, and further confirms the importance of TFAM and mitochondrial function in neuronal integrity.

In order to investigate the role of neuronal mitochondrial dysfunction in neurodegeneration, *TFAM* overexpression and expression of the mitochondrially-targeted restriction enzyme *mitoXhoI,* were used to induce mitochondrial dysfunction in *Drosophila melanogaster*. Microarray gene expression analysis revealed that mitochondrial dysfunction in third instar larvae post-mitotic neurons triggered a mitochondrial retrograde response. This response included a metabolic shift demonstrated by upregulated glycolysis as well as a downregulation of the mTOR pathway, resulting in elevated expression of the cap-dependent translation repressor 4E-BP1. The transcription factor HIF1α was found to play a critical role in modulating the mTOR pathway response; *HIF1α* knockdown restored *4E-BP1* expression to control levels and rescued climbing and wing inflation phenotypes, following mitochondrial dysfunction.

In conclusion, mitochondrial dysfunction in *Drosophila* triggers a mitochondrial retrograde response which induces a downregulation of cap-dependent mRNA translation, modulated by the transcription factor HIF1α.

6.2. General discussion

Parkinson's disease (PD) is a devastating neurodegenerative disease that affects 1 in 20 people over the age of 85. It is characterised by reduced motor function due to a dopaminergic deficit in the substantia nigra. PD patients however, also exhibit a set of non-motor symptoms including cognitive decline, which may lead to PDD in approximately 80% of cases (Buter et al., 2008). To date, there is no known cure for PD or PDD and the treatments available are solely symptomatic.

PDD symptoms show considerable similarity to those exhibited in another form of dementia, dementia with Lewy bodies (DLB). The two are in fact commonly misdiagnosed at clinical presentation, and there is little known regarding factors which may differentiate between the two. Currently, the two dementia forms are distinguished primarily based on the temporal onset of cognitive decline in relation to motor symptoms. This 'one year rule' diagnosis, as it is commonly known, states that patients who exhibit cognitive decline within the same year of motor symptoms are diagnosed as having DLB, whilst those who exhibit cognitive decline at a later stage are classified as PDD patients (McKeith, 2006).

As in other neurodegenerative diseases, several studies provide evidence of mitochondrial dysfunction contributing to the onset and progression of PD. Perhaps the most convincing piece of evidence is the decrease in activity of ETC complex I which has been repeatedly observed in PD patients (Parker et al., 1989; Schapira et al., 1990a; Shoffner et al., 1991). However, not much is known regarding the role of mitochondrial dysfunction during the onset of cognitive decline in PD patients and whether mitochondrial function is differentially affected in PDD compared to DLB.

Autere and colleagues have provided evidence that polymorphisms in mtDNA-encoded Complex I genes may exert a susceptibility to PD, but that this risk is mostly dependent on the number of non-synonymous substitutions in these genes in the various mtDNA lineages (Autere et al., 2004). They found that there is a greater presence of non-synonymous substitutions in mtDNA-encoded Complex I genes in the haplogroup supercluster JTWIX compared to other clusters and that this group exhibits an increased risk of PD and advancement to PDD. In fact, this study revealed a greater number of amino acid replacements in these genes in the JTWIX group which may lead to a greater decline in Complex I activity and an increased risk of progression of PD onto PDD. Furthermore, in mtDNA, polymorphisms are routinely accompanied by other polymorphisms. Therefore, the increased risk of pathology could be due to a combination of polymorphisms occurring together rather than directly due to a single mutation. In fact, there are several lines of evidence which show that combinations of otherwise harmless individual mtDNA polymorphisms in a particular lineage may increase susceptibility to complex diseases when present together (Wallace et al., 1999; Chinnery et al., 2000; Ruiz-Pesini et al., 2000).

MtDNA works in conjunction with the nuclear genome to maintain cellular hometostasis. Therefore, coordinated interplay between mitochondrial and nuclear factors is indispensable for functional mitochondrial activity. Several studies have also assessed the risk attributed to polymorphisms in nuclear genes which have roles in mitochondrial function and biogenesis including the transcription factor TFAM. Studies discussed all throughout this thesis have highlighted the necessity of TFAM for efficient mitochondrial function. Homozygous *TFAM* mutant mice, which were devoid of mtDNA, died *in utero* in a 1998 study carried out by Larsson and colleagues (Larsson et al., 1998). Therefore, it is not surprising that no pathogenic *TFAM* mutations have been identified in AD or PD patients. One would assume that mutations in such a crucial factor for mtDNA stability would lead to much earlier symptoms, and presumably earlier lethality. Any alterations in TFAM

associated with AD and PD must therefore only result in a weak functional consequence, as individuals carrying the mutation would have survived well into adulthood with relatively efficient mitochondrial function.

A SNP in intron 4 of the *TFAM* transcript, *TFAM* SNP rs2306604 A>G has, however, been shown to be significantly associated with a higher risk of AD (Bertram et al., 2007; Laumet et al., 2010). Results obtained from studies of this SNP in association with PD, however, have not been very robust; GWAS and meta-analysis have found no association of the SNP with an increased risk of PD, (Belin et al., 2007; Alvarez et al., 2008b; Pankratz et al., 2009; Simon-Sanchez et al., 2009; Lill et al., 2012) whilst one study suggested that rs2306604 G/G is an independent risk factor for PD (Gaweda-Walerych et al., 2010). The study presented in this thesis is the first reported investigation of the association of *TFAM* rs2306604 A>G with PD and PDD.

Results presented in Chapter 2 suggest that this SNP exhibits significant association with PD in males but not in females, and that it is the A/A genotype that presents itself as the risk factor for disease development, as is found in AD cases. Furthermore, results obtained from this cohort study suggest that the association is much greater in PDD patients with the rs2306604 A>G SNP being much more strongly associated in PDD males than controls. This association was not significant in DLB cases. Therefore, this study is the first to imply there might be genetic polymorphisms which might distinguish PDD from DLB. This suggests that there might be a genetic predisposition which plays a role in determining the temporal onset of cognitive decline following presentation of motor symptoms.

It is important to note that this study does not take into account mtDNA genetic background of the cohort cases. As discussed above, mtDNA lineages are important in determining mitochondrial function as well as affecting the expression of nuclear genes which regulate mitochondrial function, such as TFAM. Therefore, additional study is

required to investigate whether the fact that *TFAM* SNP rs2306604 A>G is associated with PDD but not with DLB is due to an underlying difference in mtDNA background, or whether it is a distinguishing feature which is independent of mtDNA lineage.

Additionally, studies have suggested that the combined presence of *TFAM* rs2306604 SNP G/G and parkin variant, *PARK2* G/G V380L present an increased risk of PD in a mitochondrial HV cluster background (Gaweda-Walerych et al., 2010; Gaweda-Walerych et al., 2012). Again, this confirms that there are multiple factors which are to be taken into account when analysing SNP genetic associations and there might be a multitude of factors which contribute to the result obtained in this study. Unfortunately, due to unavailability of additional information, the association study was thereby limited to the data presented in chapters 2 and 3.

PDD patients in the cohort studies also had a significantly lower mtDNA copy number in the pre-frontal cortex compared to controls, and this mtDNA reduction was even greater than in PD patients. This was an interesting finding, considering that little is known regarding the role of mtDNA copy number in PD progression to PDD. A reduction in mtDNA levels in the prefrontal cortex is similarly observed in AD cases (Rodriguez-Santiago et al., 2001). This further supports the hypothesis that AD and PDD exhibit similar neuropathological characteristics and that mitochondrial dysfunction in this brain region might be indicative of a general form of cognitive decline.

Interestingly, we found no association between mtDNA copy number and rs2306604 genotype in the cohort used, suggesting that *TFAM* SNP rs2306604 A>G does not influence mtDNA copy number. *TFAM* SNP rs2306604 A>G was also found to bear no effect on mitochondrial-associated protein levels. According to the statistical analyses used, any changes observed in these parameters were purely due to the different diagnosis and not due to the rs2306604 genotype of the individual. Alternatively, such an association might

exist but is not traceable utilising the methods we used for measurement of mtDNA copy number and protein levels. Analysing levels in whole brain tissue homogenate in fact, might have provided misleading results as it could be diluting an effect, thereby masking an association. Measurement of mtDNA and protein levels in individual neurons from the prefrontal cortex might provide a clearer identification of such an association.

Previous studies have suggested that the presence of this SNP could lead to an alternative splice form of *TFAM*, leading to the generation of a truncated 22kDa form of the protein. Western blot analysis carried out in this thesis only revealed the presence of the mature 24kDa form of the protein, suggesting that this truncated form is not present within any of the cohort cases, or that it is not traceable using the technique we utilised, as discussed in section 3.5.3. The functional consequences of *in vivo* presence of *TFAM* SNP rs2306604 A>G therefore remain unknown.

It is important to note that PD pathogenesis may result from a particular genetic predisposition, environmental factors as well as changes associated with ageing. Mitochondrial dysfunction is only one of the molecular mechanisms associated with PD. Inflammation, impairment of the ubiquitin-proteosome system, impairment of the protein folding system and abnormalities in cellular transport are additional mechanisms which are associated with PD and which could equally contribute to disease progression.

Individual association studies may bring something new to the field in terms of uncovering new potential therapeutic avenues and identifying genetic risk factors. However, in order for robust reliable statistical power to be inferred from these studies, there needs to be a much greater case number utilised. Furthermore, the need for exhaustive clinical, demographic and lifestyle information is imperative. Recent studies have highlighted that caffeine intake, smoking and exposure to mitochondrial toxins might all be contributing to risk of the disease. It would therefore be crucial to have such information available as it

could shed light on confounding factors that might be interfering with the results obtained from the study. As argued by Gaweda-Walerych et al., a holistic approach, comprising all of the factors available, including mitochondrial dynamics and bioenergetic data, oxidative stress information, as well as a clearly understood mtDNA genetic background, would be the best way of carrying out and interpreting association studies (Gaweda-Walerych and Zekanowski, 2013). This might be the only way to ultimately determine whether specific genetic variants might be causing a susceptibility to PD or PDD risk and whether their identification could be useful in establishing methods of therapy that are based on these genetic markers. Therefore, I propose that a higher number of cases as well as more comprehensive medical history information would be required to further extend the study outlined in this thesis, and to better apprehend the involvement of *TFAM* SNP rs2306604 A>G in different forms of neurodegeneration.

Ultimately, human post-mortem tissue studies serve to obtain correlative data and determine genetic associations. *In vivo* models are required to better understand the role of mitochondrial biogenesis, dynamics and overall function in the progression of the disease. Indeed, mitochondrial dysfunction has been investigated in several neurodegenerative disease models, which have been covered in detail in sections 1.10 and 1.12. However, the initial response of neurons to mitochondrial dysfunction and the downstream mechanism which elicits neuronal death is still not well understood. Since mitochondrial dysfunction and synapse loss appear to be early hallmarks of neurodegenerative disease, mitochondria might well be an efficient therapeutic target. If mitochondrial dysfunction is an early symptom that might lead to a downward spiral, then trying to understand this mechanism could uncover the truth behind the process of neurodegeneration.

Recently generated mouse models of mitochondrial dysfunction include the MitoPark mouse, in which *TFAM* is conditionally knocked out in dopaminergic neurons. This animal exhibits adult-onset parkinsonian phenotypes including loss of motor ability and tremors, neuronal loss in the substantia nigra, as well as intraneuronal inclusions (Ekstrand et al., 2007). Similarly, the expression of a mitochondrially targeted endonuclease – *mito-PstI* in mouse dopaminergic neurons, generated parkinsonian like phenotypes. As in mitoPark mice, motor ability was reduced, dopamine levels were reduced and there was neuronal loss in the substantia nigra (Pickrell et al., 2011). Furthermore, both models exhibited reduced levels of mtDNA copy number.

TFAM is a major regulator of mtDNA transcription and replication, which controls mtDNA copy number in cells. As discussed in section 1.7.2, TFAM binds to mtDNA and is responsible for its bending into a particular conformation, and ratios of TFAM to mtDNA are particularly important in maintaining optimal efficiency of transcription and replication of the genome. MtDNA decline is generally observed upon *TFAM* knockdown, consistent with the fact that TFAM is required for mtDNA transcription and replication. Subsequently, studies have shown that *TFAM* overexpression might attenuate certain mitochondrial dysfunction phenotypes observed in neurodegenerative disorders. For example, *TFAM* overexpression has been shown to reduce oxidative damage induced by β-amyloid treatment in SH-SY5Y cells (Xu et al., 2009). Similarly, in a mouse model of ALS, overexpression of human *TFAM* was found to reduce oxidative stress and motor neuron cell death and generally delayed onset of disease (Morimoto et al., 2012).

However, as previously argued, the beneficial aspects of TFAM overexpression are highly dependent on cell type, model organism and most importantly on an efficient balance of TFAM to mtDNA. Studies have shown that *TFAM* overexpression in mice results in an increased proportion of mtDNA deletions and reduced respiration in muscle and heart

tissue (Ylikallio et al., 2010). Consistent with these findings, data presented in this thesis suggests that excess TFAM in *Drosophila* does not alter mtDNA copy number, however, it does result in the suppression of mitochondrial gene expression, as levels of a mitochondrial-encoded protein were significantly reduced. As also previously argued (section 4.5.1), one must note that due to the highly dynamic nature of mitochondrial processes, the over-expression of several mitochondrial proteins could result in an alteration of mitochondrial gene expression. Therefore, a caveat of this study is that no 'unreactive' mitochondrial-targeted control was used to validate this tool. The expression of mitochondrial-targeted constructs such as mitoGFP or other mitochondrial proteins, could help determine whether the mitochondrial dysfunction observed is due to alterations of TFAM or whether it is simply due to alterations in the general balance of mitochondrial proteins.

In this thesis, an additional tool for inducing mitochondrial dysfunction - expression of a mitochondrially-target restriction enzyme *mitoXhoI*, which cuts mtDNA at the *CoI* site, resulted in linearization of mtDNA. MtDNA undergoes transcription as two polycistronic mRNAs. Therefore, linearization of the genome leads to reduced transcription of mitochondrially-encoded genes, leading to mitochondrial dysfunction.

In order to better understand the initial role of mitochondrial dysfunction in neurodegeneration at the cellular and functional level, we triggered mitochondrial dysfunction specifically in *Drosophila* motor neurons and investigated the NMJ, which has been repeatedly praised as the ideal structure for studying synaptic mechanisms (Katz, 1996; Ribchester, 2009). Overexpression of *TFAM* and expression of the mitochondrially-targeted restriction enzyme *mitoXhoI*, resulted in a severe loss of mitochondria at the synapses and behavioural defects. A third model of mitochondrial dysfunction, knockdown of coupling factor 6 of ATP synthase, which targets the respiratory chain, was also utilised.

Microarray gene expression analysis on larvae overexpressing *TFAM* and *ATPSyn-Cf6* dsRNA revealed a differential regulation of hundreds of nuclear genes. Approximately half of the genes that were differentially regulated differed depending on whether mitochondrial dysfunction was induced by overexpression of *TFAM* or knockdown of *ATPSyn-Cf6*. This confirmed that different forms of mitochondrial dysfunction do affect nuclear gene expression differently. A previous study, investigating changes in nuclear transcription upon mtDNA loss (ρ^o cells) or the presence of a 3243 A>G mutation also identified differences in the retrograde response depending on the specific mitochondrial insult (Jahangir Tafrechi et al., 2005). Similarly, a later study also identified a differential response in transcription dependent on a 3243 A>G mutation load in mtDNA, which is a mutation associated with maternally inherited diabetes and deafness (MIDD) as well as the neuromuscular MELAS syndrome (van den Ouweland et al., 1992; Jacobs, 2003). The study found that nuclear gene expression changes differently according to mtDNA 3243A>G heteroplasmy in transmitochondrial cybrids (Picard et al., 2014). The possibility of interference due to previously discussed issues of karyotype instability in cybrids (section 1.12.1) was excluded for several reasons. Firstly, changes in cybrid nuclear DNA genes were non-random in relation to mtDNA 3243A>G heteroplasmy. Secondly, transcriptional gene expression phases were found to be independent of clonal origins of the 143B (TK^-) nuclei. Lastly, the 3243G heteroplasmic mtDNAs were transferred from 143B (TK^-) cybrids into SH-SY5Y neuroblastoma cybrids and similar gene expression profiles were obtained (Picard et al., 2014). Similar to findings obtained in the Picard study, differences in compensatory retrograde response have also been reported depending on which components of the TCA cycle are mutated in yeast (McCammon et al., 2003). Together with my work, these studies confirm that different forms of mitochondrial dysfunction do affect nuclear gene expression differently.

The microarray carried out in this study, however, revealed that there was also a set of 142 genes which were commonly differentially regulated, suggesting that there is a series of genes whose regulation is commonly conserved in different cases of mitochondrial dysfunction. I therefore focused on identifying this conserved mitochondrial retrograde mechanism.

Analysis of the microarray data revealed a conspicuous upregulated expression of glycolytic genes in response to both forms of mitochondrial dysfunction. As discussed in section 4.5.3, this is a commonly reported phenomenon that has been observed in yeast, *Drosophila* and mammalian systems, and is a method by which the organism compensates for loss of mitochondrial activity by shifting from oxidative phosphorylation to aerobic glycolysis. Additionally, differential regulation of the Insulin-like growth factor 1 receptor/mechanistic target of rapamycin (IGF-1/mTOR) pathway was also apparent, with mitochondrial dysfunction causing a downregulated expression of two of the eight Ilps; *Ilp1* and *Ilp3* and an upregulation of the mTOR downstream factor, *Thor*, the *Drosophila* homologue of *4E-BP1*.

In yeast, the organism most thoroughly studied in respect to mitochondrial retrograde signalling, mTOR complex 1 (mTORC1) is known to be inactivated in response to mitochondrial dysfunction. Indeed, recruitment of retrograde factors RTG1, RTG2 and RTG3 inhibits mTOR signals, downregulating the pathway activity. An additional study carried out in yeast has shown that treatment with a protonophore or mutations in the mitochondrial genome trigger a downregulation of mTORC1 (Kawai et al., 2011). Several further studies have demonstrated a link between the TOR pathway and RTG proteins (Komeili et al., 2000; Dilova et al., 2002; Dilova et al., 2004; Giannattasio et al., 2005), including a 2010 study which thoroughly investigated the mTORC1 interaction network in yeast, and established several links with the mitochondrial retrograde pathway (Breitkreutz et al., 2010). mTOR

signalling is a highly conserved pathway and its inactivation upon mitochondrial dysfunction is indicative of evolutionary conservation in the mitochondrial retrograde signalling pathway.

mTOR signalling plays a key role in protein synthesis, cell growth, synaptic plasticity and function, and is a key player in maintaining cellular homeostasis. However, mTOR hyperactivity is known to be detrimental and causes cognitive decline in several animal models (Ehninger et al., 2008; Puighermanal et al., 2009; Ehninger, 2013). Indeed, diabetes, known to cause an increase in mTOR activity, is known to be a risk factor for AD, via an mTOR mediated mechanism (Ma et al., 2013b; Orr et al., 2014). Additionally, mTOR signalling has been found to be elevated in AD patients, and increased mTOR activity has also been shown to increase tau levels and phosphorylation in *Drosophila* and mice (Khurana et al., 2006; Caccamo et al., 2013; Tang et al., 2013). A recent study carried out on an AD mouse model has identified that a reduction in mTOR signalling restores gene expression to wild-type levels in the mouse hippocampus as well as reducing Aβ aggregates and improving memory function (Caccamo et al., 2014). Indeed accumulation of Aβ is sufficient to cause an increase in mTOR activity (Caccamo et al., 2011). Additional studies have also shown that treatment with Rapamycin, an mTOR inhibitor, alleviates AD symptoms in animal models (Harrison et al., 2009; Spilman et al., 2010). What's more, reduction in mTOR activity is thought to cause an increase in lifespan in several animal species (Lamming et al., 2013). A recent report has also identified that a reduced activity of the mTOR downstream factor, eukaryotic initiation factor 2 α-subunit (eIF2α) ameliorates AD-like pathology and improves memory (Ma et al., 2013a; Caccamo et al., 2014). Similarly in 2009, Tain et al., showed that overexpression of *Thor* can suppress dopaminergic degeneration in a *Drosophila* model of Parkinson's disease, leading the authors to suggest that pharmacological stimulation of 4E-BP activity could be a potential therapeutic strategy against PD (Tain et al., 2009).

Taken together, these findings suggest that downregulation of mTOR and reduction in protein translation might be a neuroprotective mechanism which could be an initial response to mitochondrial dysfunction, as an attempt to protect against neuronal death. Does this neuroprotective mitochondrial retrograde response fail in a longterm scenario of mitochondrial dysfunction, resulting in a hyperactivity of the mTORC1 pathway, leading to neurodegeneration symptoms and consequent neuronal death? Additionally, what are the transcription factors responsible for modulating this initial response, including the downregulation of the mTORC1 pathway?

Mitochondrial retrograde studies carried out in yeast identified Rtg1 and Rtg3 as transcription factors which regulate this response (Butow and Avadhani, 2004). However, these factors are not conserved in other species. In mammalian cells, mitochondrial dysfunction activates a series of transcription factors including nuclear factor of activated T-cells (NFAT), CAAT/enhancer binding protein δ (C/EBPδ), cAMP-responsive element binding protein (CREB), and a novel IκBβ-dependent nuclear factor κB (NFκB) c-Rel/p50 (Amuthan et al., 2001; Biswas et al., 2005; Guha et al., 2007). In this study I have identified *sima*, the *Drosophila* ortholog of *HIF1α*, as a transcriptional regulator of the mitochondrial retrograde response, which was found to be required for the downregulation of *Ilp3* and the upregulation of *Thor* upon mitochondrial dysfunction. Additional studies have also implicated *HIF1α* in the regulation of mRNA translation (Wouters et al., 2005; Koritzinsky et al., 2006; Liu et al., 2006). In conditions of hypoxia which stimulate HIF1α, protein synthesis is reduced, via an upregulation of 4E-BP, in preference to an upregulation of stress-combating techniques which includes an upregulation of chaperones, antioxidants and transcription factors (Lin et al., 2014). Furthermore, when PINK1 is recruited to mitochondria in response to mitochondrial dysfunction, 4E-BP1 levels are upregulated and this occurs via activation of HIF1α (Lin et al., 2014).

There are several reasons which justify the proposition of HIF1α as an important transcription factor mediating the mitochondrial retrograde response. Firstly, oxygen is the final electron acceptor in the mitochondrial ETC, and HIF1α activity is based upon levels of ambient oxygen. Therefore, it makes sense that HIF1α responds upon changes in mitochondrial efficiency. Secondly, HIF1α controls the expression of cytochrome oxidase genes which comprise complex IV of the ETC. Lastly, HIF1α plays a major role in regulating glycolytic activity and indeed, HIF1α is known to upregulate several glycolytic genes including *Impl3* expression, a gene encoding for lactate dehydrogenase, which is also upregulated in the microarray analysis described in this thesis (Bruick and McKnight, 2001; Freije et al., 2012).

It is important to note that studies have implicated a role of HIF1α in regulating mitochondrial ROS signalling (Majmundar et al., 2010; Young and Simon, 2012). Contrastingly, other studies suggest that there are additional ROS-responsive pathways which act in initiating a mitochondrial retrograde response that are independent of HIF1α (Chae et al., 2013). Furthermore, other studies have suggested that conversely, mitochondria are important regulators of HIF1α stability by regulating intracellular oxygen availability, and that mitochondrially-generated ROS are an important redox signal integrating mitochondrial function with the rest of the cell (Murphy, 2009). A study published by Chandel et al., in 1998 was the first to report that HIF1-DNA binding and consequent HIF1 mediated transcription requires mitochondrial generated ROS (Chandel et al., 1998). A later study, reported in 2007 further showed that ROS generated by mitochondrial ETC complex III is required for the transduction of a hypoxia signal and for stabilisation of HIF1α (Bell et al., 2007). This study also suggested that mitochondrial oxygen consumption plays no role in modulating the hypoxic signal. A later *in vitro* study, however, found contrasting evidence to the Bell study, showing that ETC inhibitors targeting different complexes of the respiratory chain decreased HIF1α stability to a similar

degree (Chua et al., 2010). Furthermore, the study found that there was no effect on HIF1α when ROS levels were increased or decreased, and that re-establishing mitochondrial oxygen consumption upon inhibition of complex III restored HIF1α stabilisation (Chua et al., 2010). The study therefore concluded that mitochondrial oxygen consumption rate is the main determinant of HIF1α stability in hypoxic conditions.

As stated in section 4.4.3, most glutathione was present in a reduced state in the mitochondrial matrix of the described models of induced mitochondrial dysfunction, compared to a wildtype scenario. Further work will be required to determine whether ROS are acting as a retrograde signal in this system. The results outlined in chapter 5 of this thesis confirm the role of HIF1α in mediating the mitochondrial retrograde response, suggesting that HIF1α could be modulating the mitochondrial retrograde pathway independent of any alterations in ROS levels. Alterations in HIF1α stability might therefore be due to alterations in mitochondrial oxygen consumption, as suggested by Chua et al. (Chua et al., 2010).

Knockdown of *sima* in flies having mitochondrial dysfunction was found to inhibit the mitochondrial retrograde response which triggers downregulation cap-dependent mRNA translation. Furthermore, *sima* knockdown also rescues climbing ability and wing inflation phenotypes in the context of mitochondrial dysfunction. This suggests that knockdown of *sima* restores motor neuronal and CCAP neuronal activity. Surely, this implies that *sima* knockdown is neuroprotective and should be investigated as a potential avenue for therapeutic treatment of neurodegeneration. However, one must also keep in mind that increased neuronal activity and restoration of cap-dependent translation might not be energetically sustainable in the long term. Therefore, if mitochondria continue to be dysfunctional for a prolonged period of time, there needs to be a mechanism which is able to counteract this dysfunction for the same timeframe. If the stress response mechanism is

only beneficial in the short term, then this is what ultimately leads to neuronal death occurring anyway.

It is unknown, however, how does this metabolic switch triggered by HIF1α would apply to the neurodegenerative diseases that are associated with mitochondrial dysfunction. The SNpc, predominantly affected in PD, appears to be more energy-dependent than other brain areas and is richer in metabolism-related and mitochondrial-associated genes. The Snpc also expresses more hypoxia-related genes (Lin et al., 2014). Therefore, in the case of PD, is this brain region more sensitive to a bioenergetic deficit? This might suggest that the SNpc is particularly responsive to mitochondrial dysfunction, and subsequent alterations in HIF1α levels. This strengthens the need of further investigation into the potential role of HIFα as a therapeutic agent for PD and other neurodegenerative diseases.

Considering the multi-branched nature of the mTOR pathway and its many inputs and outputs and considering the heterogeneity of the mitochondrial network, it is not surprising that variations and different degrees of mitochondrial dysfunction lead to a great variety of symptoms and pathologies and that this also suggests a probable variation in retrograde triggers. Therefore, the role of mTORC1 in mitochondrial dysfunction is probably not a clear cut process – the downregulation of translation might be an instinctual sudden stress response which might be altered over time with possibly elevated levels of mitochondrial dysfunction. Additionally, as previously argued, mtDNA and nuclear DNA background play a huge role in determining the retrograde response to mitochondrial dysfunction, thereby adding additional parameters to take into consideration and further complicating the process.

Ultimately, the mitochondrial retrograde response is a highly complex process. Therefore, while some aspects might be conserved in the different neurodegenerative disorders, others might vary greatly depending on the individual and the degree of mitochondrial

dysfunction. It is therefore imperative for more research to be carried out to better understand what factors are required to initiate this retrograde response, and how its activation or inhibition could worsen or alleviate symptoms pertaining to diseases which are associated with mitochondrial dysfunction.

6.3. Future directions

This thesis presents convincing evidence which further supports a role of mitochondrial dysfunction in neurodegeneration. However, additional work is required to better understand the mechanisms underlying all aspects of the studies outlined. Brief descriptions of the future work which I deem to be required for this purpose are listed below.

1. Measuring mitochondrial-associated protein levels and Complex I activity, and associations with *TFAM* SNP rs2306604 A>G, in other brain regions apart from the pre-frontal cortex.

2. Investigating the frequency of *TFAM* SNP rs2306604 A>G in additional PD and PDD cases, which would strengthen the statistical power of any significant associations.

3. Investigating the presence of *TFAM* SNP rs2306604 A>G in PD and PDD, in combination with additional polymorphisms. This would help to further elucidate whether the presence of *TFAM* SNP rs2306604 A>G as a lone polymorphism is sufficient to induce greater risk for PD and PDD, or whether the risk is increased by a combination of polymorphisms.

4. Polysomal profiling at different developmental stages in *Drosophila* mitochondrial dysfunction would need to be carried out in order to follow changes in mRNA translation upon mitochondrial dysfunction. Additionally, this assay could be used to investigate alterations in mRNA translation rates upon inhibition of the mitochondrial retrograde response by *sima* knockdown.

5. HIF1α acts in combination with HIF1β to form a heterodimeric complex which binds to hypoxia responsive elements in the genome, in response to hypoxia. It would be of interest to investigate whether Tango, the *Drosophila* homologue of HIF1β, is also required in modulating the mitochondrial retrograde response. Monitoring of *Thor-lacZ* expression upon knockdown or overexpression of *tgo* would indicate its requirement on mRNA translation regulation. Similarly, climbing and wing inflation assays would indicate the effect of altering *tgo* expression levels on neuronal activity.

6. Since neurodegeneration is an age-related process, it would be important to establish the role of *sima* in aged fly models of mitochondrial dysfunction compared to aged wild-type control flies. Lifespan assays would need to be carried out in order to investigate whether knockdown of *sima*, and subsequent upregulated mRNA translation and neuronal activity, ameliorates or aggravates health-span. Furthermore this would help to better establish the role of the mitochondrial retrograde mechanism throughout ageing and progression of disease, and could outline different coping mechanisms in the larval and adult stages of the fly models. This could shed some light on different metabolic responses to initial versus prolonged mitochondrial dysfunction.

7. How does HIF1α involvement in the mitochondrial retrograde mechanism translate in human examples of neurodegeneration? One way of investigating this, is to carry out western blot analysis on PD and PDD cases and analyse protein levels of 4E-BP1 and HIF1α. Unfortunately, this would only provide information about levels of these proteins of interest at the progressive end of the disease; however, it would still be of major interest to observe whether there are significant changes in these protein levels upon progression from PD to PDD.

8. An investigation into the mechanism underlying the mitochondrial retrograde response upon mitochondrial dysfunction in the CNS. Use of a genetic screen *in vitro* as well as *in vivo* in *Drosophila* could identify novel regulators of this retrograde response.

9. Finally, I conclude that investigating the effects of alterations in HIF1α levels on the mitochondrial retrograde signalling pathway in rodent models of mitochondrial dysfunction, would be the next step in unfolding this mechanism in a mammalian system.

7. References

Aarsland D, Kvaloy JT, Andersen K, Larsen JP, Tang MX, Lolk A, Kragh-Sorensen P, Marder K (2007) The effect of age of onset of PD on risk of dementia. Journal of neurology 254:38-45.

Aasly JO, Vilarino-Guell C, Dachsel JC, Webber PJ, West AB, Haugarvoll K, Johansen KK, Toft M, Nutt JG, Payami H, Kachergus JM, Lincoln SJ, Felic A, Wider C, Soto-Ortolaza AI, Cobb SA, White LR, Ross OA, Farrer MJ (2010) Novel pathogenic LRRK2 p.Asn1437His substitution in familial Parkinson's disease. Movement disorders : official journal of the Movement Disorder Society 25:2156-2163.

Abrahams JP, Leslie AG, Lutter R, Walker JE (1994) Structure at 2.8 A resolution of F1-ATPase from bovine heart mitochondria. Nature 370:621-628.

Alafuzoff I et al. (2009) Staging/typing of Lewy body related alpha-synuclein pathology: a study of the BrainNet Europe Consortium. Acta neuropathologica 117:635-652.

Albrecht M (2005) LRRK2 mutations and Parkinsonism. Lancet 365:1230.

Albrecht Simone C, Barata Ana G, Großhans J, Teleman Aurelio A, Dick Tobias P (2011) In Vivo Mapping of Hydrogen Peroxide and Oxidized Glutathione Reveals Chemical and Regional Specificity of Redox Homeostasis. Cell Metabolism 14:819-829.

Aleardi AM, Benard G, Augereau O, Malgat M, Talbot JC, Mazat JP, Letellier T, Dachary-Prigent J, Solaini GC, Rossignol R (2005) Gradual alteration of mitochondrial structure and function by beta-amyloids: importance of membrane viscosity changes, energy deprivation, reactive oxygen species production, and cytochrome c release. Journal of bioenergetics and biomembranes 37:207-225.

Allen JF (1993) Control of gene expression by redox potential and the requirement for chloroplast and mitochondrial genomes. Journal of theoretical biology 165:609-631.

Alvarez G, Munoz-Montano JR, Satrustegui J, Avila J, Bogonez E, Diaz-Nido J (1999) Lithium protects cultured neurons against beta-amyloid-induced neurodegeneration. FEBS letters 453:260-264.

Alvarez V, Corao AI, Alonso-Montes C, Sanchez-Ferrero E, De Mena L, Morales B, Garcia-Castro M, Coto E (2008a) Mitochondrial transcription factor A (TFAM) gene variation and risk of late-onset Alzheimer's disease. Journal of Alzheimer's disease : JAD 13:275-280.

Alvarez V, Corao AI, Sanchez-Ferrero E, De Mena L, Alonso-Montes C, Huerta C, Blazquez M, Ribacoba R, Guisasola LM, Salvador C, Garcia-Castro M, Coto E (2008b) Mitochondrial transcription factor A (TFAM) gene variation in Parkinson's disease. Neurosci Lett 432:79-82.

Amo T, Sato S, Saiki S, Wolf AM, Toyomizu M, Gautier CA, Shen J, Ohta S, Hattori N (2011) Mitochondrial membrane potential decrease caused by loss of PINK1 is not due to proton leak, but to respiratory chain defects. Neurobiol Dis 41:111-118.

Amuthan G, Biswas G, Zhang SY, Klein-Szanto A, Vijayasarathy C, Avadhani NG (2001) Mitochondria-to-nucleus stress signaling induces phenotypic changes, tumor progression and cell invasion. The EMBO journal 20:1910-1920.

Amuthan G, Biswas G, Ananadatheerthavarada HK, Vijayasarathy C, Shephard HM, Avadhani NG (2002) Mitochondrial stress-induced calcium signaling, phenotypic changes and invasive behavior in human lung carcinoma A549 cells. Oncogene 21:7839-7849.

Andersen K, Launer LJ, Dewey ME, Letenneur L, Ott A, Copeland JR, Dartigues JF, Kragh-Sorensen P, Baldereschi M, Brayne C, Lobo A, Martinez-Lage JM, Stijnen T, Hofman A (1999) Gender differences in the incidence of AD and vascular dementia: The EURODEM Studies. EURODEM Incidence Research Group. Neurology 53:1992-1997.

Anderson JP, Walker DE, Goldstein JM, de Laat R, Banducci K, Caccavello RJ, Barbour R, Huang J, Kling K, Lee M, Diep L, Keim PS, Shen X, Chataway T, Schlossmacher MG, Seubert P, Schenk D, Sinha S, Gai WP, Chilcote TJ (2006) Phosphorylation of Ser-129 is the dominant pathological modification of alpha-synuclein in familial and sporadic Lewy body disease. The Journal of biological chemistry 281:29739-29752.

Andersson SG, Karlberg O, Canback B, Kurland CG (2003) On the origin of mitochondria: a genomics perspective. Philosophical transactions of the Royal Society of London Series B, Biological sciences 358:165-177; discussion 177-169.

Andres-Mateos E, Perier C, Zhang L, Blanchard-Fillion B, Greco TM, Thomas B, Ko HS, Sasaki M, Ischiropoulos H, Przedborski S, Dawson TM, Dawson VL (2007) DJ-1 gene deletion reveals that DJ-1 is an atypical peroxiredoxin-like peroxidase. Proceedings of the National Academy of Sciences of the United States of America 104:14807-14812.

Andreyev AY, Kushnareva YE, Starkov AA (2005) Mitochondrial metabolism of reactive oxygen species. Biochemistry Biokhimiia 70:200-214.

Appel-Cresswell S, Vilarino-Guell C, Encarnacion M, Sherman H, Yu I, Shah B, Weir D, Thompson C, Szu-Tu C, Trinh J, Aasly JO, Rajput A, Rajput AH, Jon Stoessl A, Farrer MJ (2013) Alpha-synuclein p.H50Q, a novel pathogenic mutation for Parkinson's disease. Movement disorders : official journal of the Movement Disorder Society 28:811-813.

Arnold RS, Sun Q, Sun CQ, Richards JC, O'Hearn S, Osunkoya AO, Wallace DC, Petros JA (2013) An inherited heteroplasmic mutation in mitochondrial gene COI in a patient with prostate cancer alters reactive oxygen, reactive nitrogen and proliferation. BioMed research international 2013:239257.

Arriagada PV, Growdon JH, Hedley-Whyte ET, Hyman BT (1992) Neurofibrillary tangles but not senile plaques parallel duration and severity of Alzheimer's disease. Neurology 42:631-639.

Atamna H, Boyle K (2006) Amyloid-beta peptide binds with heme to form a peroxidase: relationship to the cytopathologies of Alzheimer's disease. Proceedings of the National Academy of Sciences of the United States of America 103:3381-3386.

Athauda D, Foltynie T (2015) The ongoing pursuit of neuroprotective therapies in Parkinson disease. Nat Rev Neurol 11:25-40.

Autere J, Moilanen JS, Finnila S, Soininen H, Mannermaa A, Hartikainen P, Hallikainen M, Majamaa K (2004) Mitochondrial DNA polymorphisms as risk factors for Parkinson's disease and Parkinson's disease dementia. Human genetics 115:29-35.

Bai H, Kang P, Tatar M (2012) Drosophila insulin-like peptide-6 (dilp6) expression from fat body extends lifespan and represses secretion of Drosophila insulin-like peptide-2 from the brain. Aging cell 11:978-985.

Ballard C, Kahn Z, Corbett A (2011) Treatment of dementia with Lewy bodies and Parkinson's disease dementia. Drugs & aging 28:769-777.

Ballard C, Ziabreva I, Perry R, Larsen JP, O'Brien J, McKeith I, Perry E, Aarsland D (2006) Differences in neuropathologic characteristics across the Lewy body dementia spectrum. Neurology 67:1931-1934.

Baloh RH, Schmidt RE, Pestronk A, Milbrandt J (2007) Altered axonal mitochondrial transport in the pathogenesis of Charcot-Marie-Tooth disease from mitofusin 2 mutations. The Journal of neuroscience : the official journal of the Society for Neuroscience 27:422-430.

Barja G (2014) The mitochondrial free radical theory of aging. Progress in molecular biology and translational science 127:1-27.

Belarbi S, Hecham N, Lesage S, Kediha MI, Smail N, Benhassine T, Ysmail-Dahlouk F, Lohman E, Benhabyles B, Hamadouche T, Assami S, Brice A, Tazir M (2010) LRRK2

G2019S mutation in Parkinson's disease: a neuropsychological and neuropsychiatric study in a large Algerian cohort. Parkinsonism Relat Disord 16:676-679.

Belfort MA, Saade GR, Snabes M, Dunn R, Moise KJ, Jr., Cruz A, Young R (1995) Hormonal status affects the reactivity of the cerebral vasculature. American journal of obstetrics and gynecology 172:1273-1278.

Belin AC, Björk BF, Westerlund M, Galter D, Sydow O, Lind C, Pernold K, Rosvall L, Håkansson A, Winblad B, Nissbrandt H, Graff C, Olson L (2007) Association study of two genetic variants in mitochondrial transcription factor A (TFAM) in Alzheimer's and Parkinson's disease. Neuroscience Letters 420:257-262.

Bell EL, Klimova TA, Eisenbart J, Moraes CT, Murphy MP, Budinger GR, Chandel NS (2007) The Qo site of the mitochondrial complex III is required for the transduction of hypoxic signaling via reactive oxygen species production. J Cell Biol 177:1029-1036.

Bellizzi D, D'Aquila P, Giordano M, Montesanto A, Passarino G (2012) Global DNA methylation levels are modulated by mitochondrial DNA variants. Epigenomics 4:17-27.

Ben Sassi S, Nabli F, Hentati E, Nahdi H, Trabelsi M, Ben Ayed H, Amouri R, Duda JE, Farrer MJ, Hentati F (2012) Cognitive dysfunction in Tunisian LRRK2 associated Parkinson's disease. Parkinsonism Relat Disord 18:243-246.

Benda C (1898) Ueber die spermatogenese der vertebraten und höherer evertebraten, II. Theil: Die histiogenese der spermien. Arch Aat Physiol 73:393-398.

Bender A, Krishnan KJ, Morris CM, Taylor GA, Reeve AK, Perry RH, Jaros E, Hersheson JS, Betts J, Klopstock T, Taylor RW, Turnbull DM (2006) High levels of mitochondrial DNA deletions in substantia nigra neurons in aging and Parkinson disease. Nature genetics 38:515-517.

Bertram L, McQueen MB, Mullin K, Blacker D, Tanzi RE (2007) Systematic meta-analyses of Alzheimer disease genetic association studies: the AlzGene database. Nature genetics 39:17-23.

Bertram L, Blacker D, Mullin K, Keeney D, Jones J, Basu S, Yhu S, McInnis MG, Go RC, Vekrellis K, Selkoe DJ, Saunders AJ, Tanzi RE (2000) Evidence for genetic linkage of Alzheimer's disease to chromosome 10q. Science 290:2302-2303.

Bialecka M, Kurzawski M, Roszmann A, Robowski P, Sitek EJ, Honczarenko K, Mak M, Deptula-Jarosz M, Golab-Janowska M, Drozdzik M, Slawek J (2014) BDNF G196A (Val66Met) polymorphism associated with cognitive impairment in Parkinson's disease. Neurosci Lett 561:86-90.

Bierer LM, Hof PR, Purohit DP, Carlin L, Schmeidler J, Davis KL, Perl DP (1995) Neocortical neurofibrillary tangles correlate with dementia severity in Alzheimer's disease. Arch Neurol 52:81-88.

Bir A, Sen O, Anand S, Khemka VK, Banerjee P, Cappai R, Sahoo A, Chakrabarti S (2014) alpha-synuclein-induced mitochondrial dysfunction in isolated preparation and intact cells: Implications in the pathogenesis of Parkinson's disease. Journal of neurochemistry 131:868-877.

Biswas G, Anandatheerthavarada HK, Avadhani NG (2005) Mechanism of mitochondrial stress-induced resistance to apoptosis in mitochondrial DNA-depleted C2C12 myocytes. Cell death and differentiation 12:266-278.

Biswas G, Adebanjo OA, Freedman BD, Anandatheerthavarada HK, Vijayasarathy C, Zaidi M, Kotlikoff M, Avadhani NG (1999) Retrograde Ca2+ signaling in C2C12 skeletal myocytes in response to mitochondrial genetic and metabolic stress: a novel mode of inter-organelle crosstalk. The EMBO journal 18:522-533.

Blalock EM, Geddes JW, Chen KC, Porter NM, Markesbery WR, Landfield PW (2004) Incipient Alzheimer's disease: microarray correlation analyses reveal major

transcriptional and tumor suppressor responses. Proceedings of the National Academy of Sciences of the United States of America 101:2173-2178.

Bolstad BM, Irizarry RA, Astrand M, Speed TP (2003) A comparison of normalization methods for high density oligonucleotide array data based on variance and bias. Bioinformatics 19:185-193.

Braak H, Braak E (1991) Neuropathological stageing of Alzheimer-related changes. Acta neuropathologica 82:239-259.

Braak H, Rub U, Jansen Steur EN, Del Tredici K, de Vos RA (2005) Cognitive status correlates with neuropathologic stage in Parkinson disease. Neurology 64:1404-1410.

Braak H, Del Tredici K, Rub U, de Vos RA, Jansen Steur EN, Braak E (2003) Staging of brain pathology related to sporadic Parkinson's disease. Neurobiol Aging 24:197-211.

Brand AH, Perrimon N (1993) Targeted gene expression as a means of altering cell fates and generating dominant phenotypes. Development 118:401-415.

Breitkreutz A, Choi H, Sharom JR, Boucher L, Neduva V, Larsen B, Lin ZY, Breitkreutz BJ, Stark C, Liu G, Ahn J, Dewar-Darch D, Reguly T, Tang X, Almeida R, Qin ZS, Pawson T, Gingras AC, Nesvizhskii AI, Tyers M (2010) A global protein kinase and phosphatase interaction network in yeast. Science 328:1043-1046.

Broadstock M, Ballard C, Corbett A (2014) Latest treatment options for Alzheimer's disease, Parkinson's disease dementia and dementia with Lewy bodies. Expert opinion on pharmacotherapy 15:1797-1810.

Brogiolo W, Stocker H, Ikeya T, Rintelen F, Fernandez R, Hafen E (2001) An evolutionarily conserved function of the Drosophila insulin receptor and insulin-like peptides in growth control. Current biology : CB 11:213-221.

Broughton S, Alic N, Slack C, Bass T, Ikeya T, Vinti G, Tommasi AM, Driege Y, Hafen E, Partridge L (2008) Reduction of DILP2 in Drosophila triages a metabolic phenotype from lifespan revealing redundancy and compensation among DILPs. PloS one 3:e3721.

Bruick RK, McKnight SL (2001) A conserved family of prolyl-4-hydroxylases that modify HIF. Science 294:1337-1340.

Buchkovich NJ, Yu Y, Zampieri CA, Alwine JC (2008) The TORrid affairs of viruses: effects of mammalian DNA viruses on the PI3K-Akt-mTOR signalling pathway. Nature reviews Microbiology 6:266-275.

Busto GU, Cervantes-Sandoval I, Davis RL (2010) Olfactory learning in Drosophila. Physiology 25:338-346.

Buter TC, van den Hout A, Matthews FE, Larsen JP, Brayne C, Aarsland D (2008) Dementia and survival in Parkinson disease: a 12-year population study. Neurology 70:1017-1022.

Butow RA, Avadhani NG (2004) Mitochondrial signaling: the retrograde response. Mol Cell 14:1-15.

Butow RA, Docherty R, Parikh VS (1988) A path from mitochondria to the yeast nucleus. Philosophical transactions of the Royal Society of London Series B, Biological sciences 319:127-133.

Caccamo A, De Pinto V, Messina A, Branca C, Oddo S (2014) Genetic reduction of mammalian target of rapamycin ameliorates Alzheimer's disease-like cognitive and pathological deficits by restoring hippocampal gene expression signature. The Journal of neuroscience : the official journal of the Society for Neuroscience 34:7988-7998.

Caccamo A, Maldonado MA, Majumder S, Medina DX, Holbein W, Magri A, Oddo S (2011) Naturally secreted amyloid-beta increases mammalian target of rapamycin (mTOR) activity via a PRAS40-mediated mechanism. The Journal of biological chemistry 286:8924-8932.

Caccamo A, Magri A, Medina DX, Wisely EV, Lopez-Aranda MF, Silva AJ, Oddo S (2013) mTOR regulates tau phosphorylation and degradation: implications for Alzheimer's disease and other tauopathies. Aging cell 12:370-380.

Caccappolo E et al. (2011) Neuropsychological Profile of Parkin Mutation Carriers with and without Parkinson Disease: The CORE-PD Study. Journal of the International Neuropsychological Society : JINS 17:91-100.

Cadenas E, Davies KJ (2000) Mitochondrial free radical generation, oxidative stress, and aging. Free radical biology & medicine 29:222-230.

Cagin U (2013) Investigating neuronal mitochondrial DNA loss in Drosophila melanogaster. In: King's College London (University of London).

Campbell CT, Kolesar JE, Kaufman BA (2012) Mitochondrial transcription factor A regulates mitochondrial transcription initiation, DNA packaging, and genome copy number. Biochimica et biophysica acta 1819:921-929.

Canevari L, Clark JB, Bates TE (1999) beta-Amyloid fragment 25-35 selectively decreases complex IV activity in isolated mitochondria. FEBS letters 457:131-134.

Cannon MV, Dunn DA, Irwin MH, Brooks AI, Bartol FF, Trounce IA, Pinkert CA (2011) Xenomitochondrial mice: investigation into mitochondrial compensatory mechanisms. Mitochondrion 11:33-39.

Canugovi C, Maynard S, Bayne AC, Sykora P, Tian J, de Souza-Pinto NC, Croteau DL, Bohr VA (2010) The mitochondrial transcription factor A functions in mitochondrial base excision repair. DNA repair 9:1080-1089.

Cardoso SM, Pereira CF, Moreira PI, Arduino DM, Esteves AR, Oliveira CR (2010) Mitochondrial control of autophagic lysosomal pathway in Alzheimer's disease. Exp Neurol 223:294-298.

Celotto AM, Chiu WK, Van Voorhies W, Palladino MJ (2011) Modes of metabolic compensation during mitochondrial disease using the Drosophila model of ATP6 dysfunction. PloS one 6:e25823.

Cerpa W, Toledo EM, Varela-Nallar L, Inestrosa NC (2009) The role of Wnt signaling in neuroprotection. Drug news & perspectives 22:579-591.

Chae S, Ahn BY, Byun K, Cho YM, Yu MH, Lee B, Hwang D, Park KS (2013) A systems approach for decoding mitochondrial retrograde signaling pathways. Science signaling 6:rs4.

Chandel NS, Maltepe E, Goldwasser E, Mathieu CE, Simon MC, Schumacker PT (1998) Mitochondrial reactive oxygen species trigger hypoxia-induced transcription. Proceedings of the National Academy of Sciences of the United States of America 95:11715-11720.

Chang CJ, Yin PH, Yang DM, Wang CH, Hung WY, Chi CW, Wei YH, Lee HC (2009) Mitochondrial dysfunction-induced amphiregulin upregulation mediates chemo-resistance and cell migration in HepG2 cells. Cellular and molecular life sciences : CMLS 66:1755-1765.

Chartier-Harlin MC, Crawford F, Houlden H, Warren A, Hughes D, Fidani L, Goate A, Rossor M, Roques P, Hardy J, et al. (1991) Early-onset Alzheimer's disease caused by mutations at codon 717 of the beta-amyloid precursor protein gene. Nature 353:844-846.

Chartier-Harlin MC, Kachergus J, Roumier C, Mouroux V, Douay X, Lincoln S, Levecque C, Larvor L, Andrieux J, Hulihan M, Waucquier N, Defebvre L, Amouyel P, Farrer M, Destee A (2004) Alpha-synuclein locus duplication as a cause of familial Parkinson's disease. Lancet 364:1167-1169.

Chinnery PF, Johnson MA, Wardell TM, Singh-Kler R, Hayes C, Brown DT, Taylor RW, Bindoff LA, Turnbull DM (2000) The epidemiology of pathogenic mitochondrial DNA mutations. Ann Neurol 48:188-193.

Choi SH, Kim YH, Hebisch M, Sliwinski C, Lee S, D'Avanzo C, Chen H, Hooli B, Asselin C, Muffat J, Klee JB, Zhang C, Wainger BJ, Peitz M, Kovacs DM, Woolf CJ, Wagner SL, Tanzi RE, Kim DY (2014) A three-dimensional human neural cell culture model of Alzheimer's disease. Nature.

Chua YL, Dufour E, Dassa EP, Rustin P, Jacobs HT, Taylor CT, Hagen T (2010) Stabilization of hypoxia-inducible factor-1alpha protein in hypoxia occurs independently of mitochondrial reactive oxygen species production. The Journal of biological chemistry 285:31277-31284.

Clark-Walker G, Linnane AW (1966) Invivo differentiation of yeast cytoplasmic and mitochondrial protein synthesis with antibiotics. Biochemical and biophysical research communications 25:8-13.

Claude A (1946) Fractionation of mammalian liver cells by differential centrifugation; experimental procedures and results. The Journal of experimental medicine 84:61-89.

Clayton DA (1982) Replication of animal mitochondrial DNA. Cell 28:693-705.

Cocheme HM, Quin C, McQuaker SJ, Cabreiro F, Logan A, Prime TA, Abakumova I, Patel JV, Fearnley IM, James AM, Porteous CM, Smith RA, Saeed S, Carre JE, Singer M, Gems D, Hartley RC, Partridge L, Murphy MP (2011) Measurement of H2O2 within living Drosophila during aging using a ratiometric mass spectrometry probe targeted to the mitochondrial matrix. Cell Metab 13:340-350.

Colinet H, Renault D (2012) Metabolic effects of CO(2) anaesthesia in Drosophila melanogaster. Biology letters 8:1050-1054.

Colombani J, Andersen DS, Leopold P (2012) Secreted peptide Dilp8 coordinates Drosophila tissue growth with developmental timing. Science 336:582-585.

Conway KA, Harper JD, Lansbury PT, Jr. (2000) Fibrils formed in vitro from alpha-synuclein and two mutant forms linked to Parkinson's disease are typical amyloid. Biochemistry 39:2552-2563.

Cookson MR (2012) Cellular effects of LRRK2 mutations. Biochemical Society transactions 40:1070-1073.

Copeland JM, Cho J, Lo T, Jr., Hur JH, Bahadorani S, Arabyan T, Rabie J, Soh J, Walker DW (2009) Extension of Drosophila life span by RNAi of the mitochondrial respiratory chain. Current biology : CB 19:1591-1598.

Copeland WC (2008) Inherited mitochondrial diseases of DNA replication. Annual review of medicine 59:131-146.

Corbett A, Ballard C (2012) New and emerging treatments for Alzheimer's disease. Expert opinion on emerging drugs 17:147-156.

Corral-Debrinski M, Horton T, Lott MT, Shoffner JM, McKee AC, Beal MF, Graham BH, Wallace DC (1994) Marked changes in mitochondrial DNA deletion levels in Alzheimer brains. Genomics 23:471-476.

Correia SC, Santos RX, Perry G, Zhu X, Moreira PI, Smith MA (2012) Mitochondrial importance in Alzheimer's, Huntington's and Parkinson's diseases. In: Neurodegenerative Diseases, pp 205-221: Springer.

Coskun PE, Beal MF, Wallace DC (2004) Alzheimer's brains harbor somatic mtDNA control-region mutations that suppress mitochondrial transcription and replication. Proceedings of the National Academy of Sciences of the United States of America 101:10726-10731.

Coskun PE, Wyrembak J, Derbereva O, Melkonian G, Doran E, Lott IT, Head E, Cotman CW, Wallace DC (2010) Systemic mitochondrial dysfunction and the etiology of Alzheimer's disease and down syndrome dementia. Journal of Alzheimer's disease : JAD 20 Suppl 2:S293-310.

Cotzias GC (1968) L-Dopa for Parkinsonism. The New England journal of medicine 278:630.

Crouch PJ, Blake R, Duce JA, Ciccotosto GD, Li QX, Barnham KJ, Curtain CC, Cherny RA, Cappai R, Dyrks T, Masters CL, Trounce IA (2005) Copper-dependent inhibition of human cytochrome c oxidase by a dimeric conformer of amyloid-beta1-42. The Journal of neuroscience : the official journal of the Society for Neuroscience 25:672-679.

Cruts M, Hendriks L, Van Broeckhoven C (1996) The presenilin genes: a new gene family involved in Alzheimer disease pathology. Hum Mol Genet 5 Spec No:1449-1455.

Cui L, Jeong H, Borovecki F, Parkhurst CN, Tanese N, Krainc D (2006) Transcriptional repression of PGC-1alpha by mutant huntingtin leads to mitochondrial dysfunction and neurodegeneration. Cell 127:59-69.

Dagda RK, Cherra SJ, 3rd, Kulich SM, Tandon A, Park D, Chu CT (2009) Loss of PINK1 function promotes mitophagy through effects on oxidative stress and mitochondrial fission. The Journal of biological chemistry 284:13843-13855.

Dairaghi DJ, Shadel GS, Clayton DA (1995a) Addition of a 29 residue carboxyl-terminal tail converts a simple HMG box-containing protein into a transcriptional activator. Journal of molecular biology 249:11-28.

Dairaghi DJ, Shadel GS, Clayton DA (1995b) Human mitochondrial transcription factor A and promoter spacing integrity are required for transcription initiation. Biochimica et biophysica acta 1271:127-134.

de Lau LM, Breteler MM (2006) Epidemiology of Parkinson's disease. Lancet neurology 5:525-535.

Dell'agnello C, Leo S, Agostino A, Szabadkai G, Tiveron C, Zulian A, Prelle A, Roubertoux P, Rizzuto R, Zeviani M (2007) Increased longevity and refractoriness to Ca(2+)-dependent neurodegeneration in Surf1 knockout mice. Hum Mol Genet 16:431-444.

Deshpande A, Mina E, Glabe C, Busciglio J (2006) Different conformations of amyloid beta induce neurotoxicity by distinct mechanisms in human cortical neurons. The Journal of neuroscience : the official journal of the Society for Neuroscience 26:6011-6018.

Devi L, Raghavendran V, Prabhu BM, Avadhani NG, Anandatheerthavarada HK (2008) Mitochondrial import and accumulation of alpha-synuclein impair complex I in human dopaminergic neuronal cultures and Parkinson disease brain. The Journal of biological chemistry 283:9089-9100.

Dickson DW, Uchikado H, Fujishiro H, Tsuboi Y (2010) Evidence in favor of Braak staging of Parkinson's disease. Movement disorders : official journal of the Movement Disorder Society 25 Suppl 1:S78-82.

Dilova I, Chen CY, Powers T (2002) Mks1 in concert with TOR signaling negatively regulates RTG target gene expression in S. cerevisiae. Current biology : CB 12:389-395.

Dilova I, Aronova S, Chen JC, Powers T (2004) Tor signaling and nutrient-based signals converge on Mks1p phosphorylation to regulate expression of Rtg1.Rtg3p-dependent target genes. The Journal of biological chemistry 279:46527-46535.

Dinardo MM, Musicco C, Fracasso F, Milella F, Gadaleta MN, Gadaleta G, Cantatore P (2003) Acetylation and level of mitochondrial transcription factor A in several organs of young and old rats. Biochemical and biophysical research communications 301:187-191.

Distelmaier F, Valsecchi F, Liemburg-Apers DC, Lebiedzinska M, Rodenburg RJ, Heil S, Keijer J, Fransen J, Imamura H, Danhauser K, Seibt A, Viollet B, Gellerich FN, Smeitink JA, Wieckowski MR, Willems PH, Koopman WJ (2015) Mitochondrial dysfunction in primary human fibroblasts triggers an adaptive cell survival program that requires AMPK-alpha. Biochimica et biophysica acta 1852:529-540.

Dodson MW, Guo M (2007) Pink1, Parkin, DJ-1 and mitochondrial dysfunction in Parkinson's disease. Current opinion in neurobiology 17:331-337.

Dooley CT, Dore TM, Hanson GT, Jackson WC, Remington SJ, Tsien RY (2004) Imaging dynamic redox changes in mammalian cells with green fluorescent protein indicators. The Journal of biological chemistry 279:22284-22293.

Du H, Guo L, Yan SS (2012) Synaptic mitochondrial pathology in Alzheimer's disease. Antioxidants & redox signaling 16:1467-1475.

Du H, Guo L, Fang F, Chen D, Sosunov AA, McKhann GM, Yan Y, Wang C, Zhang H, Molkentin JD, Gunn-Moore FJ, Vonsattel JP, Arancio O, Chen JX, Yan SD (2008) Cyclophilin D deficiency attenuates mitochondrial and neuronal perturbation and ameliorates learning and memory in Alzheimer's disease. Nature medicine 14:1097-1105.

Durieux J, Wolff S, Dillin A (2011) The cell-non-autonomous nature of electron transport chain-mediated longevity. Cell 144:79-91.

Eckert A, Hauptmann S, Scherping I, Rhein V, Muller-Spahn F, Gotz J, Muller WE (2008) Soluble beta-amyloid leads to mitochondrial defects in amyloid precursor protein and tau transgenic mice. Neuro-degenerative diseases 5:157-159.

Ehninger D (2013) From genes to cognition in tuberous sclerosis: implications for mTOR inhibitor-based treatment approaches. Neuropharmacology 68:97-105.

Ehninger D, Han S, Shilyansky C, Zhou Y, Li W, Kwiatkowski DJ, Ramesh V, Silva AJ (2008) Reversal of learning deficits in a Tsc2+/- mouse model of tuberous sclerosis. Nature medicine 14:843-848.

Ekstrand MI, Falkenberg M, Rantanen A, Park CB, Gaspari M, Hultenby K, Rustin P, Gustafsson CM, Larsson NG (2004) Mitochondrial transcription factor A regulates mtDNA copy number in mammals. Hum Mol Genet 13:935-944.

Ekstrand MI, Terzioglu M, Galter D, Zhu S, Hofstetter C, Lindqvist E, Thams S, Bergstrand A, Hansson FS, Trifunovic A, Hoffer B, Cullheim S, Mohammed AH, Olson L, Larsson N-G (2007) Progressive parkinsonism in mice with respiratory-chain-deficient dopamine neurons. Proceedings of the National Academy of Sciences 104:1325-1330.

Emre M, Tsolaki M, Bonuccelli U, Destee A, Tolosa E, Kutzelnigg A, Ceballos-Baumann A, Zdravkovic S, Bladstrom A, Jones R (2010) Memantine for patients with Parkinson's disease dementia or dementia with Lewy bodies: a randomised, double-blind, placebo-controlled trial. Lancet neurology 9:969-977.

Emre M, Aarsland D, Albanese A, Byrne EJ, Deuschl G, De Deyn PP, Durif F, Kulisevsky J, van Laar T, Lees A, Poewe W, Robillard A, Rosa MM, Wolters E, Quarg P, Tekin S, Lane R (2004) Rivastigmine for dementia associated with Parkinson's disease. The New England journal of medicine 351:2509-2518.

Emre M et al. (2007) Clinical diagnostic criteria for dementia associated with Parkinson's disease. Mov Disord 22:1689-1707; quiz 1837.

Falkenberg M, Gaspari M, Rantanen A, Trifunovic A, Larsson NG, Gustafsson CM (2002) Mitochondrial transcription factors B1 and B2 activate transcription of human mtDNA. Nature genetics 31:289-294.

Farlow MR, Cummings JL (2007) Effective pharmacologic management of Alzheimer's disease. The American journal of medicine 120:388-397.

Fereshtehnejad SM, Religa D, Westman E, Aarsland D, Lokk J, Eriksdotter M (2013) Demography, diagnostics, and medication in dementia with Lewy bodies and Parkinson's disease with dementia: data from the Swedish Dementia Quality Registry (SveDem). Neuropsychiatric disease and treatment 9:927-935.

Fernandez R, Tabarini D, Azpiazu N, Frasch M, Schlessinger J (1995) The Drosophila insulin receptor homolog: a gene essential for embryonic development encodes two

receptor isoforms with different signaling potential. The EMBO journal 14:3373-3384.

Firth JD, Ebert BL, Ratcliffe PJ (1995) Hypoxic regulation of lactate dehydrogenase A. Interaction between hypoxia-inducible factor 1 and cAMP response elements. The Journal of biological chemistry 270:21021-21027.

Fischer A, Sananbenesi F, Wang X, Dobbin M, Tsai LH (2007) Recovery of learning and memory is associated with chromatin remodelling. Nature 447:178-182.

Fisher RP, Clayton DA (1988) Purification and characterization of human mitochondrial transcription factor 1. Molecular and cellular biology 8:3496-3509.

Foltynie T, Cheeran B, Williams-Gray CH, Edwards MJ, Schneider SA, Weinberger D, Rothwell JC, Barker RA, Bhatia KP (2009) BDNF val66met influences time to onset of levodopa induced dyskinesia in Parkinson's disease. Journal of neurology, neurosurgery, and psychiatry 80:141-144.

Formentini L, Sanchez-Arago M, Sanchez-Cenizo L, Cuezva JM (2012) The mitochondrial ATPase inhibitory factor 1 triggers a ROS-mediated retrograde prosurvival and proliferative response. Mol Cell 45:731-742.

Forny-Germano L, Lyra ESNM, Batista AF, Brito-Moreira J, Gralle M, Boehnke SE, Coe BC, Lablans A, Marques SA, Martinez AM, Klein WL, Houzel JC, Ferreira ST, Munoz DP, De Felice FG (2014) Alzheimer's Disease-Like Pathology Induced by Amyloid-beta Oligomers in Nonhuman Primates. The Journal of neuroscience : the official journal of the Society for Neuroscience 34:13629-13643.

Frank CA, Wang X, Collins CA, Rodal AA, Yuan Q, Verstreken P, Dickman DK (2013) New approaches for studying synaptic development, function, and plasticity using Drosophila as a model system. The Journal of neuroscience : the official journal of the Society for Neuroscience 33:17560-17568.

Freije WA, Mandal S, Banerjee U (2012) Expression profiling of attenuated mitochondrial function identifies retrograde signals in Drosophila. G3 (Bethesda) 2:843-851.

Freyer C, Park CB, Ekstrand MI, Shi Y, Khvorostova J, Wibom R, Falkenberg M, Gustafsson CM, Larsson NG (2010) Maintenance of respiratory chain function in mouse hearts with severely impaired mtDNA transcription. Nucleic Acids Res 38:6577-6588.

Fuchs J, Nilsson C, Kachergus J, Munz M, Larsson EM, Schule B, Langston JW, Middleton FA, Ross OA, Hulihan M, Gasser T, Farrer MJ (2007) Phenotypic variation in a large Swedish pedigree due to SNCA duplication and triplication. Neurology 68:916-922.

Fujiwara H, Hasegawa M, Dohmae N, Kawashima A, Masliah E, Goldberg MS, Shen J, Takio K, Iwatsubo T (2002) alpha-Synuclein is phosphorylated in synucleinopathy lesions. Nature cell biology 4:160-164.

Fukui H, Diaz F, Garcia S, Moraes CT (2007) Cytochrome c oxidase deficiency in neurons decreases both oxidative stress and amyloid formation in a mouse model of Alzheimer's disease. Proceedings of the National Academy of Sciences of the United States of America 104:14163-14168.

Fuste JM, Wanrooij S, Jemt E, Granycome CE, Cluett TJ, Shi Y, Atanassova N, Holt IJ, Gustafsson CM, Falkenberg M (2010) Mitochondrial RNA polymerase is needed for activation of the origin of light-strand DNA replication. Mol Cell 37:67-78.

Garelli A, Gontijo AM, Miguela V, Caparros E, Dominguez M (2012) Imaginal discs secrete insulin-like peptide 8 to mediate plasticity of growth and maturation. Science 336:579-582.

Garrido N, Griparic L, Jokitalo E, Wartiovaara J, van der Bliek AM, Spelbrink JN (2003) Composition and dynamics of human mitochondrial nucleoids. Mol Biol Cell 14:1583-1596.

Gasca-Salas C, Estanga A, Clavero P, Aguilar-Palacio I, Gonzalez-Redondo R, Obeso JA, Rodriguez-Oroz MC (2014) Longitudinal Assessment of the Pattern of Cognitive

Decline in Non-Demented Patients with Advanced Parkinson's Disease. Journal of Parkinson's disease.

Gaspari M, Falkenberg M, Larsson NG, Gustafsson CM (2004) The mitochondrial RNA polymerase contributes critically to promoter specificity in mammalian cells. The EMBO journal 23:4606-4614.

Gatt AP, Jones EL, Francis PT, Ballard C, Bateman JM (2013) Association of a polymorphism in mitochondrial transcription factor A (TFAM) with Parkinson's disease dementia but not dementia with Lewy bodies. Neurosci Lett 557 Pt B:177-180.

Gauthier BR, Wiederkehr A, Baquie M, Dai C, Powers AC, Kerr-Conte J, Pattou F, MacDonald RJ, Ferrer J, Wollheim CB (2009) PDX1 deficiency causes mitochondrial dysfunction and defective insulin secretion through TFAM suppression. Cell Metab 10:110-118.

Gautier CA, Kitada T, Shen J (2008) Loss of PINK1 causes mitochondrial functional defects and increased sensitivity to oxidative stress. Proceedings of the National Academy of Sciences of the United States of America 105:11364-11369.

Gaweda-Walerych K, Zekanowski C (2013) The impact of mitochondrial DNA and nuclear genes related to mitochondrial functioning on the risk of Parkinson's disease. Current genomics 14:543-559.

Gaweda-Walerych K, Safranow K, Maruszak A, Bialecka M, Klodowska-Duda G, Czyzewski K, Slawek J, Rudzinska M, Styczynska M, Opala G, Drozdzik M, Kurzawski M, Szczudlik A, Canter JA, Barcikowska M, Zekanowski C (2010) Mitochondrial transcription factor A variants and the risk of Parkinson's disease. Neuroscience Letters 469:24-29.

Gaweda-Walerych K, Safranow K, Jasinska-Myga B, Bialecka M, Klodowska-Duda G, Rudzinska M, Czyzewski K, Cobb SA, Slawek J, Styczynska M, Opala G, Drozdzik M, Nishioka K, Farrer MJ, Ross OA, Wszolek ZK, Barcikowska M, Zekanowski C (2012) PARK2 variability in Polish Parkinson's disease patients--interaction with mitochondrial haplogroups. Parkinsonism Relat Disord 18:520-524.

Gegg ME, Cooper JM, Chau KY, Rojo M, Schapira AH, Taanman JW (2010) Mitofusin 1 and mitofusin 2 are ubiquitinated in a PINK1/parkin-dependent manner upon induction of mitophagy. Hum Mol Genet 19:4861-4870.

Geminard C, Rulifson EJ, Leopold P (2009) Remote control of insulin secretion by fat cells in Drosophila. Cell Metab 10:199-207.

Giannattasio S, Liu Z, Thornton J, Butow RA (2005) Retrograde response to mitochondrial dysfunction is separable from TOR1/2 regulation of retrograde gene expression. The Journal of biological chemistry 280:42528-42535.

Giasson BI, Murray IV, Trojanowski JQ, Lee VM (2001) A hydrophobic stretch of 12 amino acid residues in the middle of alpha-synuclein is essential for filament assembly. The Journal of biological chemistry 276:2380-2386.

Giasson BI, Duda JE, Murray IV, Chen Q, Souza JM, Hurtig HI, Ischiropoulos H, Trojanowski JQ, Lee VM (2000) Oxidative damage linked to neurodegeneration by selective alpha-synuclein nitration in synucleinopathy lesions. Science 290:985-989.

Gillies GE, McArthur S (2010) Estrogen actions in the brain and the basis for differential action in men and women: a case for sex-specific medicines. Pharmacological reviews 62:155-198.

Goate A, Chartier-Harlin MC, Mullan M, Brown J, Crawford F, Fidani L, Giuffra L, Haynes A, Irving N, James L, et al. (1991) Segregation of a missense mutation in the amyloid precursor protein gene with familial Alzheimer's disease. Nature 349:704-706.

Goedert M, Spillantini MG, Del Tredici K, Braak H (2013) 100 years of Lewy pathology. Nat Rev Neurol 9:13-24.

Goldman JG, Holden S, Bernard B, Ouyang B, Goetz CG, Stebbins GT (2013) Defining optimal cutoff scores for cognitive impairment using Movement Disorder Society Task

Force criteria for mild cognitive impairment in Parkinson's disease. Movement disorders : official journal of the Movement Disorder Society 28:1972-1979.
Goldwurm S et al. (2006) LRRK2 G2019S mutation and Parkinson's disease: a clinical, neuropsychological and neuropsychiatric study in a large Italian sample. Parkinsonism Relat Disord 12:410-419.
Goto Y, Nonaka I, Horai S (1990) A mutation in the tRNA(Leu)(UUR) gene associated with the MELAS subgroup of mitochondrial encephalomyopathies. Nature 348:651-653.
Gouras GK, Almeida CG, Takahashi RH (2005) Intraneuronal Abeta accumulation and origin of plaques in Alzheimer's disease. Neurobiology of aging 26:1235-1244.
Graff J, Tsai LH (2013) Histone acetylation: molecular mnemonics on the chromatin. Nat Rev Neurosci 14:97-111.
Gronke S, Clarke DF, Broughton S, Andrews TD, Partridge L (2010) Molecular evolution and functional characterization of Drosophila insulin-like peptides. PLoS Genet 6:e1000857.
Guerini FR, Beghi E, Riboldazzi G, Zangaglia R, Pianezzola C, Bono G, Casali C, Di Lorenzo C, Agliardi C, Nappi G, Clerici M, Martignoni E (2009) BDNF Val66Met polymorphism is associated with cognitive impairment in Italian patients with Parkinson's disease. European journal of neurology : the official journal of the European Federation of Neurological Societies 16:1240-1245.
Guha M, Avadhani NG (2013) Mitochondrial retrograde signaling at the crossroads of tumor bioenergetics, genetics and epigenetics. Mitochondrion 13:577-591.
Guha M, Srinivasan S, Biswas G, Avadhani NG (2007) Activation of a novel calcineurin-mediated insulin-like growth factor-1 receptor pathway, altered metabolism, and tumor cell invasion in cells subjected to mitochondrial respiratory stress. The Journal of biological chemistry 282:14536-14546.
Guha M, Fang JK, Monks R, Birnbaum MJ, Avadhani NG (2010) Activation of Akt is essential for the propagation of mitochondrial respiratory stress signaling and activation of the transcriptional coactivator heterogeneous ribonucleoprotein A2. Mol Biol Cell 21:3578-3589.
Günther C, Hadeln Kv, Müller-Thomsen T, Alberici A, Binetti G, Hock C, Nitsch RM, Stoppe G, Reiss J, Gal A, Finckh U (2004) Possible association of mitochondrial transcription factor A (TFAM) genotype with sporadic Alzheimer disease. Neuroscience Letters 369:219-223.
Gura T (2008) Hope in Alzheimer's fight emerges from unexpected places. Nature medicine 14:894.
Gutterman DD (2005) Mitochondria and reactive oxygen species: an evolution in function. Circulation research 97:302-304.
Haass C, Selkoe DJ (2007) Soluble protein oligomers in neurodegeneration: lessons from the Alzheimer's amyloid beta-peptide. Nature reviews Molecular cell biology 8:101-112.
Hamilton RL (2000) Lewy bodies in Alzheimer's disease: a neuropathological review of 145 cases using alpha-synuclein immunohistochemistry. Brain Pathol 10:378-384.
Hanagasi HA, Ayribas D, Baysal K, Emre M (2005) Mitochondrial complex I, II/III, and IV activities in familial and sporadic Parkinson's disease. The International journal of neuroscience 115:479-493.
Hance N, Ekstrand MI, Trifunovic A (2005) Mitochondrial DNA polymerase gamma is essential for mammalian embryogenesis. Hum Mol Genet 14:1775-1783.
Hanson GT, Aggeler R, Oglesbee D, Cannon M, Capaldi RA, Tsien RY, Remington SJ (2004) Investigating mitochondrial redox potential with redox-sensitive green fluorescent protein indicators. The Journal of biological chemistry 279:13044-13053.

Hansson CA, Frykman S, Farmery MR, Tjernberg LO, Nilsberth C, Pursglove SE, Ito A, Winblad B, Cowburn RF, Thyberg J, Ankarcrona M (2004) Nicastrin, presenilin, APH-1, and PEN-2 form active gamma-secretase complexes in mitochondria. The Journal of biological chemistry 279:51654-51660.

Hansson Petersen CA, Alikhani N, Behbahani H, Wiehager B, Pavlov PF, Alafuzoff I, Leinonen V, Ito A, Winblad B, Glaser E, Ankarcrona M (2008) The amyloid beta-peptide is imported into mitochondria via the TOM import machinery and localized to mitochondrial cristae. Proceedings of the National Academy of Sciences of the United States of America 105:13145-13150.

Harding AJ, Halliday GM (2001) Cortical Lewy body pathology in the diagnosis of dementia. Acta neuropathologica 102:355-363.

Harding AJ, Broe GA, Halliday GM (2002) Visual hallucinations in Lewy body disease relate to Lewy bodies in the temporal lobe. Brain 125:391-403.

Hardy J, Mayer J (2011) The Amyloid Cascade Hypothesis Has Misled the Pharmaceutical Industry. Biochemical Society transactions 39:920-923.

Hardy JA, Higgins GA (1992) Alzheimer's disease: the amyloid cascade hypothesis. Science 256:184-185.

Harrison DE, Strong R, Sharp ZD, Nelson JF, Astle CM, Flurkey K, Nadon NL, Wilkinson JE, Frenkel K, Carter CS, Pahor M, Javors MA, Fernandez E, Miller RA (2009) Rapamycin fed late in life extends lifespan in genetically heterogeneous mice. Nature 460:392-395.

Hattori N, Tanaka M, Ozawa T, Mizuno Y (1991) Immunohistochemical studies on complexes I, II, III, and IV of mitochondria in Parkinson's disease. Ann Neurol 30:563-571.

Hayashi G, Cortopassi G (2015) Oxidative stress in inherited mitochondrial diseases. Free radical biology & medicine.

Hayashi Y, Yoshida M, Yamato M, Ide T, Wu Z, Ochi-Shindou M, Kanki T, Kang D, Sunagawa K, Tsutsui H, Nakanishi H (2008) Reverse of age-dependent memory impairment and mitochondrial DNA damage in microglia by an overexpression of human mitochondrial transcription factor a in mice. The Journal of neuroscience : the official journal of the Society for Neuroscience 28:8624-8634.

Haynes CM, Ron D (2010) The mitochondrial UPR - protecting organelle protein homeostasis. J Cell Sci 123:3849-3855.

Haynes CM, Fiorese CJ, Lin YF (2013) Evaluating and responding to mitochondrial dysfunction: the mitochondrial unfolded-protein response and beyond. Trends Cell Biol 23:311-318.

Haynes CM, Yang Y, Blais SP, Neubert TA, Ron D (2010) The matrix peptide exporter HAF-1 signals a mitochondrial UPR by activating the transcription factor ZC376.7 in C. elegans. Mol Cell 37:529-540.

Higgins CM, Jung C, Xu Z (2003) ALS-associated mutant SOD1G93A causes mitochondrial vacuolation by expansion of the intermembrane space and by involvement of SOD1 aggregation and peroxisomes. BMC neuroscience 4:16.

Holt IJ, Lorimer HE, Jacobs HT (2000) Coupled leading- and lagging-strand synthesis of mammalian mitochondrial DNA. Cell 100:515-524.

Horan MP, Cooper DN (2014) The emergence of the mitochondrial genome as a partial regulator of nuclear function is providing new insights into the genetic mechanisms underlying age-related complex disease. Human genetics 133:435-458.

Houtkooper RH, Mouchiroud L, Ryu D, Moullan N, Katsyuba E, Knott G, Williams RW, Auwerx J (2013) Mitonuclear protein imbalance as a conserved longevity mechanism. Nature 497:451-457.

Howell N, Bindoff LA, McCullough DA, Kubacka I, Poulton J, Mackey D, Taylor L, Turnbull DM (1991) Leber hereditary optic neuropathy: identification of the same mitochondrial ND1 mutation in six pedigrees. American journal of human genetics 49:939-950.

Howlett DR, Whitfield D, Johnson M, Attems J, O'Brien JT, Aarsland D, Lai MK, Lee JH, Chen C, Ballard C, Hortobagyi T, Francis PT (2014) Regional Multiple Pathology Scores are Associated with Cognitive Decline in Lewy Body Dementias. Brain Pathol.

Huang da W, Sherman BT, Lempicki RA (2009) Systematic and integrative analysis of large gene lists using DAVID bioinformatics resources. Nature protocols 4:44-57.

Huang JK, Ma PL, Ji SY, Zhao XL, Tan JX, Sun XJ, Huang FD (2013) Age-dependent alterations in the presynaptic active zone in a Drosophila model of Alzheimer's disease. Neurobiol Dis 51:161-167.

Hughes AJ, Daniel SE, Lees AJ (2001) Improved accuracy of clinical diagnosis of Lewy body Parkinson's disease. Neurology 57:1497-1499.

Humphrey DM, Parsons RB, Ludlow ZN, Riemensperger T, Esposito G, Verstreken P, Jacobs HT, Birman S, Hirth F (2012) Alternative oxidase rescues mitochondria-mediated dopaminergic cell loss in Drosophila. Human Molecular Genetics 21:2698-2712.

Hung WY, Wu CW, Yin PH, Chang CJ, Li AF, Chi CW, Wei YH, Lee HC (2010) Somatic mutations in mitochondrial genome and their potential roles in the progression of human gastric cancer. Biochimica et biophysica acta 1800:264-270.

Hurtig HI, Trojanowski JQ, Galvin J, Ewbank D, Schmidt ML, Lee VM, Clark CM, Glosser G, Stern MB, Gollomp SM, Arnold SE (2000) Alpha-synuclein cortical Lewy bodies correlate with dementia in Parkinson's disease. Neurology 54:1916-1921.

Hutton M, Perez-Tur J, Hardy J (1998) Genetics of Alzheimer's disease. Essays in biochemistry 33:117-131.

Hwang KS, Beyer MK, Green AE, Chung C, Thompson PM, Janvin C, Larsen JP, Aarsland D, Apostolova LG (2013) Mapping cortical atrophy in Parkinson's disease patients with dementia. Journal of Parkinson's disease 3:69-76.

Ibanez P, Bonnet AM, Debarges B, Lohmann E, Tison F, Pollak P, Agid Y, Durr A, Brice A (2004) Causal relation between alpha-synuclein gene duplication and familial Parkinson's disease. Lancet 364:1169-1171.

Ikeda K, Ikeda S, Yoshimura T, Kato H, Namba M (1978) Idiopathic Parkinsonism with Lewy-type inclusions in cerebral cortex. A case report. Acta neuropathologica 41:165-168.

Ikeya T, Galic M, Belawat P, Nairz K, Hafen E (2002) Nutrient-dependent expression of insulin-like peptides from neuroendocrine cells in the CNS contributes to growth regulation in Drosophila. Current biology : CB 12:1293-1300.

Ikeuchi M, Matsusaka H, Kang D, Matsushima S, Ide T, Kubota T, Fujiwara T, Hamasaki N, Takeshita A, Sunagawa K, Tsutsui H (2005) Overexpression of mitochondrial transcription factor a ameliorates mitochondrial deficiencies and cardiac failure after myocardial infarction. Circulation 112:683-690.

Inczedy-Farkas G, Trampush JW, Perczel Forintos D, Beech D, Andrejkovics M, Varga Z, Remenyi V, Bereznai B, Gal A, Molnar MJ (2014) Mitochondrial DNA mutations and cognition: a case-series report. Archives of clinical neuropsychology : the official journal of the National Academy of Neuropsychologists 29:315-321.

Inestrosa NC, Marzolo MP, Bonnefont AB (1998) Cellular and molecular basis of estrogen's neuroprotection. Potential relevance for Alzheimer's disease. Molecular neurobiology 17:73-86.

Irrcher I et al. (2010) Loss of the Parkinson's disease-linked gene DJ-1 perturbs mitochondrial dynamics. Human Molecular Genetics 19:3734-3746.

Irwin DJ, Lee VM, Trojanowski JQ (2013) Parkinson's disease dementia: convergence of alpha-synuclein, tau and amyloid-beta pathologies. Nat Rev Neurosci 14:626-636.

Iseki E (2004) Dementia with Lewy bodies: reclassification of pathological subtypes and boundary with Parkinson's disease or Alzheimer's disease. Neuropathology : official journal of the Japanese Society of Neuropathology 24:72-78.

Ishikawa K, Motoi Y, Mizuno Y, Kubo S, Hattori N (2014) Effects of donepezil dose escalation in Parkinson's patients with dementia receiving long-term donepezil treatment: an exploratory study. Psychogeriatrics : the official journal of the Japanese Psychogeriatric Society 14:93-100.

Ishikawa K, Takenaga K, Akimoto M, Koshikawa N, Yamaguchi A, Imanishi H, Nakada K, Honma Y, Hayashi J (2008) ROS-generating mitochondrial DNA mutations can regulate tumor cell metastasis. Science 320:661-664.

Iyengar B, Roote J, Campos AR (1999) The tamas gene, identified as a mutation that disrupts larval behavior in Drosophila melanogaster, codes for the mitochondrial DNA polymerase catalytic subunit (DNApol-gamma125). Genetics 153:1809-1824.

Iyengar B, Luo N, Farr CL, Kaguni LS, Campos AR (2002) The accessory subunit of DNA polymerase gamma is essential for mitochondrial DNA maintenance and development in Drosophila melanogaster. Proceedings of the National Academy of Sciences of the United States of America 99:4483-4488.

Jacobs HT (2003) Disorders of mitochondrial protein synthesis. Hum Mol Genet 12 Spec No 2:R293-301.

Jahangir Tafrechi RS, Svensson PJ, Janssen GM, Szuhai K, Maassen JA, Raap AK (2005) Distinct nuclear gene expression profiles in cells with mtDNA depletion and homoplasmic A3243G mutation. Mutation research 578:43-52.

Jan LY, Jan YN (1982) Antibodies to horseradish peroxidase as specific neuronal markers in Drosophila and in grasshopper embryos. Proceedings of the National Academy of Sciences of the United States of America 79:2700-2704.

Janetzky B, Hauck S, Youdim MB, Riederer P, Jellinger K, Pantucek F, Zochling R, Boissl KW, Reichmann H (1994) Unaltered aconitase activity, but decreased complex I activity in substantia nigra pars compacta of patients with Parkinson's disease. Neurosci Lett 169:126-128.

Jenner P (2008) Molecular mechanisms of L-DOPA-induced dyskinesia. Nat Rev Neurosci 9:665-677.

Jia Y, Rothermel B, Thornton J, Butow RA (1997) A basic helix-loop-helix-leucine zipper transcription complex in yeast functions in a signaling pathway from mitochondria to the nucleus. Molecular and cellular biology 17:1110-1117.

Jimenez S, Torres M, Vizuete M, Sanchez-Varo R, Sanchez-Mejias E, Trujillo-Estrada L, Carmona-Cuenca I, Caballero C, Ruano D, Gutierrez A, Vitorica J (2011) Age-dependent accumulation of soluble amyloid beta (Abeta) oligomers reverses the neuroprotective effect of soluble amyloid precursor protein-alpha (sAPP(alpha)) by modulating phosphatidylinositol 3-kinase (PI3K)/Akt-GSK-3beta pathway in Alzheimer mouse model. The Journal of biological chemistry 286:18414-18425.

Johns DR, Neufeld MJ, Park RD (1992) An ND-6 mitochondrial DNA mutation associated with Leber hereditary optic neuropathy. Biochemical and biophysical research communications 187:1551-1557.

Jones AW, Yao Z, Vicencio JM, Karkucinska-Wieckowska A, Szabadkai G (2012) PGC-1 family coactivators and cell fate: roles in cancer, neurodegeneration, cardiovascular disease and retrograde mitochondria-nucleus signalling. Mitochondrion 12:86-99.

Jonsson T et al. (2012) A mutation in APP protects against Alzheimer/'s disease and age-related cognitive decline. Nature advance online publication.

Kachergus J, Mata IF, Hulihan M, Taylor JP, Lincoln S, Aasly J, Gibson JM, Ross OA, Lynch T, Wiley J, Payami H, Nutt J, Maraganore DM, Czyzewski K, Styczynska M, Wszolek ZK, Farrer MJ, Toft M (2005) Identification of a novel LRRK2 mutation linked to autosomal dominant parkinsonism: evidence of a common founder across European populations. American journal of human genetics 76:672-680.

Kaipparettu BA, Ma Y, Park JH, Lee TL, Zhang Y, Yotnda P, Creighton CJ, Chan WY, Wong LJ (2013) Crosstalk from non-cancerous mitochondria can inhibit tumor properties of metastatic cells by suppressing oncogenic pathways. PloS one 8:e61747.

Kane M, Cook L (2013) Dementia 2013: The hidden voice of loneliness. London: Alzheimers Society.

Kang JS, Tian JH, Pan PY, Zald P, Li C, Deng C, Sheng ZH (2008) Docking of axonal mitochondria by syntaphilin controls their mobility and affects short-term facilitation. Cell 132:137-148.

Kanki T, Ohgaki K, Gaspari M, Gustafsson CM, Fukuoh A, Sasaki N, Hamasaki N, Kang D (2004) Architectural role of mitochondrial transcription factor A in maintenance of human mitochondrial DNA. Molecular and cellular biology 24:9823-9834.

Kao LP, Ovchinnikov D, Wolvetang E (2012) The effect of ethidium bromide and chloramphenicol on mitochondrial biogenesis in primary human fibroblasts. Toxicology and applied pharmacology 261:42-49.

Karran E, Mercken M, De Strooper B (2011) The amyloid cascade hypothesis for Alzheimer's disease: an appraisal for the development of therapeutics. Nature reviews Drug discovery 10:698-712.

Katz B (1996) Neural transmitter release: from quantal secretion to exocytosis and beyond. The Fenn Lecture. Journal of neurocytology 25:677-686.

Kaufman BA, Durisic N, Mativetsky JM, Costantino S, Hancock MA, Grutter P, Shoubridge EA (2007) The mitochondrial transcription factor TFAM coordinates the assembly of multiple DNA molecules into nucleoid-like structures. Mol Biol Cell 18:3225-3236.

Kawai S, Urban J, Piccolis M, Panchaud N, De Virgilio C, Loewith R (2011) Mitochondrial genomic dysfunction causes dephosphorylation of Sch9 in the yeast Saccharomyces cerevisiae. Eukaryotic cell 10:1367-1369.

Kayalar C, Rosing J, Boyer PD (1977) An alternating site sequence for oxidative phosphorylation suggested by measurement of substrate binding patterns and exchange reaction inhibitions. The Journal of biological chemistry 252:2486-2491.

Kaye D, Shah SJ, Borlaug BA, Gustafsson F, Komtebedde J, Kubo S, Magnin C, Maurer MS, Feldman T, Burkhoff D (2014) Effects of an interatrial shunt on rest and exercise hemodynamics: results of a computer simulation in heart failure. Journal of cardiac failure 20:212-221.

Keeney PM, Quigley CK, Dunham LD, Papageorge CM, Iyer S, Thomas RR, Schwarz KM, Trimmer PA, Khan SM, Portell FR, Bergquist KE, Bennett JP, Jr. (2009) Mitochondrial gene therapy augments mitochondrial physiology in a Parkinson's disease cell model. Human gene therapy 20:897-907.

Kelly RD, Mahmud A, McKenzie M, Trounce IA, St John JC (2012) Mitochondrial DNA copy number is regulated in a tissue specific manner by DNA methylation of the nuclear-encoded DNA polymerase gamma A. Nucleic Acids Res 40:10124-10138.

Kempster PA, O'Sullivan SS, Holton JL, Revesz T, Lees AJ (2010) Relationships between age and late progression of Parkinson's disease: a clinico-pathological study. Brain 133:1755-1762.

Kennedy EP, Lehninger AL (1949) Oxidation of fatty acids and tricarboxylic acid cycle intermediates by isolated rat liver mitochondria. The Journal of biological chemistry 179:957-972.

Khrapko K, Vijg J (2009) Mitochondrial DNA mutations and aging: devils in the details? Trends in genetics : TIG 25:91-98.

Khrapko K, Bodyak N, Thilly WG, van Orsouw NJ, Zhang X, Coller HA, Perls TT, Upton M, Vijg J, Wei JY (1999) Cell-by-cell scanning of whole mitochondrial genomes in aged human heart reveals a significant fraction of myocytes with clonally expanded deletions. Nucleic Acids Res 27:2434-2441.

Khurana V, Lu Y, Steinhilb ML, Oldham S, Shulman JM, Feany MB (2006) TOR-mediated cell-cycle activation causes neurodegeneration in a Drosophila tauopathy model. Current biology : CB 16:230-241.

Kim Y, Park J, Kim S, Song S, Kwon SK, Lee SH, Kitada T, Kim JM, Chung J (2008) PINK1 controls mitochondrial localization of Parkin through direct phosphorylation. Biochemical and biophysical research communications 377:975-980.

Kirvell SL, Esiri M, Francis PT (2006) Down-regulation of vesicular glutamate transporters precedes cell loss and pathology in Alzheimer's disease. Journal of neurochemistry 98:939-950.

Kittel RJ, Wichmann C, Rasse TM, Fouquet W, Schmidt M, Schmid A, Wagh DA, Pawlu C, Kellner RR, Willig KI, Hell SW, Buchner E, Heckmann M, Sigrist SJ (2006) Bruchpilot promotes active zone assembly, Ca2+ channel clustering, and vesicle release. Science 312:1051-1054.

Koczor CA, Torres RA, Fields EJ, Boyd A, He S, Patel N, Lee EK, Samarel AM, Lewis W (2013) Thymidine kinase and mtDNA depletion in human cardiomyopathy: epigenetic and translational evidence for energy starvation. Physiological genomics 45:590-596.

Komeili A, Wedaman KP, O'Shea EK, Powers T (2000) Mechanism of metabolic control. Target of rapamycin signaling links nitrogen quality to the activity of the Rtg1 and Rtg3 transcription factors. J Cell Biol 151:863-878.

Koritzinsky M, Magagnin MG, van den Beucken T, Seigneuric R, Savelkouls K, Dostie J, Pyronnet S, Kaufman RJ, Weppler SA, Voncken JW, Lambin P, Koumenis C, Sonenberg N, Wouters BG (2006) Gene expression during acute and prolonged hypoxia is regulated by distinct mechanisms of translational control. The EMBO journal 25:1114-1125.

Kosaka K, Yoshimura M, Ikeda K, Budka H (1984) Diffuse type of Lewy body disease: progressive dementia with abundant cortical Lewy bodies and senile changes of varying degree--a new disease? Clinical neuropathology 3:185-192.

Kraytsberg Y, Simon DK, Turnbull DM, Khrapko K (2009) Do mtDNA deletions drive premature aging in mtDNA mutator mice? Aging cell 8:502-506.

Kraytsberg Y, Kudryavtseva E, McKee AC, Geula C, Kowall NW, Khrapko K (2006) Mitochondrial DNA deletions are abundant and cause functional impairment in aged human substantia nigra neurons. Nature genetics 38:518-520.

Krebiehl G, Ruckerbauer S, Burbulla LF, Kieper N, Maurer B, Waak J, Wolburg H, Gizatullina Z, Gellerich FN, Woitalla D, Riess O, Kahle PJ, Proikas-Cezanne T, Krüger R (2010) Reduced Basal Autophagy and Impaired Mitochondrial Dynamics Due to Loss of Parkinson's Disease-Associated Protein DJ-1. PloS one 5:e9367.

Krebs HA (1937) The role of fumarate in the respiration of Bacterium coli commune. The Biochemical journal 31:2095-2124.

Krishnan KJ, Greaves LC, Reeve AK, Turnbull D (2007) The ageing mitochondrial genome. Nucleic Acids Res 35:7399-7405.

Krishnan KJ, Reeve AK, Samuels DC, Chinnery PF, Blackwood JK, Taylor RW, Wanrooij S, Spelbrink JN, Lightowlers RN, Turnbull DM (2008) What causes mitochondrial DNA deletions in human cells? Nature genetics 40:275-279.

Kruger R, Kuhn W, Muller T, Woitalla D, Graeber M, Kosel S, Przuntek H, Epplen JT, Schols L, Riess O (1998) Ala30Pro mutation in the gene encoding alpha-synuclein in Parkinson's disease. Nature genetics 18:106-108.

Kukat C, Wurm CA, Spahr H, Falkenberg M, Larsson NG, Jakobs S (2011) Super-resolution microscopy reveals that mammalian mitochondrial nucleoids have a uniform size and frequently contain a single copy of mtDNA. Proceedings of the National Academy of Sciences of the United States of America 108:13534-13539.

Kukreja L, Kujoth GC, Prolla TA, Van Leuven F, Vassar R (2014) Increased mtDNA mutations with aging promotes amyloid accumulation and brain atrophy in the APP/Ld transgenic mouse model of Alzheimer's disease. Molecular neurodegeneration 9:16.

Kurland C, Andersson S (2000) Origin and evolution of the mitochondrial proteome. Microbiology and Molecular Biology Reviews 64:786-820.

LaFerla FM, Green KN, Oddo S (2007) Intracellular amyloid-beta in Alzheimer's disease. Nature reviews Neuroscience 8:499-509.

Lamming DW, Ye L, Sabatini DM, Baur JA (2013) Rapalogs and mTOR inhibitors as anti-aging therapeutics. The Journal of clinical investigation 123:980-989.

Lane N (2006) Power, sex, suicide : mitochondria and the meaning of life, Oxford University Press pbk. Edition. Oxford ; New York: Oxford University Press.

Lane N (2014) Bioenergetic constraints on the evolution of complex life. Cold Spring Harbor perspectives in biology 6:a015982.

Lapointe J, Hekimi S (2008) Early mitochondrial dysfunction in long-lived Mclk1+/- mice. The Journal of biological chemistry 283:26217-26227.

Larsson NG, Tulinius MH, Holme E, Oldfors A, Andersen O, Wahlstrom J, Aasly J (1992) Segregation and manifestations of the mtDNA tRNA(Lys) A-->G(8344) mutation of myoclonus epilepsy and ragged-red fibers (MERRF) syndrome. American journal of human genetics 51:1201-1212.

Larsson NG, Wang J, Wilhelmsson H, Oldfors A, Rustin P, Lewandoski M, Barsh GS, Clayton DA (1998) Mitochondrial transcription factor A is necessary for mtDNA maintenance and embryogenesis in mice. Nature genetics 18:231-236.

Laumet G et al. (2010) Systematic analysis of candidate genes for Alzheimer's disease in a French, genome-wide association study. Journal of Alzheimer's disease : JAD 20:1181-1188.

Lavara-Culebras E, Paricio N (2007) Drosophila DJ-1 mutants are sensitive to oxidative stress and show reduced lifespan and motor deficits. Gene 400:158-165.

Lavista-Llanos S, Centanin L, Irisarri M, Russo DM, Gleadle JM, Bocca SN, Muzzopappa M, Ratcliffe PJ, Wappner P (2002) Control of the hypoxic response in Drosophila melanogaster by the basic helix-loop-helix PAS protein similar. Molecular and cellular biology 22:6842-6853.

Lazarou M, Jin SM, Kane LA, Youle RJ (2012) Role of PINK1 binding to the TOM complex and alternate intracellular membranes in recruitment and activation of the E3 ligase Parkin. Developmental cell 22:320-333.

Lee J-Y, Nagano Y, Taylor JP, Lim KL, Yao T-P (2010) Disease-causing mutations in Parkin impair mitochondrial ubiquitination, aggregation, and HDAC6-dependent mitophagy. The Journal of Cell Biology 189:671-679.

Lee T, Luo L (1999) Mosaic analysis with a repressible cell marker for studies of gene function in neuronal morphogenesis. Neuron 22:451-461.

Lefai E, Calleja M, Ruiz de Mena I, Lagina AT, 3rd, Kaguni LS, Garesse R (2000) Overexpression of the catalytic subunit of DNA polymerase gamma results in depletion of mitochondrial DNA in Drosophila melanogaster. Molecular & general genetics : MGG 264:37-46.

Lerner C, Bitto A, Pulliam D, Nacarelli T, Konigsberg M, Van Remmen H, Torres C, Sell C (2013) Reduced mammalian target of rapamycin activity facilitates mitochondrial retrograde signaling and increases life span in normal human fibroblasts. Aging cell 12:966-977.

Lesage S, Anheim M, Letournel F, Bousset L, Honore A, Rozas N, Pieri L, Madiona K, Durr A, Melki R, Verny C, Brice A (2013) G51D alpha-synuclein mutation causes a novel parkinsonian-pyramidal syndrome. Ann Neurol 73:459-471.

Leverenz JB, Hamilton R, Tsuang DW, Schantz A, Vavrek D, Larson EB, Kukull WA, Lopez O, Galasko D, Masliah E, Kaye J, Woltjer R, Clark C, Trojanowski JQ, Montine TJ (2008) Empiric refinement of the pathologic assessment of Lewy-related pathology in the dementia patient. Brain Pathol 18:220-224.

Li Z, Okamoto K, Hayashi Y, Sheng M (2004) The importance of dendritic mitochondria in the morphogenesis and plasticity of spines and synapses. Cell 119:873-887.

Liang X, Slifer M, Martin ER, Schnetz-Boutaud N, Bartlett J, Anderson B, Zuchner S, Gwirtsman H, Gilbert JR, Pericak-Vance MA, Haines JL (2009) Genomic convergence to identify candidate genes for Alzheimer disease on chromosome 10. Human mutation 30:463-471.

Liang X, Martin ER, Schnetz-Boutaud N, Bartlett J, Anderson B, Zuchner S, Gwirtsman H, Schmechel D, Carney R, Gilbert JR, Pericak-Vance MA, Haines JL (2007) Effect of heterogeneity on the chromosome 10 risk in late-onset Alzheimer disease. Human mutation 28:1065-1073.

Liao TS, Call GB, Guptan P, Cespedes A, Marshall J, Yackle K, Owusu-Ansah E, Mandal S, Fang QA, Goodstein GL, Kim W, Banerjee U (2006) An efficient genetic screen in Drosophila to identify nuclear-encoded genes with mitochondrial function. Genetics 174:525-533.

Liao X, Butow RA (1993) RTG1 and RTG2: two yeast genes required for a novel path of communication from mitochondria to the nucleus. Cell 72:61-71.

Lill CM et al. (2012) Comprehensive research synopsis and systematic meta-analyses in Parkinson's disease genetics: The PDGene database. PLoS Genet 8:e1002548.

Lin MT, Beal MF (2006) Mitochondrial dysfunction and oxidative stress in neurodegenerative diseases. Nature 443:787-795.

Lin MT, Simon DK, Ahn CH, Kim LM, Beal MF (2002) High aggregate burden of somatic mtDNA point mutations in aging and Alzheimer's disease brain. Hum Mol Genet 11:133-145.

Lin W, Wadlington NL, Chen L, Zhuang X, Brorson JR, Kang UJ (2014) Loss of PINK1 attenuates HIF-1alpha induction by preventing 4E-BP1-dependent switch in protein translation under hypoxia. The Journal of neuroscience : the official journal of the Society for Neuroscience 34:3079-3089.

Linder T, Park CB, Asin-Cayuela J, Pellegrini M, Larsson NG, Falkenberg M, Samuelsson T, Gustafsson CM (2005) A family of putative transcription termination factors shared amongst metazoans and plants. Current genetics 48:265-269.

Ling X, Wen L, Zhou Y (2012) Role of mitochondrial translocation of telomerase in hepatocellular carcinoma cells with multidrug resistance. International journal of medical sciences 9:545-554.

Lippa CF, Fujiwara H, Mann DM, Giasson B, Baba M, Schmidt ML, Nee LE, O'Connell B, Pollen DA, St George-Hyslop P, Ghetti B, Nochlin D, Bird TD, Cairns NJ, Lee VM, Iwatsubo T, Trojanowski JQ (1998) Lewy bodies contain altered alpha-synuclein in brains of many familial Alzheimer's disease patients with mutations in presenilin and amyloid precursor protein genes. The American journal of pathology 153:1365-1370.

Lippa CF et al. (2007) DLB and PDD boundary issues: diagnosis, treatment, molecular pathology, and biomarkers. Neurology 68:812-819.

Litvan I, Goldman JG, Troster AI, Schmand BA, Weintraub D, Petersen RC, Mollenhauer B, Adler CH, Marder K, Williams-Gray CH, Aarsland D, Kulisevsky J, Rodriguez-Oroz MC, Burn DJ, Barker RA, Emre M (2012) Diagnostic criteria for mild cognitive impairment in Parkinson's disease: Movement Disorder Society Task Force guidelines. Movement disorders : official journal of the Movement Disorder Society 27:349-356.

Liu J, Wu Q, He D, Ma T, Du L, Dui W, Guo X, Jiao R (2011) Drosophila sbo regulates lifespan through its function in the synthesis of coenzyme Q in vivo. Journal of genetics and genomics = Yi chuan xue bao 38:225-234.

Liu L, Cash TP, Jones RG, Keith B, Thompson CB, Simon MC (2006) Hypoxia-induced energy stress regulates mRNA translation and cell growth. Mol Cell 21:521-531.

Liu S, Sawada T, Lee S, Yu W, Silverio G, Alapatt P, Millan I, Shen A, Saxton W, Kanao T, Takahashi R, Hattori N, Imai Y, Lu B (2012) Parkinson's disease-associated kinase PINK1 regulates Miro protein level and axonal transport of mitochondria. PLoS Genet 8:e1002537.

Liu W, Vives-Bauza C, Acin-Perez R, Yamamoto A, Tan Y, Li Y, Magrane J, Stavarache MA, Shaffer S, Chang S, Kaplitt MG, Huang XY, Beal MF, Manfredi G, Li C (2009) PINK1 defect causes mitochondrial dysfunction, proteasomal deficit and alpha-synuclein aggregation in cell culture models of Parkinson's disease. PloS one 4:e4597.

Liu X, Jiang N, Hughes B, Bigras E, Shoubridge E, Hekimi S (2005) Evolutionary conservation of the clk-1-dependent mechanism of longevity: loss of mclk1 increases cellular fitness and lifespan in mice. Genes & development 19:2424-2434.

Liu Z, Sekito T, Spirek M, Thornton J, Butow RA (2003) Retrograde signaling is regulated by the dynamic interaction between Rtg2p and Mks1p. Mol Cell 12:401-411.

Lohmann K (1929) Über die pyrophosphatfraktion im muskel. Naturwissenschaften 17:624-625.

Lorenzen N, Nielsen SB, Yoshimura Y, Vad BS, Andersen CB, Betzer C, Kaspersen JD, Christiansen G, Pedersen JS, Jensen PH, Mulder FA, Otzen DE (2014) How epigallocatechin gallate can inhibit alpha-synuclein oligomer toxicity in vitro. The Journal of biological chemistry 289:21299-21310.

Lu B, Lee J, Nie X, Li M, Morozov Yaroslav I, Venkatesh S, Bogenhagen Daniel F, Temiakov D, Suzuki Carolyn K (2013) Phosphorylation of Human TFAM in Mitochondria Impairs DNA Binding and Promotes Degradation by the AAA+ Lon Protease. Molecular Cell 49:121-132.

Lu T, Aron L, Zullo J, Pan Y, Kim H, Chen Y, Yang TH, Kim HM, Drake D, Liu XS, Bennett DA, Colaiacovo MP, Yankner BA (2014) REST and stress resistance in ageing and Alzheimer's disease. Nature 507:448-454.

Luan H, Lemon WC, Peabody NC, Pohl JB, Zelensky PK, Wang D, Nitabach MN, Holmes TC, White BH (2006) Functional dissection of a neuronal network required for cuticle tanning and wing expansion in Drosophila. The Journal of neuroscience : the official journal of the Society for Neuroscience 26:573-584.

Lustbader JW et al. (2004) ABAD directly links Abeta to mitochondrial toxicity in Alzheimer's disease. Science 304:448-452.

Lutz AK, Exner N, Fett ME, Schlehe JS, Kloos K, Lammermann K, Brunner B, Kurz-Drexler A, Vogel F, Reichert AS, Bouman L, Vogt-Weisenhorn D, Wurst W, Tatzelt J, Haass C, Winklhofer KF (2009) Loss of parkin or PINK1 function increases Drp1-dependent mitochondrial fragmentation. The Journal of biological chemistry 284:22938-22951.

Ma T, Trinh MA, Wexler AJ, Bourbon C, Gatti E, Pierre P, Cavener DR, Klann E (2013a) Suppression of eIF2alpha kinases alleviates Alzheimer's disease-related plasticity and memory deficits. Nat Neurosci 16:1299-1305.

Ma YQ, Wu DK, Liu JK (2013b) mTOR and tau phosphorylated proteins in the hippocampal tissue of rats with type 2 diabetes and Alzheimer's disease. Molecular medicine reports 7:623-627.

Macdonald A, Briggs K, Poppe M, Higgins A, Velayudhan L, Lovestone S (2008) A feasibility and tolerability study of lithium in Alzheimer's disease. International journal of geriatric psychiatry 23:704-711.

Mackenzie IR (2001) The pathology of Parkinson's disease. BRITISH COLUMBIA MEDICAL JOURNAL 43:142-147.

Maher-Edwards G, Zvartau-Hind M, Hunter AJ, Gold M, Hopton G, Jacobs G, Davy M, Williams P (2010) Double-blind, controlled phase II study of a 5-HT6 receptor antagonist, SB-742457, in Alzheimer's disease. Current Alzheimer research 7:374-385.

Maier D, Farr CL, Poeck B, Alahari A, Vogel M, Fischer S, Kaguni LS, Schneuwly S (2001) Mitochondrial single-stranded DNA-binding protein is required for mitochondrial DNA replication and development in Drosophila melanogaster. Mol Biol Cell 12:821-830.

Majmundar AJ, Wong WJ, Simon MC (2010) Hypoxia-inducible factors and the response to hypoxic stress. Mol Cell 40:294-309.

Malik AN, Shahni R, Rodriguez-de-Ledesma A, Laftah A, Cunningham P (2011) Mitochondrial DNA as a non-invasive biomarker: accurate quantification using real time quantitative PCR without co-amplification of pseudogenes and dilution bias. Biochemical and biophysical research communications 412:1-7.

Manczak M, Anekonda TS, Henson E, Park BS, Quinn J, Reddy PH (2006) Mitochondria are a direct site of A beta accumulation in Alzheimer's disease neurons: implications for free radical generation and oxidative damage in disease progression. Human molecular genetics 15:1437-1449.

Mandal S, Guptan P, Owusu-Ansah E, Banerjee U (2005) Mitochondrial regulation of cell cycle progression during development as revealed by the tenured mutation in Drosophila. Developmental cell 9:843-854.

Mandal S, Freije WA, Guptan P, Banerjee U (2010) Metabolic control of G1-S transition: cyclin E degradation by p53-induced activation of the ubiquitin-proteasome system. J Cell Biol 188:473-479.

Mandel H, Szargel R, Labay V, Elpeleg O, Saada A, Shalata A, Anbinder Y, Berkowitz D, Hartman C, Barak M, Eriksson S, Cohen N (2001) The deoxyguanosine kinase gene is mutated in individuals with depleted hepatocerebral mitochondrial DNA. Nature genetics 29:337-341.

Maniura-Weber K, Goffart S, Garstka HL, Montoya J, Wiesner RJ (2004) Transient overexpression of mitochondrial transcription factor A (TFAM) is sufficient to stimulate mitochondrial DNA transcription, but not sufficient to increase mtDNA copy number in cultured cells. Nucleic Acids Res 32:6015-6027.

Mann DM, Jones D, Snowden JS, Neary D, Hardy J (1992) Pathological changes in the brain of a patient with familial Alzheimer's disease having a missense mutation at codon 717 in the amyloid precursor protein gene. Neurosci Lett 137:225-228.

Margulis L (1981) Symbiosis in cell evolution : life and its environment on the early Earth. San Francisco: W. H. Freeman.

Martin W, Muller M (1998) The hydrogen hypothesis for the first eukaryote. Nature 392:37-41.

Martinez-Azorin F, Calleja M, Hernandez-Sierra R, Farr CL, Kaguni LS, Garesse R (2008) Over-expression of the catalytic core of mitochondrial DNA (mtDNA) polymerase in the nervous system of Drosophila melanogaster reduces median life span by inducing mtDNA depletion. Journal of neurochemistry 105:165-176.

Martinez-Azorin F, Calleja M, Hernandez-Sierra R, Farr CL, Kaguni LS, Garesse R (2013) Muscle-specific overexpression of the catalytic subunit of DNA polymerase gamma induces pupal lethality in Drosophila melanogaster. Archives of insect biochemistry and physiology 83:127-137.

Martinus RD, Garth GP, Webster TL, Cartwright P, Naylor DJ, Hoj PB, Hoogenraad NJ (1996) Selective induction of mitochondrial chaperones in response to loss of the mitochondrial genome. European journal of biochemistry / FEBS 240:98-103.

Marusich MF, Robinson BH, Taanman JW, Kim SJ, Schillace R, Smith JL, Capaldi RA (1997) Expression of mtDNA and nDNA encoded respiratory chain proteins in chemically and genetically-derived Rho0 human fibroblasts: a comparison of subunit proteins in normal fibroblasts treated with ethidium bromide and fibroblasts from a patient with mtDNA depletion syndrome. Biochimica et biophysica acta 1362:145-159.

Massaad CA, Amin SK, Hu L, Mei Y, Klann E, Pautler RG (2010) Mitochondrial superoxide contributes to blood flow and axonal transport deficits in the Tg2576 mouse model of Alzheimer's disease. PloS one 5:e10561.

Matsushima Y, Goto Y, Kaguni LS (2010) Mitochondrial Lon protease regulates mitochondrial DNA copy number and transcription by selective degradation of mitochondrial transcription factor A (TFAM). Proceedings of the National Academy of Sciences of the United States of America 107:18410-18415.

Mattila PM, Rinne JO, Helenius H, Dickson DW, Roytta M (2000) Alpha-synuclein-immunoreactive cortical Lewy bodies are associated with cognitive impairment in Parkinson's disease. Acta neuropathologica 100:285-290.

Mayer A, Lahr G, Swaab DF, Pilgrim C, Reisert I (1998) The Y-chromosomal genes SRY and ZFY are transcribed in adult human brain. neurogenetics 1:281-288.

McCammon MT, Epstein CB, Przybyla-Zawislak B, McAlister-Henn L, Butow RA (2003) Global transcription analysis of Krebs tricarboxylic acid cycle mutants reveals an alternating pattern of gene expression and effects on hypoxic and oxidative genes. Mol Biol Cell 14:958-972.

McKeith I, Del Ser T, Spano P, Emre M, Wesnes K, Anand R, Cicin-Sain A, Ferrara R, Spiegel R (2000a) Efficacy of rivastigmine in dementia with Lewy bodies: a randomised, double-blind, placebo-controlled international study. Lancet 356:2031-2036.

McKeith I, Mintzer J, Aarsland D, Burn D, Chiu H, Cohen-Mansfield J, Dickson D, Dubois B, Duda JE, Feldman H, Gauthier S, Halliday G, Lawlor B, Lippa C, Lopez OL, Machado JC, O'Brien J, Playfer J (2004) Dementia with Lewy bodies. The Lancet Neurology 3:19-28.

McKeith IG (2006) Consensus guidelines for the clinical and pathologic diagnosis of dementia with Lewy bodies (DLB): report of the Consortium on DLB International Workshop. Journal of Alzheimer's disease : JAD 9:417-423.

McKeith IG, Ballard CG, Perry RH, Ince PG, O'Brien JT, Neill D, Lowery K, Jaros E, Barber R, Thompson P, Swann A, Fairbairn AF, Perry EK (2000b) Prospective validation of consensus criteria for the diagnosis of dementia with Lewy bodies. Neurology 54:1050-1058.

McKeith IG et al. (1996) Consensus guidelines for the clinical and pathologic diagnosis of dementia with Lewy bodies (DLB): report of the consortium on DLB international workshop. Neurology 47:1113-1124.

McKeith IG et al. (2005) Diagnosis and management of dementia with Lewy bodies: third report of the DLB Consortium. Neurology 65:1863-1872.

McKinney EA, Oliveira MT (2013) Replicating animal mitochondrial DNA. Genetics and molecular biology 36:308-315.

Michikawa Y, Laderman K, Richter K, Attardi G (1999a) Role of nuclear background and in vivo environment in variable segregation behavior of the aging-dependent T414G mutation at critical control site for human fibroblast mtDNA replication. Somatic cell and molecular genetics 25:333-342.

Michikawa Y, Mazzucchelli F, Bresolin N, Scarlato G, Attardi G (1999b) Aging-dependent large accumulation of point mutations in the human mtDNA control region for replication. Science 286:774-779.

Mirra SS, Heyman A, McKeel D, Sumi SM, Crain BJ, Brownlee LM, Vogel FS, Hughes JP, van Belle G, Berg L (1991) The Consortium to Establish a Registry for Alzheimer's Disease (CERAD). Part II. Standardization of the neuropathologic assessment of Alzheimer's disease. Neurology 41:479-486.

Misko A, Jiang S, Wegorzewska I, Milbrandt J, Baloh RH (2010) Mitofusin 2 is necessary for transport of axonal mitochondria and interacts with the Miro/Milton complex. The Journal of neuroscience : the official journal of the Society for Neuroscience 30:4232-4240.

Mitchell P (1961) Coupling of phosphorylation to electron and hydrogen transfer by a chemi-osmotic type of mechanism. Nature 191:144-148.

Monoranu CM, Apfelbacher M, Grunblatt E, Puppe B, Alafuzoff I, Ferrer I, Al-Saraj S, Keyvani K, Schmitt A, Falkai P, Schittenhelm J, Halliday G, Kril J, Harper C, McLean C, Riederer P, Roggendorf W (2009) pH measurement as quality control on human post mortem brain tissue: a study of the BrainNet Europe consortium. Neuropathology and applied neurobiology 35:329-337.

Mooradian AD (1993) Antioxidant properties of steroids. The Journal of steroid biochemistry and molecular biology 45:509-511.

Moraes CT, DiMauro S, Zeviani M, Lombes A, Shanske S, Miranda AF, Nakase H, Bonilla E, Werneck LC, Servidei S, et al. (1989) Mitochondrial DNA deletions in progressive external ophthalmoplegia and Kearns-Sayre syndrome. The New England journal of medicine 320:1293-1299.

Morais VA, Verstreken P, Roethig A, Smet J, Snellinx A, Vanbrabant M, Haddad D, Frezza C, Mandemakers W, Vogt-Weisenhorn D, Van Coster R, Wurst W, Scorrano L, De Strooper B (2009) Parkinson's disease mutations in PINK1 result in decreased Complex I activity and deficient synaptic function. EMBO molecular medicine 1:99-111.

Moreno H, Yu E, Pigino G, Hernandez AI, Kim N, Moreira JE, Sugimori M, Llinas RR (2009) Synaptic transmission block by presynaptic injection of oligomeric amyloid beta. Proceedings of the National Academy of Sciences of the United States of America 106:5901-5906.

Morimoto N, Miyazaki K, Kurata T, Ikeda Y, Matsuura T, Kang D, Ide T, Abe K (2012) Effect of mitochondrial transcription factor a overexpression on motor neurons in amyotrophic lateral sclerosis model mice. Journal of Neuroscience Research:n/a-n/a.

Morozov YI, Agaronyan K, Cheung AC, Anikin M, Cramer P, Temiakov D (2014) A novel intermediate in transcription initiation by human mitochondrial RNA polymerase. Nucleic Acids Res 42:3884-3893.

Morris RL, Hollenbeck PJ (1993) The regulation of bidirectional mitochondrial transport is coordinated with axonal outgrowth. J Cell Sci 104 (Pt 3):917-927.

Mortiboys H, Johansen KK, Aasly JO, Bandmann O (2010) Mitochondrial impairment in patients with Parkinson disease with the G2019S mutation in LRRK2. Neurology 75:2017-2020.

Mortiboys H, Thomas KJ, Koopman WJ, Klaffke S, Abou-Sleiman P, Olpin S, Wood NW, Willems PH, Smeitink JA, Cookson MR, Bandmann O (2008) Mitochondrial function and morphology are impaired in parkin-mutant fibroblasts. Ann Neurol 64:555-565.

Murdock DG, Christacos NC, Wallace DC (2000) The age-related accumulation of a mitochondrial DNA control region mutation in muscle, but not brain, detected by a sensitive PNA-directed PCR clamping based method. Nucleic Acids Res 28:4350-4355.

Murphy MP (2009) How mitochondria produce reactive oxygen species. The Biochemical journal 417:1-13.

Murrell J, Farlow M, Ghetti B, Benson MD (1991) A mutation in the amyloid precursor protein associated with hereditary Alzheimer's disease. Science 254:97-99.

Myers A et al. (2002) Full genome screen for Alzheimer disease: stage II analysis. American journal of medical genetics 114:235-244.

Naftolin F, Leranth C, Perez J, Garcia-Segura LM (1993) Estrogen induces synaptic plasticity in adult primate neurons. Neuroendocrinology 57:935-939.

Narendra D, Tanaka A, Suen D-F, Youle RJ (2009) Parkin-induced mitophagy in the pathogenesis of Parkinson disease. Autophagy 5:706-708.

Narendra DP, Jin SM, Tanaka A, Suen DF, Gautier CA, Shen J, Cookson MR, Youle RJ (2010) PINK1 is selectively stabilized on impaired mitochondria to activate Parkin. PLoS biology 8:e1000298.

Nargund AM, Pellegrino MW, Fiorese CJ, Baker BM, Haynes CM (2012) Mitochondrial import efficiency of ATFS-1 regulates mitochondrial UPR activation. Science 337:587-590.

Naruse S, Igarashi S, Kobayashi H, Aoki K, Inuzuka T, Kaneko K, Shimizu T, Iihara K, Kojima T, Miyatake T, et al. (1991) Mis-sense mutation Val----Ile in exon 17 of amyloid precursor protein gene in Japanese familial Alzheimer's disease. Lancet 337:978-979.

Nass MM, Nass S (1963) Intramitochondrial Fibers with DNA Characteristics. I. Fixation and Electron Staining Reactions. J Cell Biol 19:593-611.

Nassel DR, Kubrak OI, Liu Y, Luo J, Lushchak OV (2013) Factors that regulate insulin producing cells and their output in Drosophila. Frontiers in physiology 4:252.

Ngo HB, Kaiser JT, Chan DC (2011) The mitochondrial transcription and packaging factor Tfam imposes a U-turn on mitochondrial DNA. Nature structural & molecular biology 18:1290-1296.

Nicholas A, Kraytsberg Y, Guo X, Khrapko K (2009) On the timing and the extent of clonal expansion of mtDNA deletions: evidence from single-molecule PCR. Exp Neurol 218:316-319.

Nishino I, Spinazzola A, Hirano M (1999) Thymidine phosphorylase gene mutations in MNGIE, a human mitochondrial disorder. Science 283:689-692.

Nishioka K, Ross OA, Ishii K, Kachergus JM, Ishiwata K, Kitagawa M, Kono S, Obi T, Mizoguchi K, Inoue Y, Imai H, Takanashi M, Mizuno Y, Farrer MJ, Hattori N (2009) Expanding the clinical phenotype of SNCA duplication carriers. Movement disorders : official journal of the Movement Disorder Society 24:1811-1819.

Niu J, Yu M, Wang C, Xu Z (2012) Leucine-rich repeat kinase 2 disturbs mitochondrial dynamics via Dynamin-like protein. Journal of neurochemistry 122:650-658.

O'Brien JT, Burns A (2011) Clinical practice with anti-dementia drugs: a revised (second) consensus statement from the British Association for Psychopharmacology. J Psychopharmacol 25:997-1019.

O'Hagan HM, Wang W, Sen S, Destefano Shields C, Lee SS, Zhang YW, Clements EG, Cai Y, Van Neste L, Easwaran H, Casero RA, Sears CL, Baylin SB (2011) Oxidative damage

targets complexes containing DNA methyltransferases, SIRT1, and polycomb members to promoter CpG Islands. Cancer cell 20:606-619.
Obeso JA, Rodriguez-Oroz MC, Goetz CG, Marin C, Kordower JH, Rodriguez M, Hirsch EC, Farrer M, Schapira AH, Halliday G (2010) Missing pieces in the Parkinson's disease puzzle. Nature medicine 16:653-661.
Orr ME, Salinas A, Buffenstein R, Oddo S (2014) Mammalian target of rapamycin hyperactivity mediates the detrimental effects of a high sucrose diet on Alzheimer's disease pathology. Neurobiol Aging 35:1233-1242.
Owusu-Ansah E, Song W, Perrimon N (2013) Muscle mitohormesis promotes longevity via systemic repression of insulin signaling. Cell 155:699-712.
Owusu-Ansah E, Yavari A, Mandal S, Banerjee U (2008) Distinct mitochondrial retrograde signals control the G1-S cell cycle checkpoint. Nature genetics 40:356-361.
Paisan-Ruiz C et al. (2004) Cloning of the gene containing mutations that cause PARK8-linked Parkinson's disease. Neuron 44:595-600.
Palacino JJ, Sagi D, Goldberg MS, Krauss S, Motz C, Wacker M, Klose J, Shen J (2004) Mitochondrial dysfunction and oxidative damage in parkin-deficient mice. The Journal of biological chemistry 279:18614-18622.
Palade GE (1953) An electron microscope study of the mitochondrial structure. The journal of histochemistry and cytochemistry : official journal of the Histochemistry Society 1:188-211.
Pankratz N, Nichols WC, Uniacke SK, Halter C, Rudolph A, Shults C, Conneally PM, Foroud T (2002) Genome screen to identify susceptibility genes for Parkinson disease in a sample without parkin mutations. American journal of human genetics 71:124-135.
Pankratz N, Wilk JB, Latourelle JC, DeStefano AL, Halter C, Pugh EW, Doheny KF, Gusella JF, Nichols WC, Foroud T, Myers RH (2009) Genomewide association study for susceptibility genes contributing to familial Parkinson disease. Human genetics 124:593-605.
Parikh VS, Morgan MM, Scott R, Clements LS, Butow RA (1987) The mitochondrial genotype can influence nuclear gene expression in yeast. Science 235:576-580.
Parisi MA, Clayton DA (1991) Similarity of human mitochondrial transcription factor 1 to high mobility group proteins. Science 252:965-969.
Parker WD, Jr., Boyson SJ, Parks JK (1989) Abnormalities of the electron transport chain in idiopathic Parkinson's disease. Ann Neurol 26:719-723.
Parkinson J (1817) An essay on the shaking palsy: Whittingham and Rowland.
Pasinelli P, Belford ME, Lennon N, Bacskai BJ, Hyman BT, Trotti D, Brown RH, Jr. (2004) Amyotrophic lateral sclerosis-associated SOD1 mutant proteins bind and aggregate with Bcl-2 in spinal cord mitochondria. Neuron 43:19-30.
Pavlov PF, Wiehager B, Sakai J, Frykman S, Behbahani H, Winblad B, Ankarcrona M (2011) Mitochondrial gamma-secretase participates in the metabolism of mitochondria-associated amyloid precursor protein. FASEB journal : official publication of the Federation of American Societies for Experimental Biology 25:78-88.
Perier C, Vila M (2012) Mitochondrial biology and Parkinson's disease. Cold Spring Harb Perspect Med 2:a009332.
Perl DP (2010) Neuropathology of Alzheimer's disease. The Mount Sinai journal of medicine, New York 77:32-42.
Perrin RJ, Woods WS, Clayton DF, George JM (2000) Interaction of human alpha-Synuclein and Parkinson's disease variants with phospholipids. Structural analysis using site-directed mutagenesis. The Journal of biological chemistry 275:34393-34398.
Perrin L, Bloyer S, Ferraz C, Agrawal N, Sinha P, Dura JM (2003) The leucine zipper motif of the Drosophila AF10 homologue can inhibit PRE-mediated repression: implications

for leukemogenic activity of human MLL-AF10 fusions. Molecular and cellular biology 23:119-130.

Perry EK, McKeith I, Thompson P, Marshall E, Kerwin J, Jabeen S, Edwardson JA, Ince P, Blessed G, Irving D, et al. (1991) Topography, extent, and clinical relevance of neurochemical deficits in dementia of Lewy body type, Parkinson's disease, and Alzheimer's disease. Annals of the New York Academy of Sciences 640:197-202.

Petros JA, Baumann AK, Ruiz-Pesini E, Amin MB, Sun CQ, Hall J, Lim S, Issa MM, Flanders WD, Hosseini SH, Marshall FF, Wallace DC (2005) mtDNA mutations increase tumorigenicity in prostate cancer. Proceedings of the National Academy of Sciences of the United States of America 102:719-724.

Phillips NR, Sprouse ML, Roby RK (2014) Simultaneous quantification of mitochondrial DNA copy number and deletion ratio: a multiplex real-time PCR assay. Scientific reports 4:3887.

Piao Y, Kim HG, Oh MS, Pak YK (2012) Overexpression of TFAM, NRF-1 and myr-AKT protects the MPP(+)-induced mitochondrial dysfunctions in neuronal cells. Biochimica et biophysica acta 1820:577-585.

Picard M, Zhang J, Hancock S, Derbeneva O, Golhar R, Golik P, O'Hearn S, Levy S, Potluri P, Lvova M, Davila A, Lin CS, Perin JC, Rappaport EF, Hakonarson H, Trounce IA, Procaccio V, Wallace DC (2014) Progressive increase in mtDNA 3243A>G heteroplasmy causes abrupt transcriptional reprogramming. Proceedings of the National Academy of Sciences of the United States of America 111:E4033-4042.

Pickrell AM, Pinto M, Hida A, Moraes CT (2011) Striatal dysfunctions associated with mitochondrial DNA damage in dopaminergic neurons in a mouse model of Parkinson's disease. The Journal of neuroscience : the official journal of the Society for Neuroscience 31:17649-17658.

Pinho CM, Teixeira PF, Glaser E (2014) Mitochondrial import and degradation of amyloid-beta peptide. Biochimica et biophysica acta.

Pinto M, Moraes CT (2015) Mechanisms linking mtDNA damage and aging. Free radical biology & medicine 85:250-258.

Pohjoismaki JL, Wanrooij S, Hyvarinen AK, Goffart S, Holt IJ, Spelbrink JN, Jacobs HT (2006) Alterations to the expression level of mitochondrial transcription factor A, TFAM, modify the mode of mitochondrial DNA replication in cultured human cells. Nucleic Acids Res 34:5815-5828.

Poletti M, Bonuccelli U (2013) Acute and chronic cognitive effects of levodopa and dopamine agonists on patients with Parkinson's disease: a review. Therapeutic advances in psychopharmacology 3:101-113.

Polymeropoulos MH, Lavedan C, Leroy E, Ide SE, Dehejia A, Dutra A, Pike B, Root H, Rubenstein J, Boyer R, Stenroos ES, Chandrasekharappa S, Athanassiadou A, Papapetropoulos T, Johnson WG, Lazzarini AM, Duvoisin RC, Di Iorio G, Golbe LI, Nussbaum RL (1997) Mutation in the alpha-synuclein gene identified in families with Parkinson's disease. Science 276:2045-2047.

Pospisilik JA et al. (2010) Drosophila genome-wide obesity screen reveals hedgehog as a determinant of brown versus white adipose cell fate. Cell 140:148-160.

Poulton J, Morten K, Freeman-Emmerson C, Potter C, Sewry C, Dubowitz V, Kidd H, Stephenson J, Whitehouse W, Hansen FJ, et al. (1994) Deficiency of the human mitochondrial transcription factor h-mtTFA in infantile mitochondrial myopathy is associated with mtDNA depletion. Hum Mol Genet 3:1763-1769.

Prelli F, Castano E, Glenner GG, Frangione B (1988) Differences between vascular and plaque core amyloid in Alzheimer's disease. Journal of neurochemistry 51:648-651.

Prince M, Prina M, Guerchet M (2013) World alzheimer report 2013. An analysis of long-term care for dementia Alzheimer’s Disease International, London.

Proukakis C, Dudzik CG, Brier T, MacKay DS, Cooper JM, Millhauser GL, Houlden H, Schapira AH (2013) A novel alpha-synuclein missense mutation in Parkinson disease. Neurology 80:1062-1064.

Puighermanal E, Marsicano G, Busquets-Garcia A, Lutz B, Maldonado R, Ozaita A (2009) Cannabinoid modulation of hippocampal long-term memory is mediated by mTOR signaling. Nat Neurosci 12:1152-1158.

Ramirez-Bermudez J (2012) Alzheimer's disease: critical notes on the history of A medical concept. Archives of medical research 43:595-599.

Ramsey CP, Giasson BI (2008) The E163K DJ-1 mutant shows specific antioxidant deficiency. Brain research 1239:1-11.

Rebrin I, Bayne AC, Mockett RJ, Orr WC, Sohal RS (2004) Free aminothiols, glutathione redox state and protein mixed disulphides in aging Drosophila melanogaster. The Biochemical journal 382:131-136.

Reddy PH (2013) Is the mitochondrial outermembrane protein VDAC1 therapeutic target for Alzheimer's disease? Biochimica et biophysica acta 1832:67-75.

Reddy PH, Beal MF (2008) Amyloid beta, mitochondrial dysfunction and synaptic damage: implications for cognitive decline in aging and Alzheimer's disease. Trends in molecular medicine 14:45-53.

Reddy PH, Tripathi R, Troung Q, Tirumala K, Reddy TP, Anekonda V, Shirendeb UP, Calkins MJ, Reddy AP, Mao P, Manczak M (2012) Abnormal mitochondrial dynamics and synaptic degeneration as early events in Alzheimer's disease: implications to mitochondria-targeted antioxidant therapeutics. Biochimica et biophysica acta 1822:639-649.

Reeve A, Simcox E, Turnbull D (2014) Ageing and Parkinson's disease: Why is advancing age the biggest risk factor? Ageing Res Rev 14C:19-30.

Reyes A, Yang MY, Bowmaker M, Holt IJ (2005) Bidirectional replication initiates at sites throughout the mitochondrial genome of birds. The Journal of biological chemistry 280:3242-3250.

Ribchester RR (2009) Mammalian neuromuscular junctions: modern tools to monitor synaptic form and function. Current opinion in pharmacology 9:297-305.

Rivera-Oliver M, Diaz-Rios M (2014) Using caffeine and other adenosine receptor antagonists and agonists as therapeutic tools against neurodegenerative diseases: a review. Life sciences 101:1-9.

Robinson BH (2006) Lactic acidemia and mitochondrial disease. Molecular genetics and metabolism 89:3-13.

Rodriguez-Santiago B, Casademont J, Nunes V (2001) Is mitochondrial DNA depletion involved in Alzheimer's disease? European journal of human genetics : EJHG 9:279-285.

Ronan JL, Wu W, Crabtree GR (2013) From neural development to cognition: unexpected roles for chromatin. Nature reviews Genetics 14:347-359.

Ross OA, Braithwaite AT, Skipper LM, Kachergus J, Hulihan MM, Middleton FA, Nishioka K, Fuchs J, Gasser T, Maraganore DM, Adler CH, Larvor L, Chartier-Harlin MC, Nilsson C, Langston JW, Gwinn K, Hattori N, Farrer MJ (2008) Genomic investigation of alpha-synuclein multiplication and parkinsonism. Ann Neurol 63:743-750.

Rothermel BA, Thornton JL, Butow RA (1997) Rtg3p, a basic helix-loop-helix/leucine zipper protein that functions in mitochondrial-induced changes in gene expression, contains independent activation domains. The Journal of biological chemistry 272:19801-19807.

Rothermel BA, Shyjan AW, Etheredge JL, Butow RA (1995) Transactivation by Rtg1p, a basic helix-loop-helix protein that functions in communication between mitochondria and the nucleus in yeast. The Journal of biological chemistry 270:29476-29482.

Rotig A, Cormier V, Blanche S, Bonnefont JP, Ledeist F, Romero N, Schmitz J, Rustin P, Fischer A, Saudubray JM, et al. (1990) Pearson's marrow-pancreas syndrome. A multisystem mitochondrial disorder in infancy. The Journal of clinical investigation 86:1601-1608.

Rubio-Cosials A, Sidow JF, Jimenez-Menendez N, Fernandez-Millan P, Montoya J, Jacobs HT, Coll M, Bernado P, Sola M (2011) Human mitochondrial transcription factor A induces a U-turn structure in the light strand promoter. Nature structural & molecular biology 18:1281-1289.

Rui Y, Tiwari P, Xie Z, Zheng JQ (2006) Acute impairment of mitochondrial trafficking by beta-amyloid peptides in hippocampal neurons. The Journal of neuroscience : the official journal of the Society for Neuroscience 26:10480-10487.

Ruiz-Pesini E, Lapena AC, Diez-Sanchez C, Perez-Martos A, Montoya J, Alvarez E, Diaz M, Urries A, Montoro L, Lopez-Perez MJ, Enriquez JA (2000) Human mtDNA haplogroups associated with high or reduced spermatozoa motility. American journal of human genetics 67:682-696.

Ruthel G, Hollenbeck PJ (2003) Response of mitochondrial traffic to axon determination and differential branch growth. The Journal of neuroscience : the official journal of the Society for Neuroscience 23:8618-8624.

Saada A, Shaag A, Mandel H, Nevo Y, Eriksson S, Elpeleg O (2001) Mutant mitochondrial thymidine kinase in mitochondrial DNA depletion myopathy. Nature genetics 29:342-344.

Saha S, Guillily MD, Ferree A, Lanceta J, Chan D, Ghosh J, Hsu CH, Segal L, Raghavan K, Matsumoto K, Hisamoto N, Kuwahara T, Iwatsubo T, Moore L, Goldstein L, Cookson M, Wolozin B (2009) LRRK2 modulates vulnerability to mitochondrial dysfunction in Caenorhabditis elegans. The Journal of neuroscience : the official journal of the Society for Neuroscience 29:9210-9218.

Sanchez-Martinez A, Calleja M, Peralta S, Matsushima Y, Hernandez-Sierra R, Whitworth AJ, Kaguni LS, Garesse R (2012) Modeling pathogenic mutations of human twinkle in Drosophila suggests an apoptosis role in response to mitochondrial defects. PloS one 7:e43954.

Sanders LH, McCoy J, Hu X, Mastroberardino PG, Dickinson BC, Chang CJ, Chu CT, Van Houten B, Greenamyre JT (2014) Mitochondrial DNA damage: Molecular marker of vulnerable nigral neurons in Parkinson's disease. Neurobiol Dis 70:214-223.

Schapira AH, Cooper JM, Dexter D, Clark JB, Jenner P, Marsden CD (1990a) Mitochondrial complex I deficiency in Parkinson's disease. Journal of neurochemistry 54:823-827.

Schapira AH, Mann VM, Cooper JM, Dexter D, Daniel SE, Jenner P, Clark JB, Marsden CD (1990b) Anatomic and disease specificity of NADH CoQ1 reductase (complex I) deficiency in Parkinson's disease. Journal of neurochemistry 55:2142-2145.

Schatz G, Haslbrunner E, Tuppy H (1964) Deoxyribonucleic acid associated with yeast mitochondria. Biochemical and biophysical research communications 15:127-132.

Schneider LS (2013) Alzheimer disease pharmacologic treatment and treatment research. Continuum (Minneap Minn) 19:339-357.

Schroeder EA, Raimundo N, Shadel GS (2013) Epigenetic silencing mediates mitochondria stress-induced longevity. Cell Metab 17:954-964.

Sekito T, Thornton J, Butow RA (2000) Mitochondria-to-nuclear signaling is regulated by the subcellular localization of the transcription factors Rtg1p and Rtg3p. Mol Biol Cell 11:2103-2115.

Selkoe DJ (2002) Alzheimer's disease is a synaptic failure. Science 298:789-791.

Seppi K, Weintraub D, Coelho M, Perez-Lloret S, Fox SH, Katzenschlager R, Hametner EM, Poewe W, Rascol O, Goetz CG, Sampaio C (2011) The Movement Disorder Society Evidence-Based Medicine Review Update: Treatments for the non-motor

symptoms of Parkinson's disease. Movement disorders : official journal of the Movement Disorder Society 26 Suppl 3:S42-80.

Sha D, Chin LS, Li L (2010) Phosphorylation of parkin by Parkinson disease-linked kinase PINK1 activates parkin E3 ligase function and NF-kappaB signaling. Hum Mol Genet 19:352-363.

Shanker V, Groves M, Heiman G, Palmese C, Saunders-Pullman R, Ozelius L, Raymond D, Bressman S (2011) Mood and cognition in leucine-rich repeat kinase 2 G2019S Parkinson's disease. Movement disorders : official journal of the Movement Disorder Society 26:1875-1880.

Sheng B, Wang X, Su B, Lee HG, Casadesus G, Perry G, Zhu X (2012) Impaired mitochondrial biogenesis contributes to mitochondrial dysfunction in Alzheimer's disease. Journal of neurochemistry 120:419-429.

Sheng ZH (2014) Mitochondrial trafficking and anchoring in neurons: New insight and implications. J Cell Biol 204:1087-1098.

Sheng ZH, Cai Q (2012) Mitochondrial transport in neurons: impact on synaptic homeostasis and neurodegeneration. Nat Rev Neurosci 13:77-93.

Shi Y, Dierckx A, Wanrooij PH, Wanrooij S, Larsson N-G, Wilhelmsson LM, Falkenberg M, Gustafsson CM (2012) Mammalian transcription factor A is a core component of the mitochondrial transcription machinery. Proceedings of the National Academy of Sciences 109:16510-16515.

Shidara Y, Yamagata K, Kanamori T, Nakano K, Kwong JQ, Manfredi G, Oda H, Ohta S (2005) Positive contribution of pathogenic mutations in the mitochondrial genome to the promotion of cancer by prevention from apoptosis. Cancer research 65:1655-1663.

Shoffner JM, Watts RL, Juncos JL, Torroni A, Wallace DC (1991) Mitochondrial oxidative phosphorylation defects in Parkinson's disease. Ann Neurol 30:332-339.

Shoffner JM, Lott MT, Lezza AM, Seibel P, Ballinger SW, Wallace DC (1990) Myoclonic epilepsy and ragged-red fiber disease (MERRF) is associated with a mitochondrial DNA tRNA(Lys) mutation. Cell 61:931-937.

Shoffner JM, Fernhoff PM, Krawiecki NS, Caplan DB, Holt PJ, Koontz DA, Takei Y, Newman NJ, Ortiz RG, Polak M, et al. (1992) Subacute necrotizing encephalopathy: oxidative phosphorylation defects and the ATPase 6 point mutation. Neurology 42:2168-2174.

Shoubridge EA, Wai T (2007) Mitochondrial DNA and the mammalian oocyte. Current topics in developmental biology 77:87-111.

Shutt TE, Lodeiro MF, Cotney J, Cameron CE, Shadel GS (2010) Core human mitochondrial transcription apparatus is a regulated two-component system in vitro. Proceedings of the National Academy of Sciences of the United States of America 107:12133-12138.

Silva DF, Selfridge JE, Lu J, E L, Roy N, Hutfles L, Burns JM, Michaelis EK, Yan S, Cardoso SM, Swerdlow RH (2013) Bioenergetic flux, mitochondrial mass and mitochondrial morphology dynamics in AD and MCI cybrid cell lines. Hum Mol Genet 22:3931-3946.

Simon-Sanchez J et al. (2009) Genome-wide association study reveals genetic risk underlying Parkinson's disease. Nature genetics 41:1308-1312.

Singleton AB et al. (2003) alpha-Synuclein locus triplication causes Parkinson's disease. Science 302:841.

Somme JH, Gomez-Esteban JC, Molano A, Tijero B, Lezcano E, Zarranz JJ (2011) Initial neuropsychological impairments in patients with the E46K mutation of the alpha-synuclein gene (PARK 1). Journal of the neurological sciences 310:86-89.

Spatola M, Wider C (2014) Genetics of Parkinson's disease: the yield. Parkinsonism Relat Disord 20 Suppl 1:S35-38.

Spillantini MG, Schmidt ML, Lee VM, Trojanowski JQ, Jakes R, Goedert M (1997) Alpha-synuclein in Lewy bodies. Nature 388:839-840.

Spilman P, Podlutskaya N, Hart MJ, Debnath J, Gorostiza O, Bredesen D, Richardson A, Strong R, Galvan V (2010) Inhibition of mTOR by rapamycin abolishes cognitive deficits and reduces amyloid-beta levels in a mouse model of Alzheimer's disease. PloS one 5:e9979.

Suarez J, Hu Y, Makino A, Fricovsky E, Wang H, Dillmann WH (2008) Alterations in mitochondrial function and cytosolic calcium induced by hyperglycemia are restored by mitochondrial transcription factor A in cardiomyocytes. American journal of physiology Cell physiology 295:C1561-1568.

Swerdlow RH, Khan SM (2004) A "mitochondrial cascade hypothesis" for sporadic Alzheimer's disease. Medical hypotheses 63:8-20.

Swerdlow RH (2007) Mitochondria in cybrids containing mtDNA from persons with mitochondriopathies. Journal of neuroscience research 85:3416-3428.

Swerdlow RH, Burns JM, Khan SM (2013) The Alzheimer's disease mitochondrial cascade hypothesis: Progress and perspectives. Biochimica et biophysica acta.

Szabados T, Dul C, Majtenyi K, Hargitai J, Penzes Z, Urbanics R (2004) A chronic Alzheimer's model evoked by mitochondrial poison sodium azide for pharmacological investigations. Behavioural brain research 154:31-40.

Tain LS, Mortiboys H, Tao RN, Ziviani E, Bandmann O, Whitworth AJ (2009) Rapamycin activation of 4E-BP prevents parkinsonian dopaminergic neuron loss. Nat Neurosci 12:1129-1135.

Takashima A, Noguchi K, Sato K, Hoshino T, Imahori K (1993) Tau protein kinase I is essential for amyloid beta-protein-induced neurotoxicity. Proceedings of the National Academy of Sciences of the United States of America 90:7789-7793.

Takashima A, Noguchi K, Michel G, Mercken M, Hoshi M, Ishiguro K, Imahori K (1996) Exposure of rat hippocampal neurons to amyloid beta peptide (25-35) induces the inactivation of phosphatidyl inositol-3 kinase and the activation of tau protein kinase I/glycogen synthase kinase-3 beta. Neurosci Lett 203:33-36.

Tang Z, Bereczki E, Zhang H, Wang S, Li C, Ji X, Branca RM, Lehtio J, Guan Z, Filipcik P, Xu S, Winblad B, Pei JJ (2013) Mammalian target of rapamycin (mTor) mediates tau protein dyshomeostasis: implication for Alzheimer disease. The Journal of biological chemistry 288:15556-15570.

Tanner CM, Goldman SM (1996) Epidemiology of Parkinson's disease. Neurologic clinics 14:317-335.

Tatsuta T, Langer T (2008) Quality control of mitochondria: protection against neurodegeneration and ageing. The EMBO journal 27:306-314.

Taylor RW, Turnbull DM (2005) Mitochondrial DNA mutations in human disease. Nature reviews Genetics 6:389-402.

Thiffault C, Bennett Jr JP (2005) Cyclical mitochondrial ΔΨM fluctuations linked to electron transport, F0F1 ATP-synthase and mitochondrial Na+/Ca+2 exchange are reduced in Alzheimer's disease cybrids. Mitochondrion 5:109-119.

Thomas KJ, McCoy MK, Blackinton J, Beilina A, van der Brug M, Sandebring A, Miller D, Maric D, Cedazo-Minguez A, Cookson MR (2011) DJ-1 acts in parallel to the PINK1/parkin pathway to control mitochondrial function and autophagy. Hum Mol Genet 20:40-50.

Thomas RR, Keeney PM, Bennett JP (2012) Impaired complex-I mitochondrial biogenesis in Parkinson disease frontal cortex. Journal of Parkinson's disease 2:67-76.

Thorburn DR, Rahman S (1993) Mitochondrial DNA-associated Leigh syndrome and NARP.

Tofaris GK, Razzaq A, Ghetti B, Lilley KS, Spillantini MG (2003) Ubiquitination of alpha-synuclein in Lewy bodies is a pathological event not associated with impairment of proteasome function. The Journal of biological chemistry 278:44405-44411.

Tominaga K, Hayashi J, Kagawa Y, Ohta S (1993) Smaller isoform of human mitochondrial transcription factor 1: its wide distribution and production by alternative splicing. Biochemical and biophysical research communications 194:544-551.

Trifunovic A, Wredenberg A, Falkenberg M, Spelbrink JN, Rovio AT, Bruder CE, Bohlooly YM, Gidlof S, Oldfors A, Wibom R, Tornell J, Jacobs HT, Larsson NG (2004) Premature ageing in mice expressing defective mitochondrial DNA polymerase. Nature 429:417-423.

Trimmer PA, Borland MK (2005) Differentiated Alzheimer's disease transmitochondrial cybrid cell lines exhibit reduced organelle movement. Antioxidants & redox signaling 7:1101-1109.

Tuppen HA, Blakely EL, Turnbull DM, Taylor RW (2010) Mitochondrial DNA mutations and human disease. Biochimica et biophysica acta 1797:113-128.

Tyynismaa H, Suomalainen A (2009) Mouse models of mitochondrial DNA defects and their relevance for human disease. EMBO reports 10:137-143.

Tyynismaa H, Mjosund KP, Wanrooij S, Lappalainen I, Ylikallio E, Jalanko A, Spelbrink JN, Paetau A, Suomalainen A (2005) Mutant mitochondrial helicase Twinkle causes multiple mtDNA deletions and a late-onset mitochondrial disease in mice. Proceedings of the National Academy of Sciences of the United States of America 102:17687-17692.

Tyynismaa H, Sembongi H, Bokori-Brown M, Granycome C, Ashley N, Poulton J, Jalanko A, Spelbrink JN, Holt IJ, Suomalainen A (2004) Twinkle helicase is essential for mtDNA maintenance and regulates mtDNA copy number. Hum Mol Genet 13:3219-3227.

van den Ouweland JM, Lemkes HH, Ruitenbeek W, Sandkuijl LA, de Vijlder MF, Struyvenberg PA, van de Kamp JJ, Maassen JA (1992) Mutation in mitochondrial tRNA(Leu)(UUR) gene in a large pedigree with maternally transmitted type II diabetes mellitus and deafness. Nature genetics 1:368-371.

van Duijn CM, Hendriks L, Cruts M, Hardy JA, Hofman A, Van Broeckhoven C (1991) Amyloid precursor protein gene mutation in early-onset Alzheimer's disease. Lancet 337:978.

Vanden Broeck L, Naval-Sanchez M, Adachi Y, Diaper D, Dourlen P, Chapuis J, Kleinberger G, Gistelinck M, Van Broeckhoven C, Lambert JC, Hirth F, Aerts S, Callaerts P, Dermaut B (2013) TDP-43 loss-of-function causes neuronal loss due to defective steroid receptor-mediated gene program switching in Drosophila. Cell reports 3:160-172.

Vermulst M, Wanagat J, Kujoth GC, Bielas JH, Rabinovitch PS, Prolla TA, Loeb LA (2008) DNA deletions and clonal mutations drive premature aging in mitochondrial mutator mice. Nature genetics 40:392-394.

Verstreken P, Ly CV, Venken KJT, Koh T-W, Zhou Y, Bellen HJ (2005) Synaptic Mitochondria Are Critical for Mobilization of Reserve Pool Vesicles at Drosophila Neuromuscular Junctions. Neuron 47:365-378.

Vijayvergiya C, Beal MF, Buck J, Manfredi G (2005) Mutant superoxide dismutase 1 forms aggregates in the brain mitochondrial matrix of amyotrophic lateral sclerosis mice. The Journal of neuroscience : the official journal of the Society for Neuroscience 25:2463-2470.

Vincow ES, Merrihew G, Thomas RE, Shulman NJ, Beyer RP, MacCoss MJ, Pallanck LJ (2013) The PINK1-Parkin pathway promotes both mitophagy and selective respiratory chain turnover in vivo. Proceedings of the National Academy of Sciences of the United States of America 110:6400-6405.

Vives-Bauza C, Zhou C, Huang Y, Cui M, de Vries RL, Kim J, May J, Tocilescu MA, Liu W, Ko HS, Magrane J, Moore DJ, Dawson VL, Grailhe R, Dawson TM, Li C, Tieu K, Przedborski S (2010) PINK1-dependent recruitment of Parkin to mitochondria in mitophagy. Proceedings of the National Academy of Sciences of the United States of America 107:378-383.

Vossel KA, Zhang K, Brodbeck J, Daub AC, Sharma P, Finkbeiner S, Cui B, Mucke L (2010) Tau reduction prevents Abeta-induced defects in axonal transport. Science 330:198.

Wagh DA, Rasse TM, Asan E, Hofbauer A, Schwenkert I, Durrbeck H, Buchner S, Dabauvalle MC, Schmidt M, Qin G, Wichmann C, Kittel R, Sigrist SJ, Buchner E (2006) Bruchpilot, a protein with homology to ELKS/CAST, is required for structural integrity and function of synaptic active zones in Drosophila. Neuron 49:833-844.

Wallace DC (1992) Mitochondrial genetics: a paradigm for aging and degenerative diseases? Science 256:628-632.

Wallace DC, Brown MD, Lott MT (1999) Mitochondrial DNA variation in human evolution and disease. Gene 238:211-230.

Wallace DC, Zheng XX, Lott MT, Shoffner JM, Hodge JA, Kelley RI, Epstein CM, Hopkins LC (1988a) Familial mitochondrial encephalomyopathy (MERRF): genetic, pathophysiological, and biochemical characterization of a mitochondrial DNA disease. Cell 55:601-610.

Wallace DC, Singh G, Lott MT, Hodge JA, Schurr TG, Lezza AM, Elsas LJ, 2nd, Nikoskelainen EK (1988b) Mitochondrial DNA mutation associated with Leber's hereditary optic neuropathy. Science 242:1427-1430.

Wang H, Morais R (1997) Up-regulation of nuclear genes in response to inhibition of mitochondrial DNA expression in chicken cells. Biochimica et biophysica acta 1352:325-334.

Wang J, Markesbery WR, Lovell MA (2006) Increased oxidative damage in nuclear and mitochondrial DNA in mild cognitive impairment. Journal of neurochemistry 96:825-832.

Wang KZ, Zhu J, Dagda RK, Uechi G, Cherra SJ, 3rd, Gusdon AM, Balasubramani M, Chu CT (2014) ERK-mediated phosphorylation of TFAM downregulates mitochondrial transcription: Implications for Parkinson's disease. Mitochondrion 17:132-140.

Wang X, Su B, Siedlak SL, Moreira PI, Fujioka H, Wang Y, Casadesus G, Zhu X (2008) Amyloid-beta overproduction causes abnormal mitochondrial dynamics via differential modulation of mitochondrial fission/fusion proteins. Proceedings of the National Academy of Sciences of the United States of America 105:19318-19323.

Wang X, Winter D, Ashrafi G, Schlehe J, Wong YL, Selkoe D, Rice S, Steen J, LaVoie MJ, Schwarz TL (2011) PINK1 and Parkin target Miro for phosphorylation and degradation to arrest mitochondrial motility. Cell 147:893-906.

Wanrooij S, Goffart S, Pohjoismaki JL, Yasukawa T, Spelbrink JN (2007) Expression of catalytic mutants of the mtDNA helicase Twinkle and polymerase POLG causes distinct replication stalling phenotypes. Nucleic Acids Res 35:3238-3251.

Wanrooij S, Miralles Fuste J, Stewart JB, Wanrooij PH, Samuelsson T, Larsson NG, Gustafsson CM, Falkenberg M (2012) In vivo mutagenesis reveals that OriL is essential for mitochondrial DNA replication. EMBO reports 13:1130-1137.

Warburg O (1913) über sauerstoffatmende Körnchen aus Leberzellen und über Sauerstoffatmung in Berkefeld-Filtraten wässriger Leberextrakte. Pflüger's Archiv für die gesamte Physiologie des Menschen und der Tiere 154:599-617.

Weihofen A, Thomas KJ, Ostaszewski BL, Cookson MR, Selkoe DJ (2009) Pink1 forms a multiprotein complex with Miro and Milton, linking Pink1 function to mitochondrial trafficking. Biochemistry 48:2045-2052.

Weinreb O, Amit T, Bar-Am O, Youdim MB (2011) A novel anti-Alzheimer's disease drug, ladostigil neuroprotective, multimodal brain-selective monoamine oxidase and cholinesterase inhibitor. International review of neurobiology 100:191-215.

Williams-Gray CH, Evans JR, Goris A, Foltynie T, Ban M, Robbins TW, Brayne C, Kolachana BS, Weinberger DR, Sawcer SJ, Barker RA (2009) The distinct cognitive syndromes of Parkinson's disease: 5 year follow-up of the CamPaIGN cohort. Brain 132:2958-2969.

Williamson D (2002) The curious history of yeast mitochondrial DNA. Nature reviews Genetics 3:475-481.

Wirz KT, Keitel S, Swaab DF, Verhaagen J, Bossers K (2014) Early molecular changes in Alzheimer disease: can we catch the disease in its presymptomatic phase? Journal of Alzheimer's disease : JAD 38:719-740.

Wooten GF, Currie LJ, Bovbjerg VE, Lee JK, Patrie J (2004) Are men at greater risk for Parkinson's disease than women? Journal of neurology, neurosurgery, and psychiatry 75:637-639.

Wouters BG, van den Beucken T, Magagnin MG, Koritzinsky M, Fels D, Koumenis C (2005) Control of the hypoxic response through regulation of mRNA translation. Seminars in cell & developmental biology 16:487-501.

Wright AF, Chakarova CF, Abd El-Aziz MM, Bhattacharya SS (2010) Photoreceptor degeneration: genetic and mechanistic dissection of a complex trait. Nature reviews Genetics 11:273-284.

Xiong H, Wang D, Chen L, Choo YS, Ma H, Tang C, Xia K, Jiang W, Ronai Z, Zhuang X, Zhang Z (2009) Parkin, PINK1, and DJ-1 form a ubiquitin E3 ligase complex promoting unfolded protein degradation. The Journal of clinical investigation 119:650-660.

Xu H, DeLuca SZ, O'Farrell PH (2008) Manipulating the metazoan mitochondrial genome with targeted restriction enzymes. Science 321:575-577.

Xu S, Zhong M, Zhang L, Wang Y, Zhou Z, Hao Y, Zhang W, Yang X, Wei A, Pei L, Yu Z (2009) Overexpression of Tfam protects mitochondria against beta-amyloid-induced oxidative damage in SH-SY5Y cells. The FEBS journal 276:3800-3809.

Yakubovskaya E, Guja KE, Eng ET, Choi WS, Mejia E, Beglov D, Lukin M, Kozakov D, Garcia-Diaz M (2014) Organization of the human mitochondrial transcription initiation complex. Nucleic Acids Research.

Yang MY, Bowmaker M, Reyes A, Vergani L, Angeli P, Gringeri E, Jacobs HT, Holt IJ (2002) Biased incorporation of ribonucleotides on the mitochondrial L-strand accounts for apparent strand-asymmetric DNA replication. Cell 111:495-505.

Yang Y, Ouyang Y, Yang L, Beal MF, McQuibban A, Vogel H, Lu B (2008) Pink1 regulates mitochondrial dynamics through interaction with the fission/fusion machinery. Proceedings of the National Academy of Sciences 105:7070-7075.

Yao J, Irwin RW, Zhao L, Nilsen J, Hamilton RT, Brinton RD (2009) Mitochondrial bioenergetic deficit precedes Alzheimer's pathology in female mouse model of Alzheimer's disease. Proceedings of the National Academy of Sciences of the United States of America 106:14670-14675.

Yasukawa T, Reyes A, Cluett TJ, Yang MY, Bowmaker M, Jacobs HT, Holt IJ (2006) Replication of vertebrate mitochondrial DNA entails transient ribonucleotide incorporation throughout the lagging strand. The EMBO journal 25:5358-5371.

Ylikallio E, Tyynismaa H, Tsutsui H, Ide T, Suomalainen A (2010) High mitochondrial DNA copy number has detrimental effects in mice. Hum Mol Genet 19:2695-2705.

Yoneda T, Benedetti C, Urano F, Clark SG, Harding HP, Ron D (2004) Compartment-specific perturbation of protein handling activates genes encoding mitochondrial chaperones. J Cell Sci 117:4055-4066.

Young RM, Simon MC (2012) Untuning the tumor metabolic machine: HIF-alpha: pro- and antitumorigenic? Nature medicine 18:1024-1025.

Yu W, Sun Y, Guo S, Lu B (2011) The PINK1/Parkin pathway regulates mitochondrial dynamics and function in mammalian hippocampal and dopaminergic neurons. Human Molecular Genetics 20:3227-3240.

Zarranz JJ, Alegre J, Gomez-Esteban JC, Lezcano E, Ros R, Ampuero I, Vidal L, Hoenicka J, Rodriguez O, Atares B, Llorens V, Gomez Tortosa E, del Ser T, Munoz DG, de Yebenes JG (2004) The new mutation, E46K, of alpha-synuclein causes Parkinson and Lewy body dementia. Ann Neurol 55:164-173.

Zeviani M, Moraes CT, DiMauro S, Nakase H, Bonilla E, Schon EA, Rowland LP (1988) Deletions of mitochondrial DNA in Kearns-Sayre syndrome. Neurology 38:1339-1346.

Zhang CL, Ho PL, Kintner DB, Sun D, Chiu SY (2010) Activity-dependent regulation of mitochondrial motility by calcium and Na/K-ATPase at nodes of Ranvier of myelinated nerves. The Journal of neuroscience : the official journal of the Society for Neuroscience 30:3555-3566.

Zhang X, Heng X, Li T, Li L, Yang D, Du Y, Doody RS, Le W (2011) Long-term treatment with lithium alleviates memory deficits and reduces amyloid-beta production in an aged Alzheimer's disease transgenic mouse model. Journal of Alzheimer's disease : JAD 24:739-749.

Zhao Q, Wang J, Levichkin IV, Stasinopoulos S, Ryan MT, Hoogenraad NJ (2002) A mitochondrial specific stress response in mammalian cells. The EMBO journal 21:4411-4419.

Zhao XL, Wang WA, Tan JX, Huang JK, Zhang X, Zhang BZ, Wang YH, YangCheng HY, Zhu HL, Sun XJ, Huang FD (2010) Expression of beta-amyloid induced age-dependent presynaptic and axonal changes in Drosophila. The Journal of neuroscience : the official journal of the Society for Neuroscience 30:1512-1522.

Zhu XH, Qiao H, Du F, Xiong Q, Liu X, Zhang X, Ugurbil K, Chen W (2012) Quantitative imaging of energy expenditure in human brain. NeuroImage 60:2107-2117.

Zimorski V, Ku C, Martin WF, Gould SB (2014) Endosymbiotic theory for organelle origins. Current opinion in microbiology 22C:38-48.

Zimprich A et al. (2004) Mutations in LRRK2 cause autosomal-dominant parkinsonism with pleomorphic pathology. Neuron 44:601-607.

Ziviani E, Tao RN, Whitworth AJ (2010) Drosophila parkin requires PINK1 for mitochondrial translocation and ubiquitinates mitofusin. Proceedings of the National Academy of Sciences of the United States of America 107:5018-5023.

Zoncu R, Efeyan A, Sabatini DM (2011) mTOR: from growth signal integration to cancer, diabetes and ageing. Nature reviews Molecular cell biology 12:21-35.

Zubenko GS, Hughes HB, Stiffler JS, Hurtt MR, Kaplan BB (1998) A genome survey for novel Alzheimer disease risk loci: results at 10-cM resolution. Genomics 50:121-128.

Appendix 1. Full list of demographic and clinical information of cases used in the studies outlined in chapters 2 and 3.

Case no.	BA9 Tissue available	Diagnosis	Gender	Age at death	CERAD	Tau BRAAK stage	Lewy body score	*TFAM* SNP rs2306604 A>G
096/02	Y	Control	M	87				AG
101/97	Y	Control	F	83				A
122/94	Y	Control	F	72				AG
123/03	Y	Control	M	64	0	0		AG
144/94	Y	Control	F	86				A
161/00	Y	Control	M	60				AG
163/90	Y	Control	F	91				A
178/95	Y	Control	F	63				G
181/94	Y	Control	M	75				G
185/04	Y	Control	M	80	1			A
185/96	Y	Control	M	87				A
188/96	Y	Control	F	82				A
191/94	Y	Control	F	94				AG
196/94	Y	Control	M	95				AG
288/99	Y	Control	F	62				G
64/96	Y	Control	F	72		1		G
843/84	Y	Control	M	76				AG
922/88	Y	Control	F	84				AG
96/02	Y	Control	M	87				AG
97/97	Y	Control	M	72		1		A
A011/06	Y	Control	F	82	0	2		AG
A047/02	Y	Control	F	87				A
A048/09	Y	Control	M	81				G
A049/03	Y	Control	M	79				AG
A063/10	Y	Control	F	90				AG
A124/04	Y	Control	M	59				AG
A133/95	Y	Control	M	85				G
A134/00	Y	Control	M	86	0	2		AG
A136/10	Y	Control	F	89				G
A145/02	Y	Control	M	55				AG
A153/01	Y	Control	M	71	0	0		AG
A153/04	Y	Control	M	71				AG
A170/00	Y	Control	F	68	0	0		AG
A185/04	Y	Control	M	80	1	4		A
A219/97	Y	Control	F	76	0	0		A
A223/96	Y	Control	M	80	0	0		AG
A239/03	Y	Control	M	78	0	1		G
A239/95	Y	Control	F	79	1	3		AG
A283/96	Y	Control	M	77	0	1		AG
A308/09	Y	Control	M	66				AG
A31/96	Y	Control	M	70	0	0		AG

Case no.	BA9 Tissue available	Diagnosis	Gender	Age at death	CERAD	Tau BRAAK stage	Lewy body score	*TFAM* SNP rs2306604 A>G
A316/95	Y	Control	M	80	0	1		G
A33/96	Y	Control	F	96	0	2		A
A359/08	Y	Control	F	80				AG
A401/97	Y	Control	M	85	0	3		G
A47/02	Y	Control	F	87	0	0		A
A61/96	Y	Control	M	65	0	0		AG
A94/95	Y	Control	F	80	0	1		A
P001	N	Control	F	81				AG
P002	N	Control	F	74				AG
P003	N	Control	M	74				A
P004	N	Control	M	77				AG
P005	N	Control	F	84				AG
P006	N	Control	F	70				G
P007	N	Control	M	82				G
P008	N	Control	F	76				AG
P009	N	Control	F	70				G
P010	N	Control	M	76				G
P011	N	Control	F	90				AG
P012	N	Control	F	70				G
P014	N	Control	F	84				A
P015	N	Control	F	71				AG
P016	N	Control	M	76				G
P017	N	Control	M	83				AG
P018	N	Control	F	82				A
P019	N	Control	F	69				AG
P020	N	Control	M	84				AG
P022	N	Control	F	75				AG
P023	N	Control	M	73				AG
P024	N	Control	F	86				A
P025	N	Control	M	73				G
P026	N	Control	M	75				AG
P027	N	Control	F	84				AG
P028	N	Control	F	79				A
P029	N	Control	M	72				AG
P030	N	Control	M	82				AG
P031	N	Control	M	80				A
P032	N	Control	F	73				AG
P033	N	Control	M	72				AG
P034	N	Control	F	71				AG
P035	N	Control	F	70				AG
P036	N	Control	F	71				AG

Case no.	BA9 Tissue available	Diagnosis	Gender	Age at death	CERAD	Tau BRAAK stage	Lewy body score	*TFAM* SNP rs2306604 A>G
P037	N	Control	F	87				G
P038	N	Control	F	73				AG
P039	N	Control	M	68				AG
P040	N	Control	F	67				AG
P041	N	Control	F	83				A
P042	N	Control	F	80				A
P043	N	Control	M	89				G
P044	N	Control	F	86				AG
P045	N	Control	F	77				AG
P046	N	Control	F	67				G
P048	N	Control	F	77				A
P050	N	Control	M	65				G
P051	N	Control	F	72				A
P052	N	Control	M	71				G
P053	N	Control	M	75				G
P055	N	Control	F	72				A
P056	N	Control	F	70				AG
P057	N	Control	M	78				AG
P058	N	Control	F	65				A
P059	N	Control	F	84				G
P061	N	Control	M	67				A
P062	N	Control	F	70				AG
P063	N	Control	F	84				G
P064	N	Control	M	88				A
P065	N	Control	F	82				A
P066	N	Control	F	67				A
P067	N	Control	F	80				A
P068	N	Control	F	77				A
P070	N	Control	F	81				AG
P071	N	Control	M	71				G
P072	N	Control	F	71				AG
P073	N	Control	F	71				A
P074	N	Control	F	81				AG
P076	N	Control	F	72				AG
P077	N	Control	F	73				AG
P079	N	Control	M	74				AG
P080	N	Control	M	65				A
P083	N	Control	F	78				AG
P084	N	Control	M	66				G
P085	N	Control	F	81				A
P086	N	Control	F	72				A

Case no.	BA9 Tissue available	Diagnosis	Gender	Age at death	CERAD	Tau BRAAK stage	Lewy body score	*TFAM* SNP rs2306604 A>G
P087	N	Control	F	72				G
P088	N	Control	F	77				A
P089	N	Control	F	79				A
P090	N	Control	F	67				G
P094	N	Control	M	80				AG
P095	N	Control	F	84				AG
P097	N	Control	F	71				G
P098	N	Control	F	71				AG
P099	N	Control	M	72				AG
P100	N	Control	F	60				AG
P101	N	Control	F	74				AG
P102	N	Control	F	81				AG
P103	N	Control	F	75				A
P104	N	Control	F	85				AG
P105	N	Control	F	72				AG
P106	N	Control	F	65				G
P107	N	Control	M	67				G
P108	N	Control	F	72				A
004/03	Y	DLB	F	69	1	2		G
007/03	Y	DLB	F	88	3	3		A
016/01	Y	DLB	F	81				G
019/98	Y	DLB	M	79	0			AG
020/00	Y	DLB	M	74	3	4		AG
024/99	Y	DLB	M	88	5			A
040/97	Y	DLB	F	85	5	6		AG
047/98	Y	DLB	M	73				AG
050/95	Y	DLB	F	81	3	2		A
060/98	Y	DLB	F	77	3			A
061/98	Y	DLB	F	83				A
075/97	Y	DLB	F	82	5			AG
080/01	Y	DLB	M	92	3	4		AG
113/03	Y	DLB	M	77	1	3		A
125/97	Y	DLB	M	86				A
129/03	Y	DLB	M	79	1	4		G
133/90	Y	DLB	M	67		1		G
136/98	Y	DLB	M	77				AG
143/97	Y	DLB	M	63	3	6		AG
153/96	Y	DLB	F	79	5	2		G
192/96	Y	DLB	M	79	5			AG
290/99	Y	DLB	F	85				G
D120	N	DLB	M	69				A

Case no.	BA9 Tissue available	Diagnosis	Gender	Age at death	CERAD	Tau BRAAK stage	Lewy body score	*TFAM* SNP rs2306604 A>G
D124	N	DLB	F	69				AG
D126	N	DLB	M	68				AG
D129	N	DLB	M	72				G
D13	N	DLB	M	77				AG
D134	N	DLB	F	80				AG
D136	N	DLB	M	72				AG
D14	N	DLB	F	81				G
D140	N	DLB	F	80				G
D147	N	DLB	M	73				AG
D156	N	DLB	M					A
D160	N	DLB	M	73				G
D162	N	DLB	F	76				A
D165	N	DLB	F	84				AG
D171	N	DLB	M	69				A
D173	N	DLB	M	77				AG
D174	N	DLB	M	76				AG
D177	N	DLB	M	86				G
D182	N	DLB	F	82				AG
D186	N	DLB	F	77				G
D189	N	DLB	M	79				A
D26	N	DLB	M	78				G
D37	N	DLB	M	70				A
D44	N	DLB	M	64				AG
D51	N	DLB	M	71				G
D66	N	DLB	F	84				AG
D7	N	DLB	F	58				G
D80	N	DLB	F	79				A
D81	N	DLB	M	72				AG
D85	N	DLB	M	69				A
D87	N	DLB	F	71				AG
D93	N	DLB	F	92				AG
D95	N	DLB	M	66				G
M04	N	DLB	F	82				A
M07	N	DLB	F	81				AG
M22	N	DLB	M	81				AG
M23	N	DLB	F	72				AG
M26	N	DLB	F	74				G
M27	N	DLB	M	77				AG
M33	N	DLB	F	73				A
M36	N	DLB	F	76				A
M38	N	DLB	F	68				A

Case no.	BA9 Tissue available	Diagnosis	Gender	Age at death	CERAD	Tau BRAAK stage	Lewy body score	*TFAM* SNP rs2306604 A>G
M46	N	DLB	F	68				A
M47	N	DLB	F	80				AG
M49	N	DLB	M	69				A
M54	N	DLB	F	70				G
M56	N	DLB	F	74				AG
M57	N	DLB	F	81				A
M59	N	DLB	M	71				A
M67	N	DLB	F	75				A
017/99	Y	PDD	M	76				A
111/03	Y	PDD	M	81				A
183/96	Y	PDD	M	85				A
20020080	Y	PDD	M	70	0	1	2	A
20050099	Y	PDD	M	89	1	2	3	A
A143/00	Y	PDD	F	89	0	1	0	A
D118	N	PDD	M	64				A
D178	N	PDD	M	80				A
D183	N	PDD	M	74				A
D34	N	PDD	M	70				A
M11	N	PDD	F	79				A
M15	N	PDD	F	81				A
M34	N	PDD	M	69				A
M37	N	PDD	F	68				A
M40	N	PDD	F	63				A
M64	N	PDD	F	73				A
M66	N	PDD	F	73				A
PD002	Y	PDD	M	84	0	0	3	A
PD014	Y	PDD	M	79		1		A
PD067	Y	PDD	M	83		0		A
PD081	Y	PDD	M	73		0		A
PD099	Y	PDD	M	82		1		A
PD102	Y	PDD	M	81	1	1		A
ST02/01	Y	PDD	M	82	0	1	2	A
ST04/01	Y	PDD	F	85	3	2	3	A
ST10/02	Y	PDD	M	82	1	1	3	A
ST13/02	Y	PDD	F	81	1	1		A
ST14/02	Y	PDD	M	78	2	2		A
ST17/02	Y	PDD	M	72	0	1		A
ST19/02	Y	PDD	F	84	0	1	2	A
ST20/02	Y	PDD	F	84	2	1	3	A
ST22/02	Y	PDD	F	79	3	1	2	A
ST24/03	Y	PDD	M	88	1	2		A

Case no.	BA9 Tissue available	Diagnosis	Gender	Age at death	CERAD	Tau BRAAK stage	Lewy body score	*TFAM* SNP rs2306604 A>G
ST25/04	Y	PDD	F	86	1	1		A
ST30/04	Y	PDD	M	86	0	0		A
123/97	Y	PDD	F	76				AG
151/98	Y	PDD	M	64				AG
183/91	Y	PDD	M	79				AG
20030103	Y	PDD	F	73	1	2	3	AG
20030134	Y	PDD	M	75	1	2	3	AG
D74	N	PDD	F	55				AG
M14	N	PDD	F	74				AG
M20	N	PDD	F	82				AG
M31	N	PDD	F	75				AG
M32	N	PDD	M	79				AG
M50	N	PDD	M	81				AG
M55	N	PDD	F	79				AG
M58	N	PDD	F	76				AG
PD013	Y	PDD	M	78	0	1	2	AG
PD063	Y	PDD	F	80	0	0		AG
PD093	Y	PDD	F	81		1		AG
ST03/01	Y	PDD	M	75	1	1	3	AG
ST09/02	Y	PDD	M	78	3	3	2	AG
ST11/02	Y	PDD	F	73	1	1		AG
ST12/02	Y	PDD	F	80	0	1	2	AG
ST15/02	Y	PDD	F	88	0	1		AG
ST16/02	Y	PDD	M	80	0	1		AG
ST18/02	Y	PDD	M	79	1	1	1	AG
ST23/03	Y	PDD	F	82	2	1	3	AG
20040022	Y	PDD	M	79	1	2	3	G
20040076	Y	PDD	M	76	0	1	3	G
20040105	Y	PDD	M	68	3	3	3	G
20050096	Y	PDD	M	73	0	0	2	G
D154	N	PDD	M	69				G
D94	N	PDD	F	78				G
M05	N	PDD	M	69				G
M21	N	PDD	F	81				G
M28	N	PDD	F	80				G
M29	N	PDD	F	76				G
M39	N	PDD	F	82				G
M44	N	PDD	F	71				G
ST01/01	Y	PDD	F	83	2	1	3	G
ST21/03	Y	PDD	F	83	3	1	3	G
ST29/04	Y	PDD	F	88	1	2		u

Case no.	BA9 Tissue available	Diagnosis	Gender	Age at death	CERAD	Tau BRAAK stage	Lewy body score	*TFAM* SNP rs2306604 A>G
PD022	Y	PD	F	76				A
PD023	Y	PD	M	82	1	1	2	A
PD036	Y	PD	M	76	0	1		A
PD050	Y	PD	F	82				A
PD051	Y	PD	M	80	0	1	2	A
PD086	Y	PD	F	87	0	1	1	A
PD106	Y	PD	M	75	2	1	1	A
PD109	Y	PD	M	72	0	1	1	A
PD114	Y	PD	M	61	2	1	2	A
PD132	Y	PD	M	78	1	1	2	A
PD154	Y	PD	F	79	2	1	2	A
PD160	Y	PD	M	65	0	1	2	A
PD184	Y	PD	M	71	0	1	2	A
PD354	Y	PD	F	89	1	1		A
PD356	Y	PD	F	86				A
PD368	Y	PD	F	83				A
PD423	Y	PD	F	66				A
PD436	Y	PD	M	80				A
PD074	Y	PD	M	85				AG
PD175	Y	PD	M	87	0	1	2	AG
PD187	Y	PD	M	71				AG
PD197	Y	PD	F	80	0	1	2	AG
PD201	Y	PD	M	87				AG
PD203	Y	PD	F	84	1	1	2	AG
PD204	Y	PD	F	86	2	1	2	AG
PD216	Y	PD	M	78	1	1	2	AG
PD239	Y	PD	M	81	2	1	2	AG
PD275	Y	PD	M	79	1	1		AG
PD305	Y	PD	M	86	1	1		AG
PD317	Y	PD	M	70				AG
PD348	Y	PD	M	78	1	1		AG
PD377	Y	PD	F	84				AG
PD398	Y	PD	M	74				AG
PD009	Y	PD	F	86				G
PD032	Y	PD	M	89	0	1	1	G
PD121	Y	PD	M	69	3	3	2	G
PD183	Y	PD	M	69	2	2	3	G
PD387	Y	PD	M	82				G
PD416	Y	PD	F	85				G
PD007	Y	PD	M	78				unknown
PD229	Y	PD	F	86				unknown

Case no.	MMSE	Years of dementia at death	Years of PD at death	Years of PD till dementia onset	Years of dementia till PD onset	PMD	BA9 pH
096/02							
101/97							
122/94							
123/03							
144/94							
161/00							
163/90							
178/95							
181/94							
185/04							
185/96							
188/96							
191/94							
196/94							
288/99							
64/96							
843/84							
922/88							
96/02							
97/97							
A011/06						43	6.37
A047/02						21.5	6
A048/09						42	6.73
A049/03						34	6.28
A063/10						74	6.57
A124/04						50	
A133/95						48	7.02
A134/00						6	6.78
A136/10						65	6.43
A145/02							
A153/01						5	6.42
A153/04							
A170/00						9	6.61
A185/04						48	6.57
A219/97						63	6.04
A223/96						11	6.72
A239/03						9.5	6.63
A239/95						38	6.48
A283/96						29	6.52
A308/09						52	6.66
A31/96						45	6.8

Case no.	MMSE	Years of dementia at death	Years of PD at death	Years of PD till dementia onset	Years of dementia till PD onset	PMD	BA9 pH
A316/95						35	6.44
A33/96						72	6.1
A359/08						22	6.5
A401/97						42	6.05
A47/02							
A61/96						29	6.84
A94/95						31	6.15
P001							
P002							
P003							
P004							
P005							
P006							
P007							
P008							
P009							
P010							
P011							
P012							
P014							
P015							
P016							
P017							
P018							
P019							
P020							
P022							
P023							
P024							
P025							
P026							
P027							
P028							
P029							
P030							
P031							
P032							
P033							
P034							
P035							
P036							

Case no.	MMSE	Years of dementia at death	Years of PD at death	Years of PD till dementia onset	Years of dementia till PD onset	PMD	BA9 pH
P037							
P038							
P039							
P040							
P041							
P042							
P043							
P044							
P045							
P046							
P048							
P050							
P051							
P052							
P053							
P055							
P056							
P057							
P058							
P059							
P061							
P062							
P063							
P064							
P065							
P066							
P067							
P068							
P070							
P071							
P072							
P073							
P074							
P076							
P077							
P079							
P080							
P083							
P084							
P085							
P086							

Case no.	MMSE	Years of dementia at death	Years of PD at death	Years of PD till dementia onset	Years of dementia till PD onset	PMD	BA9 pH
P087							
P088							
P089							
P090							
P094							
P095							
P097							
P098							
P099							
P100							
P101							
P102							
P103							
P104							
P105							
P106							
P107							
P108							
004/03	19	10	10	0	0	45	6.66
007/03	18	4	4	0	0	16	6.45
016/01						31	6.26
019/98	25	3	2	-1	1	26	6.66
020/00	4	4	3	-1	1	6	6.23
024/99	0	2	0	-1.5	1.5	24	6.13
040/97	16	1	0	-1	1	48	6.48
047/98		5	5	0	0	58	7.6
050/95	12	2	0	-2	2	23	6.41
060/98	5	2	1	-1	1	48	6.48
061/98	0	1	0	-1	1	33	6.21
075/97	1	5	0	-5	5	75	6.73
080/01	12	9	9	0	0	20	6
113/03	12	5	5	0	0	59	6.5
125/97	9					60	6.84
129/03	22	8	19	11		64	6.32
133/90		3	3	0	0	24	5.88
136/98	19	2	15	13		33	6.23
143/97						36	6.91
153/96	23	4	4	0		64	6.48
192/96		6	1	-5.5	5.5	16	6.73
290/99		3	5	2		20	6.3
D120	28	6					

Case no.	MMSE	Years of dementia at death	Years of PD at death	Years of PD till dementia onset	Years of dementia till PD onset	PMD	BA9 pH
D124	22	1					
D126		0					
D129		4					
D13	13	10					
D134		4					
D136		3					
D14	17	1					
D140	22	3					
D147	21	1					
D156		0					
D160		5					
D162	22	0					
D165		7					
D171		6					
D173		7					
D174	20	1					
D177	16	2					
D182	23	2					
D186	18	2					
D189		1					
D26		3					
D37	30	4					
D44	23	1					
D51	21	2					
D66	24	5					
D7	18	5					
D80	24	1					
D81	20	2					
D85	11	6					
D87		3					
D93	22	3					
D95	24	2					
M04	24	8					
M07	23	5					
M22	14	2					
M23	25	5					
M26	21	8					
M27	19	2					
M33	21	0					
M36	22	1					
M38	16	2					

Case no.	MMSE	Years of dementia at death	Years of PD at death	Years of PD till dementia onset	Years of dementia till PD onset	PMD	BA9 pH
M46	24	4					
M47	18	5					
M49	20	8					
M54	25	1					
M56	27	3					
M57	21	6					
M59	13	6					
M67	24	2					
017/99		0					
111/03	6	6					
183/96	14	4					
20020080	16	5	12	7	0	17	6.19
20050099	4	3	16	13	0	64	5.99
A143/00		0				54	6.08
D118	23	1					
D178	26	6					
D183	25	3					
D34	27	1					
M11	21	8					
M15	28	15					
M34	30	8					
M37	20	10					
M40	21	8					
M64	18	3					
M66	25	8					
PD002		1	9	8			6.41
PD014		3	12	9		21	6.71
PD067		2	9	7		10	6.83
PD081		0	9	9		19	6.51
PD099		4	11	7		10	6.73
PD102		7	25	18		16	
ST02/01	16	1	15	14	0	37	6.45
ST04/01	2	4	8	4	0		6.81
ST10/02	20	1	4	3	0	24	6.44
ST13/02	26	0				28	6.85
ST14/02	5	0				24	6.48
ST17/02	27	0				9	6.9
ST19/02		0				27	6.18
ST20/02	3	2	16	14	0	36	6.36
ST22/02	12	2	7	5	0	24	7.19
ST24/03	15	6	15	9	0	24	6.49

Case no.	MMSE	Years of dementia at death	Years of PD at death	Years of PD till dementia onset	Years of dementia till PD onset	PMD	BA9 pH
ST25/04	11	7	21	14	0	24	6.3
ST30/04	16					32	6.73
123/97	11	2					
151/98	14	1					
183/91		2					
20030103	5	4	10	6	0	30	5.83
20030134	17	2	4	2	0	40	6.46
D74	27	0					
M14	13	12					
M20	22	0					
M31	19	2					
M32	18	10					
M50	24	11					
M55	27	12					
M58	27	2					
PD013		7	24	17		20	6.08
PD063		1	13	12		10	6.73
PD093		3	14	11		22	
ST03/01	16	1	13	12	0	36	6.31
ST09/02	9	1	9	8	0	72	6.8
ST11/02	25	0				60	6.68
ST12/02	29	1	6	5	0	28	6.34
ST15/02	13	0				72	5.9
ST16/02	20	0				26	6.58
ST18/02	10	5	16	11	0	30	6.8
ST23/03	6	2	14	12	0	33	6.74
20040022		9	14	5	0	30	6.78
20040076		7	11	4	0	17	6.45
20040105	9	6	8	2	0	11	6.15
20050096	19	5	23	18	0	31	5.83
D154	21	3					
D94	21	1					
M05	24	0					
M21	23	6					
M28	20	6					
M29	25	10					
M39	23	0					
M44	23	9					
ST01/01	12	4	19	15	0	24	6.63
ST21/03	14	2	26	24	0	24	6.45
ST29/04	3					32	6.15

Case no.	MMSE	Years of dementia at death	Years of PD at death	Years of PD till dementia onset	Years of dementia till PD onset	PMD	BA9 pH
PD022			10			14	6.55
PD023			7			28	6.54
PD036			10			10	6.88
PD050			14				6.46
PD051			5			7	6.77
PD086			9			22	6.76
PD106			8			3	6.63
PD109			6			9	6.4
PD114			2			12	6.73
PD132			10			11	6.69
PD154			24			19	6.85
PD160			6			14	6.6
PD184			7			24	6.57
PD354			11			8	6.7
PD356			9			19	6.79
PD368			30			14	6.58
PD423			13			19	6.99
PD436			8				6.71
PD074			9			17	6.49
PD175			19			15	6.61
PD187			8			11	6.58
PD197			22			15	6.43
PD201			7			19	6.52
PD203			18			19	
PD204			18			5	6.53
PD216			8			21	6.67
PD239			6			8	6.4
PD275			15			22	6.5
PD305			8			20	6.71
PD317			16			24	
PD348			6			31	6.81
PD377			4			15	6.53
PD398			24			12	6.71
PD009			15			6	6.43
PD032			3			16	6.52
PD121			4			9	6.74
PD183			19			22	6.59
PD387			19			14	6.62
PD416			12			17	6.77
PD007			10			22	
PD229			18			7	6.56

Appendix 2. Microarray and gene ontology (GO) analysis

Appendix 2.1 List of genes that were significantly differentially regulated upon *TFAM* overexpression.

transcript_ cluster_id	Gene Symbol	Gene Title	p-value	Fold change
18154670	dom /// snoRNA:Me28S-G2596	domino /// ncRNA	0.001216175	8.24603
18137346	snoRNA:Psi18S-640g	ncRNA	0.000575468	5.62505
18207604	CG15784	CG15784 gene product from transcript CG15784-RA	0.000193688	5.51706
18141748	CG31918	CG31918 gene product from transcript CG31918-RA	0.000214553	3.70455
18173921	ImpL3	Ecdysone-inducible gene L3	0.001970607	3.58449
18138001	Thor	CG8846 gene product from transcript CG8846-RA	0.00270655	3.235
18161305	CG13430	CG13430 gene product from transcript CG13430-RA	0.001199013	3.11299
18150198	CG18343	CG18343 gene product from transcript CG18343-RA	0.000415337	3.04329
18149383	CG2064	CG2064 gene product from transcript CG2064-RA	0.000297723	2.80085
18190022	CG31157	CG31157 gene product from transcript CG31157-RB	0.003184809	2.46274
18142755	FucTB	CG4435 gene product from transcript CG4435-RA	0.000696815	2.45558
18198470	TFAM	mitochondrial transcription factor A	9.31E-06	2.34985
18155337	CG42694	CG42694 gene product from transcript CG42694-RA	0.000948164	2.2214
18160245	Arc1	Activity-regulated cytoskeleton associated protein 1	0.000108027	2.15547
18154142	Vkor	Vitamin-K epoxide reductase	0.008863742	1.87653
18137376	snoRNA:Psi18S-525c	ncRNA	0.004784562	1.86948
18168863	CG7607	CG7607 gene product from transcript CG7607-RA	0.002469362	1.8693
18154342	snoRNA:Psi28S-3316a	ncRNA	0.001249277	1.80242
18217993	snoRNA:Me28S-U3344b	ncRNA	0.001281285	1.69847
18156120	cv-2	crossveinless 2	0.001654013	1.69341
18168794	blos4	BLOC-1 subunit 4	0.005306561	1.68943
18163719	CG34232	CG34232 gene product from transcript CG34232-RA	0.003414842	1.58253
18159512	CG7637	CG7637 gene product from transcript CG7637-RA	0.001649847	1.54785
18142869	CG5846	CG5846 gene product from transcript CG5846-RA	0.006010311	1.54681
18150644	Arc2	CG13941 gene product from transcript CG13941-RA	0.003126833	1.54564
18136839	Ada1-2	CG31866 gene product from transcript CG31866-RA	0.002951174	1.54478
18142919	CG5727	CG5727 gene product from transcript CG5727-RA	0.006773993	1.54257
18133690	mRpL28	mitochondrial ribosomal protein L28	0.003165487	1.52601

18134171	CG7191	CG7191 gene product from transcript CG7191-RA	0.002290588	1.51138
18142886	CG31714	CG31714 gene product from transcript CG31714-RB	0.008882207	1.5066
18191725	Rbp1	RNA-binding protein 1	0.001865953	1.50202
18185768	CG14715	CG14715 gene product from transcript CG14715-RA	0.004138754	1.50177
18131365	Trf	TBP-related factor	0.006783743	1.49161
18203018	mRpL37	mitochondrial ribosomal protein L37	0.000612093	1.48775
18153306	Tret1-1	Trehalose transporter 1-1	0.006335764	1.48552
18132916	CG2789	CG2789 gene product from transcript CG2789-RA	0.001765072	1.48408
18205028	CR41608	ribosomal RNA	0.000910637	1.47645
18171959	loj	logjam	0.006072274	1.47212
18165272	CG17684	CG17684 gene product from transcript CG17684-RC	0.002510032	1.46805
18204860	ND3	NADH dehydrogenase subunit 3	0.006319813	1.45411
18158130	Dgp-1	CG5729 gene product from transcript CG5729-RA	8.42E-05	1.45384
18154666	snoRNA:Me28S-A2589b	ncRNA	0.001301827	1.44864
18144739	CG31683	CG31683 gene product from transcript CG31683-RA	0.001055888	1.44807
18136832	Qtzl	Quetzalcoatl	0.001102121	1.43038
18140864	CG18095	CG18095 gene product from transcript CG18095-RB	0.001969727	1.42731
18142747	borr	borealin-related	0.001573783	1.4251
18187053	CG7342	CG7342 gene product from transcript CG7342-RB	0.005556996	1.42067
18191773	Xrp1	CG17836 gene product from transcript CG17836-RB	0.003401172	1.41121
18169539	CG17029	CG17029 gene product from transcript CG17029-RA	0.00024886	1.40792
18208447	CG2076	CG2076 gene product from transcript CG2076-RA	0.00097162	1.40643
18172683	Bet1	CG14084 gene product from transcript CG14084-RB	0.002689554	1.40435
18157874	Inos	CG11143 gene product from transcript CG11143-RA	0.000662356	1.40422
18150034	CG12942	CG12942 gene product from transcript CG12942-RA	0.004580837	1.40386
18172840	Exn	Ephexin	0.002232586	1.40107
18170573	CG11425	CG11425 gene product from transcript CG11425-RA	0.001026525	1.395
18156255	ix	intersex	0.004650343	1.39117
18176893	CG8111	CG8111 gene product from transcript CG8111-RA	0.002876667	1.38303
18182365	E(spl)	Enhancer of split	0.009645258	1.37837
18149377	CG2065	CG2065 gene product from transcript CG2065-RA	2.85E-05	1.37834
18203582	CG43448	CG43448 gene product from transcript CG43448-RA	0.001968114	1.36591
18131618	His3.3A /// His3.3B	Histone H3.3A /// Histone H3.3B	0.006127948	1.36157

18170738	GNBP1	Gram-negative bacteria binding protein 1	0.002172055	1.35968
18200063	CG11882	CG11882 gene product from transcript CG11882-RA	0.007331665	1.35229
18178466	CG14057	CG14057 gene product from transcript CG14057-RA	0.003384012	1.33997
18131738	Acer	Angiotensin-converting enzyme-related	0.005730108	1.33373
18195594	RpL35A	Ribosomal protein L35A	0.001482247	1.33139
18149426	CG1882	CG1882 gene product from transcript CG1882-RA	0.005315602	1.3218
18132393	Taf10	TBP-associated factor 10	0.000333316	1.31896
18161743	CG3501	CG3501 gene product from transcript CG3501-RA	0.009024873	1.31185
18144062	Taf13	TBP-associated factor 13	0.008836609	1.29969
18148328	Nrk	Neurospecific receptor kinase	0.008766055	1.2966
18135748	Pomp	CG9324 gene product from transcript CG9324-RA	3.46E-05	1.29456
18140409	NTPase	CG3059 gene product from transcript CG3059-RD	0.004505528	1.29295
18188448	CG5913	CG5913 gene product from transcript CG5913-RA	0.002634422	1.29038
18131668	RpS21	Ribosomal protein S21	0.005511447	1.28886
18216191	CG6123	CG6123 gene product from transcript CG6123-RB	0.007905125	1.28815
18198589	CG7044	CG7044 gene product from transcript CG7044-RA	0.002534054	1.28767
18172710	CG42588	CG42588 gene product from transcript CG42588-RA	0.007284208	1.27362
18171088	CR32027	ncRNA	0.000862496	1.26807
18135200	CG16820	CG16820 gene product from transcript CG16820-RA	0.006627346	1.26453
18168685	CG8329	CG8329 gene product from transcript CG8329-RA	0.00169095	1.25803
18193862	Nmdmc	NAD-dependent methylenetetrahydrofolate dehydrogenase	0.007290833	1.24683
18140339	dnt	doughnut on 2	0.000555652	1.24252
18148476	san	separation anxiety	0.00244481	1.24111
18134302	Scgalpha	Sarcoglycan alpha	0.002640796	1.23919
18138091	LanB1	CG7123 gene product from transcript CG7123-RA	0.000536162	1.23891
18161255	CG16868	CG16868 gene product from transcript CG16868-RA	0.003669986	1.23605
18208208	Rbm13	RNA-binding motif protein 13	0.003848889	1.23157
18154964	CG42360	CG42360 gene product from transcript CG42360-RA	0.001283464	1.22981
18178217	CG5830	CG5830 gene product from transcript CG5830-RA	0.002265748	1.2283
18211098	CG42240	CG42240 gene product from transcript CG42240-RA	0.002310454	1.22618
18156673	dpn	deadpan	0.002935974	1.22555

18142473	mon2	CG8683 gene product from transcript CG8683-RB	0.002327515	1.22338
18169736	beg	bad egg	0.007281212	1.22323
18152609	Pask	PAS kinase	0.008913397	1.22304
18198845	CG4813	CG4813 gene product from transcript CG4813-RA	0.007749747	1.2221
18133663	CG3036	CG3036 gene product from transcript CG3036-RA	0.002624977	1.2205
18142912	CG5731	CG5731 gene product from transcript CG5731-RA	0.00569152	1.21338
18135030	CG14945	CG14945 gene product from transcript CG14945-RB	0.002934221	1.21086
18172671	CG42575	CG42575 gene product from transcript CG42575-RA	0.00052047	1.20832
18197160	Ravus	CG15889 gene product from transcript CG15889-RA	0.009772333	1.20247
18203521	vret	vreteno	0.000489586	1.20105
18186795	sll	slalom	0.001986136	1.19695
18134652	eEF1delta	CG4912 gene product from transcript CG4912-RB	6.00E-05	1.19541
18217846	snoRNA:Psi18S-1854c	ncRNA	0.007834201	1.19416
18217826	snoRNA:Psi28S-1192b	ncRNA	0.003257402	1.19306
18152066	CG10306	CG10306 gene product from transcript CG10306-RA	0.009807127	1.19119
18133694	CG3792	CG3792 gene product from transcript CG3792-RA	0.004678829	1.18934
18166977	Rev1	CG12189 gene product from transcript CG12189-RA	0.001348521	1.18882
18176446	CG10671	CG10671 gene product from transcript CG10671-RB	0.004946807	1.1875
18166227	tap	target of Poxn	0.000430786	1.18613
18193002	e	ebony	0.000280314	1.18362
18194868	Irp-1B	Iron regulatory protein 1B	0.004115626	1.18148
18134667	CG4957	CG4957 gene product from transcript CG4957-RA	0.007974996	1.17479
18175769	CG2277	CG2277 gene product from transcript CG2277-RA	0.009551461	1.17452
18171399	CG32250	CG32250 gene product from transcript CG32250-RA	0.003810554	1.17446
18163882	snoRNA:Or-CD1	ncRNA	0.005321113	1.17121
18139237	l(2)37Cc	lethal (2) 37Cc	0.00468869	1.17026
18161902	Rrp4	CG3931 gene product from transcript CG3931-RA	0.008791764	1.166
18195800	MAGE	CG10059 gene product from transcript CG10059-RA	0.009854643	1.16379
18164958	Eaf /// mir-4977	ELL-associated factor /// mir-4977 stem loop	0.007504492	1.16312
18185658	CG4820	CG4820 gene product from transcript CG4820-RB	0.008969043	1.15982
18188294	Nup358	Nucleoporin 358	0.003028192	1.15963
18184683	CG1236	CG1236 gene product from transcript CG1236-RA	0.007954358	1.15883

18183587	sima	similar	0.005544955	1.15856
18166516	Trn	Transportin	0.0064983	1.15722
18169870	mRpS26	mitochondrial ribosomal protein S26	0.0074742	1.15672
18190421	CG31472	CG31472 gene product from transcript CG31472-RA	0.005420729	1.15631
18161975	Upf3	CG11184 gene product from transcript CG11184-RB	0.003284819	1.15594
18168404	CG6745	CG6745 gene product from transcript CG6745-RA	0.000305255	1.15495
18212651	shtd	shattered	0.007109925	1.15442
18148606	bonsai	CG4207 gene product from transcript CG4207-RA	0.007766797	1.15064
18179141	mRpL15	mitochondrial ribosomal protein L15	0.005618132	1.14976
18149778	CG12140	CG12140 gene product from transcript CG12140-RA	0.0097342	1.14878
18181501	CG42863	CG42863 gene product from transcript CG42863-RB	0.008660875	1.14835
18202403	Ino80	CG31212 gene product from transcript CG31212-RA	0.000386794	1.14525
18149710	Updo	CG1818 gene product from transcript CG1818-RA	0.000709967	1.14443
18160444	CG8314	CG8314 gene product from transcript CG8314-RA	0.007198857	1.14274
18143758	Atac2	ATAC complex component 2	0.00074219	1.14129
18131069	ref(2)P	refractory to sigma P	0.001678822	1.13932
18153776	CG30349	CG30349 gene product from transcript CG30349-RA	0.006824619	1.13918
18211291	CG5010	CG5010 gene product from transcript CG5010-RA	0.001078923	1.13761
18214386	lin-52	CG15929 gene product from transcript CG15929-RA	0.009150359	1.13411
18183605	Hmu	Hemomucin	0.001656483	1.13236
18142469	RpL36A	Ribosomal protein L36A	0.005787647	1.13184
18140791	Rpn11	CG18174 gene product from transcript CG18174-RA	0.008534965	1.13181
18202368	ALiX	ALG-2 interacting protein X	0.000657961	1.13079
18202099	pncr002:3R	putative noncoding RNA 002:3R	0.002366496	1.13027
18191841	scaRNA:mgU2-25	ncRNA	0.000322539	1.1268
18198619	CG3337	CG3337 gene product from transcript CG3337-RA	0.001437471	1.12652
18169698	TSG101	tumor suppressor protein 101	0.002786764	1.12584
18203499	snRNA:U4atac:82E	small nuclear RNA U4atac at 82E	0.009193095	1.12555
18160209	RpS23	Ribosomal protein S23	0.005443141	1.12516
18176994	CG7185	CG7185 gene product from transcript CG7185-RB	0.006356462	1.1241
18165468	LanB2	Laminin B2	0.003413521	1.12392
18138532	CG43403	CG43403 gene product from transcript CG43403-RA	0.007341784	1.12189
18209746	Hs3st-B	Heparan sulfate 3-O sulfotransferase-B	0.006096256	1.12106

18182995	Gnf1	Germ line transcription factor 1	0.008253461	1.11708
18195012	Noa36	CG10009 gene product from transcript CG10009-RA	0.005345982	1.11672
18160466	casp	caspar	0.008548242	1.116
18218410	Megalin	CG42611 gene product from transcript CG42611-RA	0.007663898	1.11558
18147971	RpL11	Ribosomal protein L11	0.001875604	1.11026
18192983	Dl	Delta	0.004007629	1.10785
18140503	Taf10b	TBP-associated factor 10b	0.007752123	1.10747
18132113	beta'Cop	beta'-coatomer protein	0.00260211	1.10668
18155317	CG42678	CG42678 gene product from transcript CG42678-RG	0.004533447	1.10435
18208543	CG11699	CG11699 gene product from transcript CG11699-RA	0.006352381	1.10384
18184014	gukh	GUK-holder	0.002384124	1.10109
18158284	Spn4	Serine protease inhibitor 4	0.009500507	1.10025
18216945	mRpL14	mitochondrial ribosomal protein L14	0.005031468	1.09863
18197221	yellow-e2	CG17044 gene product from transcript CG17044-RB	0.008753208	1.09802
18143402	CG9934	CG9934 gene product from transcript CG9934-RB	0.002349179	1.09698
18138997	ck	crinkled	0.004652414	1.09596
18193803	Crc	Calreticulin	0.001438407	1.09328
18140014	RpL9	Ribosomal protein L9	0.003567168	1.089
18145550	snoRNA:Psi28S-2996	ncRNA	0.000602456	1.08799
18132619	dao	down and out	0.003371475	1.08626
18186631	pad	poils au dos	0.005977259	1.08298
18208551	CG11696	CG11696 gene product from transcript CG11696-RA	0.009257201	1.0818
18156226	Hsc70-5	Heat shock protein cognate 5	0.009666787	1.08172
18141733	CG31650	CG31650 gene product from transcript CG31650-RF	0.008275916	1.08113
18134672	CG4968	CG4968 gene product from transcript CG4968-RA	0.004429893	1.07783
18137260	His2A:CG33853 ///	CG33853 gene product from transcript CG33853-RA	0.000575401	1.07699
18152039	CG10321	CG10321 gene product from transcript CG10321-RA	0.008358105	1.07699
18136473	His2A:CG31618 ///	CG31618 gene product from transcript CG31618-RA	0.000431063	1.07624
18159807	CG8858	CG8858 gene product from transcript CG8858-RA	0.004689175	1.07537
18199652	CG6073	CG6073 gene product from transcript CG6073-RA	0.000906437	1.07465
18165998	RpS4	Ribosomal protein S4	0.008137342	1.07153
18185234	Tcp-1eta	CG8351 gene product from transcript CG8351-RA	0.00438848	1.06535
18149451	CG2906	CG2906 gene product from transcript CG2906-RE	0.00044902	1.06486
18150006	CG12325	CG12325 gene product from transcript CG12325-RA	0.008055326	1.06255

18219234	kl-3	male fertility factor kl3	0.004181665	1.05968
18181860	scaRNA:pUf68-a	ncRNA	0.001229777	1.05922
18202281	CG34293	CG34293 gene product from transcript CG34293-RA	0.003821104	1.05285
18204046	Rad23	CG1836 gene product from transcript CG1836-RB	0.003041165	1.05263
18146459	gho	ghost	0.00303588	1.05171
18172904	CG42676	CG42676 gene product from transcript CG42676-RD	0.008179293	1.05052
18167940	CG4769	CG4769 gene product from transcript CG4769-RA	0.008929421	1.04681
18200552	CstF-50	CG2261 gene product from transcript CG2261-RA	0.009409992	1.02657
18173529	Notum /// mir-4941	CG13076 gene product from transcript CG13076-RB	0.001575277	0.966293
18135708	Arc-p34	CG10954 gene product from transcript CG10954-RA	0.006590619	0.952418
18201562	Unc-115a /// Unc-115b	CG31352 gene product from transcript CG31352-RA	0.005011536	0.94748
18138279	CG43051	CG43051 gene product from transcript CG43051-RB	8.61E-05	0.94549
18144790	RluA-1	CG31719 gene product from transcript CG31719-RA	0.009845629	0.940391
18158303	ced-6	CG11804 gene product from transcript CG11804-RD	0.000153626	0.937225
18169211	CG10741	CG10741 gene product from transcript CG10741-RB	0.007445609	0.920592
18183735	Ice	CG7788 gene product from transcript CG7788-RA	0.00508727	0.917428
18185865	CG17639	CG17639 gene product from transcript CG17639-RA	0.002758188	0.916263
18202739	E(var)3-9	Enhancer of variegation 3-9	0.00046223	0.915395
18169918	MYPT-75D	CG6896 gene product from transcript CG6896-RA	0.009220406	0.908841
18162975	CG30375	CG30375 gene product from transcript CG30375-RA	0.001918266	0.908442
18151744	CG11044	CG11044 gene product from transcript CG11044-RA	0.009865918	0.90175
18132017	KdelR	KDEL receptor	0.005627271	0.901146
18194562	Rab1	Rab-protein 1	0.003899471	0.894818
18202306	CG34353	CG34353 gene product from transcript CG34353-RB	0.001084427	0.894219
18214141	CG14810	CG14810 gene product from transcript CG14810-RB	0.004573251	0.890755
18184679	CG1239	CG1239 gene product from transcript CG1239-RA	0.003527111	0.887632
18136572	CG31661	CG31661 gene product from transcript CG31661-RA	0.007504383	0.878268
18150655	Dh44-R1	Diuretic hormone 44 receptor 1	0.004838241	0.87768
18158501	CG9430	CG9430 gene product from transcript CG9430-RB	0.001798084	0.874502
18144474	CG13773	CG13773 gene product from transcript CG13773-RA	0.005912821	0.873997

18177032	CG6983	CG6983 gene product from transcript CG6983-RA	0.000253572	0.873876
18154202	Yu	ncRNA	0.006841689	0.872302
18135349	CG15141	CG15141 gene product from transcript CG15141-RA	0.003168971	0.87041
18200711	CG17193	CG17193 gene product from transcript CG17193-RB	0.006929341	0.869666
18136885	CG31928	CG31928 gene product from transcript CG31928-RA	0.009896456	0.863918
18151296	CG4975 /// CG4984	CG4975 gene product from transcript CG4975-RC	0.004469496	0.8632
18149161	CG3270	CG3270 gene product from transcript CG3270-RA	0.007457679	0.859796
18158990	Mal-A7	Maltase A7	0.009089439	0.85928
18180785	snoRNA:Or-CD11a	ncRNA	0.003869643	0.85926
18177236	pall	pallbearer	0.006548162	0.858546
18189532	CG18672	CG18672 gene product from transcript CG18672-RB	0.002410554	0.854864
18153198	Uhg1	U snoRNA host gene 1	0.007311613	0.852241
18141388	CG3117	CG3117 gene product from transcript CG3117-RB	0.002587046	0.851631
18134661	CG4953	CG4953 gene product from transcript CG4953-RA	0.003357879	0.849528
18190590	CG33110	CG33110 gene product from transcript CG33110-RA	0.00789783	0.843445
18142114	Tsp	Thrombospondin	0.007679562	0.843309
18189951	CG31104	CG31104 gene product from transcript CG31104-RA	0.008487416	0.840469
18173527	CG4641 /// mir-4940 /// nwk	CG4641 gene product from transcript CG4641-RA	0.00580685	0.84012
18161416	CG4030	CG4030 gene product from transcript CG4030-RA	0.000869827	0.829569
18208082	CG15330	CG15330 gene product from transcript CG15330-RA	0.005826931	0.828649
18151269	HPS4	Hermansky-Pudlak Syndrome 4 ortholog	0.009916421	0.824848
18198913	CG17111	CG17111 gene product from transcript CG17111-RB	0.006784088	0.823458
18142760	jp	junctophilin	0.001120585	0.819984
18163038	CG30403	CG30403 gene product from transcript CG30403-RB	0.008754219	0.818053
18153463	CG30093	CG30093 gene product from transcript CG30093-RA	0.004704774	0.814056
18203546	CR43435	ncRNA	2.05E-05	0.813473
18151018	CG6262	CG6262 gene product from transcript CG6262-RB	0.008909545	0.812102
18169001	CG14125	CG14125 gene product from transcript CG14125-RA	0.000745845	0.809274
18163176	CG30486	CG30486 gene product from transcript CG30486-RB	0.004406818	0.807686
18150301	Cpr49Af	Cuticular protein 49Af	0.006460296	0.807518
18146538	CG43153	CG43153 gene product from transcript CG43153-RA	0.00134092	0.795628

18162802	CG30196	CG30196 gene product from transcript CG30196-RA	0.00131304	0.791375
18199546	alrm	astrocytic leucine-rich repeat molecule	0.007206935	0.786217
18199996	CG9997	CG9997 gene product from transcript CG9997-RA	0.002758496	0.781906
18208275	Gr8a	Gustatory receptor 8a	0.006897148	0.776487
18136813	CR31845	ncRNA	0.005849643	0.774731
18199764	Cpr97Eb	Cuticular protein 97Eb	0.003612836	0.774051
18152265	Obp59a	Odorant-binding protein 59a	0.00101205	0.773675
18162410	Gr59c	Gustatory receptor 59c	0.00026524	0.772871
18141438	CG12400	CG12400 gene product from transcript CG12400-RA	0.001159771	0.771248
18153693	CG30280	CG30280 gene product from transcript CG30280-RB	0.002378308	0.768438
18187120	CG4686	CG4686 gene product from transcript CG4686-RA	0.000265788	0.765585
18188853	CG14527	CG14527 gene product from transcript CG14527-RA	0.004489832	0.764418
18184717	CG1208	CG1208 gene product from transcript CG1208-RB	0.005183712	0.763429
18208108	CG15337	CG15337 gene product from transcript CG15337-RA	0.004026197	0.75891
18157969	Ady43A	CG1851 gene product from transcript CG1851-RA	0.00403644	0.755935
18170188	Spn77Bb	Serpin 77Bb	0.006060339	0.753598
18186801	CG14329	CG14329 gene product from transcript CG14329-RA	0.000783602	0.743154
18217872	inaF-A	CG34322 gene product from transcript CG34322-RA	0.001916919	0.722015
18176467	CG10635	CG10635 gene product from transcript CG10635-RA	0.000306441	0.720365
18154829	Mlp60A	Muscle LIM protein at 60A	0.004011238	0.71862
18147882	PebIII	Ejaculatory bulb protein III	0.008960484	0.714332
18163021	CG30392	CG30392 gene product from transcript CG30392-RA	0.004751544	0.710874
18137386	BG642163	CG34102 gene product from transcript CG34102-RA	0.003132257	0.710612
18168307	ldbr	lariat debranching enzyme	0.002333999	0.709086
18139593	Gyc32E	Guanyl cyclase at 32E	0.007608087	0.7037
18176460	Uev1A	CG10640 gene product from transcript CG10640-RA	0.002211696	0.700764
18144961	Cpr30F	Cuticular protein 30F	0.007949721	0.696969
18210372	CG32551	CG32551 gene product from transcript CG32551-RB	0.006371923	0.696004
18176606	CG10469	CG10469 gene product from transcript CG10469-RA	0.000855532	0.693676
18145396	His4:CG31611 ///	CG31611 gene product from transcript CG31611-RA	0.004083871	0.689378
18172510	Sfp79B	Seminal fluid protein 79	0.002312923	0.683762
18166767	Rh50	CG7499 gene product from transcript CG7499-RA	0.007696921	0.665234

18161134	endoB	endophilin B	0.000909184	0.648779
18203635	mir-4945	mir-4945 stem loop	0.007784818	0.627274
18153561	CG30197	CG30197 gene product from transcript CG30197-RA	3.69E-06	0.60787
18170976	Ilp1	Insulin-like peptide 1	0.009023732	0.606509
18197461	CG6912	CG6912 gene product from transcript CG6912-RA	0.006964493	0.569697
18178610	CG5506	CG5506 gene product from transcript CG5506-RA	0.00536986	0.53232
18158274	mthl3	methuselah-like 3	0.001843841	0.52145
18154241	snoRNA:U31:54Eb	ncRNA	0.000456861	0.468991
18154290	snoRNA:Or-CD4	ncRNA	0.002094688	0.432139

Appendix 2.2 List of genes that were significantly differentially regulated upon *ATPSyn-Cf6* RNAi

transcript_cluster_id	Gene Symbol	Gene Title	p-value	Fold change
18207604	CG15784	CG15784 gene product from transcript CG15784-RA	6.03E-05	10.5969
18212607	w	white	3.38E-06	9.30131
18154670	dom /// snoRNA:Me28S-G2596	domino /// ncRNA	0.00095617	8.56686
18137346	snoRNA:Psi18S-640g	ncRNA	0.00069359	8.13965
18173921	ImpL3	Ecdysone-inducible gene L3	0.00033932	7.97103
18138001	Thor	CG8846 gene product from transcript CG8846-RA	0.000565	5.83231
18141748	CG31918	CG31918 gene product from transcript CG31918-RA	0.00062151	4.37434
18190022	CG31157	CG31157 gene product from transcript CG31157-RB	0.00046312	4.28967
18149383	CG2064	CG2064 gene product from transcript CG2064-RA	0.00010561	3.81893
18205102	CG40648 /// CG43176	CG40648 gene product from transcript CG40648-RB /// CG43176 gene product from transcript CG43176-RB	0.00317208	3.51624
18151892	CG9313	CG9313 gene product from transcript CG9313-RA	0.00222925	2.88412
18161305	CG13430	CG13430 gene product from transcript CG13430-RA	0.00159555	2.86149
18153306	Tret1-1	Trehalose transporter 1-1	0.00110164	2.81272
18150198	CG18343	CG18343 gene product from transcript CG18343-RA	0.00207589	2.76453
18167718	CG14997	CG14997 gene product from transcript CG14997-RB	0.00061028	2.68688
18136417	CG13245	CG13245 gene product from transcript CG13245-RA	0.00348208	2.67462
18158130	Dgp-1	CG5729 gene product from transcript CG5729-RA	0.00096629	2.62097
18160245	Arc1	Activity-regulated cytoskeleton associated protein 1	6.11E-05	2.56448
18142755	FucTB	CG4435 gene product from transcript CG4435-RA	0.00027521	2.50122
18171047	Gr64a	Gustatory receptor 64a	0.00052089	2.47306
18156120	cv-2	crossveinless 2	1.17E-05	2.43755
18137364	snoRNA:Psi18S-525i	ncRNA	0.00115461	2.39906
18205551	Hex-A	Hexokinase A	0.00302129	2.36947
18137376	snoRNA:Psi18S-525c	ncRNA	0.00304722	2.35583
18189641	CG18731	CG18731 gene product from transcript CG18731-RA	0.00465534	2.3492
18150644	Arc2	CG13941 gene product from transcript CG13941-RA	0.00311678	2.32007
18191837	CheB98a	Chemosensory protein A 98a	0.00869434	2.19248
18180610	pncr009:3L	putative noncoding RNA 009:3L	0.00602012	2.18646
18168863	CG7607	CG7607 gene product from transcript CG7607-RA	9.01E-05	2.17674

18183289	Hsp70Bb /// Hsp70Bc	Heat-shock-protein-70Bb /// Heat-shock-protein-70Bc	0.00424289	2.14216
18177602	CG5946	CG5946 gene product from transcript CG5946-RB	0.00495456	2.1346
18192562	mir-4951	mir-4951 stem loop	0.0082785	2.04486
18205963	y	yellow	0.00384956	2.01326
18149377	CG2065	CG2065 gene product from transcript CG2065-RA	0.0060389	1.97465
18140864	CG18095	CG18095 gene product from transcript CG18095-RB	0.00301527	1.90088
18137374	snoRNA:Psi18S-525d	ncRNA	0.00696082	1.878
18176479	blanks	CG10630 gene product from transcript CG10630-RA	0.00189323	1.86689
18136832	Qtzl	Quetzalcoatl	0.0001013	1.85172
18168794	blos4	BLOC-1 subunit 4	0.00618154	1.81667
18137362	snoRNA:Psi18S-525j	ncRNA	0.0092684	1.81412
18154342	snoRNA:Psi28S-3316a	ncRNA	0.00157657	1.76679
18187053	CG7342	CG7342 gene product from transcript CG7342-RB	0.00138545	1.75682
18132916	CG2789	CG2789 gene product from transcript CG2789-RA	0.00128501	1.74489
18144739	CG31683	CG31683 gene product from transcript CG31683-RA	0.00728208	1.72951
18149279	Gadd45	CG11086 gene product from transcript CG11086-RA	0.00288436	1.71983
18205073	Su(Ste):CR40820	ncRNA	0.00552004	1.71519
18191725	Rbp1	RNA-binding protein 1	0.00181542	1.71257
18135200	CG16820	CG16820 gene product from transcript CG16820-RA	0.00256896	1.70397
18208447	CG2076	CG2076 gene product from transcript CG2076-RA	0.0004414	1.68845
18154517	Rgk2	CG34390 gene product from transcript CG34390-RA	0.00093715	1.67261
18185768	CG14715	CG14715 gene product from transcript CG14715-RA	0.00069977	1.66363
18155337	CG42694	CG42694 gene product from transcript CG42694-RA	0.00155381	1.66228
18184582	CG1113	CG1113 gene product from transcript CG1113-RA	5.39E-05	1.65956
18144596	CG31600	CG31600 gene product from transcript CG31600-RA	0.00438316	1.6591
18143153	Ast-C	Allatostatin C	0.00827769	1.64893
18172683	Bet1	CG14084 gene product from transcript CG14084-RB	0.00093655	1.64152
18144038	CG13962	CG13962 gene product from transcript CG13962-RA	0.00568099	1.63233
18210964	snoRNA:Me18S-G894	ncRNA	0.00887228	1.62661
18149426	CG1882	CG1882 gene product from transcript CG1882-RA	0.0007392	1.62248
18180649	snoRNA:Me28S-A2634a	ncRNA	0.00736272	1.61945
18203018	mRpL37	mitochondrial ribosomal protein L37	0.00018822	1.61239
18163719	CG34232	CG34232 gene product from transcript CG34232-RA	0.00270732	1.60778

18134171	CG7191	CG7191 gene product from transcript CG7191-RA	0.00113077	1.60759
18176893	CG8111	CG8111 gene product from transcript CG8111-RA	0.00039659	1.60559
18189765	bai	baiser	0.0007726	1.5942
18172710	CG42588	CG42588 gene product from transcript CG42588-RA	0.00054462	1.5874
18217993	snoRNA:Me28S-U3344b	ncRNA	0.00965921	1.58092
18191773	Xrp1	CG17836 gene product from transcript CG17836-RB	0.00291055	1.5691
18170858	asparagine-synthetase	asparagine synthetase	0.00231	1.56638
18152327	asrij	CG13533 gene product from transcript CG13533-RA	0.00205478	1.55215
18142747	borr	borealin-related	0.00096301	1.54624
18165272	CG17684	CG17684 gene product from transcript CG17684-RC	0.0029367	1.5456
18133927	frj	farjavit	0.00677752	1.54303
18180900	Mst77F	Male-specific transcript 77F	0.00246547	1.54054
18131052	numb	CG3779 gene product from transcript CG3779-RB	0.00968873	1.52817
18216191	CG6123	CG6123 gene product from transcript CG6123-RB	0.00513927	1.52813
18179471	CG7130	CG7130 gene product from transcript CG7130-RA	0.00720837	1.51901
18204052	yellow-h	CG1629 gene product from transcript CG1629-RA	0.00818318	1.51537
18193862	Nmdmc	NAD-dependent methylenetetrahydrofolate dehydrogenase	0.00087647	1.50605
18172840	Exn	Ephexin	0.00131918	1.50184
18197090	CG10126	CG10126 gene product from transcript CG10126-RB	0.00437373	1.5015
18217838	snoRNA:Psi28S-1135b	ncRNA	0.00797287	1.49616
18208208	Rbm13	RNA-binding motif protein 13	0.00136745	1.49516
18200066	CG14509	CG14509 gene product from transcript CG14509-RB	0.00536327	1.49368
18171021	Gr64b /// Gr64c	Gustatory receptor 64b /// Gustatory receptor 64c	0.00131264	1.49319
18156910	l(2)not	lethal (2) neighbor of tid	0.00315373	1.48761
18178217	CG5830	CG5830 gene product from transcript CG5830-RA	0.00012407	1.47155
18150034	CG12942	CG12942 gene product from transcript CG12942-RA	0.00363334	1.4572
18178119	CG7841	CG7841 gene product from transcript CG7841-RA	0.00687607	1.45293
18132393	Taf10	TBP-associated factor 10	0.00309227	1.44266
18172671	CG42575	CG42575 gene product from transcript CG42575-RA	0.00045101	1.4426
18156255	ix	intersex	0.00538518	1.44083
18180012	CR32207	ncRNA	0.00897907	1.4405
18140409	NTPase	CG3059 gene product from transcript CG3059-RD	0.00666035	1.44036
18178470	CG6512	CG6512 gene product from transcript CG6512-RB	0.00374011	1.43897

18166086	CG32320	CG32320 gene product from transcript CG32320-RC	0.00302906	1.43359
18209015	rab3-GEF	CG5627 gene product from transcript CG5627-RC	0.00971081	1.43349
18154666	snoRNA:Me28S-A2589b	ncRNA	0.00444189	1.42975
18217830	snoRNA:Psi28S-1135f	ncRNA	0.00189759	1.42833
18205085	Su(Ste):CR42414 /// Su(Ste):CR42436 /// Su(Ste):CR42440 /// Su(Ste):CR42443	ncRNA /// ncRNA /// ncRNA /// ncRNA	0.00909222	1.42741
18157867	CG8910	CG8910 gene product from transcript CG8910-RA	0.00840028	1.42692
18142869	CG5846	CG5846 gene product from transcript CG5846-RA	0.00712039	1.42139
18159512	CG7637	CG7637 gene product from transcript CG7637-RA	2.37E-05	1.42004
18170573	CG11425	CG11425 gene product from transcript CG11425-RA	0.0003724	1.41948
18197424	CG17304	CG17304 gene product from transcript CG17304-RA	0.00609519	1.41464
18136243	TepIV	Thiolester containing protein IV	0.00584729	1.40373
18196583	Tpc1	Thiamine pyrophosphate carrier protein 1	0.00161826	1.39494
18142600	CG7627	CG7627 gene product from transcript CG7627-RB	0.00835849	1.3903
18203582	CG43448	CG43448 gene product from transcript CG43448-RA	0.00130302	1.38434
18138870	aub	aubergine	0.00814965	1.38431
18168870	CG14141	CG14141 gene product from transcript CG14141-RA	0.00293094	1.37882
18139237	l(2)37Cc	lethal (2) 37Cc	0.00496437	1.37379
18135748	Pomp	CG9324 gene product from transcript CG9324-RA	0.00041795	1.37123
18193002	e	ebony	0.00381131	1.36759
18217834	snoRNA:Psi28S-1135d	ncRNA	0.00124629	1.36645
18145749	Aats-asn	Asparaginyl-tRNA synthetase	0.00150623	1.36604
18142680	CG9510 /// CG9515	CG9510 gene product from transcript CG9510-RC	0.00611554	1.3467
18155416	mi	minus	0.00234087	1.34232
18170738	GNBP1	Gram-negative bacteria binding protein 1	0.00183648	1.34025
18172193	CG34455	CG34455 gene product from transcript CG34455-RC	0.00020333	1.33589
18206438	Hsp60	Heat shock protein 60	0.00714319	1.33496
18198589	CG7044	CG7044 gene product from transcript CG7044-RA	0.0016562	1.33324
18195692	CG2017	CG2017 gene product from transcript CG2017-RA	0.00081963	1.32884
18185466	CG8417	CG8417 gene product from transcript CG8417-RA	0.00319293	1.32724
18161743	CG3501	CG3501 gene product from transcript CG3501-RA	0.0061091	1.32455

18172798	CG42630 /// mtTFB1	CG42630 gene product from transcript CG42630-RA /// Mitochondrial Transcription Factor B1	0.00220474	1.32219
18148726	Aats-cys	Cysteinyl-tRNA synthetase	0.00416838	1.30906
18190959	CG34317 /// CG7950	CG34317 gene product from transcript CG34317-RA	0.00716466	1.30453
18179703	HBS1	CG1898 gene product from transcript CG1898-RA	0.00431613	1.30101
18180817	snoRNA:Psi28S-1837a	ncRNA	0.00445381	1.288
18213482	CG2658	CG2658 gene product from transcript CG2658-RB	0.00268513	1.28711
18176868	CG7506	CG7506 gene product from transcript CG7506-RA	0.00656835	1.27949
18142912	CG5731	CG5731 gene product from transcript CG5731-RA	0.00738243	1.27094
18174479	Rac1	CG2248 gene product from transcript CG2248-RA	0.00109148	1.26839
18144062	Taf13	TBP-associated factor 13	0.00682681	1.26757
18156673	dpn	deadpan	0.00138788	1.26742
18131618	His3.3A /// His3.3B	Histone H3.3A /// Histone H3.3B	0.00139008	1.26602
18171088	CR32027	ncRNA	0.00024312	1.26497
18143847	CG10623	CG10623 gene product from transcript CG10623-RA	0.00311502	1.26129
18134022	CG3476	CG3476 gene product from transcript CG3476-RA	0.00571236	1.2585
18164468	CG42732	CG42732 gene product from transcript CG42732-RH	0.00753201	1.25835
18143613	CG13284	CG13284 gene product from transcript CG13284-RA	0.0081904	1.25757
18202168	RpS7 /// snoRNA:Psi18S-1377b	Ribosomal protein S7 /// ncRNA	0.00680026	1.25585
18197845	ns1	nucleostemin 1	0.00309263	1.25524
18147139	mei-W68	meiotic W68	0.00522451	1.24911
18139488	CG33649 /// DNApol-gamma35	CG33649 gene product from transcript CG33649-RA /// DNA polymerase gamma 35kD	0.00909722	1.24865
18131668	RpS21	Ribosomal protein S21	0.0009991	1.24853
18195594	RpL35A	Ribosomal protein L35A	0.00332662	1.24103
18177312	iPLA2-VIA	calcium-independent phospholipase A2 VIA	0.00670401	1.23893
18154251	snoRNA:Me28S-A3407a	ncRNA	0.00613538	1.23656
18177554	CG11652	CG11652 gene product from transcript CG11652-RA	0.00504862	1.23559
18199573	CG4730	CG4730 gene product from transcript CG4730-RA	0.00943814	1.23485
18134302	Scgalpha	Sarcoglycan alpha	0.0018049	1.23211
18189252	dj-1beta	CG1349 gene product from transcript CG1349-RA	0.0012515	1.22836
18134652	eEF1delta	CG4912 gene product from transcript CG4912-RB	7.57E-06	1.22819
18193177	RpL32	Ribosomal protein L32	0.00441206	1.22686
18131738	Acer	Angiotensin-converting enzyme-related	0.00433504	1.2255

18167150	pex10	peroxin 10	0.00876471	1.224
18147760	Cct5	T-complex Chaperonin 5	0.00821256	1.22208
18133656	CG3008	CG3008 gene product from transcript CG3008-RA	0.00306654	1.21796
18153973	CG30493	CG30493 gene product from transcript CG30493-RB	0.00162682	1.21512
18131069	ref(2)P	refractory to sigma P	0.00077173	1.21195
18195800	MAGE	CG10059 gene product from transcript CG10059-RA	0.00238993	1.21033
18199695	CG6425	CG6425 gene product from transcript CG6425-RA	0.00425993	1.20876
18162584	CG30022	CG30022 gene product from transcript CG30022-RB	0.00211952	1.20863
18176446	CG10671	CG10671 gene product from transcript CG10671-RB	0.00265446	1.20623
18176903	CG7565	CG7565 gene product from transcript CG7565-RA	0.00152064	1.20286
18161255	CG16868	CG16868 gene product from transcript CG16868-RA	0.00114234	1.2
18144167	Mtp	Microsomal triacylglycerol transfer protein	0.00669395	1.19753
18168832	CG7638	CG7638 gene product from transcript CG7638-RA	0.00293392	1.194
18173983	sti	sticky	0.00694341	1.19397
18209406	CG4872	CG4872 gene product from transcript CG4872-RA	0.00972829	1.19077
18202403	Ino80	CG31212 gene product from transcript CG31212-RA	0.00096217	1.18948
18211291	CG5010	CG5010 gene product from transcript CG5010-RA	0.0013282	1.18921
18215857	Anxb11	Annexin B11	0.0090365	1.18819
18183166	ppan	peter pan	0.00768755	1.18775
18168404	CG6745	CG6745 gene product from transcript CG6745-RA	0.00262462	1.18726
18149710	Updo	CG1818 gene product from transcript CG1818-RA	0.00185684	1.18709
18184429	CG9791	CG9791 gene product from transcript CG9791-RC	0.00301038	1.18611
18160444	CG8314	CG8314 gene product from transcript CG8314-RA	0.00719811	1.18408
18156106	clt	cricklet	0.00695968	1.1826
18216945	mRpL14	mitochondrial ribosomal protein L14	0.00192108	1.18015
18208818	CG1662	CG1662 gene product from transcript CG1662-RA	0.009885	1.17947
18185658	CG4820	CG4820 gene product from transcript CG4820-RB	0.00818575	1.17384
18133694	CG3792	CG3792 gene product from transcript CG3792-RA	0.0048409	1.17191
18172723	BHD	Birt-Hogg-Dube homolog	0.00447945	1.17091
18148801	Adam	CG12131 gene product from transcript CG12131-RA	0.00960811	1.16681
18181128	Vti1	CG3279 gene product from transcript CG3279-RA	0.00757214	1.16538
18218902	CR43497	ncRNA	0.00655982	1.16395
18209746	Hs3st-B	Heparan sulfate 3-O sulfotransferase-B	0.00510486	1.15955
18198845	CG4813	CG4813 gene product from	0.00566563	1.15835

		transcript CG4813-RA		
18166977	Rev1	CG12189 gene product from transcript CG12189-RA	0.00022847	1.15824
18198545	CG3822	CG3822 gene product from transcript CG3822-RA	0.00570564	1.15778
18171098	CG32038	CG32038 gene product from transcript CG32038-RA	0.00624537	1.15746
18173198	Ect4	CG43119 gene product from transcript CG43119-RI	0.00268206	1.15669
18168918	PCID2	PCI domain-containing protein 2	0.0029372	1.15495
18200680	granny-smith	granny smith	0.00846738	1.15439
18200647	Ugt86Di	CG6658 gene product from transcript CG6658-RA	0.00557256	1.15426
18178350	CG4573	CG4573 gene product from transcript CG4573-RA	0.0061076	1.15069
18178624	Prestin	CG5485 gene product from transcript CG5485-RA	0.00751566	1.14997
18138091	LanB1	CG7123 gene product from transcript CG7123-RA	0.00103271	1.14679
18179951	Ndfip	Nedd4 family interacting protein	0.00510313	1.14499
18198619	CG3337	CG3337 gene product from transcript CG3337-RA	0.00157063	1.14388
18139077	Eno	Enolase	0.00278226	1.14032
18167629	IntS10	Integrator 10	0.00520661	1.13987
18200852	Spec2	CG14672 gene product from transcript CG14672-RA	0.00519965	1.13968
18191841	scaRNA:mgU2-25	ncRNA	0.00219448	1.13847
18199548	CG4553	CG4553 gene product from transcript CG4553-RA	0.00838847	1.13349
18150646	Tfb1	CG8151 gene product from transcript CG8151-RB	0.00480318	1.13328
18213842	CG13364	CG13364 gene product from transcript CG13364-RA	0.00796648	1.13032
18218609	CG42854	CG42854 gene product from transcript CG42854-RA	0.00298705	1.12967
18187225	Srp14	Signal recognition particle protein 14	0.00966718	1.12933
18145550	snoRNA:Psi28S-2996	ncRNA	0.00736528	1.1287
18195950	CG2747	CG2747 gene product from transcript CG2747-RD	0.00499733	1.12542
18183720	RpS20	Ribosomal protein S20	0.00145545	1.1235
18174496	RpS9	Ribosomal protein S9	0.00074463	1.11832
18169698	TSG101	tumor suppressor protein 101	0.00377256	1.11832
18206908	Crag	Calmodulin-binding protein related to a Rab3 GDP/GTP exchange protein	0.00349223	1.11757
18216512	CG12702	CG12702 gene product from transcript CG12702-RA	0.00671461	1.11718
18179216	CG11396	CG11396 gene product from transcript CG11396-RA	0.00046612	1.11695
18141576	CG3702	CG3702 gene product from transcript CG3702-RA	0.00078896	1.11157
18161975	Upf3	CG11184 gene product from transcript CG11184-RB	0.00845278	1.10988
18217347	Rab9Fb	Rab GTPase 9Fb	0.00608404	1.10913
18147971	RpL11	Ribosomal protein L11	0.0050975	1.10583

18138004	wb	wing blister	0.00256153	1.10399
18184118	CG11970	CG11970 gene product from transcript CG11970-RA	0.00262973	1.10346
18201535	CG31320	CG31320 gene product from transcript CG31320-RA	0.00746204	1.10315
18192983	Dl	Delta	0.00737701	1.10056
18202744	CG12163	CG12163 gene product from transcript CG12163-RB	0.00576503	1.10012
18176994	CG7185	CG7185 gene product from transcript CG7185-RB	0.00124625	1.08631
18202368	ALiX	ALG-2 interacting protein X	0.00751174	1.08523
18156419	sub	subito	0.00331387	1.079
18150743	pcs	parcas	0.00973699	1.07868
18169390	CG6859	CG6859 gene product from transcript CG6859-RA	0.00560458	1.07861
18206728	CG11412	CG11412 gene product from transcript CG11412-RC	0.00781226	1.07719
18137618	l(2)37Cd	lethal (2) 37Cd	0.00064376	1.07103
18184106	rha	CG11908 gene product from transcript CG11908-RA	0.00394443	1.06965
18200820	CG18766	CG18766 gene product from transcript CG18766-RB	0.00837091	1.06713
18140954	Spn27A	Serpin 27A	0.00351791	1.06012
18195295	Snap24	Synapse protein 24	0.00035428	1.05726
18175627	Tudor-SN	CG7008 gene product from transcript CG7008-RA	8.11E-05	1.05531
18188169	Trf4-2	CG17462 gene product from transcript CG17462-RA	0.00268128	1.05424
18172904	CG42676	CG42676 gene product from transcript CG42676-RD	0.00339452	1.0464
18147725	Dcp-1	Death caspase-1	0.00239293	1.04464
18158416	SCAP	SREBP cleavage activating protein	0.00394888	1.04304
18217114	Stim	Stromal interaction molecule	0.00984113	1.03939
18205430	dwg	deformed wings	0.00139099	1.02453
18193931	pll	pelle	0.00641721	0.975716
18205631	Met	Methoprene-tolerant	0.0046752	0.962239
18201562	Unc-115a /// Unc-115b	CG31352 gene product from transcript CG31352-RA /// CG31332 gene product from transcript CG31332-RD	0.00463604	0.962239
18148900	CSN7	COP9 complex homolog subunit 7	0.0060013	0.956608
18208148	Trf4-1	CG11265 gene product from transcript CG11265-RE	0.00813735	0.955724
18192319	lute	CG43226 gene product from transcript CG43226-RC	0.00661157	0.947304
18209615	CG6106	CG6106 gene product from transcript CG6106-RA	0.00172427	0.945839
18169918	MYPT-75D	CG6896 gene product from transcript CG6896-RA	0.00205447	0.945249
18139621	Uch	Ubiquitin carboxy-terminal hydrolase	0.00611991	0.932817
18182528	ort	ora transientless	0.00370002	0.927295
18162975	CG30375	CG30375 gene product from transcript CG30375-RA	0.00098599	0.926502
18188844	CG1647	CG1647 gene product from	0.0086378	0.904734

		transcript CG1647-RA		
18181251	CG42638 /// trpml	CG42638 gene product from transcript CG42638-RA /// transient receptor potential mucolipin	0.00620619	0.904609
18169211	CG10741	CG10741 gene product from transcript CG10741-RB	0.00489654	0.899898
18168169	sec63	CG8583 gene product from transcript CG8583-RA	0.0034034	0.897385
18202739	E(var)3-9	Enhancer of variegation 3-9	0.00016396	0.896784
18178107	Best3	Bestrophin 3	0.00838554	0.894136
18135414	CG5783	CG5783 gene product from transcript CG5783-RA	0.00377317	0.893372
18131918	SA	Stromalin	0.00950391	0.892258
18199795	CG5984	CG5984 gene product from transcript CG5984-RA	0.00187497	0.890055
18179489	CG12546 /// CG14452	CG12546 gene product from transcript CG12546-RA /// CG14452 gene product from transcript CG14452-RA	0.00933525	0.884581
18208454	CG18292	CG18292 gene product from transcript CG18292-RA	0.00883178	0.878065
18177236	pall	pallbearer	0.00449977	0.876039
18183735	Ice	CG7788 gene product from transcript CG7788-RA	0.00049642	0.872968
18151296	CG4975 /// CG4984	CG4975 gene product from transcript CG4975-RC /// CG4984 gene product from transcript CG4984-RD	0.0044309	0.868863
18133960	Tango1	Transport and Golgi organization 1	0.00635577	0.867038
18146561	CG43271	CG43271 gene product from transcript CG43271-RA	0.00709926	0.866657
18190590	CG33110	CG33110 gene product from transcript CG33110-RA	0.00824954	0.862701
18174438	Con	Connectin	0.00108219	0.861287
18203667	CR43633	ncRNA	0.0071896	0.858526
18170822	exex	extra-extra	0.00768239	0.857871
18213573	CG3081	CG3081 gene product from transcript CG3081-RA	0.00308284	0.857812
18177541	CG11660	CG11660 gene product from transcript CG11660-RA	0.00540736	0.856129
18134661	CG4953	CG4953 gene product from transcript CG4953-RA	0.00247443	0.852556
18213037	CG15865	CG15865 gene product from transcript CG15865-RA	0.00235208	0.851414
18212788	Yp2	Yolk protein 2	0.00519328	0.846374
18155451	CG42753	CG42753 gene product from transcript CG42753-RA	0.00280996	0.846061
18152302	CG13532	CG13532 gene product from transcript CG13532-RA	0.00831944	0.844791
18160593	CG15710	CG15710 gene product from transcript CG15710-RA	0.00444053	0.842452
18176606	CG10469	CG10469 gene product from transcript CG10469-RA	0.00454781	0.842121
18144474	CG13773	CG13773 gene product from transcript CG13773-RA	0.00502971	0.838801
18198913	CG17111	CG17111 gene product from	0.00620576	0.837542

		transcript CG17111-RB		
18142760	jp	junctophilin	0.00014847	0.836092
18179124	CG13248	CG13248 gene product from transcript CG13248-RA	0.00911344	0.8353
18188368	CG5111	CG5111 gene product from transcript CG5111-RA	0.00711398	0.833873
18151739	CG11041	CG11041 gene product from transcript CG11041-RB	0.00960347	0.83343
18141765	CG7742	CG7742 gene product from transcript CG7742-RA	0.00374987	0.832256
18141159	CG5126	CG5126 gene product from transcript CG5126-RA	0.00263721	0.831834
18135349	CG15141	CG15141 gene product from transcript CG15141-RA	0.0021022	0.830719
18209672	Pvf1	PDGF- and VEGF-related factor 1	0.00307256	0.830278
18195203	CG2082	CG2082 gene product from transcript CG2082-RO	0.00890957	0.828343
18203136	CG42789	CG42789 gene product from transcript CG42789-RA	0.00459018	0.827865
18201884	dpr11	CG33202 gene product from transcript CG33202-RB	0.00664696	0.82226
18156074	Amy-p	Amylase proximal	0.00814662	0.818545
18162410	Gr59c	Gustatory receptor 59c	0.00852015	0.817033
18179191	cmpy	crimpy	0.00178677	0.81592
18162802	CG30196	CG30196 gene product from transcript CG30196-RA	0.00031754	0.80735
18181428	CG42764	CG42764 gene product from transcript CG42764-RB	0.00763566	0.802441
18198922	CG13830	CG13830 gene product from transcript CG13830-RD	0.00188221	0.802181
18163509	SIP2	Syntaxin Interacting Protein 2	0.00666661	0.801533
18183946	Pcd	pterin-4a-carbinolamine dehydratase	0.00644948	0.801459
18161542	CG4386	CG4386 gene product from transcript CG4386-RA	0.00460361	0.797008
18181599	CG43085	CG43085 gene product from transcript CG43085-RA	0.00685298	0.792418
18163038	CG30403	CG30403 gene product from transcript CG30403-RB	0.00806516	0.78629
18136813	CR31845	ncRNA	0.00707127	0.78252
18141282	CG9967	CG9967 gene product from transcript CG9967-RA	0.00817463	0.78131
18208108	CG15337	CG15337 gene product from transcript CG15337-RA	0.00444608	0.781075
18199996	CG9997	CG9997 gene product from transcript CG9997-RA	0.00043183	0.780029
18186801	CG14329	CG14329 gene product from transcript CG14329-RA	0.00029947	0.778517
18138259	mir-932	mir-932 stem loop	0.00577106	0.778265
18165176	CG40191	CG40191 gene product from transcript CG40191-RC	5.62E-05	0.775788
18133006	CG4577	CG4577 gene product from transcript CG4577-RA	0.00056071	0.775572
18165134	rl	rolled	0.00981922	0.774677
18188326	CG11878	CG11878 gene product from transcript CG11878-RA	0.00376345	0.773014
18172510	Sfp79B	Seminal fluid protein 79	0.00698367	0.769735

18182945	Ccp84Ad	CG2341 gene product from transcript CG2341-RA	0.00340661	0.768953
18144721	CG31677	CG31677 gene product from transcript CG31677-RA	0.00921253	0.76771
18144961	Cpr30F	Cuticular protein 30F	0.0008396	0.762671
18162910	CG30355	CG30355 gene product from transcript CG30355-RA	0.00464086	0.762407
18203546	CR43435	ncRNA	3.68E-05	0.759067
18179679	CG18808	CG18808 gene product from transcript CG18808-RA	0.00162533	0.745906
18175772	CG9186	CG9186 gene product from transcript CG9186-RB	0.00441964	0.742348
18135911	CG3262	CG3262 gene product from transcript CG3262-RD	0.0040742	0.741251
18184717	CG1208	CG1208 gene product from transcript CG1208-RB	0.00880127	0.740908
18146538	CG43153	CG43153 gene product from transcript CG43153-RA	0.00592774	0.738891
18208275	Gr8a	Gustatory receptor 8a	0.0052984	0.735824
18165215	Yeti	CG40218 gene product from transcript CG40218-RA	0.00577918	0.726886
18161134	endoB	endophilin B	0.0050366	0.714497
18170976	Ilp1	Insulin-like peptide 1	0.0084955	0.711269
18211888	CR43461	ncRNA	0.00867789	0.710874
18210372	CG32551	CG32551 gene product from transcript CG32551-RB	0.00167094	0.709824
18168307	ldbr	lariat debranching enzyme	0.00245015	0.709398
18188457	CG14540	CG14540 gene product from transcript CG14540-RA	0.00098635	0.704872
18176460	Uev1A	CG10640 gene product from transcript CG10640-RA	0.00056549	0.703522
18193731	Takr86C	Tachykinin-like receptor at 86C	0.00059545	0.696583
18194075	l(3)neo43	lethal (3) neo43	0.00178335	0.695955
18199618	CcapR	Cardioacceleratory peptide receptor	0.00395267	0.692795
18186833	CG14321	CG14321 gene product from transcript CG14321-RA	0.00247061	0.691595
18137386	BG642163	CG34102 gene product from transcript CG34102-RA	0.00255612	0.68677
18153561	CG30197	CG30197 gene product from transcript CG30197-RA	0.0077143	0.672047
18186402	CG3987	CG3987 gene product from transcript CG3987-RA	0.00406746	0.66688
18217872	inaF-A	CG34322 gene product from transcript CG34322-RA	0.00227378	0.662167
18202229	CG34148	CG34148 gene product from transcript CG34148-RA	0.00752868	0.660471
18187120	CG4686	CG4686 gene product from transcript CG4686-RA	0.00016307	0.65299
18189926	CG31086 /// CG31323	CG31086 gene product from transcript CG31086-RB /// CG31323 gene product from transcript CG31323-RA	0.00516557	0.649454
18157969	Ady43A	CG1851 gene product from transcript CG1851-RA	0.00070362	0.649214
18178610	CG5506	CG5506 gene product from transcript CG5506-RA	0.00832784	0.647671
18143158	Ast-CC	Allatostatin double C	0.00416383	0.64646

18159092	CG8216	CG8216 gene product from transcript CG8216-RA	0.00038131	0.635721
18171921	CG34002	CG34002 gene product from transcript CG34002-RB	0.00613068	0.628173
18149246	Tsp42El	Tetraspanin 42El	0.00710957	0.615843
18137535	CG34351	CG34351 gene product from transcript CG34351-RC	0.00878067	0.61506
18137557	CG34381	CG34381 gene product from transcript CG34381-RB	2.70E-05	0.614294
18190260	CG31323	CG31323 gene product from transcript CG31323-RA	0.00899695	0.60462
18197509	CG6654	CG6654 gene product from transcript CG6654-RA	0.00311757	0.594878
18158274	mthl3	methuselah-like 3	0.0001988	0.584942
18166767	Rh50	CG7499 gene product from transcript CG7499-RA	0.00072599	0.569184
18186662	Gyc-89Da	Guanylyl cyclase at 89Da	0.002398	0.558076
18197611	CG14871	CG14871 gene product from transcript CG14871-RB	0.00681125	0.541112
18176817	pst	pastrel	0.00108573	0.540126
18154290	snoRNA:Or-CD4	ncRNA	0.00840178	0.527594
18154336	snoRNA:Psi28S-3316d	ncRNA	0.00963706	0.514913
18179739	Ilp3	Insulin-like peptide 3	0.00043264	0.499792
18197461	CG6912	CG6912 gene product from transcript CG6912-RA	0.00023605	0.0827881

Appendix 2.3 List of genes that were commonly regulated upon *TFAM* overexpression and *ATPSyn-Cf6* RNAi

			TFAM o/e		*ATPSyn-Cf6* RNAi	
transcript_id	**Gene Symbol**	**Gene Title**	**p-value**	**Fold change**	**p-value**	**Fold change**
18154670	dom /// snoRNA:Me28S-G2596	domino /// ncRNA	0.001216175	8.24603	0.000956175	8.56686
18137346	snoRNA:Psi18S-640g	ncRNA	0.000575468	5.62505	0.000693591	8.13965
18207604	CG15784	CG15784 gene product from transcript CG15784-RA	0.000193688	5.51706	6.03E-05	10.5969
18141748	CG31918	CG31918 gene product from transcript CG31918-RA	0.000214553	3.70455	0.000621511	4.37434
18173921	ImpL3	Ecdysone-inducible gene L3	0.001970607	3.58449	0.000339321	7.97103
18138001	Thor	CG8846 gene product from transcript CG8846-RA	0.00270655	3.235	0.000564999	5.83231
18161305	CG13430	CG13430 gene product from transcript CG13430-RA	0.001199013	3.11299	0.001595547	2.86149
18150198	CG18343	CG18343 gene product from transcript CG18343-RA	0.000415337	3.04329	0.002075888	2.76453
18149383	CG2064	CG2064 gene product from transcript CG2064-RA	0.000297723	2.80085	0.000105611	3.81893
18190022	CG31157	CG31157 gene product from transcript CG31157-RB	0.003184809	2.46274	0.000463122	4.28967
18142755	FucTB	CG4435 gene product from transcript CG4435-RA	0.000696815	2.45558	0.000275209	2.50122
18155337	CG42694	CG42694 gene product from transcript CG42694-RA	0.000948164	2.2214	0.001553813	1.66228
18160245	Arc1	Activity-regulated cytoskeleton associated protein 1	0.000108027	2.15547	6.11E-05	2.56448
18137376	snoRNA:Psi18S-525c	ncRNA	0.004784562	1.86948	0.003047217	2.35583
18168863	CG7607	CG7607 gene product from transcript CG7607-RA	0.002469362	1.8693	9.01E-05	2.17674
18154342	snoRNA:Psi28S-3316a	ncRNA	0.001249277	1.80242	0.001576574	1.76679

18217993	snoRNA:Me28S-U3344b	ncRNA	0.001281285	1.69847	0.009659213	1.58092
18156120	cv-2	crossveinless 2	0.001654013	1.69341	1.17E-05	2.43755
18168794	blos4	BLOC-1 subunit 4	0.005306561	1.68943	0.006181543	1.81667
18163719	CG34232	CG34232 gene product from transcript CG34232-RA	0.003414842	1.58253	0.002707323	1.60778
18159512	CG7637	CG7637 gene product from transcript CG7637-RA	0.001649847	1.54785	2.37E-05	1.42004
18142869	CG5846	CG5846 gene product from transcript CG5846-RA	0.006010311	1.54681	0.007120388	1.42139
18150644	Arc2	CG13941 gene product from transcript CG13941-RA	0.003126833	1.54564	0.003116782	2.32007
18134171	CG7191	CG7191 gene product from transcript CG7191-RA	0.002290588	1.51138	0.001130766	1.60759
18191725	Rbp1	RNA-binding protein 1	0.001865953	1.50202	0.001815417	1.71257
18185768	CG14715	CG14715 gene product from transcript CG14715-RA	0.004138754	1.50177	0.000699772	1.66363
18203018	mRpL37	mitochondrial ribosomal protein L37	0.000612093	1.48775	0.000188217	1.61239
18153306	Tret1-1	Trehalose transporter 1-1	0.006335764	1.48552	0.001101639	2.81272
18132916	CG2789	CG2789 gene product from transcript CG2789-RA	0.001765072	1.48408	0.00128501	1.74489
18165272	CG17684	CG17684 gene product from transcript CG17684-RC	0.002510032	1.46805	0.002936703	1.5456
18158130	Dgp-1	CG5729 gene product from transcript CG5729-RA	8.42E-05	1.45384	0.000966286	2.62097
18154666	snoRNA:Me28S-A2589b	ncRNA	0.001301827	1.44864	0.004441888	1.42975
18144739	CG31683	CG31683 gene product from transcript CG31683-RA	0.001055888	1.44807	0.007282082	1.72951
18136832	Qtzl	Quetzalcoatl	0.001102121	1.43038	0.000101296	1.85172
18140864	CG18095	CG18095 gene product from transcript CG18095-RB	0.001969727	1.42731	0.003015274	1.90088
18142747	borr	borealin-related	0.001573783	1.4251	0.000963011	1.54624
18187053	CG7342	CG7342 gene product from transcript CG7342-RB	0.005556996	1.42067	0.001385446	1.75682

18191773	Xrp1	CG17836 gene product from transcript CG17836-RB	0.003401172	1.41121	0.002910549	1.5691
18208447	CG2076	CG2076 gene product from transcript CG2076-RA	0.00097162	1.40643	0.000441403	1.68845
18172683	Bet1	CG14084 gene product from transcript CG14084-RB	0.002689554	1.40435	0.000936547	1.64152
18150034	CG12942	CG12942 gene product from transcript CG12942-RA	0.004580837	1.40386	0.003633341	1.4572
18172840	Exn	Ephexin	0.002232586	1.40107	0.001319182	1.50184
18170573	CG11425	CG11425 gene product from transcript CG11425-RA	0.001026525	1.395	0.000372403	1.41948
18156255	ix	intersex	0.004650343	1.39117	0.00538518	1.44083
18176893	CG8111	CG8111 gene product from transcript CG8111-RA	0.002876667	1.38303	0.000396588	1.60559
18149377	CG2065	CG2065 gene product from transcript CG2065-RA	2.85E-05	1.37834	0.006038904	1.97465
18203582	CG43448	CG43448 gene product from transcript CG43448-RA	0.001968114	1.36591	0.001303025	1.38434
18131618	His3.3A /// His3.3B	Histone H3.3A /// Histone H3.3B	0.006127948	1.36157	0.001390081	1.26602
18170738	GNBP1	Gram-negative bacteria binding protein 1	0.002172055	1.35968	0.001836479	1.34025
18131738	Acer	Angiotensin-converting enzyme-related	0.005730108	1.33373	0.004335039	1.2255
18195594	RpL35A	Ribosomal protein L35A	0.001482247	1.33139	0.003326623	1.24103
18149426	CG1882	CG1882 gene product from transcript CG1882-RA	0.005315602	1.3218	0.000739204	1.62248
18132393	Taf10	TBP-associated factor 10	0.000333316	1.31896	0.003092271	1.44266
18161743	CG3501	CG3501 gene product from transcript CG3501-RA	0.009024873	1.31185	0.006109095	1.32455
18144062	Taf13	TBP-associated factor 13	0.008836609	1.29969	0.006826809	1.26757
18135748	Pomp	CG9324 gene product from transcript CG9324-RA	3.46E-05	1.29456	0.000417946	1.37123
18140409	NTPase	CG3059 gene product from transcript CG3059-RD	0.004505528	1.29295	0.006660345	1.44036

18131668	RpS21	Ribosomal protein S21	0.005511447	1.28886	0.000999105	1.24853
18216191	CG6123	CG6123 gene product from transcript CG6123-RB	0.007905125	1.28815	0.00513927	1.52813
18198589	CG7044	CG7044 gene product from transcript CG7044-RA	0.002534054	1.28767	0.001656204	1.33324
18172710	CG42588	CG42588 gene product from transcript CG42588-RA	0.007284208	1.27362	0.000544616	1.5874
18171088	CR32027	ncRNA	0.000862496	1.26807	0.000243117	1.26497
18135200	CG16820	CG16820 gene product from transcript CG16820-RA	0.006627346	1.26453	0.002568962	1.70397
18193862	Nmdmc	NAD-dependent methylenetetrahydrofolate dehydrogenase	0.007290833	1.24683	0.000876472	1.50605
18134302	Scgalpha	Sarcoglycan alpha	0.002640796	1.23919	0.001804896	1.23211
18138091	LanB1	CG7123 gene product from transcript CG7123-RA	0.000536162	1.23891	0.00103271	1.14679
18161255	CG16868	CG16868 gene product from transcript CG16868-RA	0.003669986	1.23605	0.001142343	1.2
18208208	Rbm13	RNA-binding motif protein 13	0.003848889	1.23157	0.001367455	1.49516
18178217	CG5830	CG5830 gene product from transcript CG5830-RA	0.002265748	1.2283	0.000124072	1.47155
18156673	dpn	deadpan	0.002935974	1.22555	0.001387883	1.26742
18198845	CG4813	CG4813 gene product from transcript CG4813-RA	0.007749747	1.2221	0.005665626	1.15835
18142912	CG5731	CG5731 gene product from transcript CG5731-RA	0.00569152	1.21338	0.007382428	1.27094
18172671	CG42575	CG42575 gene product from transcript CG42575-RA	0.00052047	1.20832	0.00045101	1.4426
18134652	eEF1delta	CG4912 gene product from transcript CG4912-RB	6.00E-05	1.19541	7.57E-06	1.22819
18133694	CG3792	CG3792 gene product from transcript CG3792-RA	0.004678829	1.18934	0.004840898	1.17191
18166977	Rev1	CG12189 gene product from transcript CG12189-RA	0.001348521	1.18882	0.000228467	1.15824
18176446	CG10671	CG10671 gene product from transcript CG10671RB	0.004946807	1.1875	0.002654463	1.20623

18193002	e	ebony	0.000280314	1.18362	0.003811313	1.36759
18139237	l(2)37Cc	lethal (2) 37Cc	0.00468869	1.17026	0.004964366	1.37379
18195800	MAGE	CG10059 gene product from transcript CG10059-RA	0.009854643	1.16379	0.002389928	1.21033
18185658	CG4820	CG4820 gene product from transcript CG4820-RB	0.008969043	1.15982	0.008185746	1.17384
18161975	Upf3	CG11184 gene product from transcript CG11184-RB	0.003284819	1.15594	0.00845278	1.10988
18168404	CG6745	CG6745 gene product from transcript CG6745-RA	0.000305255	1.15495	0.002624616	1.18726
18202403	Ino80	CG31212 gene product from transcript CG31212-RA	0.000386794	1.14525	0.000962166	1.18948
18149710	Updo	CG1818 gene product from transcript CG1818-RA	0.000709967	1.14443	0.001856843	1.18709
18160444	CG8314	CG8314 gene product from transcript CG8314-RA	0.007198857	1.14274	0.007198113	1.18408
18131069	ref(2)P	refractory to sigma P	0.001678822	1.13932	0.000771726	1.21195
18211291	CG5010	CG5010 gene product from transcript CG5010-RA	0.001078923	1.13761	0.001328196	1.18921
18202368	ALiX	ALG-2 interacting protein X	0.000657961	1.13079	0.007511745	1.08523
18191841	scaRNA:mgU2-25	ncRNA	0.000322539	1.1268	0.00219448	1.13847
18198619	CG3337	CG3337 gene product from transcript CG3337-RA	0.001437471	1.12652	0.001570632	1.14388
18169698	TSG101	tumor suppressor protein 101	0.002786764	1.12584	0.00377256	1.11832
18176994	CG7185	CG7185 gene product from transcript CG7185-RB	0.006356462	1.1241	0.001246255	1.08631
18209746	Hs3st-B	Heparan sulfate 3-O sulfotransferase-B	0.006096256	1.12106	0.005104865	1.15955
18147971	RpL11	Ribosomal protein L11	0.001875604	1.11026	0.005097498	1.10583
18192983	Dl	Delta	0.004007629	1.10785	0.007377014	1.10056
18216945	mRpL14	mitochondrial ribosomal protein L14	0.005031468	1.09863	0.001921077	1.18015
18145550	snoRNA:Psi28S-2996	ncRNA	0.000602456	1.08799	0.007365283	1.1287
18172904	CG42676	CG42676 gene product from transcript CG42676-RD	0.008179293	1.05052	0.003394525	1.0464

18201562	Unc-115a /// Unc-115b	CG31352 gene product from transcript CG31352-RA /// CG31332 gene product from transcript CG31332-RD	0.005011536	0.94748	0.004636045	0.96229
18169211	CG10741	CG10741 gene product from transcript CG10741-RB	0.007445609	0.92059	0.004896538	0.89988
18183735	Ice	CG7788 gene product from transcript CG7788-RA	0.00508727	0.91742	0.000496423	0.87298
18202739	E(var)3-9	Enhancer of variegation 3-9	0.00046223	0.91535	0.000163963	0.89674
18169918	MYPT-75D	CG6896 gene product from transcript CG6896-RA	0.009220406	0.90884	0.002054466	0.94529
18162975	CG30375	CG30375 gene product from transcript CG30375-RA	0.001918266	0.90844	0.000985989	0.92652
18144474	CG13773	CG13773 gene product from transcript CG13773-RA	0.005912821	0.87399	0.005029706	0.83881
18135349	CG15141	CG15141 gene product from transcript CG15141-RA	0.003168971	0.87041	0.002102202	0.83079
18151296	CG4975 /// CG4984	CG4975 gene product from transcript CG4975-RC /// CG4984 gene product from transcript CG4984-RD	0.004469496	0.8632	0.004430902	0.86883
18177236	pall	pallbearer	0.006548162	0.85856	0.004499772	0.87609
18134661	CG4953	CG4953 gene product from transcript CG4953-RA	0.003357879	0.84958	0.002474428	0.85256
18190590	CG33110	CG33110 gene product from transcript CG33110-RA	0.00789783	0.84345	0.008249538	0.86271
18198913	CG17111	CG17111 gene product from transcript CG17111-RB	0.006784088	0.82348	0.006205757	0.83752
18142760	jp	junctophilin	0.001120585	0.81994	0.00014847	0.83602
18163038	CG30403	CG30403 gene product from transcript CG30403-RB	0.008754219	0.81803	0.008065165	0.78629
18203546	CR43435	ncRNA	2.05E-05	0.81343	3.68E-05	0.75907
18146538	CG43153	CG43153 gene product from transcript CG43153-RA	0.00134092	0.79568	0.005927741	0.73881

18162802	CG30196	CG30196 gene product from transcript CG30196-RA	0.00131304	0.79135	0.000317538	0.80735
18199996	CG9997	CG9997 gene product from transcript CG9997-RA	0.002758496	0.78196	0.000431832	0.78009
18208275	Gr8a	Gustatory receptor 8a	0.006897148	0.77487	0.005298401	0.73584
18136813	CR31845	ncRNA	0.005849643	0.77471	0.007071271	0.78252
18162410	Gr59c	Gustatory receptor 59c	0.00026524	0.77281	0.008520147	0.81703
18187120	CG4686	CG4686 gene product from transcript CG4686-RA	0.000265788	0.76555	0.000163074	0.65299
18184717	CG1208	CG1208 gene product from transcript CG1208-RB	0.005183712	0.76349	0.008801269	0.74098
18208108	CG15337	CG15337 gene product from transcript CG15337-RA	0.004026197	0.75891	0.004446084	0.78105
18157969	Ady43A	CG1851 gene product from transcript CG1851-RA	0.00403644	0.75595	0.000703617	0.64924
18186801	CG14329	CG14329 gene product from transcript CG14329-RA	0.000783602	0.74314	0.000299468	0.77857
18217872	inaF-A	CG34322 gene product from transcript CG34322-RA	0.001916919	0.72205	0.002273785	0.66217
18137386	BG642163	CG34102 gene product from transcript CG34102-RA	0.003132257	0.71062	0.002556117	0.68677
18168307	ldbr	lariat debranching enzyme	0.002333999	0.70906	0.002450148	0.70938
18176460	Uev1A	CG10640 gene product from transcript CG10640-RA	0.002211696	0.70074	0.000565487	0.70352
18144961	Cpr30F	Cuticular protein 30F	0.007949721	0.69699	0.000839597	0.76261
18210372	CG32551	CG32551 gene product from transcript CG32551-RB	0.006371923	0.69604	0.001670935	0.70984
18176606	CG10469	CG10469 gene product from transcript CG10469-RA	0.000855532	0.69366	0.004547806	0.84211
18172510	Sfp79B	Seminal fluid protein 79	0.002312923	0.68372	0.006983671	0.76975
18166767	Rh50	CG7499 gene product from transcript CG7499-RA	0.007696921	0.66524	0.000725993	0.56914
18161134	endoB	endophilin B	0.000909184	0.64879	0.005036597	0.71447

18153561	CG30197	CG30197 gene product from transcript CG30197-RA	3.69E-06	0.60787	0.007714296	0.67207
18170976	Ilp1	Insulin-like peptide 1	0.009023732	0.60659	0.008495497	0.71129
18197461	CG6912	CG6912 gene product from transcript CG6912-RA	0.006964493	0.56967	0.000236046	0.08281
18178610	CG5506	CG5506 gene product from transcript CG5506-RA	0.00536986	0.53232	0.00832784	0.64761
18158274	mthl3	methuselah-like 3	0.001843841	0.52145	0.000198802	0.58492
18154290	snoRNA:Or-CD4	ncRNA	0.002094688	0.43219	0.008401781	0.52754

Appendix 2.4 GO functional clustering chart for the most enriched genes in larvae overexpressing *TFAM*

Term	Count	%	PValue	Genes	List Total	Fold Enrichment
GO:0043232~intracellular non-membrane-bounded organelle	27	1.01161	0.05351372	HIS2A:CG33823, RPL36A, HIS4:CG33871, HIS2A:CG33826, HIS2A:CG33820, KL-3, INO80, HIS4:CG33873, HIS2A:CG31618, RPS4, HIS4:CG33875, HIS2A:CG33862, HIS3.3B, HIS3.3A, MRPL37, RPL11, HIS2A:CG33817, HIS2A:CG33865, HIS2A:CG33814, RPL35A, HIS4:CG33905, HIS4:CG33883, HIS4:CG33903, HIS4:CG33909, HIS4:CG33907, HIS4:CG31611, HIS4:CG33889, HIS4:CG33887, HIS4:CG33885, HIS2A:CG33850, GNF1, HIS2A:CG33856, HIS2A:CG33859, HIS2A:CG33853, HIS2A:CG33808, HIS4:CG33895, HIS2A:CG33838, HIS4:CG33897, HIS4:CG33899, BONSAI, ARC-P34, HIS4:CG33891, TRF, HIS4:CG33893, SAN, MRPL15, MRPL14, HIS4R, RPL9, HIS2A:CG33844, HIS4:CG33901, HIS2A:CG33841, HIS2A:CG33847, RPS23, MRPS26, HIS2A:CG33829, CG7637, BORR, MRPL28, NOA36, RAVUS, LIN-52, HIS2A:CG33832, HIS2A:CG33835, CK	98	1.3983
GO:0043228~non-membrane-bounded organelle	27	1.01161	0.05351372	HIS2A:CG33823, RPL36A, HIS4:CG33871, HIS2A:CG33826, HIS2A:CG33820, KL-3, INO80, HIS4:CG33873, HIS2A:CG31618, RPS4, HIS4:CG33875, HIS2A:CG33862, HIS3.3B, HIS3.3A, MRPL37, RPL11, HIS2A:CG33817, HIS2A:CG33865, HIS2A:CG33814, RPL35A, HIS4:CG33905, HIS4:CG33883, HIS4:CG33903, HIS4:CG33909, HIS4:CG33907, HIS4:CG31611, HIS4:CG33889, HIS4:CG33887, HIS4:CG33885, HIS2A:CG33850, GNF1, HIS2A:CG33856, HIS2A:CG33859, HIS2A:CG33853, HIS2A:CG33808, HIS4:CG33895, HIS2A:CG33838, HIS4:CG33897, HIS4:CG33899, BONSAI, ARC-P34, HIS4:CG33891, TRF, HIS4:CG33893, SAN, MRPL15,	98	1.3983

				MRPL14, HIS4R, RPL9, HIS2A:CG33844, HIS4:CG33901, HIS2A:CG33841, HIS2A:CG33847, RPS23, MRPS26, HIS2A:CG33829, CG7637, BORR, MRPL28, NOA36, RAVUS, LIN-52, HIS2A:CG33832, HIS2A:CG33835, CK			
nucleus	23	0.86175	0.06453947	HIS2A:CG33823, TAF10B, HIS4:CG33871, HIS2A:CG33826, HIS2A:CG33820, INO80, MLP60A, HIS4:CG33873, HIS2A:CG31618, HIS4:CG33875, HIS2A:CG33862, HIS3.3B, HIS3.3A, E(SPL), HIS2A:CG33817, HIS2A:CG33865, EAF, HIS2A:CG33814, HIS4:CG33905, HIS4:CG33883, HIS4:CG33903, HIS4:CG33909, HIS4:CG33907, TAP, HIS4:CG31611, HIS4:CG33889, HIS4:CG33887, HIS4:CG33885, IX, TAF10, HIS2A:CG33850, DOM, GNF1, HIS2A:CG33856, HIS2A:CG33859, HIS2A:CG33853, HIS2A:CG33808, HIS4:CG33895, HIS2A:CG33838, HIS4:CG33897, RBP1, HIS4:CG33899, HIS4:CG33891, TRF, LDBR, HIS4:CG33893, DPN, HIS4R, HIS2A:CG33844, HIS4:CG33901, HIS2A:CG33841, HIS2A:CG33847, REF(2)P, HIS2A:CG33829, CG7185, CG7637, SIMA, BORR, NOA36, HIS2A:CG33832, HIS2A:CG33835	234	1.4681	
phosphoprotein	21	0.78681	0.09608717	HIS2A:CG33823, HIS4:CG33871, HIS2A:CG33826, HIS2A:CG33820, INO80, HIS4:CG33873, HIS2A:CG31618, HIS4:CG33875, HIS2A:CG33862, HIS3.3B, HIS3.3A, DNT, HIS2A:CG33817, HIS2A:CG33865, EAF, HIS2A:CG33814, HIS4:CG33905, HIS4:CG33883, HIS4:CG33903, HIS4:CG33909, HIS4:CG33907, HIS4:CG31611, HIS4:CG33889, HIS4:CG33887, HIS4:CG33885, INOS, DOM, HIS2A:CG33850, CG8858, GNF1, HIS2A:CG33856, NRK, HIS2A:CG33859, HIS2A:CG33853, HIS2A:CG33808, HIS4:CG33895, HIS2A:CG33838, HSC70-5, HIS4:CG33897, RBP1, HIS4:CG33899, HIS4:CG33891, HIS4:CG33893, CED-6, DPN,	234	1.4293	

				HIS4R, HIS2A:CG33844, HIS4:CG33901, HIS2A:CG33841, HIS2A:CG33847, REF(2)P, HIS2A:CG33829, CG7185, BORR, HIS2A:CG33832, MTHL3, HIS2A:CG33835, CK, EEF1DELTA			
GO:0070013~intracellular organelle lumen	18	0.67441	0.05277352	MRPS26, TAF10B, CG7185, CG7637, RRP4, BONSAI, TRF, IX, TAF10, TAF13, DOM, MRPL28, NOA36, MRPL15, MRPL14, CG31650, EAF, CSTF-50	98	1.581	
GO:0043233~organelle lumen	18	0.67441	0.05277352	MRPS26, TAF10B, CG7185, CG7637, RRP4, BONSAI, TRF, IX, TAF10, TAF13, DOM, MRPL28, NOA36, MRPL15, MRPL14, CG31650, EAF, CSTF-50	98	1.581	
GO:0031974~membrane-enclosed lumen	18	0.67441	0.06482678	MRPS26, TAF10B, CG7185, CG7637, RRP4, BONSAI, TRF, IX, TAF10, TAF13, DOM, MRPL28, NOA36, MRPL15, MRPL14, CG31650, EAF, CSTF-50	98	1.5395	
GO:0005198~structural molecule activity	15	0.56201	0.05981311	MRPS26, RPL35A, RPL36A, CPR97EB, BONSAI, RPS4, SCGALPHA, CPR49AF, MRPL28, MRPL15, MRPL14, RPL9, CPR30F, RPL11, RPS23	155	1.6804	
GO:0030529~ribonucleoprotein complex	14	0.52454	0.04092536	MRPS26, RPL35A, RPL36A, CG7637, BONSAI, RPS4, SNRNA:U4ATAC:82E, MRPL28, MRPL15, MRPL14, RPL9, MRPL37, RPL11, RPS23	98	1.804	
cytoplasm	14	0.52454	0.05106217	TAF10B, IMPL3, TCP-1ETA, MLP60A, ARC-P34, UPDO, INOS, TAF10, BORR, SAN, CED-6, CG8858, CG10306, CK	234	1.7811	
GO:0006350~transcription	14	0.52454	0.08273623	TAF10B, INO80, TAP, SIMA, TRF, IX, TAF10, TAF13, DOM, DPN, E(SPL), CG13773, GNF1, EAF	148	1.6357	
ribosomal protein	12	0.44961	1.24E-04	MRPS26, RPL35A, RPL36A, MRPL28, MRPL15, MRPL14, RPL9, BONSAI, MRPL37, RPL11, RPS23, RPS4	234	4.2398	
GO:0005840~ribosome	12	0.44961	0.0012175	MRPS26, RPL35A, RPL36A, MRPL28, MRPL15, MRPL14, RPL9, BONSAI, MRPL37, RPL11, RPS23, RPS4	98	3.1508	

GO:0005811~lipid particle	12	0.44961	0.0113257	HIS2A:CG33823, CG4769, HIS4:CG33871, HIS2A:CG33826, HIS2A:CG33820, HIS4:CG33873, HIS2A:CG31618, HIS4:CG33875, RPS4, HIS2A:CG33862, RPL11, HIS2A:CG33817, HIS2A:CG33865, HIS2A:CG33814, HIS4:CG33905, HIS4:CG33883, HIS4:CG33903, HIS4:CG33909, HIS4:CG33907, HIS4:CG31611, CG12140, HIS4:CG33889, HIS4:CG33887, HIS4:CG33885, HMU, HIS2A:CG33850, HIS2A:CG33856, HIS2A:CG33859, HIS2A:CG33853, HIS2A:CG33808, HIS4:CG33895, HIS2A:CG33838, HSC70-5, HIS4:CG33897, L(2)37CC, HIS4:CG33899, HIS4:CG33891, HIS4:CG33893, NUP358, HIS4R, HIS2A:CG33844, HIS4:CG33901, HIS2A:CG33841, HIS2A:CG33847, HIS2A:CG33829, CG1882, RAB1, HIS2A:CG33832, HIS2A:CG33835	98	2.3536	
transcription regulation	12	0.44961	0.09043216	TAF10B, TAF10, DOM, DPN, E(SPL), GNF1, TAP, INO80, SIMA, TRF, EAF, IX	234	1.72	
Transcription	12	0.44961	0.09704439	TAF10B, TAF10, DOM, DPN, E(SPL), GNF1, TAP, INO80, SIMA, TRF, EAF, IX	234	1.6937	
GO:0033279~ribosomal subunit	11	0.41214	0.00162793	MRPS26, RPL35A, RPL36A, MRPL28, MRPL15, MRPL14, RPL9, BONSAI, RPL11, RPS23, RPS4	98	3.2756	
GO:0003735~structural constituent of ribosome	11	0.41214	0.00240841	MRPS26, RPL35A, RPL36A, MRPL28, MRPL15, MRPL14, RPL9, BONSAI, RPL11, RPS23, RPS4	155	3.1569	

GO:0005694~chromosome	11	0.41214	0.08638137	HIS2A:CG33823, HIS4:CG33871, HIS2A:CG33826, HIS2A:CG33820, INO80, HIS4:CG33873, HIS2A:CG31618, HIS4:CG33875, HIS2A:CG33862, HIS3.3B, HIS3.3A, HIS2A:CG33817, HIS2A:CG33865, HIS2A:CG33814, HIS4:CG33905, HIS4:CG33883, HIS4:CG33903, HIS4:CG33909, HIS4:CG33907, HIS4:CG31611, HIS4:CG33889, HIS4:CG33887, HIS4:CG33885, HIS2A:CG33850, GNF1, HIS2A:CG33856, HIS2A:CG33859, HIS2A:CG33853, HIS2A:CG33808, HIS4:CG33895, HIS2A:CG33838, HIS4:CG33897, HIS4:CG33899, HIS4:CG33891, TRF, HIS4:CG33893, SAN, HIS4R, HIS2A:CG33844, HIS4:CG33901, HIS2A:CG33841, HIS2A:CG33847, HIS2A:CG33829, BORR, NOA36, RAVUS, LIN-52, HIS2A:CG33832, HIS2A:CG33835	98	1.7671	
ribonucleoprotein	10	0.37467	5.88E-04	MRPS26, RPL36A, MRPL28, MRPL14, RPL9, CG7637, BONSAI, RPL11, RPS23, RPS4	234	4.2344	
GO:0044427~chromosomal part	10	0.37467	0.05643296	HIS2A:CG33823, HIS4:CG33895, HIS4:CG33871, HIS2A:CG33838, HIS4:CG33897, HIS2A:CG33826, HIS2A:CG33820, HIS4:CG33899, INO80, HIS4:CG33873, HIS2A:CG31618, HIS4:CG33891, HIS4:CG33875, HIS4:CG33893, HIS2A:CG33862, SAN, HIS3.3B, HIS3.3A, HIS4R, HIS2A:CG33844, HIS4:CG33901, HIS2A:CG33841, HIS2A:CG33817, HIS2A:CG33865, HIS2A:CG33847, HIS2A:CG33814, HIS4:CG33883, HIS4:CG33905, HIS2A:CG33829, HIS4:CG33903, HIS4:CG33909, HIS4:CG33907, HIS4:CG31611, HIS4:CG33889, HIS4:CG33887, HIS4:CG33885, BORR, HIS2A:CG33850, RAVUS, NOA36, LIN-52, GNF1, HIS2A:CG33856, HIS2A:CG33859, HIS2A:CG33832, HIS2A:CG33808, HIS2A:CG33853, HIS2A:CG33835	98	2.0097	

Appendix 2.5 GO functional clustering chart for the most enriched genes in larvae expressing *ATPSyn-Cf6* dsRNA

Term	Count	PValue	Genes	List Total	Fold Enrichment
GO:0043232~intracellular non-membrane-bounded organelle	27	0.0535137	HIS2A:CG33823, RPL36A, HIS4:CG33871, HIS2A:CG33826, HIS2A:CG33820, KL-3, INO80, HIS4:CG33873, HIS2A:CG31618, RPS4, HIS4:CG33875, HIS2A:CG33862, HIS3.3B, HIS3.3A, MRPL37, RPL11, HIS2A:CG33817, HIS2A:CG33865, HIS2A:CG33814, RPL35A, HIS4:CG33905, HIS4:CG33883, HIS4:CG33903, HIS4:CG33909, HIS4:CG33907, HIS4:CG31611, HIS4:CG33889, HIS4:CG33887, HIS4:CG33885, HIS2A:CG33850, GNF1, HIS2A:CG33856, HIS2A:CG33859, HIS2A:CG33853, HIS2A:CG33808, HIS4:CG33895, HIS2A:CG33838, HIS4:CG33897, HIS4:CG33899, BONSAI, ARC-P34, HIS4:CG33891, TRF, HIS4:CG33893, SAN, MRPL15, MRPL14, HIS4R, RPL9, HIS2A:CG33844, HIS4:CG33901, HIS2A:CG33841, HIS2A:CG33847, RPS23, MRPS26, HIS2A:CG33829, CG7637, BORR, MRPL28, NOA36, RAVUS, LIN-52, HIS2A:CG33832, HIS2A:CG33835, CK	98	1.398294631
GO:0043228~non-membrane-bounded organelle	27	0.0535137	HIS2A:CG33823, RPL36A, HIS4:CG33871, HIS2A:CG33826, HIS2A:CG33820, KL-3, INO80, HIS4:CG33873, HIS2A:CG31618, RPS4, HIS4:CG33875, HIS2A:CG33862, HIS3.3B, HIS3.3A, MRPL37, RPL11, HIS2A:CG33817, HIS2A:CG33865, HIS2A:CG33814, RPL35A, HIS4:CG33905, HIS4:CG33883, HIS4:CG33903, HIS4:CG33909, HIS4:CG33907, HIS4:CG31611, HIS4:CG33889, HIS4:CG33887, HIS4:CG33885, HIS2A:CG33850, GNF1, HIS2A:CG33856, HIS2A:CG33859, HIS2A:CG33853, HIS2A:CG33808, HIS4:CG33895, HIS2A:CG33838, HIS4:CG33897, HIS4:CG33899, BONSAI, ARC-P34, HIS4:CG33891, TRF, HIS4:CG33893, SAN, MRPL15, MRPL14, HIS4R, RPL9, HIS2A:CG33844, HIS4:CG33901, HIS2A:CG33841, HIS2A:CG33847, RPS23, MRPS26, HIS2A:CG33829, CG7637, BORR, MRPL28, NOA36, RAVUS, LIN-52, HIS2A:CG33832, HIS2A:CG33835, CK	98	1.398294631

nucleus	23	0.0645395	HIS2A:CG33823, TAF10B, HIS4:CG33871, HIS2A:CG33826, HIS2A:CG33820, INO80, MLP60A, HIS4:CG33873, HIS2A:CG31618, HIS4:CG33875, HIS2A:CG33862, HIS3.3B, HIS3.3A, E(SPL), HIS2A:CG33817, HIS2A:CG33865, EAF, HIS2A:CG33814, HIS4:CG33905, HIS4:CG33883, HIS4:CG33903, HIS4:CG33909, HIS4:CG33907, TAP, HIS4:CG31611, HIS4:CG33889, HIS4:CG33887, HIS4:CG33885, IX, TAF10, HIS2A:CG33850, DOM, GNF1, HIS2A:CG33856, HIS2A:CG33859, HIS2A:CG33853, HIS2A:CG33808, HIS4:CG33895, HIS2A:CG33838, HIS4:CG33897, RBP1, HIS4:CG33899, HIS4:CG33891, TRF, LDBR, HIS4:CG33893, DPN, HIS4R, HIS2A:CG33844, HIS4:CG33901, HIS2A:CG33841, HIS2A:CG33847, REF(2)P, HIS2A:CG33829, CG7185, CG7637, SIMA, BORR, NOA36, HIS2A:CG33832, HIS2A:CG33835	234	1.46813805
phospho protein	21	0.0960872	HIS2A:CG33823, HIS4:CG33871, HIS2A:CG33826, HIS2A:CG33820, INO80, HIS4:CG33873, HIS2A:CG31618, HIS4:CG33875, HIS2A:CG33862, HIS3.3B, HIS3.3A, DNT, HIS2A:CG33817, HIS2A:CG33865, EAF, HIS2A:CG33814, HIS4:CG33905, HIS4:CG33883, HIS4:CG33903, HIS4:CG33909, HIS4:CG33907, HIS4:CG31611, HIS4:CG33889, HIS4:CG33887, HIS4:CG33885, INOS, DOM, HIS2A:CG33850, CG8858, GNF1, HIS2A:CG33856, NRK, HIS2A:CG33859, HIS2A:CG33853, HIS2A:CG33808, HIS4:CG33895, HIS2A:CG33838, HSC70-5, HIS4:CG33897, RBP1, HIS4:CG33899, HIS4:CG33891, HIS4:CG33893, CED-6, DPN, HIS4R, HIS2A:CG33844, HIS4:CG33901, HIS2A:CG33841, HIS2A:CG33847, REF(2)P, HIS2A:CG33829, CG7185, BORR, HIS2A:CG33832, MTHL3, HIS2A:CG33835, CK, EEF1DELTA	234	1.429290546
GO:0043233~organelle lumen	18	0.0527735	MRPS26, TAF10B, CG7185, CG7637, RRP4, BONSAI, TRF, IX, TAF10, TAF13, DOM, MRPL28, NOA36, MRPL15, MRPL14, CG31650, EAF, CSTF-50	98	1.581045368
GO:0070013~intracellular organelle lumen	18	0.0527735	MRPS26, TAF10B, CG7185, CG7637, RRP4, BONSAI, TRF, IX, TAF10, TAF13, DOM, MRPL28, NOA36, MRPL15, MRPL14, CG31650, EAF, CSTF-50	98	1.581045368
GO:0031974~membrane-enclosed lumen	18	0.0648268	MRPS26, TAF10B, CG7185, CG7637, RRP4, BONSAI, TRF, IX, TAF10, TAF13, DOM, MRPL28, NOA36, MRPL15, MRPL14, CG31650, EAF, CSTF-50	98	1.539511777

GO:0005198~structural molecule activity	15	0.059831	MRPS26, RPL35A, RPL36A, CPR97EB, BONSAI, RPS4, SCGALPHA, CPR49AF, MRPL28, MRPL15, MRPL14, RPL9, CPR30F, RPL11, RPS23	155	1.680390492
GO:0030529~ribonucleoprotein complex	14	0.040925	MRPS26, RPL35A, RPL36A, CG7637, BONSAI, RPS4, SNRNA:U4ATAC:82E, MRPL28, MRPL15, MRPL14, RPL9, MRPL37, RPL11, RPS23	98	1.803995477
cytoplasm	14	0.051062	TAF10B, IMPL3, TCP-1ETA, MLP60A, ARC-P34, UPDO, INOS, TAF10, BORR, SAN, CED-6, CG8858, CG10306, CK	234	1.781149533
GO:0006350~transcription	14	0.082736	TAF10B, INO80, TAP, SIMA, TRF, IX, TAF10, TAF13, DOM, DPN, E(SPL), CG13773, GNF1, EAF	148	1.635723959
ribosomal protein	12	1.24E-04	MRPS26, RPL35A, RPL36A, MRPL28, MRPL15, MRPL14, RPL9, BONSAI, MRPL37, RPL11, RPS23, RPS4	234	4.239751756
GO:0005840~ribosome	12	0.001217	MRPS26, RPL35A, RPL36A, MRPL28, MRPL15, MRPL14, RPL9, BONSAI, MRPL37, RPL11, RPS23, RPS4	98	3.150757077
GO:0005811~lipid particle	12	0.011325	HIS2A:CG33823, CG4769, HIS4:CG33871, HIS2A:CG33826, HIS2A:CG33820, HIS4:CG33873, HIS2A:CG31618, HIS4:CG33875, RPS4, HIS2A:CG33862, RPL11, HIS2A:CG33817, HIS2A:CG33865, HIS2A:CG33814, HIS4:CG33905, HIS4:CG33883, HIS4:CG33903, HIS4:CG33909, HIS4:CG33907, HIS4:CG31611, CG12140, HIS4:CG33889, HIS4:CG33887, HIS4:CG33885, HMU, HIS2A:CG33850, HIS2A:CG33856, HIS2A:CG33859, HIS2A:CG33853, HIS2A:CG33808, HIS4:CG33895, HIS2A:CG33838, HSC70-5, HIS4:CG33897, L(2)37CC, HIS4:CG33899, HIS4:CG33891, HIS4:CG33893, NUP358, HIS4R, HIS2A:CG33844, HIS4:CG33901, HIS2A:CG33841, HIS2A:CG33847, HIS2A:CG33829, CG1882, RAB1, HIS2A:CG33832, HIS2A:CG33835	98	2.353577576
transcription regulation	12	0.090432	TAF10B, TAF10, DOM, DPN, E(SPL), GNF1, TAP, INO80, SIMA, TRF, EAF, IX	234	1.72000265
Transcription	12	0.097044	TAF10B, TAF10, DOM, DPN, E(SPL), GNF1, TAP, INO80, SIMA, TRF, EAF, IX	234	1.693743068
GO:0033279~ribosomal subunit	11	0.001627	MRPS26, RPL35A, RPL36A, MRPL28, MRPL15, MRPL14, RPL9, BONSAI, RPL11, RPS23, RPS4	98	3.275634644

GO:0003735~structural constituent of ribosome	11	0.0024084	MRPS26, RPL35A, RPL36A, MRPL28, MRPL15, MRPL14, RPL9, BONSAI, RPL11, RPS23, RPS4	155	3.156868431
GO:0005694~chromosome	11	0.0863814	HIS2A:CG33823, HIS4:CG33871, HIS2A:CG33826, HIS2A:CG33820, INO80, HIS4:CG33873, HIS2A:CG31618, HIS4:CG33875, HIS2A:CG33862, HIS3.3B, HIS3.3A, HIS2A:CG33817, HIS2A:CG33865, HIS2A:CG33814, HIS4:CG33905, HIS4:CG33883, HIS4:CG33903, HIS4:CG33909, HIS4:CG33907, HIS4:CG31611, HIS4:CG33889, HIS4:CG33887, HIS4:CG33885, HIS2A:CG33850, GNF1, HIS2A:CG33856, HIS2A:CG33859, HIS2A:CG33853, HIS2A:CG33808, HIS4:CG33895, HIS2A:CG33838, HIS4:CG33897, HIS4:CG33899, HIS4:CG33891, TRF, HIS4:CG33893, SAN, HIS4R, HIS2A:CG33844, HIS4:CG33901, HIS2A:CG33841, HIS2A:CG33847, HIS2A:CG33829, BORR, NOA36, RAVUS, LIN-52, HIS2A:CG33832, HIS2A:CG33835	98	1.76711869
ribonucleoprotein	10	5.88E-04	MRPS26, RPL36A, MRPL28, MRPL14, RPL9, CG7637, BONSAI, RPL11, RPS23, RPS4	234	4.234357669
GO:0044427~chromosomal part	10	0.056433	HIS2A:CG33823, HIS4:CG33895, HIS4:CG33871, HIS2A:CG33838, HIS4:CG33897, HIS2A:CG33826, HIS2A:CG33820, HIS4:CG33899, INO80, HIS4:CG33873, HIS2A:CG31618, HIS4:CG33891, HIS4:CG33875, HIS4:CG33893, HIS2A:CG33862, SAN, HIS3.3B, HIS3.3A, HIS4R, HIS2A:CG33844, HIS4:CG33901, HIS2A:CG33841, HIS2A:CG33817, HIS2A:CG33865, HIS2A:CG33847, HIS2A:CG33814, HIS4:CG33883, HIS4:CG33905, HIS2A:CG33829, HIS4:CG33903, HIS4:CG33909, HIS4:CG33907, HIS4:CG31611, HIS4:CG33889, HIS4:CG33887, HIS4:CG33885, BORR, HIS2A:CG33850, RAVUS, NOA36, LIN-52, GNF1, HIS2A:CG33856, HIS2A:CG33859, HIS2A:CG33832, HIS2A:CG33808, HIS2A:CG33853, HIS2A:CG33835	98	2.009742168

Appendix 2.6 GO functional clustering chart for the genes which are commonly most enriched in larvae overexpressing *TFAM* or expressing *ATPSyn-Cf6* dsRNA

Term	Count	%	PValue	Genes	List Total	Fold Enrichment
GO:0016251~general RNA polymerase II transcription factor activity	4	0.89286	0.03927	TAF10, TAF13, DOM, IX	68	5.2333113
Secondary metabolites biosynthesis, transport, and catabolism / General function prediction only	2	0.44643	0.05154	CG2064, CG2065	6	31.7179487
mrna processing	3	0.66964	0.06401	RBP1, CG7185, LDBR	115	7.20444033
glycoprotein	8	1.78571	0.08838	CG16868, GR59C, FUCTB, LANB1, GNBP1, GR8A, MTHL3, ACER	115	2.07576212